

Interference Reduction in Multiuser Relay Networks

Dissertation

zur

Erlangung des akademischen Grades

Doktor-Ingenieur (Dr.-Ing.)

der Fakultät für Informatik und Elektrotechnik

der Universität Rostock

vorgelegt von

Hussein Al-Shatri, geb. am 01.01.1980 in Jeddah

aus Rostock

Tag der Abgabe: 5. November 2013

Als Dissertation genehmigt von
der Fakultät für Informatik und Elektrotechnik
der Universität Rostock

Gutachter:

Prof. Dr.-Ing. habil. Tobias Weber (Universität Rostock)
Prof. Dr.-Ing. Anja Klein (Technische Universität Darmstadt)
Prof. Dr.-Ing. habil. Volker Kühn (Universität Rostock)

Tag der öffentlichen Verteidigung:

04. April 2014

Acknowledgement

First of all, I would like to express the full of praise and grateful to Allah for this grace and achievement. Then, worm thanks from my heart to my mother who supports me all the way since my undergraduate studies till I become a doctor. Furthermore, I would never forget the unlimited support and patience of my wife – Fatima Al-Aidaros – during the last five years. I think living and doing research in Rostock would be really tough without her.

Furthermore, I would like to express my honest, sincere appreciation and gratitude to my supervisor Prof. Tobias Weber. His insights, suggestions, comments and unlimited support have added a meaningful value to this work. I would like to thank Prof. Anja Klein (Technische Universität Darmstadt) for her great interest in my research and for our close and very successful collaboration in several aspects documented in this work especially on interference alignment. I also thank Prof. Volker Kühn for his fruitful discussions during our institute seminars.

Moreover, I would like to thank my present and former colleagues especially M.Sc. Behailu Shikur who spent his precious time in carefully proofreading a draft of this manuscript. Special thank goes to M.Sc. Karsten Wiedmann for his tireless assistance and essential comments during the writing phase of this manuscript especially in writing the summary section in German language. Furthermore, I would like to express my worm thanks to M.Sc. Xiang Li and M. Sc. Rakash SivaSiva Ganesan (Technische Universität Darmstadt) for the fruitful discussions on topic of interference alignment.

Rostock, 16. April 2014

Hussein Al-Shatri

Contents

1	Introduction	1
1.1	Interference in cellular systems	1
1.2	Degrees of freedom of interference channels and the concept of interference alignment	2
1.3	State of the art and open problems	5
1.4	Outline of the dissertation	10
2	System model and reference scheme	12
2.1	System model and transmission technique	12
2.1.1	Cellular system model	12
2.1.2	One-way relaying transmission technique	14
2.2	Reference scheme and channel normalization	17
2.2.1	Single cell relaying algorithm	17
2.2.2	Channel model and normalization	22
3	Interference alignment	26
3.1	Interference alignment conditions	26
3.2	System of multivariate polynomial equations	27
3.3	Interference alignment with fixed transmit and receive filters	30
3.3.1	Inhomogeneous system of linear equations	30
3.3.2	Feasibility of interference alignment	32
3.3.3	Closed form solution with minimum relays retransmit energy	33
3.4	Interference alignment with partially adapted transmit and receive filters	35
3.4.1	Homogeneous system of linear equations	35
3.4.2	Feasibility of interference alignment	35
3.4.3	Closed form solution with minimum sum mean square error	36
3.5	Complexity and performance of interference alignment algorithms	38
3.5.1	Preliminary remarks	38
3.5.2	Complexity analysis	39
3.5.3	Performance analysis	41
4	Energy allocation for interference alignment systems	44
4.1	Preliminaries	44
4.2	Energy allocation for a single resource in an interference alignment system	48
4.3	Energy allocation for multiple orthogonal resources in an interference alignment system	50
4.3.1	Motivation and problem statement	50

4.3.2	Fairness constrained maximum sum rate energy allocation	51
4.4	Complexity and performance of the energy allocation algorithms	55
4.4.1	Complexity analysis	55
4.4.2	Performance analysis	56
5	Interference mitigation	61
5.1	Preliminaries	61
5.2	Interference mitigation with fixed transmit and receive filters	62
5.3	Interference mitigation with partially adapted transmit and receive filters	64
5.3.1	Energy constrained minimum sum mean square error	64
5.3.1.1	Problem statement	64
5.3.1.2	Quadratically constrained quadratic minimization problem	65
5.3.2	Energy constrained maximum sum rate	70
5.3.2.1	Problem statement and the concept of multi-convex op- timization	70
5.3.2.2	Signal to interference plus noise ratio	72
5.3.2.3	Sum rate maximization based on multi-convex optimi- zation	74
5.3.2.4	Some comments on the sum rate maximization algorithm	77
5.4	Complexity and performance of the interference mitigation algorithms .	77
5.4.1	Complexity analysis	77
5.4.2	Performance analysis	80
6	Energy allocation for interference mitigation systems	86
6.1	Preliminaries	86
6.2	Energy allocation for a single resource in an interference mitigation system	89
6.2.1	Problem statement and reformulation	89
6.2.2	Branch and bound algorithm – basic idea	92
6.2.3	Branching the feasible region	94
6.2.4	Bounding the maximum sum rate	96
6.3	Energy allocation for multiple orthogonal resources in an interference mitigation system	101
6.4	Complexity and performance of the energy allocation algorithms	105
6.4.1	Complexity analysis	105
6.4.2	Performance analysis	106
7	Summaries	110
7.1	Summary in English language	110
7.2	Kurzfassung in deutscher Sprache	112

A	Linear algebra	114
A.1	The Kronecker product and the vectorization operator	114
A.2	Some properties of the Kronecker product and the vectorization operator	114
A.3	Woodbury matrix inversion lemma	115
B	Proofs of propositions	116
B.1	Proof of Proposition 1	116
B.2	Proof of Proposition 2	118
C	Computational complexity	120
C.1	Complexity measure	120
C.2	Complexity of some mathematical operations and functions	120
D	Acronyms and symbols	123
	Bibliography	127

Chapter 1

Introduction

1.1 Interference in cellular systems

In the last few years, advances in electronics and digital signal processing have triggered the telecommunications industry to flood the market with high-technology smart terminals such as smart phones, tablets and laptops. These smart terminals support many different packet-based data application services such as interactive gaming, mobile TV and high definition video services. The high density of users in cells with such broadband services results in huge traffic demands which have to be satisfied. Therefore, system operators have to utilize the limited available bandwidth effectively and extensively to serve as many users as they can with a sufficiently high throughput. In the following, an overview of some of the key solutions and challenges in the design of future cellular systems are discussed.

The orthogonal frequency division multiplexing (OFDM) technique is employed to the physical layer of modern cellular systems [CT65, Cha66, WE71, Bel76, PR80, Cim85]. The OFDM technique splits the available frequency band into a large number of tightly spaced orthogonal subcarriers [Cha66, WE71]. It is immune to intersymbol interference as the cyclic prefix is selected longer than the channel impulse response or the multipath delay [PR80, RCK92]. In modern wireless cellular systems, users are served with two dimensional orthogonal time/frequency resource blocks. In a certain time instant, the resource blocks contain different sets of OFDM subcarriers where the split of the subcarriers among the resource blocks is unique [DPSB08]. The interference within the same cell, i.e., intra-cell interference, is avoided by serving users belonging to the same cell with different resource blocks. However, inter-cell interference is the major performance limiting factor of current cellular systems [EAH09]. Inter-cell interference occurs when at least two users, each of which belongs to a different cell, are served simultaneously with the same resource block. The received interference power can be severe and even comparable to the useful signal power especially for the cell-edge users. A low signal to interference plus noise ratio (SINR) results and thus, low throughput is achieved by the cell-edge users.

Future cellular systems will introduce small cells which cover some parts of the existing cells and aim at improving the achievable throughput of the cell-edge users. For

instance, relays will be employed for extending the cell coverage and for enhancing the achievable throughput [YHXM09, BNC⁺12]. The relays communicate with the base stations (BSs) and the users through wireless links. As a relay receives a signal from a BS/user and retransmits it to a user/BS, the relay needs to avoid self-interference using some sort of separation between its receiver and its transmitter. This separation is usually done in frequency domain or in time domain [HCM⁺12]. In other words, relays can receive and retransmit either in different frequency bands or in different time periods. Mainly two relaying protocols are proposed for future cellular systems [YHXM09, HCM⁺12]. The first one is the amplify and forward relaying protocol in which the relay simply amplifies the received signal including the received noise and retransmits it. The second relaying protocol is the decode and forward relaying protocol where the relay decodes the received message, applies error correction techniques to it and retransmits it after encoding the corrected message.

The coexistence of different types of cells sharing the same limited resource blocks with different overlapping coverage areas and different maximum transmit powers complicates the interference problem. Furthermore, adding relays to the system increases the received power of the useful signal as a user is closer to the relay than to the BS but it also causes an additional inter-cell interference as the relays are using the same set of resource blocks as other BSs [LPGD⁺11]. Based on the above discussion, there are vital demands for developing smart transmission schemes which aim at reducing the inter-cell interferences and increasing the throughput of the individual users.

1.2 Degrees of freedom of interference channels and the concept of interference alignment

Obviously, improving the user satisfaction with a variety of broadband application services is the main goal when designing any communication system. For realtime services such as interactive gaming, video conferencing and video streaming, minimizing transmission delay and packet loss plays a critical role in the system performance. In non-realtime services such as web-browsing, emailing and file transfer, it is required to maximize the throughput for optimizing the packet transmission [She95].

From an information theory perspective, the channel capacity in a system consisting of several node pairs and relays sharing the same medium is not known. A more fundamental problem is the capacity of an interference channel (IC) [Ahl74, Car78]. In an IC, a number of source-destination node pairs communicate with each other through a

shared medium. Any transmission of a source node will not just result in a useful signal at its corresponding destination node but also in interference signals at all the other destination nodes. Moreover, the capacity region of a channel can be defined as the closure of the set of all achievable rate tuples. For the general IC, the capacity region has been an open problem for more than 30 years even for a two node pair scenario. It is known only for special cases such as strong interference [Car75, Sat81, Cos85]. The best known inner bound of the capacity region of a two node pair Gaussian IC is based on rate splitting and joint decoding which is due to Han and Kobayashi (HK) [HK81]. However, the HK bound is valid only for two node pairs and it involves complicated calculations. As a result, a simpler technique to calculate the HK bound and a simplified form of the HK bound are proposed in [Sas04] and in [Kra06, CMGG08], respectively. Moreover, among the outer bounds of the capacity region of a two node pair Gaussian IC proposed in [Sat77, Car83, Kra04, ETW08], the one proposed by Etkin, Tse and Wang in [ETW08] is tight within 1 bit.

The sum capacity of ICs is not known in general as well. It is known that by treating the received interference as noise, the sum capacity of a Gaussian IC is achieved only for the weak interference case [MK09, SKC09, AV09]. In [WT08, MK09], the sum capacity of a Gaussian IC for mixed interference is found. However, several upper bounds of the sum capacity of a Gaussian IC are proposed in [ETW08, MK09, SKC09, AV09, Etk09].

In recent years, a distinguishable direction of research on information theory has been initiated which concentrates on investigating the degrees of freedom (DoFs) of communication networks which is also known as the multiplexing gain or the pre-log factor [TV05]. For a communication network, if γ is considered to be the received signal to noise ratio (SNR) at a destination node, the DoFs are defined as

$$d_{\text{dof}} = \lim_{\gamma \rightarrow \infty} \left\{ \frac{C(\gamma)}{\text{ld}(\gamma)} \right\}, \quad (1.1)$$

where $C(\gamma)$ is the sum capacity of the network as a function of the received SNR [JS08, CJ08]. As the DoFs are defined at infinite SNR, they do not depend on neither the power allocation, the absolute values of the channel coefficients nor the received noise powers but rather they depend only on the network topology [Jaf11]. The DoFs are a measure of the achievable interference free useful signal space dimensions in a communication network [CJ08]. For instance, the capacity of a single source-destination node pair, see Fig. 1.1a, can be written as

$$C = \text{ld}(1 + \gamma) \quad (1.2)$$

[CT06]. By substituting (1.2) in (1.1), 1 DoF is achieved which implies that the whole received signal space of the destination node can be exploited interference-freely. Fig.

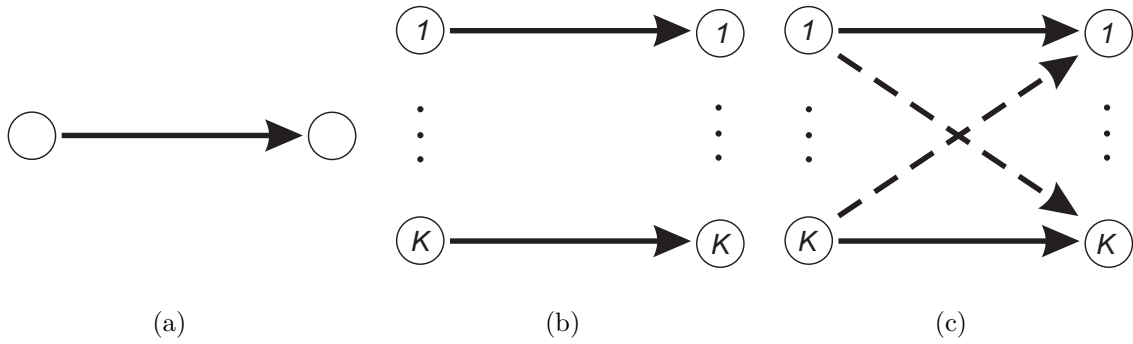


Fig. 1.1: Unidirectional communications through a shared medium between (a) a single node pair, (b) K node pairs with no cross links, and (c) K node pairs with cross links.

1.1b shows simultaneous unidirectional transmissions in a shared medium of K source-destination node pairs but there are no cross links among different node pairs. Assuming equal received SNRs γ at the destination nodes, The sum capacity of this network is calculated as

$$C = K \log(1 + \gamma). \quad (1.3)$$

Hence, the achieved DoFs are K which means that the received signal spaces at all destination nodes can be used simultaneously with no interferences. If there are cross links among the node pairs, i.e., the network topology represents an IC, as illustrated in Fig. 1.1c, $K/2$ DoFs can be achieved at the best [CJ08]. This means that independently of the number of node pairs, half of the received signal space of every destination node can be exploited interference-freely for the useful signals.

The DoFs of ICs are achievable using a transmission scheme called interference alignment (IA) [CJ08]. The DoFs of ICs are achieved when the received interference signals are aligned such that they cover just half of the signal space of each destination node while the other half is exploited interference-freely by the useful signals. IA can be realized in time [CJ08, NGJV09], frequency [SHMV08], spatial dimensions [TGR09, PJ09] or using multilevel structured codes [MOGMAK09, BPT10]. For instance, a toy example of IA is shown in Fig. 1.2. A scenario consisting of three node pairs each of which is equipped with two antennas is considered. Each source node wants to transmit a single data symbol to its corresponding destination node through a time invariant channel. As the source nodes and the destination nodes are equipped with two antennas each, every source node and destination node has two dimensional transmit and receive signal spaces, respectively. In this example, IA is achieved if the transmit filters at the source nodes are designed in such a way that the interference signals received at each destination node span only a one dimensional subspace known as the interference subspace of

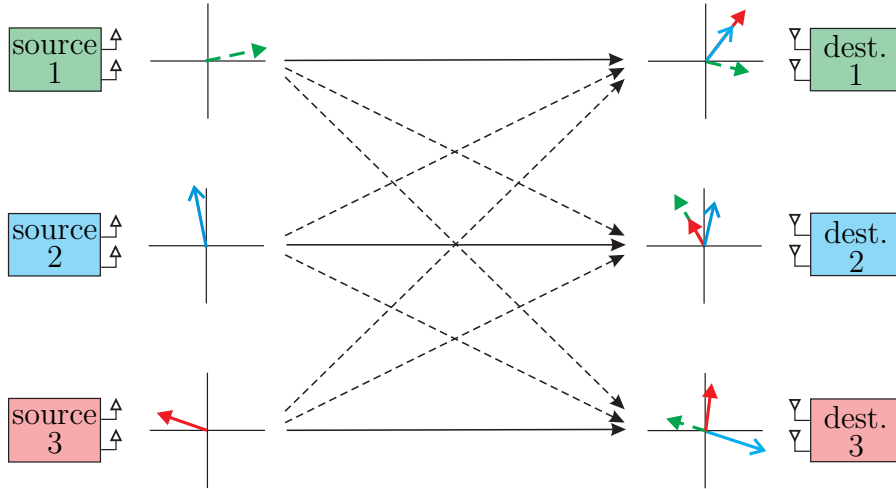


Fig. 1.2: Illustration of aligning the received interference signals at the destination nodes in spatial domain for a three node pair scenario.

the two dimensional received signal space. Furthermore, the useful signal received at a destination node has to be linearly independent of the interference subspace as shown in Fig. 1.2. Accordingly, every destination node can apply the zero forcing processing technique [UK08] to get rid of the received interferences and hence, the useful signal is decoded interference-freely.

In principle, the IA problem is an over-determined problem as the number of alignment constraints related to the number of interference signals, increases quadratically with the number of node pairs. Therefore, the number of variables, i.e., transmit filters, has to increase while attaining the number of constraints by transmitting over many time extensions [CJ08] or multiple antennas [TGR09].

1.3 State of the art and open problems

In this section, the problem tackled in the present dissertation is motivated pointing out the related contributions and the open problems. A wireless system consisting of an equal number of source nodes and destination nodes each of which being equipped with a single antenna is considered. Each of the source nodes wants to transmit a data symbol to its corresponding destination node. If the communication between the node pairs takes place simultaneously through a shared medium, the system is interference limited. A number of half duplex relays are added to the system for interference reduction rather than for the conventional purpose of range extension, see Section 1.1. Without loss of

generality, it is assumed that there are not enough antennas at the relays so that the relays cannot decode the received signals. As a result, the amplify and forward relaying protocol is considered. A transmission technique realized in two subsequent time slots is considered. The source nodes transmit to both the relays and the destination nodes in the first time slot. In the second time slot, both the source nodes and the relays retransmit to the destination nodes. At the nodes, there are filters with two coefficients each because the source nodes and the destination nodes transmit and receive twice, respectively. The present work mainly focuses on how the filter and the relay coefficients can be optimized such that the system performance is improved at all SNRs. Within this context, several problems are of interest, namely IA, sum mean square error (MSE) minimization, sum rate maximization, and energy allocation. In the following, each of these problems is discussed highlighting the open issues which are addressed in the present dissertation.

In general, relays cannot increase the DoFs of interference networks when the network is fully connected [CJ09]. However, in some special cases such as the network being partially connected [GG11], the relays being full duplex [GMGK09, LJ11] or the relays being cognitive [CS12], relays can increase the DoFs of interference networks beyond the DoFs bound shown in [CJ08]. Nevertheless, relays can help for achieving IA [GCJ11]. Employing relays for IA achievement in wireless systems is a more realistic proposal as compared to other techniques such as employing many time extensions or employing multiple antennas at the nodes for realizing IA. For a multiple node pair scenario with no relays, IA can be realized by designing the temporal transmit filters at the source nodes over many time extensions of a time variant channel [CJ08]. The main difficulty of realizing IA over many time extensions is that the channel knowledge is required to be available at the source nodes in advance. In scenarios with multiple antenna node pairs with no relays, IA can be realized in spatial dimensions over a time invariant channel [TGR09, PJ09, KX10, PD10, LD10, GCJ11]. However, the achieved DoFs are limited by the number of node pairs as shown in [YGJK10, BCT11, RLL12]. The authors normalize the Dofs over the number of the antennas at a destination node. Based on this, the number of antennas at the nodes has to be increased when new node pairs are added to these scenarios which increases the received signal space dimensionality at the destination nodes and thus, decreases the normalized DoFs.

In multiple node pair scenarios with relays, zero forcing techniques are usually applied at the relays using either joint signal processing methods if the relays can exchange their data and the channel knowledge [UK08] or distributed signal processing methods if the relays exchange only the channel knowledge [BNzOP06, MB07, RW07, BKW⁺09, EW10]. In these zero forcing techniques, the direct links are not exploited. However, the relay coefficients are adapted to the channel in such a way that no interference

is received at the destination nodes. Hence, there is no interference subspace at the received signal space of each destination node. If the direct links are considered and if the number of relays is insufficient for nullifying the interference signals, the transmit filters at the source nodes and the receive filters at the destination nodes should be adapted to the channel as well to nullify the interferences at the output of the receive filter of each destination node. As a result, at least half of the dimensions of the received signal space at the destination nodes shall be occupied by the interference signals, i.e., the received interferences shall be aligned at the destination nodes in this case [CJ08]. The problem of adapting the transmit filters at the source nodes, the receive filters at the destination nodes, and the relay coefficients to the channel aiming at getting rid of the interferences is a tri-affine problem, i.e., it is linear either in the transmit filters, in the receive filters or in the relay coefficients [AW11b, AGKW12a, AGKW12b].

During the last few years, several research groups have considered the relay aided IA problem. For instance, a three node pair scenario with single relay is considered in [GCJ11]. Each of the nodes and the relay is equipped with a single antenna. Gomadam et. al. conjecture in [GCJ11] that by designing proper temporal transmit filters at both the source nodes and the relay, IA is almost surely achievable with $3/2$ DoFs without a need for time extensions. This scenario is extended to consider K node pairs with a multiple antenna relay in [NMK10, CC10]. In [NMK10], it is shown that $K/2$ DoFs are achievable if the number of antennas at the relay is at least $\sqrt{(K-1)(K-2)}$. However, no IA algorithm is proposed. In [CC10], the authors propose an algorithm which adapts the relay coefficients such that the interference links through the relay are linearly dependent of the direct interference links. $K/2$ DoFs are achieved requiring at least $K-1$ antennas at the relay. However, the direct links are not exploited during the second time slot. Based on the above discussion, IA is achievable in multiple node pair scenarios with relays but all of the above contributions consider special case scenarios, i.e., a single relay with multiple antennas and specific designs of the filters. In this work, a multiple node pair scenario with an arbitrary number of relays and relay antennas is considered. First, the IA problem for the considered scenario is investigated. It is shown that a single variable representing the direction of the vector of each filter can help in solving the IA problem [AW11b]. Therefore, two cases of fixed filters and partially adapted filters are studied. For each case, the IA feasibility is investigated and an IA algorithm is proposed.

IA maximizes the DoFs of the interference channels and the DoFs are defined at infinite SNRs. Accordingly, the IA algorithms achieve significantly high sum rates only at high SNRs as compared to the sum rates achieved by algorithms which treat the interference as noise. In practice, energies are limited and most of the wireless systems operate at a range between low and moderate SNRs. In this range, noise

reduction in addition to interference reduction should be taken into account. Therefore, other transmission schemes which aim at minimizing the sum MSE or maximizing the sum rate should be applied. By minimizing the sum MSE, both the noise and the interference are mitigated keeping only the useful signals. Several previous contributions consider minimizing the sum MSE problem in interference networks [SSB⁺09, SLTW10, MXF⁺10, GAWK13, ALG⁺13a]. For multiple input multiple output (MIMO) ICs, the sum MSE is a convex function either of the transmit filters with fixed receive filters or of the receive filters with fixed transmit filters. This biconvexity property of the sum MSE function is exploited by alternately minimizing the sum MSE over the transmit filters and then over the receive filters. Moreover, iterative algorithms which guarantee achieving a local minimum are proposed in [SSB⁺09, SLTW10]. The authors of [SSB⁺09] show that the minimum sum MSE is implicitly an IA solution at the high SNR regime, i.e., a zero forcing solution. For multiple node pair scenarios with relays, the sum MSE is a tri-convex function of either the transmit filters, the receive filters or the relay coefficients and thus, an iterative alternate minimization algorithm is proposed in [MXF⁺10, GAWK13]. Apart from the iterative algorithms proposed in [SSB⁺09, SLTW10, MXF⁺10, GAWK13], closed form solutions for minimizing the sum MSE for the considered scenario are also of interest. By fixing part of the filter coefficients, the sum MSE becomes a convex function of the relay coefficients and the unfixed part of the filter coefficients. With the constraint of some of the filter coefficients being fixed, closed form solutions of the minimum sum MSE problem with either an IA constraint or a total energy constraint are proposed [ALG⁺13a].

Apart from solving a tri-affine problem for maximizing the DoFs, i.e., achieving the IA, or solving a tri-convex optimization problem for minimizing the sum MSE, maximizing the sum rate is the ultimate goal for improving the system performance. In multiple node pair scenarios with relays, optimizing the transmit filters, the receive filters and the relay coefficients aiming at maximizing the sum rate with a total energy constraint is a non-convex problem. Even individually optimizing either the transmit filters, the receive filters or the relay coefficients for sum rate maximization results in non-convex optimization problems. In [CA_dCC08, SRLH11, TH11], the authors optimize the receive filters aiming at minimizing the MSE for fixed transmit filters and relay coefficients. Using the optimized receive filters and by adding a set of scaling factors, they wrote the sum rate as a tri-concave function of the transmit filters, the relay coefficients and the added scaling factors. In the present work, the sum rate maximization problem for the considered scenario is addressed. The goal is to optimize both the filters and the relay coefficients for maximizing the sum rate with a total energy constraint. By adding two sets of scaling factors, a novel formulation of the sum rate maximization problem as a multi-convex optimization problem is presented [ALG⁺13b].

This new multi-convex problem formulation is quite general as it can be applied to any communication system in which the estimated data symbols are multi-linear functions of the system variables.

In multiple node pair scenarios with relays, optimizing the transmit energies of the source nodes and the relays is studied. Due to the existence of the direct links among the node pairs, an IA solution cannot be simply scaled for satisfying an energy constraint. Furthermore, the joint problem of achieving IA and optimizing the energy allocation is a non-convex problem. If the filter and the relay coefficients are determined using an IA solution, one can see that the effective channel including the filters and the relays as an interference free channel because the system is linear. Accordingly, the task is on how to allocate energies among the source nodes and the relays such that the sum rate is maximized. At high SNRs, sum rates being close to the optimum can be achieved by transmitting the data symbols with equal energies, i.e., received noise powers are very small as compared to the useful signal powers [APW09]. In low and moderate SNRs, energy allocation plays a key role in enhancing the system performance. Assuming a total energy constraint among the source nodes and the relays, the waterfilling algorithm certainly achieves the maximum sum rate [Sha49]. In this work, energy allocation on the top of an IA solution is addressed. Moreover, energy allocation in scenarios with multiple orthogonal resources is studied. For these scenarios, a rate fairness constraint among the node pairs is added [AW10].

The objectives of minimizing the sum MSE and maximizing the sum rate find a compromise between interference reduction and noise reduction and they do not necessarily align the interferences at the destination nodes especially at the noise dominant regime. Accordingly, the unaligned interferences are treated as noise. For the resulting IC, several energy allocation algorithms have been proposed. Some well known suboptimum energy allocation algorithms which try to maximize the sum rate with individual energy constraints are proposed in [YGC01, YGC02, CYM⁺06]. Considering fairness among the node pairs, a common approach in energy allocation is the signal to interference ratio (SIR) balancing [Aei73, AN82, NA83, Zan92a, Zan92b, GVGZ93, GZ94, GVG94]. For the SIR balancing, energies are allocated to the source nodes in such a way that the SIRs at the destination nodes are equal. By applying this algorithm, destination nodes achieve equal rates only at the interference dominant regime. An energy allocation algorithm which equalizes the received SINRs among the destination nodes and thus, equalizes the achieved data rates is proposed in [Ibe04]. This algorithm is fair in terms of the achieved rates at the destination nodes at all SNRs.

In ICs, the sum rate as a function of the allocated energies is not a concave function when the interference is treated as noise, i.e., the sum rate function has many

local maxima and a global maximum. As a result, this energy allocation optimization problem is non-convex [LZ08, HL09]. In the last decade, several research groups have tackled this energy allocation optimization problem with total and individual energy constraints. Firstly, a suboptimal iterative algorithm is proposed in [APW09]. In every iteration, this algorithm calculates the interference from the energy allocation being found in the previous iteration and solving the resulting energy allocation problem in a similar way as the waterfilling algorithm. In [CTP⁺07], the sum rate function is formulated as a convex geometric program which is guaranteed to converge to a global optimum only at the high SINR regime. Likewise at the high SINR regime, tools from nonnegative matrix theory are applied to find the global optimum with a polynomial complexity [TCS11]. Furthermore, the monotonicity of the sum rate function is exploited in [QZH09]. From monotonic programming, an algorithm called polyblock algorithm [Tuy00] is applied to find the global optimum at all SNRs. However, the polyblock algorithm has a high computational complexity which limits the applicability of the proposed method to only few node pair energy allocation problems. In the present work, the energy allocation optimization problem aiming at maximizing the sum rate with a total energy constraint is addressed. Unlike the previous contributions which are either valid only for a certain range of the SNRs or encounter expensive computational complexity, an algorithm which efficiently finds the global maximum sum rate for all SNRs is of interest. Basically, the structure of the sum rate function is exploited and formulated as a difference of two concave functions. Accordingly tools from difference of two convex functions (DC) programming [HPTd91, HT99, HPT00] are applied. Moreover, a branch and bound algorithm which converges to the global optimum is proposed. Moreover, energy allocation in scenarios with multiple orthogonal resources are studied.

1.4 Outline of the dissertation

In this section, the structure of the present dissertation is presented. In the following, the contents of the next chapters are outlined.

Chapter 2 starts by introducing the system model on which the analyses in the following chapters are based on. The system model is based on a cellular layout and it considers several relays each of which is equipped with an arbitrary number of antennas. In Section 2.1.2, a two time slot transmission technique is explained. To assess the performances of the proposed algorithms, Section 2.2.1 proposes an interference limited transmission scheme as a reference scheme. Basically, the reference scheme ignores the

inter-cell interferences and optimizes the transmission for each cell individually. Finally, a channel model and a channel normalization method are detailed in Section 2.2.2.

Chapter 3 concentrates on IA. Section 3.1 and Section 3.2 discuss the IA problem in general and show its solvability within the scope of the considered system model. Then, two IA algorithms are proposed and investigated. Firstly, an IA algorithm with fixed transmit and receive filters is detailed in Section 3.3. For the IA algorithm with fixed filters, the IA solution with the minimum retransmit energy of the relays is found in a closed form. Secondly, an IA algorithm with partially adapted transmit and receive filters is detailed in Section 3.4. An IA solution with the minimum sum MSE is selected in a closed form for the IA algorithm with partially adapted filters. Section 3.5 discusses the complexities and the performances of the proposed IA algorithms.

Energy allocation in the context of IA is investigated in Chapter 4. Basically, the IA algorithms being proposed in Chapter 3 employ equal energy allocation. Therefore, the energy allocation on the top of an IA solution is investigated in Section 4.2. Moreover, Section 4.3 extends the scenario and considers simultaneous transmissions through several orthogonal resources. For the multi-resource systems, an algorithm which maximizes the sum rate and guarantees equal rates achieved at the destination nodes is proposed. Section 4.4 discusses the complexities and the performances of the proposed energy allocation algorithms.

Chapter 5 focuses on interference mitigation. In contrast to the IA algorithms which aim at nullifying the interferences at the output of the receive filters, the interference mitigation algorithms do not necessarily nullify the interferences. Section 5.2 proposes an interference mitigation algorithm assuming fixed transmit and receive filters which minimizes the total unaligned interference power. In Section 5.3.1, an algorithm which minimizes the sum MSE with a total energy constraint is proposed. In Section 5.3.2, the sum rate maximization problem is formulated as a multi-convex optimization problem and a low complexity iterative algorithm which guarantees a local maximum is proposed. Section 5.4 discusses the complexities and the performances of the proposed interference mitigation algorithms.

The main focus in Chapter 6 is the energy allocation on the top of an interference mitigation solution. Section 6.1 explains the non-convex energy allocation problem of maximizing the sum rate with a total energy constraint. In Section 6.2, the problem is reformulated as a DC problem and solved using the branch and bound algorithm. Furthermore, the case of having several orthogonal resources is considered in Section 6.3. Section 6.4 discusses the complexity and the performance of the proposed energy allocation algorithm. Chapter 7 summaries the contributions of the dissertation.

Chapter 2

System model and reference scheme

2.1 System model and transmission technique

2.1.1 Cellular system model

In this section, a cellular system model on which the investigations in the later chapters are based on is introduced. The downlink of a cellular scenario consisting of K hexagonal cells is considered. As discussed in Section 1.1, users belonging to the same cell are served with different orthogonal resources. Therefore, it is reasonable to consider a single user per cell for investigating the interference reduction schemes. An illustration of a three cell scenario is shown in Fig. 2.1. Each cell contains a central BS termed source node and a single user termed destination node. Each of the source nodes and the destination nodes is equipped with a single antenna. The communication among the node pairs is aided by R relays being distributed among the cells. Each relay is equipped with M antennas which is less than the number K of node pairs. The amplify and forward relaying protocol is used.

The communication among the source nodes and the destination nodes as well as among the nodes and the relays is done using a single resource. Note that an extension of the system model to consider multiple orthogonal resources is explained in Sections 4.1 and 6.1. For a transmission through a single resource, let $\underline{h}_{\text{DS}}^{(k,l)}$ denote the channel coefficient between the l -th source node and the k -th destination node. Also, the $M \times 1$ channel vector between the l -th source node and the r -th relay is denoted as $\underline{\mathbf{h}}_{\text{RS}}^{(r,l)}$. The

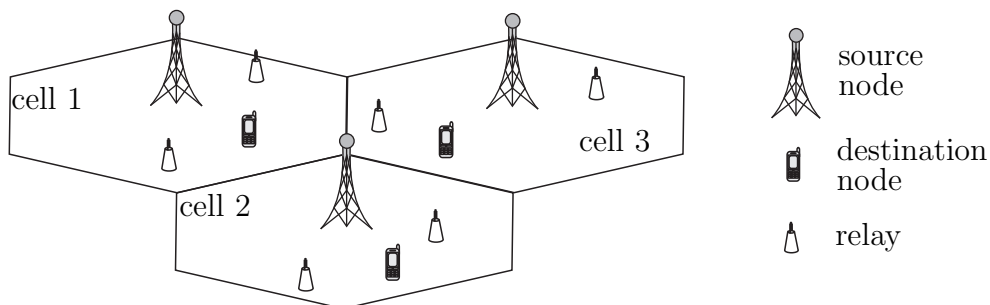


Fig. 2.1: Example of a three cell scenario.

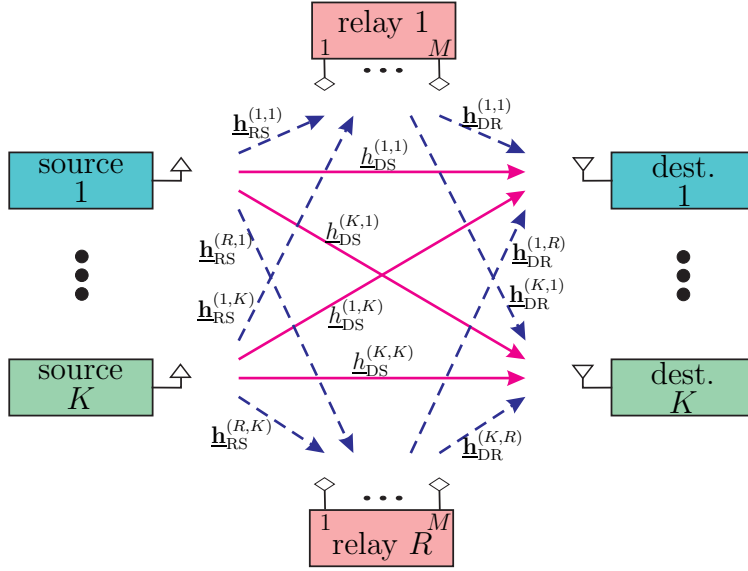


Fig. 2.2: a scenario with K source-destination node pairs and R relays.

$1 \times M$ channel vector between the r -th relay and the k -th destination node is denoted as $\underline{\mathbf{h}}_{DR}^{(k,r)}$. This means that the m -th element in $\underline{\mathbf{h}}_{RS}^{(r,l)}$ or $\underline{\mathbf{h}}_{DR}^{(k,r)}$ corresponds to the channel coefficient between the m -th antenna at the r -th relay and the l -th source node or the k -th destination node, respectively. It is assumed that the considered scenario is fully connected, i.e., channels have nonzero coefficients. The considered scenario is shown in Fig. 2.2. Concerning the channel knowledge availability, two cases are considered. In the first case, full channel state information (CSI) is available only at the relays and the filters of the nodes are fixed. In the second case, full CSI is available at the nodes and at the relays and the filters of the nodes are adapted to the channel as well. The structure of the filters at the nodes will be described in the next section. The downlink transmission takes place in two subsequent time slots and $\tau = 1, 2$ denotes the time slot index. Moreover, it is assumed that the channel remains constant within the two time slot transmission period.

Let $\underline{\mathbf{n}}_D^{(k,\tau)}$ be the received noise signal at the k -th destination node in the τ -th time slot. The received noise signals at the antennas of the r -th relay are stacked in the $M \times 1$ vector $\underline{\mathbf{n}}_R^{(r)}$. It is assumed that the noise signals received at different time slots or at different antennas of a destination node or a relay are i.i.d. Gaussian noise with zero mean and variance σ^2 . In practical wireless systems, individual energy constraints per source node and relay are usually assumed because every source node and relay

- has its own limited energy and
- is equipped with a power amplifier which has a limited dynamic range.

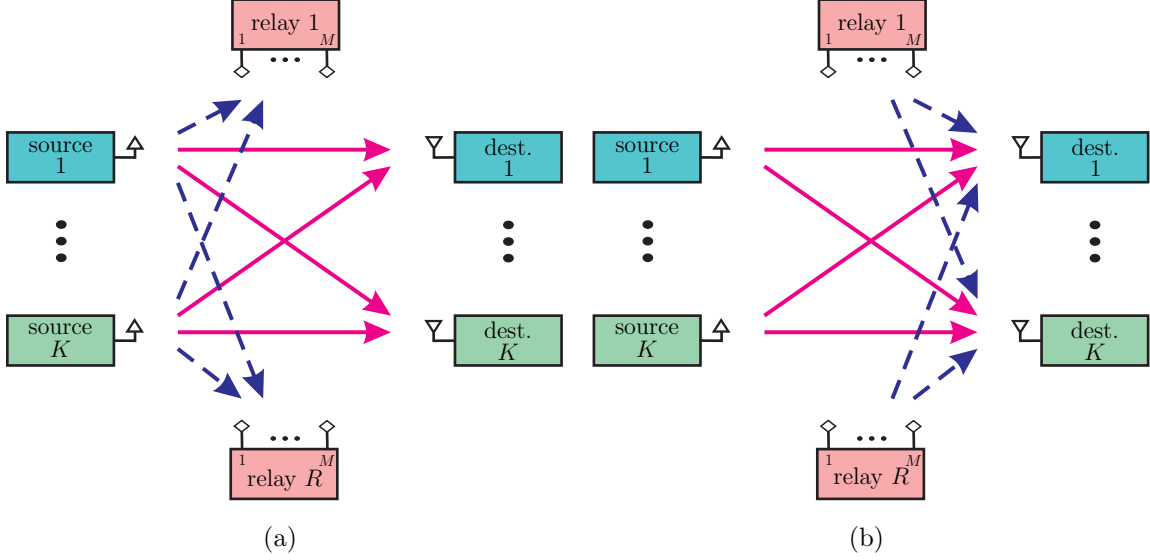


Fig. 2.3: Two time slot transmission technique: (a) the source nodes transmit to both the relays and the destination nodes in the first time slot, (b) both the source nodes and the relays retransmit to the destination nodes in the second time slot.

From the theoretical point of view, a total energy constraint is a more suitable measure as it is related to the total interference caused by the system to other systems. Therefore, a total energy constraint E_{tot} is considered here. Throughout this work, the total energy used in the τ -th time slot and the total energy used for transmitting the k -th data symbol are denoted by $E_{\text{tot}}^{(\tau)}$ and $E_{\text{tot}k}^{(k)}$, respectively. In Section 6.3, a per-resource energy constraint $E_{\text{tot}n}^{(n)}$ is used where n denotes the resource index.

2.1.2 One-way relaying transmission technique

In this section, the considered transmission technique is described. The transmission takes place in two subsequent time slots as shown in Fig. 2.3. The source nodes transmit to both the relays and the destination nodes in the first time slot. In the second time slot, both the source nodes and the relays retransmit to the destination nodes. Let $\underline{s}^{(l,\tau)}$ denote the transmitted signal of the l -th source node in the τ -th time slot. Note that the transmitted signal $\underline{s}^{(l,\tau)}$ is a linear function of the transmitted data symbol $\underline{d}^{(l)}$ as will be described later in this section. The received signals at the antennas of the r -th relay are stacked in a $M \times 1$ vector $\underline{\mathbf{e}}_{\text{R}}^{(r)}$. In the first time slot, the received signals at the r -th relays read

$$\underline{\mathbf{e}}_{\text{R}}^{(r)} = \sum_{l=1}^K \underline{\mathbf{h}}_{\text{RS}}^{(r,l)} \underline{s}^{(l,1)} + \underline{\mathbf{n}}_{\text{R}}^{(r)} \quad (2.1)$$

and the received signal at the k -th destination node reads

$$\underline{e}^{(k,1)} = \sum_{l=1}^K \underline{h}_{\text{DS}}^{(k,l)} \underline{s}^{(l,1)} + \underline{n}_{\text{D}}^{(k,1)}. \quad (2.2)$$

Because the number M of antennas at a relay is less than the number K of the transmitted signals, relays cannot separate the received signals of the source nodes using the receive zero forcing technique [UK08]. For this reason, each relay calculates its transmitted signal for the second time slot as a linear function of the received signal in the first time slot. With the $M \times M$ processing matrix $\underline{\mathbf{G}}^{(r)}$ of the r -th relay, the received signal at the k -th destination node in the second time slot reads

$$\underline{e}^{(k,2)} = \sum_{l=1}^K \underline{h}_{\text{DS}}^{(k,l)} \underline{s}^{(l,2)} + \sum_{r=1}^R \underline{\mathbf{h}}_{\text{DR}}^{(k,r)} \underline{\mathbf{G}}^{(r)} \underline{\mathbf{e}}_{\text{R}}^{(r)} + \underline{n}_{\text{D}}^{(k,2)}. \quad (2.3)$$

The received signals at the k -th destination node of both time slots of (2.2) and (2.3) can be combined as

$$\begin{pmatrix} \underline{e}^{(k,1)} \\ \underline{e}^{(k,2)} \end{pmatrix} = \sum_{l=1}^K \underline{\mathbf{H}}^{(k,l)} \begin{pmatrix} \underline{s}^{(l,1)} \\ \underline{s}^{(l,2)} \end{pmatrix} + \begin{pmatrix} \underline{n}_{\text{D}}^{(k,1)} \\ \sum_{r=1}^R \underline{\mathbf{h}}_{\text{DR}}^{(k,r)} \underline{\mathbf{G}}^{(r)} \underline{\mathbf{n}}_{\text{R}}^{(r)} + \underline{n}_{\text{D}}^{(k,2)} \end{pmatrix}, \quad (2.4)$$

where

$$\underline{\mathbf{H}}^{(k,l)} = \begin{pmatrix} \underline{h}_{\text{DS}}^{(k,l)} & 0 \\ \sum_{r=1}^R \underline{\mathbf{h}}_{\text{DR}}^{(k,r)} \underline{\mathbf{G}}^{(r)} \underline{\mathbf{h}}_{\text{RS}}^{(r,l)} & \underline{h}_{\text{DS}}^{(k,l)} \end{pmatrix} \quad (2.5)$$

is the effective channel between the l -th source node and the k -th destination node including the relays. The last term of (2.4) describes the effective noise received at the k -th destination node which contains a linear combination of the retransmitted noise signals by the relays. The effective channel described in (2.5) forms a virtual 2×2 MIMO channel between the l -th source node and the k -th destination node with equal diagonal elements $\underline{h}_{\text{DS}}^{(k,l)}$ and a single nonzero off-diagonal element $\sum_{r=1}^R \underline{\mathbf{h}}_{\text{DR}}^{(k,r)} \underline{\mathbf{G}}^{(r)} \underline{\mathbf{h}}_{\text{RS}}^{(r,l)}$ which results from the indirect signal paths through the relays. Accordingly, the received signal space at each destination node has two dimensions. To achieve IA, the interferences have to be aligned at a one dimensional subspace of the received signal space of each destination node leaving a one dimensional subspace of the received signal space of each destination node for the useful signals. Therefore, a single data symbol $\underline{d}^{(l)}$ is transmitted by each source node l . It is assumed that the data symbols transmitted by different source nodes are uncorrelated and have equal average energies

$$\text{E} \left\{ \left| \underline{d}^{(l)} \right|^2 \right\} = E_{\text{d}}, \quad \forall l, \quad (2.6)$$

where $E\{\cdot\}$ denotes the expected value. Because of the two transmissions of each source node l , there are two filter coefficients which form a temporal transmit filter

$$\underline{\mathbf{v}}^{(l)} = (\underline{v}^{(l,1)}, \underline{v}^{(l,2)})^T. \quad (2.7)$$

Additionally, each destination node k has a temporal receive filter

$$\underline{\mathbf{u}}^{(k)} = (\underline{u}^{(k,1)}, \underline{u}^{(k,2)})^T \quad (2.8)$$

as each destination node k receives twice. For the l -th source node, the transmit filter $\underline{\mathbf{v}}^{(l)}$ maps the one dimensional data symbol $\underline{d}^{(l)}$ into the two dimensional transmit signal space

$$\begin{pmatrix} \underline{s}^{(l,1)} \\ \underline{s}^{(l,2)} \end{pmatrix} = \underline{\mathbf{v}}^{(l)} \underline{d}^{(l)}. \quad (2.9)$$

Moreover, the receive filter $\underline{\mathbf{u}}^{(k)}$ at the k -th destination node projects the received signal including the useful signal and the interferences into a one dimensional subspace. Mathematically, the estimated data symbol at the k -th destination node reads

$$\hat{\underline{d}}^{(k)} = \underline{\mathbf{u}}^{(k)*T} \begin{pmatrix} \underline{e}^{(k,1)} \\ \underline{e}^{(k,2)} \end{pmatrix}, \quad (2.10)$$

and hence using (2.4) and (2.9),

$$\begin{aligned} \hat{\underline{d}}^{(k)} &= \underline{u}^{(k,1)*} \underline{e}^{(k,1)} + \underline{u}^{(k,2)*} \underline{e}^{(k,2)} \\ &= \sum_{l=1}^K \left(\underline{u}^{(k,1)*} \underline{\mathbf{h}}_{\text{DS}}^{(k,l)} \underline{v}^{(l,1)} + \underline{u}^{(k,2)*} \underline{\mathbf{h}}_{\text{DS}}^{(k,l)} \underline{v}^{(l,2)} + \underline{u}^{(k,2)*} \underline{v}^{(l,1)} \sum_{r=1}^R \underline{\mathbf{h}}_{\text{DR}}^{(k,r)} \underline{\mathbf{G}}^{(r)} \underline{\mathbf{h}}_{\text{RS}}^{(r,l)} \right) \underline{d}^{(l)} \\ &\quad + \underline{u}^{(k,2)*} \sum_{r=1}^R \underline{\mathbf{h}}_{\text{DR}}^{(k,r)} \underline{\mathbf{G}}^{(r)} \underline{\mathbf{n}}_{\text{R}}^{(r)} + \underline{u}^{(k,1)*} \underline{n}_{\text{D}}^{(k,1)} + \underline{u}^{(k,2)*} \underline{n}_{\text{D}}^{(k,2)} \end{aligned} \quad (2.11)$$

holds. Using the effective noise signal received at the k -th destination node described in the last term of (2.4), the covariance matrix of the received noise signals at the k -th destination node is calculated as

$$\mathbf{C}_{\text{nn}}^{(k)} = \sigma^2 \begin{pmatrix} 1 & 0 \\ 0 & 1 + \sum_{r=1}^R \underline{\mathbf{h}}_{\text{DR}}^{(k,r)} \underline{\mathbf{G}}^{(r)} \underline{\mathbf{G}}^{(r)*T} \underline{\mathbf{h}}_{\text{DR}}^{(k,r)*T} \end{pmatrix}. \quad (2.12)$$

Then, the received SINR at the k -th destination node is calculated as

$$\gamma^{(k)} = \frac{E_{\text{d}} \left| \underline{\mathbf{u}}^{(k)*T} \underline{\mathbf{H}}^{(k,k)} \underline{\mathbf{v}}^{(k)} \right|^2}{\underline{\mathbf{u}}^{(k)*T} \mathbf{C}_{\text{nn}}^{(k)} \underline{\mathbf{u}}^{(k)} + \sum_{l \neq k} E_{\text{d}} \left| \underline{\mathbf{u}}^{(k)*T} \underline{\mathbf{H}}^{(k,l)} \underline{\mathbf{v}}^{(l)} \right|^2}. \quad (2.13)$$

The last term on the denominator of (2.13) describes the remaining interference powers at the output of the receive filter $\underline{\mathbf{u}}^{(k)}$ of the k -th destination node. Assuming the

antennas of the relays to be well separated so that the channel matrices between a relay and the source nodes as well as between a relay and the destination nodes are full rank, the covariance matrix of the received signals at the r -th relay reads

$$\underline{\mathbf{C}}_{\text{rr}}^{(r)} = E_{\text{d}} \sum_{l=1}^K |\underline{v}^{(l,1)}|^2 \underline{\mathbf{h}}_{\text{RS}}^{(r,l)} \underline{\mathbf{h}}_{\text{RS}}^{(r,l)*\text{T}} + \sigma^2 \mathbf{I}_M, \quad (2.14)$$

where \mathbf{I}_M is an identity matrix of size $M \times M$. Note that $\underline{\mathbf{C}}_{\text{rr}}^{(r)}$ is a positive definite matrix. Using the covariance matrix of (2.14), the total retransmitted energy of the relays is calculated as

$$E_{\text{Rtot}} = \sum_{r=1}^R \text{tr} \left(\underline{\mathbf{G}}^{(r)} \underline{\mathbf{C}}_{\text{rr}}^{(r)} \underline{\mathbf{G}}^{(r)*\text{T}} \right), \quad (2.15)$$

where $\text{tr}(\cdot)$ denotes the trace of a matrix.

2.2 Reference scheme and channel normalization

2.2.1 Single cell relaying algorithm

In this section, a reference scheme is proposed. Because our work focuses on developing interference reduction algorithms, the reference scheme is considered to be interference limited. In this reference scheme,

- the links among different cells are ignored and
- the total energy constraint is distributed equally among the cells

$$E_{\text{Ctot}} = \frac{E_{\text{tot}}}{K}. \quad (2.16)$$

Based on the above discussion, the problem of maximizing the sum rate with equal energy constraints becomes a per-cell optimization problem. For each cell k , the temporal filters at the nodes and the processing matrices at the relays belonging to the k -th cell are optimized aiming at maximizing the received SNR at the k -th destination node with the energy constraint of (2.16). Obviously, this reference scheme is suboptimal as it ignores the inter-cell signals.

Consider the k -th cell which has R_c relays with indices $r = 1, \dots, R_c$ where $R_c \leq R$. By ignoring the interference term in (2.13), the received SNR at the k -th destination node is calculated as

$$\gamma^{(k)} = \frac{E_d \underline{\mathbf{u}}^{(k)*T} \left(\underline{\mathbf{H}}^{(k,k)} \underline{\mathbf{v}}^{(k)} \underline{\mathbf{v}}^{(k)*T} \underline{\mathbf{H}}^{(k,k)*T} \right) \underline{\mathbf{u}}^{(k)}}{\underline{\mathbf{u}}^{(k)*T} \mathbf{C}_{\text{nn}}^{(k)} \underline{\mathbf{u}}^{(k)}}, \quad (2.17)$$

where the structures of $\underline{\mathbf{H}}^{(k,k)}$ and $\mathbf{C}_{\text{nn}}^{(k)}$ defined in (2.5) and (2.12) are calculated with the relay indices of $r = 1, \dots, R_c$. As the data symbol $\underline{d}^{(k)}$ is transmitted twice to the k -th destination node and the noise signals are i.i.d., the maximum ratio combining (MRC) processing technique can be applied. As described in (2.17), the received SNR at the k -th destination node when considered as a function of the receive filter $\underline{\mathbf{u}}^{(k)}$ is a Rayleigh quotient [TB97]. For a certain transmit filter $\underline{\mathbf{v}}^{(k)}$ and certain relay processing matrices $\underline{\mathbf{G}}^{(r)}$, $r = 1, \dots, R_c$, the optimum receive filter is found by

$$\underline{\mathbf{u}}_{\text{MRC}}^{(k)} = \arg \max_{\underline{\mathbf{u}}^{(k)}} \left\{ \frac{E_d \underline{\mathbf{u}}^{(k)*T} \left(\underline{\mathbf{H}}^{(k,k)} \underline{\mathbf{v}}^{(k)} \underline{\mathbf{v}}^{(k)*T} \underline{\mathbf{H}}^{(k,k)*T} \right) \underline{\mathbf{u}}^{(k)}}{\underline{\mathbf{u}}^{(k)*T} \mathbf{C}_{\text{nn}}^{(k)} \underline{\mathbf{u}}^{(k)}} \right\}. \quad (2.18)$$

The Rayleigh quotient maximization problem of (2.18) is equivalent to the eigenvalue problem of the matrix $\left(\mathbf{C}_{\text{nn}}^{(k)} \right)^{-1} \left(\underline{\mathbf{H}}^{(k,k)} \underline{\mathbf{v}}^{(k)} \underline{\mathbf{v}}^{(k)*T} \underline{\mathbf{H}}^{(k,k)*T} \right)$ [TB97]. Basically, the optimum receive filter vector $\underline{\mathbf{u}}_{\text{MRC}}^{(k)}$ must direct in the same direction as the eigenvector corresponding to the largest eigenvalue of the matrix $\left(\mathbf{C}_{\text{nn}}^{(k)} \right)^{-1} \left(\underline{\mathbf{H}}^{(k,k)} \underline{\mathbf{v}}^{(k)} \underline{\mathbf{v}}^{(k)*T} \underline{\mathbf{H}}^{(k,k)*T} \right)$. Because the matrix $\left(\underline{\mathbf{H}}^{(k,k)} \underline{\mathbf{v}}^{(k)} \underline{\mathbf{v}}^{(k)*T} \underline{\mathbf{H}}^{(k,k)*T} \right)$ is of rank one, i.e., the rank of $\underline{\mathbf{v}}^{(k)}$ is one, a single nonzero eigenvalue exists and the optimum receive filter $\underline{\mathbf{u}}_{\text{MRC}}^{(k)}$ is obtained as

$$\underline{\mathbf{u}}_{\text{MRC}}^{(k)} = \left(\mathbf{C}_{\text{nn}}^{(k)} \right)^{-1} \underline{\mathbf{H}}^{(k,k)} \underline{\mathbf{v}}^{(k)}. \quad (2.19)$$

This closed form solution of the Rayleigh quotient maximization problem is known as the Wiener solution [MHM11]. By substituting (2.19) in (2.17), the SNR at the k -th destination node is simply the summation of the individual SNRs received in each of the time slots

$$\gamma^{(k)} = \gamma^{(k,1)} + \gamma^{(k,2)}, \quad (2.20)$$

with

$$\gamma^{(k,1)} = \frac{E_d}{\sigma^2} \left| \underline{v}^{(k,1)} \right|^2 \left| \underline{h}_{\text{DS}}^{(k,k)} \right|^2 \quad (2.21)$$

being the received SNR in the first time slot and

$$\gamma^{(k,2)} = \frac{E_d}{\sigma^2} \frac{\left| \underline{v}^{(k,2)} \underline{h}_{\text{DS}}^{(k,k)} + \underline{v}^{(k,1)} \sum_{r=1}^{R_c} \underline{\mathbf{h}}_{\text{DR}}^{(k,r)} \underline{\mathbf{G}}^{(r)} \underline{\mathbf{h}}_{\text{RS}}^{(r,k)} \right|^2}{1 + \sum_{r=1}^{R_c} \underline{\mathbf{h}}_{\text{DR}}^{(k,r)} \underline{\mathbf{G}}^{(r)} \underline{\mathbf{G}}^{(r)*T} \underline{\mathbf{h}}_{\text{DR}}^{(k,r)*T}} \quad (2.22)$$

being the received SNR in the second time slot.

The optimization problem aiming at maximizing the sum SNR received at the k -th destination node with a total energy constraint can be stated as

$$\left(\underline{v}_{\text{opt}}^{(k,1)}, \underline{v}_{\text{opt}}^{(k,2)}, \underline{\mathbf{G}}_{\text{opt}}^{(1)}, \dots, \underline{\mathbf{G}}_{\text{opt}}^{(R_c)} \right) = \arg \max_{\substack{\underline{v}^{(k,1)}, \underline{v}^{(k,2)}, \\ \underline{\mathbf{G}}^{(1)}, \dots, \underline{\mathbf{G}}^{(R_c)}}} \{ \gamma^{(k,1)} + \gamma^{(k,2)} \} \quad (2.23)$$

subject to

$$E_d \left(|\underline{v}^{(k,1)}|^2 + |\underline{v}^{(k,2)}|^2 \right) + \sum_{r=1}^{R_c} \text{tr} \left(\underline{\mathbf{G}}^{(r)} \underline{\mathbf{C}}_{\text{rr}}^{(r)} \underline{\mathbf{G}}^{(r)*\text{T}} \right) = E_{\text{Ctot}}, \quad (2.24)$$

where the covariance matrix $\underline{\mathbf{C}}_{\text{rr}}^{(r)}$ is calculated from (2.14) with $K = 1$. The optimization problem of (2.23)–(2.24) is non-convex because $\gamma^{(k,2)}$ is not a concave function of the variables $\underline{\mathbf{G}}^{(1)}, \dots, \underline{\mathbf{G}}^{(R_c)}, \underline{v}^{(k,1)}$ and $\underline{v}^{(k,2)}$. In the first step, the transmit filter coefficient $\underline{v}^{(k,1)}$ is considered to be a priori known. Then, the SNR in the second time slot can be maximized over the remaining variables $\underline{\mathbf{G}}^{(1)}, \dots, \underline{\mathbf{G}}^{(R_c)}$ and $\underline{v}^{(k,2)}$. The optimization problem of (2.23)–(2.24) can be reformulated for optimizing the remaining variables $\underline{\mathbf{G}}^{(1)}, \dots, \underline{\mathbf{G}}^{(R_c)}$ and $\underline{v}^{(k,2)}$ as

$$\left(\underline{v}_{\text{opt}}^{(k,2)}, \underline{\mathbf{G}}_{\text{opt}}^{(1)}, \dots, \underline{\mathbf{G}}_{\text{opt}}^{(R_c)} \right) = \arg \max_{\substack{\underline{v}^{(k,2)}, \underline{\mathbf{G}}^{(1)}, \\ \dots, \underline{\mathbf{G}}^{(R_c)}}} \{ \gamma^{(k,2)} \} \quad (2.25)$$

subject to

$$E_d |\underline{v}^{(k,2)}|^2 + \sum_{r=1}^{R_c} \text{tr} \left(\underline{\mathbf{G}}^{(r)} \underline{\mathbf{C}}_{\text{rr}}^{(r)} \underline{\mathbf{G}}^{(r)*\text{T}} \right) = E_{\text{Ctot}} - E_d |\underline{v}^{(k,1)}|^2, \quad (2.26)$$

where $\underline{v}^{(k,1)}$ is fixed.

The main idea of the following derivation is that the SNR $\gamma^{(k,2)}$ can be rewritten as a Rayleigh quotient of the variables $\underline{\mathbf{G}}^{(1)}, \dots, \underline{\mathbf{G}}^{(R_c)}$ and $\underline{v}^{(k,2)}$. By making use of (A.10) at the nominator and the denominator of (2.22), the SNR in the second time slot can be rewritten as

$$\gamma^{(k,2)} = \frac{E_d \left| \underline{v}^{(k,2)} \underline{h}_{\text{DS}}^{(k,k)} + \underline{v}^{(k,1)} \sum_{r=1}^{R_c} \text{tr} \left(\underline{\mathbf{G}}^{(r)} \underline{\mathbf{h}}_{\text{RS}}^{(r,k)} \underline{\mathbf{h}}_{\text{DR}}^{(k,r)} \right) \right|^2}{\sigma^2 \left(1 + \sum_{r=1}^{R_c} \text{tr} \left(\underline{\mathbf{G}}^{(r)} \underline{\mathbf{G}}^{(r)*\text{T}} \underline{\mathbf{h}}_{\text{DR}}^{(k,r)*\text{T}} \underline{\mathbf{h}}_{\text{DR}}^{(k,r)} \right) \right)}. \quad (2.27)$$

The vectorization property of (A.11) and the trace property of (A.14) are applied to the nominator and at the denominator of (2.27), respectively. Hence, (2.27) can be

rewritten as

$$\gamma^{(k,2)} = \frac{E_d}{\sigma^2} \frac{\left| \underline{v}^{(k,2)} \underline{h}_{\text{DS}}^{(k,k)} + \underline{v}^{(k,1)} \sum_{r=1}^{R_c} \text{vec} \left(\underline{\mathbf{G}}^{(r)*\text{T}} \right)^{*T} \text{vec} \left(\underline{\mathbf{h}}_{\text{RS}}^{(r,k)} \underline{\mathbf{h}}_{\text{DR}}^{(k,r)} \right) \right|^2}{1 + \sum_{r=1}^{R_c} \text{tr} \left(\underline{\mathbf{G}}^{(r)*\text{T}} \underline{\mathbf{h}}_{\text{DR}}^{(k,r)*\text{T}} \underline{\mathbf{h}}_{\text{DR}}^{(k,r)} \underline{\mathbf{G}}^{(r)} \right)}, \quad (2.28)$$

where $\text{vec}(\cdot)$ denotes the vectorization operator described in Appendix A.1. Applying the vectorization property of (A.8) at the denominator of (2.28) yields

$$\gamma^{(k,2)} = \frac{E_d}{\sigma^2} \frac{\left| \underline{v}^{(k,2)} \underline{h}_{\text{DS}}^{(k,k)} + \underline{v}^{(k,1)} \sum_{r=1}^{R_c} \text{vec} \left(\underline{\mathbf{G}}^{(r)*\text{T}} \right)^{*T} \text{vec} \left(\underline{\mathbf{h}}_{\text{RS}}^{(r,k)} \underline{\mathbf{h}}_{\text{DR}}^{(k,r)} \right) \right|^2}{1 + \sum_{r=1}^{R_c} \text{vec} \left(\underline{\mathbf{G}}^{(r)} \right)^{*T} \left(\mathbf{I}_M \otimes \underline{\mathbf{h}}_{\text{DR}}^{(k,r)*\text{T}} \underline{\mathbf{h}}_{\text{DR}}^{(k,r)} \right) \text{vec} \left(\underline{\mathbf{G}}^{(r)} \right)}, \quad (2.29)$$

where \otimes denotes the Kronecker product described in Appendix A.1. Rewriting the denominator of (2.29) with $\text{vec} \left(\underline{\mathbf{G}}^{(r)*\text{T}} \right)$ instead of $\text{vec} \left(\underline{\mathbf{G}}^{(r)} \right)$ yields

$$\gamma^{(k,2)} = \frac{E_d}{\sigma^2} \frac{\left| \underline{v}^{(k,2)} \frac{\underline{h}_{\text{DS}}^{(k,k)}}{\underline{v}^{(k,1)}} + \sum_{r=1}^{R_c} \text{vec} \left(\underline{\mathbf{G}}^{(r)*\text{T}} \right)^{*T} \text{vec} \left(\underline{\mathbf{h}}_{\text{RS}}^{(r,k)} \underline{\mathbf{h}}_{\text{DR}}^{(k,r)} \right) \right|^2}{1 + \sum_{r=1}^{R_c} \text{vec} \left(\underline{\mathbf{G}}^{(r)*\text{T}} \right)^{*T} \left(\underline{\mathbf{h}}_{\text{DR}}^{(k,r)\text{T}} \underline{\mathbf{h}}_{\text{DR}}^{(k,r)*} \otimes \mathbf{I}_M \right) \text{vec} \left(\underline{\mathbf{G}}^{(r)*\text{T}} \right)}. \quad (2.30)$$

Rayleigh quotient maximization is typically an unconstrained problem [TB97]. Therefore, the energy constraint of (2.26) needs to be substituted in the new $\gamma^{(k,2)}$ formulation. Using (A.8), the energy constraint of (2.26) can be written as

$$E_d \left| \underline{v}^{(k,2)} \right|^2 + \sum_{r=1}^{R_c} \text{vec} \left(\underline{\mathbf{G}}^{(r)*\text{T}} \right)^{*T} \left(\mathbf{I}_M \otimes \underline{\mathbf{C}}_{\text{rr}}^{(r)} \right) \text{vec} \left(\underline{\mathbf{G}}^{(r)*\text{T}} \right) = E_{\text{Ctot}} - E_d \left| \underline{v}^{(k,1)} \right|^2. \quad (2.31)$$

The matrix $\left(\mathbf{I}_M \otimes \underline{\mathbf{C}}_{\text{rr}}^{(r)} \right)$ can be decomposed as

$$\mathbf{I}_M \otimes \underline{\mathbf{C}}_{\text{rr}}^{(r)} = \underline{\mathbf{L}}^{(k,r)} \underline{\mathbf{L}}^{(k,r)*\text{T}} \quad (2.32)$$

using Cholesky factorization [TB97], where $\underline{\mathbf{L}}^{(k,r)}$ is a lower triangular matrix. Because the covariance matrix $\underline{\mathbf{C}}_{\text{rr}}^{(r)}$ is invertible and based on the Kronecker product property of (A.5), $\underline{\mathbf{L}}^{(k,r)}$ is an invertible matrix. Define

$$\underline{\mathbf{c}}^{(k)} = \begin{pmatrix} \sqrt{E_d} \underline{v}^{(k,2)*} \\ \underline{\mathbf{L}}^{(k,1)*\text{T}} \text{vec} \left(\underline{\mathbf{G}}^{(1)*\text{T}} \right) \\ \vdots \\ \underline{\mathbf{L}}^{(k,R_c)*\text{T}} \text{vec} \left(\underline{\mathbf{G}}^{(R_c)*\text{T}} \right) \end{pmatrix} \quad (2.33)$$

as the vector of the unknowns. Accordingly, the energy constraint of (2.31) can be written with respect to the vector $\underline{\mathbf{c}}^{(k)}$ as

$$\underline{\mathbf{c}}^{(k)*\text{T}} \underline{\mathbf{c}}^{(k)} = E_{\text{Ctot}} - E_{\text{d}} \left| \underline{v}^{(k,1)} \right|^2. \quad (2.34)$$

To write (2.30) in a vector form, let

$$\underline{\mathbf{a}}^{(k)} = \begin{pmatrix} \frac{\underline{h}_{\text{DS}}^{(k,k)}}{\sqrt{E_{\text{d}}}} \underline{v}^{(k,1)} \\ \left(\underline{\mathbf{L}}^{(k,1)} \right)^{-1} \text{vec} \left(\underline{\mathbf{h}}_{\text{RS}}^{(1,k)} \underline{\mathbf{h}}_{\text{DR}}^{(k,1)} \right) \\ \vdots \\ \left(\underline{\mathbf{L}}^{(k,R_c)} \right)^{-1} \text{vec} \left(\underline{\mathbf{h}}_{\text{RS}}^{(R_c,k)} \underline{\mathbf{h}}_{\text{DR}}^{(k,R_c)} \right) \end{pmatrix} \quad (2.35)$$

be the vector of the constants at the nominator of (2.30). Let $\mathbf{B}^{(k)}$ be a block diagonal matrix where the first diagonal element is zero and the next R_c diagonal blocks are $\left(\underline{\mathbf{L}}^{(k,r)} \right)^{-1} \left(\underline{\mathbf{h}}_{\text{DR}}^{(k,r)\text{T}} \underline{\mathbf{h}}_{\text{DR}}^{(k,r)*} \otimes \mathbf{I}_M \right) \left(\underline{\mathbf{L}}^{(k,r)*\text{T}} \right)^{-1}$ with $r = 1, \dots, R_c$. Then, the SNR in the second time slot of (2.30) can be written as

$$\gamma^{(k,2)} = \frac{E_{\text{d}} \left| \underline{v}^{(k,1)} \right|^2}{\sigma^2} \frac{\underline{\mathbf{c}}^{(k)*\text{T}} \underline{\mathbf{a}}^{(k)} \underline{\mathbf{a}}^{(k)*\text{T}} \underline{\mathbf{c}}^{(k)}}{1 + \underline{\mathbf{c}}^{(k)*\text{T}} \mathbf{B}^{(k)} \underline{\mathbf{c}}^{(k)}}. \quad (2.36)$$

By exploiting the energy constraint of (2.34), (2.36) can be rewritten as a Rayleigh quotient as

$$\gamma^{(k,2)} = \frac{E_{\text{d}} \left| \underline{v}^{(k,1)} \right|^2}{\sigma^2} \frac{\underline{\mathbf{c}}^{(k)*\text{T}} \underline{\mathbf{a}}^{(k)} \underline{\mathbf{a}}^{(k)*\text{T}} \underline{\mathbf{c}}^{(k)}}{\underline{\mathbf{c}}^{(k)*\text{T}} \left(\frac{1}{E_{\text{Ctot}} - E_{\text{d}} \left| \underline{v}^{(k,1)} \right|^2} \mathbf{I}_{R_c M^2 + 1} + \mathbf{B}^{(k)} \right) \underline{\mathbf{c}}^{(k)}}, \quad (2.37)$$

which implicitly satisfies the energy constraint. Using the new formulation of the SNR in the second time slot of (2.37), the optimization problem of (2.25)–(2.26) can be reformulated as an unconstrained maximization problem as

$$\underline{\mathbf{c}}_{\text{opt}}^{(k)} = \arg \max_{\underline{\mathbf{c}}^{(k)}} \left\{ \frac{\underline{\mathbf{c}}^{(k)*\text{T}} \underline{\mathbf{a}}^{(k)} \underline{\mathbf{a}}^{(k)*\text{T}} \underline{\mathbf{c}}^{(k)}}{\underline{\mathbf{c}}^{(k)*\text{T}} \left(\frac{1}{E_{\text{Ctot}} - E_{\text{d}} \left| \underline{v}^{(k,1)} \right|^2} \mathbf{I}_{R_c M^2 + 1} + \mathbf{B}^{(k)} \right) \underline{\mathbf{c}}^{(k)}} \right\}, \quad (2.38)$$

where $E_{\text{d}} \left| \underline{v}^{(k,1)} \right|^2 / \sigma^2$ is omitted from the objective function as it is scalar and constant. The Wiener solution of the Rayleigh quotient maximization problem of (2.38) is calculated as

$$\underline{\mathbf{c}}_{\text{opt}}^{(k)} = \left(\frac{1}{E_{\text{Ctot}}^{(k)} - E_{\text{d}} \left| \underline{v}^{(k,1)} \right|^2} \mathbf{I}_{R_c M^2 + 1} + \mathbf{B}^{(k)} \right)^{-1} \underline{\mathbf{a}}^{(k)}. \quad (2.39)$$

So far, the SNR at the k -th destination node is maximized for a fixed transmit filter coefficient $\underline{v}^{(k,1)}$ in the first time slot. Now, the optimum $\underline{v}^{(k,1)}$ needs to be found.

Actually, it is not required to optimize the argument of the transmit filter coefficient at the first time slot as for an arbitrary fixed value of the argument of $\underline{v}^{(k,1)}$, the source node and the relays will accordingly adjust the amplitudes and the arguments of their transmitted signals in the second time slot such that the sum SNR is maximized using (2.39). For all transmit filter coefficient amplitudes $|\underline{v}^{(k,1)}|$, (2.39) can be used to optimize the variables of the second time slot $\underline{v}^{(k,2)}$, $\underline{\mathbf{G}}^{(1)}$, ... and $\underline{\mathbf{G}}^{(R_c)}$. Accordingly, the sum SNR with the optimized variables in the second time slot $\underline{v}^{(k,2)}$, $\underline{\mathbf{G}}^{(1)}$, ... and $\underline{\mathbf{G}}^{(R_c)}$ can be considered as a function of the transmitted energy in the first time slot $E_d |\underline{v}^{(k,1)}|^2$. In the following proposition, the structure of the sum SNR function is described.

Proposition 1. *With the total energy constraint of (2.24), the sum SNR with the optimized variables of $\underline{v}^{(k,2)}$, $\underline{\mathbf{G}}^{(1)}$, ... and $\underline{\mathbf{G}}^{(R_c)}$ in the second time slot, if considered as a function of the transmitted energy $E_d |\underline{v}^{(k,1)}|^2$ in the first time slot is a concave function.*

The proof is shown in Appendix B.1. Based on Proposition 1, conventional numerical convex optimization tools such as the interior point method [BGN00, BHN99, WMNO06] can be applied to find the optimum split of the total energy among the two time slots. To find the optimum split of the total energy constraint among the two time slots and to find the optimum transmit filter coefficients and the relay processing matrices, an iterative algorithm is applied. In every iteration, the variables $\underline{v}^{(k,2)}$, $\underline{\mathbf{G}}^{(1)}$, ... and $\underline{\mathbf{G}}^{(R_c)}$ in the second time slot are calculated using (2.39) for a given energy split calculated by the numerical method in the previous iteration. Then, the optimized variables are feedback to the numerical method to update the energy split.

The convergence of the proposed iterative algorithm depends on the convergence of the applied numerical optimization method. In [BGN00], the convergence of the interior point method is analyzed.

In summary, a reference scheme called single cell relaying is proposed. This scheme is interference limited because it ignores the inter-cell signals. After distributing the total energy equally among the cells, the single cell relaying algorithm optimizes the transmission per cell. For each cell, the optimum filter coefficients at the nodes and the optimum relay processing matrices are found using an iterative algorithm.

2.2.2 Channel model and normalization

This section describes the channel model which is applied for obtaining the simulation results presented in the later chapters. In point to point transmission, it is reasonable

to assume that a signal travels from a transmit antenna to a receive antenna through a large number of statistically independent paths where there is no dominant path, i.e., it is assumed that there is no line of sight between the transmit and the receive antennas. Accordingly, the channel coefficient corresponding to any single path can be modeled as a circularly symmetric complex random variable [TV05]. Due to the large number of paths, the channel coefficient between a transmit antenna and a receive antenna can be modeled as a circularly symmetric complex Gaussian random variable with zero mean based on the central limit theorem [PP02]. Moreover, the distributions of the amplitude and the gain of the channel follow the Rayleigh distribution and the chi-square distribution with two degrees of freedom, respectively [TV05]. In this work, the channels are assumed to be frequency flat. However, frequency selective channels are considered for multiple orthogonal resource systems in Sections 4.3 and 6.3.

To assess the performances of the proposed algorithms, one can use a system simulator which does sophisticated system-level simulations with realistic scenarios and models. However, it is sufficient to consider here a simple channel model. This model is reasonable as scenarios with few cells is considered. It is assumed that the distances among the source nodes, the relays and the destination nodes are large enough so that a receive antenna is always located in the far field of a transmit antenna. A transmitted signal from a source node or a relay experiences attenuation depending on the distance q from the transmit antenna which is modeled using the path loss exponent model [GLZ12]. Let E_{Tx} and E_{Rx} be the energy of the transmitted signal from an antenna and the energy of the received signal at an antenna, respectively. With an attenuation exponent of 2, the path loss is calculated as

$$\frac{E_{\text{Rx}}}{E_{\text{Tx}}} = \left(\frac{v_c}{4\pi q f_c} \right)^2, \quad q \geq q_0, \quad (2.40)$$

where v_c , f_c and q_0 are the speed of light, the carrier frequency and the minimum distance between a transmit antenna and a receive antenna, respectively. With a carrier frequency f_c of 1.8 GHz [GLZ12], the path loss in decibels is calculated as

$$10\log_{10} \left(\frac{E_{\text{Rx}}}{E_{\text{Tx}}} \right) = -37.5472 - 20\log_{10}(q), \quad q \geq q_0. \quad (2.41)$$

The cell radius is set to 500 m. Also, the minimum distance between a source node and a relay or a destination node is set to 50 m such that the sum rate is not dominated by a cell-center destination node achieved rate.

For the rest of this section, a channel normalization method applied in our simulations is introduced. For a single cell scenario consisting of a single node pair with no relays shown in Fig 2.4a, different channel realizations $\underline{h}_{\text{DS}}^{(k,k)}$ are normalized by $\sqrt{\mathbb{E} \left\{ \left| \underline{h}_{\text{DS}}^{(k,k)} \right|^2 \right\}}$

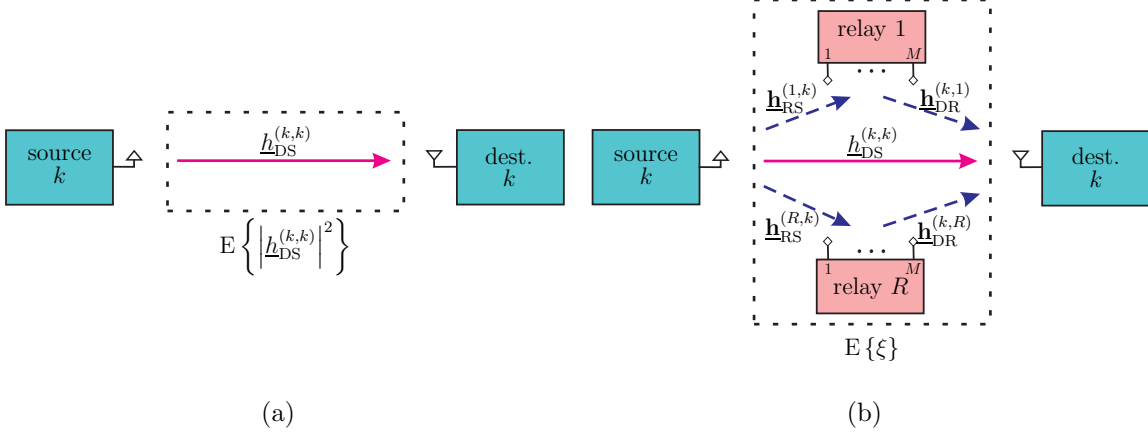


Fig. 2.4: Effective average channel gain between a node pair: (a) with no relays, (b) with relays, where ξ is the effective channel gain including the relays.

so that the average channel gain is one. Accordingly, the average SNR equals to the ratio of the transmitted signal energy and the noise power density. For scenarios with multiple cells and no relays, it is reasonable to normalize the channels corresponding to many different positions of the destination nodes such that the average gain of the intra-cell channels is one. In this case, the average gain of the inter-cell channels is less than one. For cellular scenarios with relays, channel normalization is not trivial because the effective channel between a source node and a destination node consists of both a direct link and several indirect links through the relays as shown in Fig. 2.4b. To normalize the channels in these scenarios, the effective channel gain ξ including the relays between a source node and its corresponding destination node should be derived.

Let the pseudo SNR (PSNR) be the ratio of the total transmitted energy and the noise power density at a receive antenna. Mathematically, PSNR is calculated as

$$\gamma_{\text{PSNR}} = \frac{E_d \sum_{l=1}^K \text{tr}(\mathbf{v}^{(l)} \mathbf{v}^{(l)*\text{T}}) + E_{\text{Rtot}}}{\sigma^2}. \quad (2.42)$$

The goal is to normalize the channels $\underline{h}_{\text{DS}}^{(k,k)}$, $\underline{\mathbf{h}}_{\text{RS}}^{(r,k)}$ and $\underline{\mathbf{h}}_{\text{DR}}^{(k,r)}$, $r = 1, \dots, R$ such that the received SNRs are at the same order of magnitude as the PSNR. Unfortunately, the relays contribute not only to the received SNRs at the destination node with their retransmitted noise see (2.17) but also they contribute to the PSNR with the energies of their retransmitted signals, see (2.42). Therefore, the asymptotic behavior of the SNR received at a destination node when considered as a function of PSNR will be studied. In the following, the received SNR of (2.17) will be rewritten as a function of the PSNR of (2.42) considering only the k -th node pair and all the relays. The SNR of

(2.17) can be rewritten as a function of E_d/σ^2 as

$$\gamma^{(k)} = \frac{E_d}{\sigma^2} \gamma_o^{(k)}, \quad (2.43)$$

where

$$\gamma_o^{(k)} = \frac{\left| \underline{\mathbf{u}}^{(k)*T} \underline{\mathbf{H}}^{(k,k)} \underline{\mathbf{v}}^{(k)} \right|^2}{\underline{\mathbf{u}}^{(k)*T} \begin{pmatrix} 1 & 0 \\ 0 & 1 + \sum_{r=1}^R \underline{\mathbf{h}}_{\text{DR}}^{(k,r)} \underline{\mathbf{G}}^{(r)} \underline{\mathbf{G}}^{(r)*T} \underline{\mathbf{h}}_{\text{DR}}^{(k,r)*T} \end{pmatrix} \underline{\mathbf{u}}^{(k)}}. \quad (2.44)$$

Using (2.14) and (2.15) for $K = 1$, (2.42) can be solved for E_d/σ^2 as

$$\frac{E_d}{\sigma^2} = \frac{\gamma_{\text{PSNR}} - \sum_{r=1}^R \text{tr} \left(\underline{\mathbf{G}}^{(r)} \underline{\mathbf{G}}^{(r)*T} \right)}{\text{tr} \left(\underline{\mathbf{v}}^{(k)} \underline{\mathbf{v}}^{(k)*T} \right) + |\underline{v}^{(k,1)}|^2 \sum_{r=1}^R \text{tr} \left(\underline{\mathbf{G}}^{(r)} \underline{\mathbf{h}}_{\text{RS}}^{(r,k)} \underline{\mathbf{h}}_{\text{RS}}^{(r,k)*T} \underline{\mathbf{G}}^{(r)*T} \right)}. \quad (2.45)$$

By substituting (2.45) in (2.43), the SNR as a function of PSNR is written as

$$\begin{aligned} \gamma^{(k)} &= \frac{\gamma_o^{(k)}}{\text{tr} \left(\underline{\mathbf{v}}^{(k)} \underline{\mathbf{v}}^{(k)*T} \right) + |\underline{v}^{(k,1)}|^2 \sum_{r=1}^R \text{tr} \left(\underline{\mathbf{G}}^{(r)} \underline{\mathbf{h}}_{\text{RS}}^{(r,k)} \underline{\mathbf{h}}_{\text{RS}}^{(r,k)*T} \underline{\mathbf{G}}^{(r)*T} \right)} \gamma_{\text{PSNR}} \\ &= \frac{\gamma_o^{(k)} \sum_{r=1}^R \text{tr} \left(\underline{\mathbf{G}}^{(r)} \underline{\mathbf{G}}^{(r)*T} \right)}{\text{tr} \left(\underline{\mathbf{v}}^{(k)} \underline{\mathbf{v}}^{(k)*T} \right) + |\underline{v}^{(k,1)}|^2 \sum_{r=1}^R \text{tr} \left(\underline{\mathbf{G}}^{(r)} \underline{\mathbf{h}}_{\text{RS}}^{(r,k)} \underline{\mathbf{h}}_{\text{RS}}^{(r,k)*T} \underline{\mathbf{G}}^{(r)*T} \right)}. \end{aligned} \quad (2.46)$$

It can be noted from (2.46) that the relation between $\gamma^{(k)}$ and γ_{PSNR} is linear. At high PSNRs, the second term of (2.46) can be neglected and the ratio

$$\xi = \frac{\gamma_o^{(k)}}{\text{tr} \left(\underline{\mathbf{v}}^{(k)} \underline{\mathbf{v}}^{(k)*T} \right) + |\underline{v}^{(k,1)}|^2 \sum_{r=1}^R \text{tr} \left(\underline{\mathbf{G}}^{(r)} \underline{\mathbf{h}}_{\text{RS}}^{(r,k)} \underline{\mathbf{h}}_{\text{RS}}^{(r,k)*T} \underline{\mathbf{G}}^{(r)*T} \right)} \quad (2.47)$$

can be considered as the effective channel gain between the k -th source node and the k -th destination node including the relays. Note that ξ is calculated for any channel realization with the respective optimum filters and the optimum processing matrices using the iterative algorithm proposed in the previous section. Considering the path loss model described previously in this section, different values of ξ are averaged over a large number of channel realizations corresponding to many different positions of the destination node and the relays. Hence, the channel normalization factor for multiuser relay networks is calculated as $\sqrt{\mathbb{E}\{\xi\}}$.

Chapter 3

Interference alignment

3.1 Interference alignment conditions

Based on the system model and the transmission technique introduced in Section 2.1, this chapter investigates different IA algorithms. Basically, the effective channel between the source nodes and the destination nodes including the relays is manipulated for achieving IA. As the source nodes and the destination nodes transmit twice and receive twice, respectively during the two time slots, each node has a two dimensional signal space. Accordingly, the effective channel between the source nodes and the destination nodes including the relays can be considered as a virtual MIMO interference channel with two antennas at each of the source nodes and the destination nodes. In each destination node, a single data symbol is received from the corresponding source node and thus, the useful signal spans a one dimensional subspace of the two dimensional received signal space. Therefore, the interferences received from the non-corresponding source nodes have to be aligned in a one dimensional subspace, called the interference subspace, of the received signal space.

In the proposed IA algorithms which will be discussed later in this chapter, the processing matrices at the relays and/or the temporal filters at the source nodes are adapted aiming at aligning the interferences in a one dimensional subspace of the received signal space at every destination node. Then by designing the receive filters at the destination nodes according to the zero forcing technique, the estimated data symbols at the output of the receive filters do not include any interference component. In this case, each destination node receives a single interference-free data symbol in two time slots and thus, $K/2$ DoFs are achieved in total [AW11b, AGKW12a, AGKW12b].

Define $\underline{\mathbf{u}}^{(k)*\text{T}}\underline{\mathbf{H}}^{(k,l)}\underline{\mathbf{v}}^{(l)}$ as the effective link between the l -th source node and the k -th destination node including the transmit filter at the l -th source node, the receive filter at the k -th destination node and the processing matrices at the relays. If $l \neq k$, $\underline{\mathbf{u}}^{(k)*\text{T}}\underline{\mathbf{H}}^{(k,l)}\underline{\mathbf{v}}^{(l)}$ describes the effective interference link between the l -th source node and the k -th destination node. Otherwise, it describes an effective useful link between the k -th node pair. There are two IA conditions:

1. **Interference nullifying condition:** This condition requires the interferences at the output of the receive filter of each destination node to be zero

$$\underline{\mathbf{u}}^{(k)*\text{T}}\underline{\mathbf{H}}^{(k,l)}\underline{\mathbf{v}}^{(l)} = 0, \quad l \neq k, \quad \forall k. \quad (3.1)$$

For each destination node k , this condition implies that the interferences are aligned in the interference subspace and they are nullified by the zero forcing filter $\underline{\mathbf{u}}^{(k)}$.

2. **Useful signals non-nullifying condition:** This condition ensures that there is a nonzero component of the useful signal at the output of the receive filter of each destination node

$$\underline{\mathbf{u}}^{(k)*\text{T}} \underline{\mathbf{H}}^{(k,k)} \underline{\mathbf{v}}^{(k)} \neq 0, \quad \forall k. \quad (3.2)$$

Considering the receive signal space of each destination node, this condition implies that the useful signal does not align with the interferences and thus, it has always a component being orthogonal to the interference subspace.

These two conditions are sufficient and necessary for IA regardless of whether the elements of the channel matrices are drawn randomly from a continuous distribution or the channel matrices $\underline{\mathbf{H}}^{(k,l)}$ with $k, l = 1, \dots, K$ have a special structure as in our case, see (2.5) [Jaf11].

3.2 System of multivariate polynomial equations

In this section, the IA conditions introduced in the previous section will be investigated and analyzed. In MIMO interference channels, the useful signals non-nullifying condition holds almost surely for any design of the transmit filters aiming at aligning the interferences at the destination nodes because it is usually assumed that the channel matrices have no special structure, i.e., their elements are drawn randomly and independently from a continuous distribution [GCJ11]. Unfortunately, for our considered system model and transmission technique, the effective channel between the source nodes and the destination nodes including the relays has a special structure. As a result, the useful signals non-nullifying condition of (3.2) does not necessarily hold for all interference nullifying solutions of (3.1). Therefore, the useful signals non-nullifying condition of (3.2) is taken into account in the feasibility studies in Section 3.3.1 and Section 3.4.1.

For the rest of this section, the interference nullifying condition is investigated. Using (2.5), (2.7) and (2.8), the interference nullifying equations of (3.1) can be rewritten as

$$\underline{\mathbf{u}}^{(k,1)*} \underline{\mathbf{h}}_{\text{DS}}^{(k,l)} \underline{\mathbf{v}}^{(l,1)} + \underline{\mathbf{u}}^{(k,2)*} \underline{\mathbf{h}}_{\text{DS}}^{(k,l)} \underline{\mathbf{v}}^{(l,2)} + \underline{\mathbf{u}}^{(k,2)*} \sum_{r=1}^R \underline{\mathbf{h}}_{\text{DR}}^{(k,r)} \underline{\mathbf{G}}^{(r)} \underline{\mathbf{h}}_{\text{RS}}^{(r,l)} \underline{\mathbf{v}}^{(l,1)} = 0, \quad l \neq k, \forall k. \quad (3.3)$$

From (3.3), one observes that the interference nullifying problem is a system of multivariate polynomial equations. In [YGJK10], it is claimed that a system of multivariate polynomial equations is proper, i.e., likely to be solvable, if the number of equations does not exceed the number of variables. Accordingly, the number of equations and the number of variables of (3.3) are calculated.

Each of the interference nullifying equations of (3.3) corresponds to an effective interference link. Therefore, the number of equations equals the total number of the effective interference links. Each destination node receives $K - 1$ interference signals from the non-corresponding source nodes and there are K destination nodes. As a result, the total number of equations is $K(K - 1)$.

For calculating the number of variables, one should be careful not to count the unnecessary variables which do not help in nullifying the interferences. Dividing (3.3) by $\underline{v}^{(l,1)}$ and $\underline{u}^{(k,2)*}$ yields

$$\sum_{r=1}^R \underline{\mathbf{h}}_{\text{DR}}^{(k,r)} \underline{\mathbf{G}}^{(r)} \underline{\mathbf{h}}_{\text{RS}}^{(r,l)} + \underline{h}_{\text{DS}}^{(k,l)} \left(\frac{\underline{v}^{(l,2)}}{\underline{v}^{(l,1)}} + \frac{\underline{u}^{(k,1)*}}{\underline{u}^{(k,2)*}} \right) = 0, \quad l \neq k, \forall k. \quad (3.4)$$

Section 2.1.2 introduces the temporal filters at the source nodes $\underline{\mathbf{v}}^{(k)}$ and at the destination nodes $\underline{\mathbf{u}}^{(k)}$ for $k = 1, \dots, K$. These filters are represented by two dimensional vectors as described in (2.7) and (2.8). Accordingly, each filter vector has a certain magnitude and a certain direction. By looking at the system of equations of (3.4), each equation is linear in the processing matrix $\underline{\mathbf{G}}^{(r)}$ of each relay $r = 1, \dots, R$, the ratio of the transmit filter coefficients $\underline{v}^{(l,2)}/\underline{v}^{(l,1)}$, and the ratio of the receive filter coefficients $\underline{u}^{(k,1)*}/\underline{u}^{(k,2)*}$. This means that the magnitudes or the norms of the transmit and the receive filter vectors do not play a role in solving the interference nullifying problem. It is worth to mention that the amount of energy being transmitted from a source node is the square of the norm of the transmit filter vector. Because the ratio of the coefficients of a two-dimensional vector is a function of the direction of the vector, the transmitted directions and the received directions are the relevant variables to the interference nullifying problem. Based on this discussion, each relay has a processing matrix with M^2 variables and there are R relays. Also, each of the K source nodes and each of the K destination nodes has only a single variable, i.e., this variable describing either a transmitted direction or a received direction. Therefore, the total number of variables is $M^2R + 2K$. The system of multivariate polynomial equations of (3.3) is proper if

$$K(K - 1) \leq M^2R + 2K. \quad (3.5)$$

The inequality of (3.5) holds for nullifying the interferences at the output of a receive filter at each destination node but still the useful signals may be also nullified as the useful signals non-nullifying condition has not been considered in (3.5).

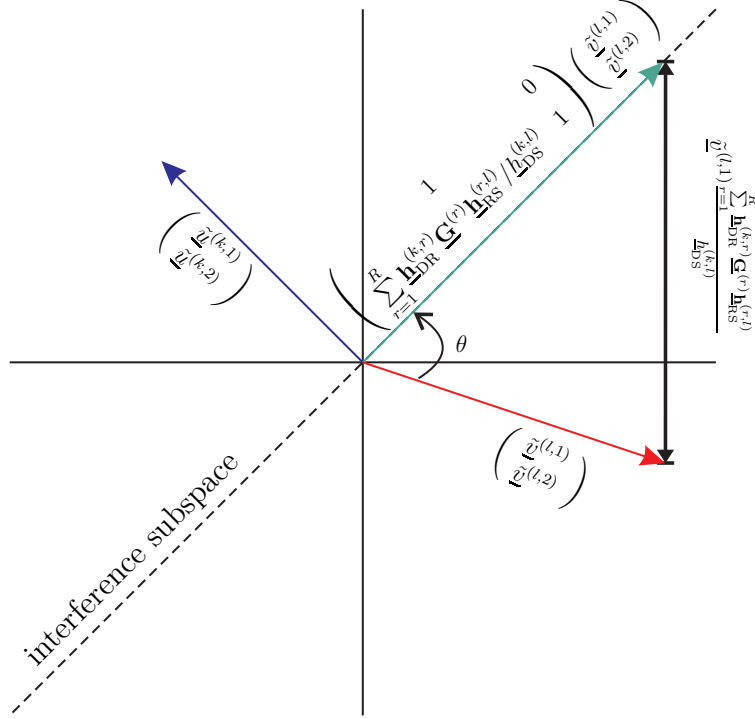


Fig. 3.1: Illustration of the process of rotating a transmit filter vector to the interference subspace using the shear matrix.

To understand how the transmitted directions, the received directions, and the relay processing matrices can be adapted to the channel such that the interferences are aligned at the received signal space of each destination node, consider the interference nullifying equation for nullifying the effective interference link between the l -th source node and the k -th destination node

$$\mathbf{u}^{(k)*T} \mathbf{H}^{(k,l)} \mathbf{v}^{(l)} = 0, \quad l \neq k. \quad (3.6)$$

An illustration of the following description is shown in Fig. 3.1. As the vector norms of the transmit filters and the receive filters do not play a role in IA, unit vectors $(\tilde{\mathbf{v}}^{(l,1)}, \tilde{\mathbf{v}}^{(l,2)})^T$ and $(\tilde{\mathbf{u}}^{(k,1)}, \tilde{\mathbf{u}}^{(k,2)})^T$ containing information of the transmitted directions and the received directions, respectively, can be used. These unit vectors can replace $\mathbf{v}^{(l)}$ and $\mathbf{u}^{(k)}$ in (3.6). Then by dividing the effective channel $\mathbf{H}^{(k,l)}$ by the channel coefficient $\mathbf{h}_{DS}^{(k,l)}$ of the direct link, (3.6) can be rewritten as

$$\left(\tilde{\mathbf{u}}^{(k,1)*} \quad \tilde{\mathbf{u}}^{(k,2)*} \right) \begin{pmatrix} 1 & 0 \\ \frac{\sum_{r=1}^R \mathbf{h}_{DR}^{(k,r)} \mathbf{G}^{(r)} \mathbf{h}_{RS}^{(r,l)}}{\mathbf{h}_{DS}^{(k,l)}} & 1 \end{pmatrix} \begin{pmatrix} \tilde{\mathbf{v}}^{(l,1)} \\ \tilde{\mathbf{v}}^{(l,2)} \end{pmatrix} = 0, \quad (3.7)$$

and

$$\left(\tilde{\mathbf{u}}^{(k,1)*} \quad \tilde{\mathbf{u}}^{(k,2)*} \right) \begin{pmatrix} \tilde{\mathbf{v}}^{(l,1)} \\ \tilde{\mathbf{v}}^{(l,2)} + \tilde{\mathbf{v}}^{(l,1)} \frac{\sum_{r=1}^R \mathbf{h}_{DR}^{(k,r)} \mathbf{G}^{(r)} \mathbf{h}_{RS}^{(r,l)}}{\mathbf{h}_{DS}^{(k,l)}} \end{pmatrix} = 0. \quad (3.8)$$

Because the receive filter $\underline{\mathbf{u}}^{(k)}$ is a zero forcing filter, the received direction determines the interference subspace which is the orthogonal complement subspace of the receive filter vector $\underline{\mathbf{u}}^{(k)}$. The matrix

$$\begin{pmatrix} 1 & 0 \\ \frac{\sum_{r=1}^R \underline{\mathbf{h}}_{\text{DR}}^{(k,r)} \underline{\mathbf{G}}^{(r)} \underline{\mathbf{h}}_{\text{RS}}^{(r,l)}}{\underline{h}_{\text{DS}}^{(k,l)}} & 1 \end{pmatrix} \quad (3.9)$$

is known as shear matrix [FvFH95]. The shear matrix of (3.9) shifts the transmit filter vector $(\tilde{\underline{v}}^{(l,1)}, \tilde{\underline{v}}^{(l,2)})^T$ parallel to the vertical axis by $\tilde{\underline{v}}^{(l,1)} \sum_{r=1}^R \underline{\mathbf{h}}_{\text{DR}}^{(k,r)} \underline{\mathbf{G}}^{(r)} \underline{\mathbf{h}}_{\text{RS}}^{(r,l)} / \underline{h}_{\text{DS}}^{(k,l)}$ till it lies on the interference subspace as shown in Fig. 3.1. Because of the special structure of the shear matrix of (3.9), the filter coefficients $\tilde{\underline{v}}^{(l,1)}$ and $\tilde{\underline{v}}^{(k,2)}$ with $k, l = 1, \dots, K$ cannot be zero otherwise the rotation will not work. The shift range is

$$-\infty < \tilde{\underline{v}}^{(l,1)} \frac{\sum_{r=1}^R \underline{\mathbf{h}}_{\text{DR}}^{(k,r)} \underline{\mathbf{G}}^{(r)} \underline{\mathbf{h}}_{\text{RS}}^{(r,l)}}{\underline{h}_{\text{DS}}^{(k,l)}} < \infty, \quad (3.10)$$

and thus, the angle θ of rotation ranges between $-\frac{\pi}{2}$ and $\frac{\pi}{2}$.

In the next two sections, IA is achieved by linearizing the system of equations of (3.3). The linearization is accomplished by two approaches. Firstly, the filter coefficients at the nodes are fixed and only the relays are adapted to the channel to achieve IA which is described in Section 3.3. The second approach is described in Section 3.4 and it is based on linearizing the system of equations by fixing part of the filter coefficients at the nodes and adapting the relays and the unfixed filter coefficients to achieve IA.

3.3 Interference alignment with fixed transmit and receive filters

3.3.1 Inhomogeneous system of linear equations

In this section, the system of multivariate polynomial equations of (3.3) is linearized by fixing the coefficients of the temporal filters at all nodes. In this case, the relay processing matrices can be adapted to manipulate the effective channel between the source nodes and the destination nodes to achieve IA [AW11b, AGKW12b]. There are some implications of fixing the transmit and the receive filters which can be summarized as follows:

- No CSI is required at the nodes. However, full CSI is required to be available only at the relays.
- For each source node l , the transmitted directions are set in certain directions as $\underline{v}^{(l,1)}$ and $\underline{v}^{(l,2)}$ are fixed. The transmitted energies at the source nodes are fixed and calculated for each source node l as $\underline{\mathbf{v}}^{(l)*\text{T}}\underline{\mathbf{v}}^{(l)}$.
- For each destination node k , fixing the receive filter coefficients $\underline{u}^{(k,1)}$ and $\underline{u}^{(k,2)}$ follows choosing the interference subspace of the received signal space, i.e., the orthogonal complement subspace of the receive filter vector $\underline{\mathbf{u}}^{(k)}$.

When designing the transmit and the receive filters, some aspects have to be taken into account. If a transmit filter vector l is chosen to be orthogonal to a receive filter vector k for any $k, l = 1, \dots, K$, then the signal received from the l -th source node at the k -th destination node through the direct link is nullified. Based on this idea and without using the relays, an invalid IA solution can be found by setting all the transmit filter vectors orthogonal to the receive filter vectors. In this case, all the interferences will be nullified at the output of the receive filters but also the useful signals will be nullified.

If the temporal filters at the nodes are fixed, the system of equations of (3.3) becomes linear in $\underline{\mathbf{G}}^{(r)}$ with $r = 1, \dots, R$. Using (A.13), (3.3) can be rewritten as

$$\underline{v}^{(l,1)}\underline{u}^{(k,2)*} \sum_{r=1}^R \left(\underline{\mathbf{h}}_{\text{RS}}^{(r,l)\text{T}} \otimes \underline{\mathbf{h}}_{\text{DR}}^{(k,r)} \right) \text{vec} \left(\underline{\mathbf{G}}^{(r)} \right) = -\underline{h}_{\text{DS}}^{(k,l)} \left(\underline{v}^{(l,1)}\underline{u}^{(k,1)*} + \underline{v}^{(l,2)}\underline{u}^{(k,2)*} \right), \quad l \neq k, \forall k. \quad (3.11)$$

Define

$$\underline{\mathbf{x}} = \begin{pmatrix} \text{vec} \left(\underline{\mathbf{G}}^{(1)} \right) \\ \vdots \\ \text{vec} \left(\underline{\mathbf{G}}^{(R)} \right) \end{pmatrix} \quad (3.12)$$

as the vector of the unknowns. Let

$$\underline{\mathbf{H}}_{\text{ff}} = \begin{pmatrix} \underline{v}^{(1,1)}\underline{u}^{(2,2)*} \left(\underline{\mathbf{h}}_{\text{RS}}^{(1,1)\text{T}} \otimes \underline{\mathbf{h}}_{\text{DR}}^{(2,1)} \right) & \dots & \underline{v}^{(1,1)}\underline{u}^{(2,2)*} \left(\underline{\mathbf{h}}_{\text{RS}}^{(R,1)\text{T}} \otimes \underline{\mathbf{h}}_{\text{DR}}^{(2,R)} \right) \\ \vdots & & \vdots \\ \underline{v}^{(1,1)}\underline{u}^{(K,2)*} \left(\underline{\mathbf{h}}_{\text{RS}}^{(1,1)\text{T}} \otimes \underline{\mathbf{h}}_{\text{DR}}^{(K,1)} \right) & \dots & \underline{v}^{(1,1)}\underline{u}^{(K,2)*} \left(\underline{\mathbf{h}}_{\text{RS}}^{(R,1)\text{T}} \otimes \underline{\mathbf{h}}_{\text{DR}}^{(K,R)} \right) \\ \vdots & & \vdots \\ \vdots & & \vdots \\ \underline{v}^{(K,1)}\underline{u}^{(1,2)*} \left(\underline{\mathbf{h}}_{\text{RS}}^{(1,K)\text{T}} \otimes \underline{\mathbf{h}}_{\text{DR}}^{(1,1)} \right) & \dots & \underline{v}^{(K,1)}\underline{u}^{(1,2)*} \left(\underline{\mathbf{h}}_{\text{RS}}^{(R,K)\text{T}} \otimes \underline{\mathbf{h}}_{\text{DR}}^{(1,R)} \right) \\ \vdots & & \vdots \\ \underline{v}^{(K,1)}\underline{u}^{(K-1,2)*} \left(\underline{\mathbf{h}}_{\text{RS}}^{(1,K)\text{T}} \otimes \underline{\mathbf{h}}_{\text{DR}}^{(K-1,1)} \right) & \dots & \underline{v}^{(K,1)}\underline{u}^{(K-1,2)*} \left(\underline{\mathbf{h}}_{\text{RS}}^{(R,K)\text{T}} \otimes \underline{\mathbf{h}}_{\text{DR}}^{(K-1,R)} \right) \end{pmatrix} \quad (3.13)$$

and

$$\underline{\mathbf{p}} = \left(\underline{h}_{\text{DS}}^{(2,1)} (\underline{v}^{(1,1)} \underline{u}^{(2,1)*} + \underline{v}^{(1,2)} \underline{u}^{(2,2)*}), \dots, \underline{h}_{\text{DS}}^{(K,1)} (\underline{v}^{(1,2)} \underline{u}^{(K,1)*} + \underline{v}^{(1,2)} \underline{u}^{(K,2)*}), \dots, \dots, \right. \\ \left. \underline{h}_{\text{DS}}^{(1,K)} (\underline{v}^{(K,1)} \underline{u}^{(1,1)*} + \underline{v}^{(K,2)} \underline{u}^{(1,2)*}), \dots, \underline{h}_{\text{DS}}^{(K-1,K)} (\underline{v}^{(K,1)} \underline{u}^{(K-1,1)*} + \underline{v}^{(K,2)} \underline{u}^{(K-1,2)*}) \right)^{\text{T}} \quad (3.14)$$

be a $K(K-1) \times M^2R$ matrix and a $K(K-1)$ dimensional vector, respectively. Each row in $\underline{\mathbf{H}}_{\text{ff}}$ and each element in $\underline{\mathbf{p}}$ corresponds to an effective interference link through the relays and an effective direct interference link, respectively. Using (3.12), (3.13) and (3.14), (3.11) can be written as an inhomogeneous system of linear equations

$$\underline{\mathbf{H}}_{\text{ff}} \underline{\mathbf{x}} = -\underline{\mathbf{p}}. \quad (3.15)$$

In general, the inhomogeneous system of linear equations of (3.15) has a unique solution if the number $K(K-1)$ of equations equals the number M^2R of variables. Moreover, if the number of equations $K(K-1)$ is less than the number M^2R of variables, there are infinitely many solutions. However, there is no solution to the system of linear equations of (3.15) when the number of equations $K(K-1)$ exceeds the number M^2R of variables.

3.3.2 Feasibility of interference alignment

In this section, the number of relays and relay antennas required for achieving IA are presented. In [LAG⁺13], the authors investigate the feasibility of IA for a scenario similar to our considered scenario but they consider single antenna relays. Based on the assumption that the relay antennas are carefully spaced such that the channel between the source nodes and a relay as well as the channel between a relay and the destination nodes are full rank, the contributions of [LAG⁺13] can be adopted for our considered scenario.

If the coefficients of the channels between the nodes and the relays are drawn randomly and independently from a continuous distribution, then the matrix $\underline{\mathbf{H}}_{\text{ff}}$ is almost surely a full rank matrix

$$\text{rank}(\underline{\mathbf{H}}_{\text{ff}}) = \min \{K(K-1), M^2R\}. \quad (3.16)$$

Moreover, by picking randomly any solution of the inhomogeneous system of linear equations of (3.15), the useful signals non-nullifying condition of (3.2) is almost surely satisfied. Accordingly, the required number of relays and relay antennas for achieving IA is calculated using

$$M^2R \geq K(K-1). \quad (3.17)$$

If the equality of (3.17) holds, then there is a unique solution for IA. Otherwise, there are infinitely many IA solutions.

3.3.3 Closed form solution with minimum relays retransmit energy

Out of the infinitely many solutions of (3.15) existing when the equality does not hold in (3.17), the one which maximizes the sum rate can be chosen. Unfortunately, the sum rate is not a concave function of the relay processing matrices, i.e., it has many local maxima and a global maximum. Therefore, no closed form solution for the relay processing matrices when aiming at maximizing the sum rate with an IA constraint can be obtained.

Alternatively, minimizing the total transmitted energy can be chosen as an objective. Because the transmitted energies of the source nodes become fixed by fixing the transmit filters, minimizing the total retransmitted energy of the relays will be considered. If there are enough relays for achieving IA, i.e., if the inequality of (3.17) holds, the set of solutions of (3.15) forms a hyperplane parallel to the subspace $\underline{\mathbf{H}}_{\text{ff}}\underline{\mathbf{x}} = \mathbf{0}$. In the solution hyperplane, solutions for the relay processing matrices which satisfy an arbitrary total energy constraint at the relays do not necessarily exist, i.e., solutions cannot be simply scaled to satisfy any total energy constraint. Therefore, minimizing the total retransmitted energy of the relays is a reasonable objective. Using (A.14), the total relay retransmitted energy of (2.15) can be rewritten as

$$E_{\text{Rtot}} = \sum_{r=1}^R \text{tr} \left(\underline{\mathbf{G}}^{(r)*\text{T}} \underline{\mathbf{G}}^{(r)} \underline{\mathbf{C}}_{\text{rr}}^{(r)} \right) \quad (3.18)$$

$$= \sum_{r=1}^R \text{tr} \left(\underline{\mathbf{G}}^{(r)*\text{T}} \mathbf{I}_M \underline{\mathbf{G}}^{(r)} \underline{\mathbf{C}}_{\text{rr}}^{(r)} \right). \quad (3.19)$$

Using (A.7) in (3.19) yields

$$E_{\text{Rtot}} = \sum_{r=1}^R \text{vec} \left(\underline{\mathbf{G}}^{(r)*} \right)^{\text{T}} \text{vec} \left(\mathbf{I}_M \underline{\mathbf{G}}^{(r)} \underline{\mathbf{C}}_{\text{rr}}^{(r)} \right). \quad (3.20)$$

By exploiting the property of (A.6), (3.20) can be expressed as

$$E_{\text{Rtot}} = \sum_{r=1}^R \text{vec} \left(\underline{\mathbf{G}}^{(r)} \right)^{* \text{T}} \left(\underline{\mathbf{C}}_{\text{rr}}^{(r)\text{T}} \otimes \mathbf{I}_M \right) \text{vec} \left(\underline{\mathbf{G}}^{(r)} \right). \quad (3.21)$$

Let $\underline{\Phi}$ be a block diagonal matrix with R diagonal blocks. The r -th diagonal block $\left(\underline{\mathbf{C}}_{\text{rr}}^{(r)\text{T}} \otimes \mathbf{I}_M\right)$ of the matrix $\underline{\Phi}$ is of size $M^2 \times M^2$. Accordingly, the total retransmitted energy of the relays can be written in a quadratic form as

$$E_{\text{Rtot}} = \underline{\mathbf{x}}^{*\text{T}} \underline{\Phi} \underline{\mathbf{x}}. \quad (3.22)$$

The optimum relay processing matrices which minimize the total retransmitted energy at the relays are found using the optimization problem

$$\underline{\mathbf{x}}_{\text{IA}} = \arg \min_{\underline{\mathbf{x}}} \{ \underline{\mathbf{x}}^{*\text{T}} \underline{\Phi} \underline{\mathbf{x}} \} \quad (3.23)$$

subject to

$$\underline{\mathbf{H}}_{\text{ff}} \underline{\mathbf{x}} + \underline{\mathbf{p}} = \mathbf{0}. \quad (3.24)$$

The objective function $\underline{\mathbf{x}}^{*\text{T}} \underline{\Phi} \underline{\mathbf{x}}$ is a convex quadratic function, i.e., $\underline{\Phi}$ is a positive definite matrix because $\underline{\mathbf{C}}_{\text{rr}}^{(r)}$ is a positive definite matrix for any $r = 1, \dots, R$. Moreover, the constraint of (3.24) is an affine set. Therefore, the optimization problem of (3.23)–(3.24) is a convex problem. The Lagrange of the optimization problem (3.23)–(3.24) is formulated as

$$L(\underline{\mathbf{x}}, \underline{\boldsymbol{\lambda}}) = \underline{\mathbf{x}}^{*\text{T}} \underline{\Phi} \underline{\mathbf{x}} + \underline{\boldsymbol{\lambda}}^{\text{T}} (\underline{\mathbf{p}} + \underline{\mathbf{H}}_{\text{ff}} \underline{\mathbf{x}}), \quad (3.25)$$

where $\underline{\boldsymbol{\lambda}}$ is the vector of Lagrangian multipliers each of which corresponds to a constraint of (3.24). The first order optimality conditions are

$$\frac{\partial L}{\partial \underline{\mathbf{x}}} \stackrel{!}{=} \mathbf{0}, \quad (3.26)$$

and

$$\frac{\partial L}{\partial \underline{\boldsymbol{\lambda}}} \stackrel{!}{=} \mathbf{0}. \quad (3.27)$$

Hence, taking the general derivatives of (3.25) with respect to $\underline{\mathbf{x}}$ and setting the result to zero yields

$$\underline{\Phi}^{*\text{T}} \underline{\mathbf{x}} + \underline{\mathbf{H}}_{\text{ff}}^{*\text{T}} \underline{\boldsymbol{\lambda}}^* = \mathbf{0}. \quad (3.28)$$

Moreover, the general derivatives of (3.25) with respect to $\underline{\boldsymbol{\lambda}}$ are taken and equalized to zero as

$$\underline{\mathbf{p}} + \underline{\mathbf{H}}_{\text{ff}} \underline{\mathbf{x}} = \mathbf{0}. \quad (3.29)$$

Solving (3.28) for $\underline{\mathbf{x}}$ yields

$$\underline{\mathbf{x}} = -(\underline{\Phi}^{*\text{T}})^{-1} \underline{\mathbf{H}}_{\text{ff}}^{*\text{T}} \underline{\boldsymbol{\lambda}}^*. \quad (3.30)$$

By substituting (3.30) in (3.29), the optimum Lagrangian multipliers are calculated as

$$\underline{\boldsymbol{\lambda}}^* = \left(\underline{\mathbf{H}}_{\text{ff}} (\underline{\Phi}^{*\text{T}})^{-1} \underline{\mathbf{H}}_{\text{ff}}^{*\text{T}} \right)^{-1} \underline{\mathbf{p}}. \quad (3.31)$$

By substituting (3.31) in (3.30), the optimum relay coefficients are calculated in a closed form using

$$\underline{\mathbf{x}}_{\text{IA}} = -(\underline{\Phi}^{*\text{T}})^{-1} \underline{\mathbf{H}}_{\text{ff}}^{*\text{T}} \left(\underline{\mathbf{H}}_{\text{ff}} (\underline{\Phi}^{*\text{T}})^{-1} \underline{\mathbf{H}}_{\text{ff}}^{*\text{T}} \right)^{-1} \underline{\mathbf{p}}. \quad (3.32)$$

3.4 Interference alignment with partially adapted transmit and receive filters

3.4.1 Homogeneous system of linear equations

Fixing the temporal filters at the nodes results in a linear problem for IA but unfortunately a large number of relays and relay antennas is required to achieve IA, see (3.17). If just part of the filter coefficients, namely $\underline{v}^{(l,1)}$ and $\underline{u}^{(k,2)}$, $k, l = 1, \dots, K$, are fixed for all the nodes, then the system of equations of (3.3) is linear in the processing matrix $\underline{\mathbf{G}}^{(r)}$ of each relay r and the remaining coefficients of the filters $\underline{v}^{(l,2)}$ and $\underline{u}^{(k,1)}$, $k, l = 1, \dots, K$ [AGKW12a]. Using (A.12), the system of equations of (3.3) can be written as

$$\underline{\mathbf{q}}^{(k,l)*\text{T}} \underline{\mathbf{y}} = 0, \quad l \neq k, \quad \forall k, \quad (3.33)$$

where

$$\underline{\mathbf{y}} = \left(\text{vec} \left(\underline{\mathbf{G}}^{(1)*\text{T}} \right)^{\text{T}}, \dots, \text{vec} \left(\underline{\mathbf{G}}^{(R)*\text{T}} \right)^{\text{T}}, \underline{v}^{(1,2)*}, \dots, \underline{v}^{(K,2)*}, \underline{u}^{(1,1)}, \dots, \underline{u}^{(K,1)} \right)^{\text{T}} \quad (3.34)$$

is the vector of the unknowns and

$$\underline{\mathbf{q}}^{(k,l)} = \left(\underline{v}^{(l,1)} \underline{u}^{(k,2)*} \left(\underline{\mathbf{h}}_{\text{DR}}^{(k,1)} \otimes \underline{\mathbf{h}}_{\text{RS}}^{(1,l)\text{T}} \right), \dots, \underline{v}^{(l,1)} \underline{u}^{(k,2)*} \left(\underline{\mathbf{h}}_{\text{DR}}^{(l,R)} \otimes \underline{\mathbf{h}}_{\text{RS}}^{(R,k)\text{T}} \right) \right. \\ \left. \underbrace{0, \dots, 0}_{l-1}, \underline{u}^{(k,2)*} \underline{h}_{\text{DS}}^{(k,l)}, \underbrace{0, \dots, 0}_{K-l}, \underbrace{0, \dots, 0}_{k-1}, \underline{v}^{(l,1)} \underline{h}_{\text{DS}}^{(k,l)}, \underbrace{0, \dots, 0}_{K-k} \right)^{\text{T}} \quad (3.35)$$

is the vector of constants. Let $\underline{\mathbf{H}}_{\text{paf}}$ be a $K(K-1) \times (M^2R + 2K)$ matrix with its rows being $\underline{\mathbf{q}}^{(k,l)*\text{T}}$ with $l \neq k$ for $k = 1, \dots, K$. Then, the interference nullifying problem can be formulated as the homogeneous system of linear equations

$$\underline{\mathbf{H}}_{\text{paf}} \underline{\mathbf{y}} = \mathbf{0}. \quad (3.36)$$

In general, the homogenous system of linear equations of (3.36) has infinitely many non-trivial solutions if the number $M^2R + 2K$ of variables exceeds the number $K(K-1)$ of equations.

3.4.2 Feasibility of interference alignment

In this section, the number of relays and relay antennas required for achieving IA is presented. As mentioned in Section 3.3.2, the contributions of [LAG⁺13] can be adopted

to our considered scenario. As it is assumed that the channel coefficients are drawn randomly and independently from a continuous distribution, the rank of the matrix $\underline{\mathbf{H}}_{\text{paf}}$ is

$$\text{rank}(\underline{\mathbf{H}}_{\text{paf}}) = \min \{K^2 - K, M^2R + 2K - 1\}. \quad (3.37)$$

Furthermore, the solution space of the homogeneous system of linear equations of (3.36) can contain invalid solutions in which at least a useful signal is nullified with the interferences. As shown in [LAG⁺13] if the number of relays and relay antennas satisfy

$$M^2R \geq K^2 - 3K + 2, \quad (3.38)$$

any randomly picked solution is almost surely a valid one, i.e., it satisfies both IA conditions.

3.4.3 Closed form solution with minimum sum mean square error

As described in Section 3.4.1, the IA problem is linearized by partially adapting the transmit filters and the receive filters. Fortunately, the sum MSE when considered as a function of the unknown vector $\underline{\mathbf{y}}$ is a quadratic convex function [ALG⁺13a] as will be shown in this section. The MSE at the k -th destination node is calculated as

$$\delta^{(k)} = \text{E} \left\{ \left| \hat{\underline{d}}^{(k)} - \underline{d}^{(k)} \right|^2 \right\}. \quad (3.39)$$

Using (A.12), the estimated data symbol at the k -th destination node described in (2.11) can be rewritten as a function of the unknown vector $\underline{\mathbf{y}}$ as

$$\hat{\underline{d}}^{(k)} = \underline{\mathbf{y}}^{*\text{T}} \left(\sum_{l=1}^K \underline{\mathbf{q}}^{(k,l)} \underline{d}^{(l)} + \underline{\mathbf{z}}^{(k)} \right) + \underline{u}^{(k,2)*} \underline{n}_D^{(k,2)}, \quad (3.40)$$

where

$$\begin{aligned} \underline{\mathbf{z}}^{(k)} = & \left(\underline{u}^{(k,2)*} \left(\underline{\mathbf{h}}_{\text{DR}}^{(k,1)} \otimes \underline{\mathbf{n}}_{\text{R}}^{(1)\text{T}} \right), \dots, \underline{u}^{(k,2)*} \left(\underline{\mathbf{h}}_{\text{DR}}^{(k,R)} \otimes \underline{\mathbf{n}}_{\text{R}}^{(R)\text{T}} \right) \right) \Big| \\ & \left(\underbrace{0, \dots, 0}_K, \underbrace{0, \dots, 0}_{k-1}, \underline{n}_D^{(k,1)}, \underbrace{0, \dots, 0}_{K-k} \right)^{\text{T}}. \end{aligned} \quad (3.41)$$

Because the received noise signals at different antennas are uncorrelated, the covariance matrix $\text{E} \{ \underline{\mathbf{z}}^{(k)} \underline{\mathbf{z}}^{(k)*\text{T}} \}$ of the received noise signals excluding $\underline{n}_D^{(k,2)}$ at the k -th destination node is a block diagonal matrix. In $\text{E} \{ \underline{\mathbf{z}}^{(k)} \underline{\mathbf{z}}^{(k)*\text{T}} \}$, the first R diagonal blocks are $\text{E} \left\{ \left| \underline{u}^{(k,2)} \right|^2 \left(\underline{\mathbf{h}}_{\text{DR}}^{(k,r)\text{T}} \otimes \underline{\mathbf{n}}_{\text{R}}^{(r)} \right) \left(\underline{\mathbf{h}}_{\text{DR}}^{(k,r)*} \otimes \underline{\mathbf{n}}_{\text{R}}^{(r)*\text{T}} \right) \right\}$ with $r = 1, \dots, R$, the $(M^2R + K + k)$ -th

diagonal element is σ^2 and the remaining elements are zeros. Using (A.3) and (A.4), the r -th diagonal block for $r = 1, \dots, R$ can be simplified as

$$\begin{aligned} \mathbb{E} \left\{ \left| \underline{u}^{(k,2)} \right|^2 \left(\underline{\mathbf{h}}_{\text{DR}}^{(k,r)\text{T}} \otimes \underline{\mathbf{n}}_{\text{R}}^{(r)} \right) \left(\underline{\mathbf{h}}_{\text{DR}}^{(k,r)*} \otimes \underline{\mathbf{n}}_{\text{R}}^{(r)*\text{T}} \right) \right\} &= \mathbb{E} \left\{ \left| \underline{u}^{(k,2)} \right|^2 \left(\underline{\mathbf{h}}_{\text{DR}}^{(k,r)\text{T}} \underline{\mathbf{h}}_{\text{DR}}^{(k,r)*} \otimes \underline{\mathbf{n}}_{\text{R}}^{(r)} \underline{\mathbf{n}}_{\text{R}}^{(r)*\text{T}} \right) \right\} \\ &= \left| \underline{u}^{(k,2)} \right|^2 \left(\underline{\mathbf{h}}_{\text{DR}}^{(k,r)\text{T}} \underline{\mathbf{h}}_{\text{DR}}^{(k,r)*} \otimes \sigma^2 \mathbf{I}_M \right) \\ &= \sigma^2 \left| \underline{u}^{(k,2)} \right|^2 \left(\underline{\mathbf{h}}_{\text{DR}}^{(k,r)\text{T}} \underline{\mathbf{h}}_{\text{DR}}^{(k,r)*} \otimes \mathbf{I}_M \right). \end{aligned} \quad (3.42)$$

By substituting (3.40) in (3.39), the MSE at the k -th destination node is calculated as

$$\begin{aligned} \delta^{(k)} &= E_{\text{d}} \left(\sum_{l=1}^K \underline{\mathbf{y}}^{*\text{T}} \underline{\mathbf{q}}^{(k,l)} \underline{\mathbf{q}}^{(k,l)*\text{T}} \underline{\mathbf{y}} - \underline{\mathbf{q}}^{(k,k)*\text{T}} \underline{\mathbf{y}} - \underline{\mathbf{y}}^{*\text{T}} \underline{\mathbf{q}}^{(k,k)} + 1 \right) \\ &\quad + \underline{\mathbf{y}}^{*\text{T}} \mathbb{E} \left\{ \underline{\mathbf{z}}^{(k)} \underline{\mathbf{z}}^{(k)*\text{T}} \right\} \underline{\mathbf{y}} + \sigma^2 \left| \underline{u}^{(k,2)} \right|^2. \end{aligned} \quad (3.43)$$

Moreover, the sum MSE is calculated as

$$\delta = \sum_{k=1}^K \delta^{(k)} = \underline{\mathbf{y}}^{*\text{T}} \underline{\mathbf{A}} \underline{\mathbf{y}} - \underline{\mathbf{b}}^{*\text{T}} \underline{\mathbf{y}} - \underline{\mathbf{y}}^{*\text{T}} \underline{\mathbf{b}} + K E_{\text{d}} + \sigma^2 \left| \underline{u}^{(k,2)} \right|^2, \quad (3.44)$$

where

$$\underline{\mathbf{A}} = \sum_{k=1}^K \sum_{l=1}^K E_{\text{d}} \underline{\mathbf{q}}^{(k,l)} \underline{\mathbf{q}}^{(k,l)*\text{T}} + \sum_{k=1}^K \mathbb{E} \left\{ \underline{\mathbf{z}}^{(k)} \underline{\mathbf{z}}^{(k)*\text{T}} \right\} \quad (3.45)$$

and

$$\underline{\mathbf{b}} = \sum_{k=1}^K E_{\text{d}} \underline{\mathbf{q}}^{(k,k)}. \quad (3.46)$$

The sum MSE function of (3.44) is a quadratic convex function because $\underline{\mathbf{A}}$ is a positive semidefinite matrix.

To find an IA solution with a zero MSE at each destination node, K more equations

$$\hat{\underline{d}}^{(k)} = \underline{d}^{(k)}, \quad \forall k \quad (3.47)$$

should be added to the homogeneous system of linear equations (3.36). In this case, an inhomogeneous system of linear equations results and the required number of relays and relay antennas becomes

$$M^2 R \geq K^2 - 2K + 1. \quad (3.48)$$

Instead of solving this new inhomogeneous system of linear equations of (3.36) and (3.47), just the required number of the relays and relay antennas of (3.48) is considered to ensure that the solution space of the homogeneous system of linear equations of

(3.36) contains an IA solution with a sum MSE goes to zero and this solution can be found using the optimization problem

$$\underline{\mathbf{y}}_{\text{IA}} = \arg \min_{\underline{\mathbf{y}}} \{ \underline{\mathbf{y}}^{*\text{T}} \underline{\mathbf{A}} \underline{\mathbf{y}} - \underline{\mathbf{b}}^{*\text{T}} \underline{\mathbf{y}} - \underline{\mathbf{y}}^{*\text{T}} \underline{\mathbf{b}} \} \quad (3.49)$$

subject to

$$\underline{\mathbf{H}}_{\text{paf}} \underline{\mathbf{y}} = \mathbf{0}. \quad (3.50)$$

Note that the last two terms of (3.44) are omitted in (3.49) as they are constants. The optimization problem of (3.49)–(3.50) is convex as the objective function is convex and the constraints form an affine set. The Lagrange is written as

$$L(\underline{\mathbf{y}}, \underline{\boldsymbol{\lambda}}) = \underline{\mathbf{y}}^{*\text{T}} \underline{\mathbf{A}} \underline{\mathbf{y}} - \underline{\mathbf{b}}^{*\text{T}} \underline{\mathbf{y}} - \underline{\mathbf{y}}^{*\text{T}} \underline{\mathbf{b}} + \underline{\boldsymbol{\lambda}} \underline{\mathbf{H}}_{\text{paf}} \underline{\mathbf{y}}, \quad (3.51)$$

where $\underline{\boldsymbol{\lambda}}$ is a vector of Lagrangian multipliers each of which corresponds to a constraint of (3.50). Taking the general derivatives of (3.51) with respect to $\underline{\mathbf{y}}$ and $\underline{\boldsymbol{\lambda}}$ and then setting the results to zero yields

$$\frac{\partial L}{\partial \underline{\mathbf{y}}} = \underline{\mathbf{A}}^{\text{T}} \underline{\mathbf{y}}^* - \underline{\mathbf{b}}^* + \underline{\mathbf{H}}_{\text{paf}}^{\text{T}} \underline{\boldsymbol{\lambda}} \stackrel{!}{=} 0 \quad (3.52)$$

and

$$\frac{\partial L}{\partial \underline{\boldsymbol{\lambda}}} = \underline{\mathbf{H}}_{\text{paf}} \underline{\mathbf{y}} \stackrel{!}{=} \mathbf{0}, \quad (3.53)$$

respectively. Solving (3.52) for $\underline{\mathbf{y}}$ and substituting the result in (3.53) yields

$$\underline{\mathbf{H}}_{\text{paf}} (\underline{\mathbf{A}}^{*\text{T}})^{-1} (\underline{\mathbf{b}} - \underline{\mathbf{H}}_{\text{paf}}^{*\text{T}} \underline{\boldsymbol{\lambda}}) = \mathbf{0}. \quad (3.54)$$

Solving (3.54) for $\underline{\boldsymbol{\lambda}}$ yields

$$\underline{\boldsymbol{\lambda}} = \underline{\mathbf{b}}^{*\text{T}} \underline{\mathbf{A}}^{-1} \underline{\mathbf{H}}_{\text{paf}}^{*\text{T}} (\underline{\mathbf{H}}_{\text{paf}} \underline{\mathbf{A}}^{-1} \underline{\mathbf{H}}_{\text{paf}}^{*\text{T}})^{-1}. \quad (3.55)$$

By substituting (3.55) in (3.52), the optimum $\underline{\mathbf{y}}_{\text{IA}}$ is obtained in a closed form as

$$\underline{\mathbf{y}}_{\text{IA}} = (\underline{\mathbf{A}}^{*\text{T}})^{-1} \underline{\mathbf{b}} - (\underline{\mathbf{A}}^{*\text{T}})^{-1} \underline{\mathbf{H}}_{\text{paf}}^{*\text{T}} \left(\underline{\mathbf{H}}_{\text{paf}} (\underline{\mathbf{A}}^{*\text{T}})^{-1} \underline{\mathbf{H}}_{\text{paf}}^{*\text{T}} \right)^{-1} \underline{\mathbf{H}}_{\text{paf}} (\underline{\mathbf{A}}^{*\text{T}})^{-1} \underline{\mathbf{b}}. \quad (3.56)$$

3.5 Complexity and performance of interference alignment algorithms

3.5.1 Preliminary remarks

In the previous two sections, two IA algorithms have been proposed. Firstly, the IA algorithm with fixed filters and the minimum total relay retransmit energy has been

proposed. Secondly, the IA algorithm with partially adapted filters and the minimum sum MSE has been proposed. Both of these IA algorithms lead to closed form solutions of (3.32) and (3.56), respectively. In this section, complexity and performance investigations for both IA algorithms are presented. For a fair assessment between the two IA algorithms, equal number K of node pairs, equal number R of relays and equal number M of relay antennas are considered in the following.

3.5.2 Complexity analysis

In this subsection, the complexity of computing the proposed IA solutions is investigated. In the complexity theory, the big-O notation $\mathcal{O}(\cdot)$ is usually considered for analyzing the complexity of an algorithm. For more information on the big-O notation, see Appendix C.1. For an IA algorithm, the complexity is a function of the number of system variables, i.e., K , R and M . The $\mathcal{O}(\cdot)$ notation studies the behavior of an algorithm at infinite dimensions, i.e., when one or all of the number of variables K , R and M go to infinity. Accordingly, only operations like multiplications and divisions are considered as they have a relatively high computational cost as compared to other operations like addition or subtraction. On the other hand, addition, subtraction, logical operations and constant coefficients are ignored in the complexity calculations. Repeated operations do not increase the complexity as the result can be stored and reused when it is needed, i.e, enough memory is always available. In the following analysis, the number of complex multiplications required for computing an IA solution is taken into account. In appendix C, Table C.1 summarizes the number of multiplications and complexities of some basic linear algebra operations which are used for calculating the complexity of the proposed IA algorithms.

The IA solutions are calculated in closed form using (3.32) and (3.56) and to calculate the complexity of the algorithms, the complexity of computing the matrices $\underline{\mathbf{H}}_{\text{ff}}$, $\underline{\mathbf{H}}_{\text{paf}}$, $\underline{\Phi}$ and $\underline{\mathbf{A}}$ are first calculated. Table 3.1 summarizes the complexity of computing the matrices and vectors involved in (3.32) and (3.56). Using the Table 3.1, the complexity of computing $\underline{\mathbf{x}}_{\text{IA}}$ and $\underline{\mathbf{y}}_{\text{IA}}$ can be calculated as

$$\mathcal{O}(RM^6 + R^2M^4K^2 + RM^2K^4 + K^6), \quad (3.57)$$

and

$$\mathcal{O}(R^3M^6 + R^2M^4K^2 + RM^2K^4 + K^6), \quad (3.58)$$

respectively. Based on the IA feasibility conditions described in Section 3.3.2 and Section 3.4.2, $M^2R > K^2$ at the asymptote and thus, the complexity of computing $\underline{\mathbf{x}}_{\text{IA}}$ and $\underline{\mathbf{y}}_{\text{IA}}$ can be expressed as shown in Table 3.2.

Expression	Complexity
$\underline{\mathbf{h}}_{\text{RS}}^{(r,l)} \underline{\mathbf{h}}_{\text{RS}}^{(r,l)*\text{T}}$	$\mathcal{O}(M^2)$
$\underline{\mathbf{C}}_{\text{rT}}^{(r)}$ in (2.14)	$\mathcal{O}(KM^2)$
$\underline{\mathbf{C}}_{\text{rT}}^{(r)} \otimes \mathbf{I}_M$	$\mathcal{O}(KM^2)$
$\underline{\Phi}$	$\mathcal{O}(RKM^2)$
$\underline{\mathbf{h}}_{\text{RS}}^{(r,l)\text{T}} \otimes \underline{\mathbf{h}}_{\text{DR}}^{(k,r)}$	$\mathcal{O}(M^2)$
$\underline{\mathbf{H}}_{\text{ff}}$ in (3.13)	$\mathcal{O}(RK^2M^2)$
$\underline{\mathbf{q}}^{(k,l)}$ in (3.35)	$\mathcal{O}(RM^2)$
$\underline{\mathbf{H}}_{\text{paf}}$	$\mathcal{O}(K^2RM^2)$
$\underline{\mathbf{q}}^{(k,l)} \underline{\mathbf{q}}^{(k,l)*\text{T}}$	$\mathcal{O}(R^2M^4 + RM^2K + K^2)$
$\underline{\mathbf{h}}_{\text{DR}}^{(k,r)\text{T}} \underline{\mathbf{h}}_{\text{DR}}^{(k,r)*} \otimes \mathbf{I}_M$ in (3.42)	$\mathcal{O}(M^2)$
$\text{E} \{ \underline{\mathbf{z}}^{(k)} \underline{\mathbf{z}}^{(k)*\text{T}} \}$	$\mathcal{O}(RM^2)$
$\underline{\mathbf{A}}$ in (3.45)	$\mathcal{O}(K^2R^2M^4 + K^3RM^2 + K^4)$
$\underline{\mathbf{b}}$ in (3.46)	$\mathcal{O}(KRM^2)$

Table 3.1: Complexity of computing the matrices involved in (3.32) and (3.56).

From Table 3.2, the complexities of both algorithms are polynomial with an order of six in terms of the number M of antennas at the relays. The complexity of computing the expression of $\underline{\mathbf{x}}_{\text{IA}}$ grows quadratically with the number K of node pairs and the number R of relays. However, the complexity of computing the expression of $\underline{\mathbf{y}}_{\text{IA}}$ is quadratical and cubical with the number K of node pairs and the number R of relays, respectively.

By comparing the computational complexities in Table 3.2, it is observed that all terms except the first terms are the same. The cost of computing the closed form solution of (3.56) with partially adapted filters is higher than the cost of computing the solution of

Expression	Complexity
$\underline{\mathbf{x}}_{\text{IA}}$ in (3.32)	$\mathcal{O}(RM^6 + R^2M^4K^2)$
$\underline{\mathbf{y}}_{\text{IA}}$ in (3.56)	$\mathcal{O}(R^3M^6 + R^2M^4K^2)$

Table 3.2: Complexity of computing the optimum IA solutions.

(3.32) with fixed filters in terms of the number R of relays. The additional complexity expenses for computing $\underline{\mathbf{y}}_{\text{IA}}$ as compared to computing $\underline{\mathbf{x}}_{\text{IA}}$ are not due to the additional variables, i.e., the adapted filter coefficients, but because of the complexity of computing the inverse the full matrix $\underline{\mathbf{A}}^{-1}$ which has a higher complexity as compared to computing the inverse of the block diagonal matrix $\underline{\mathbf{\Phi}}^{-1}$, i.e., computing the inverse of a block diagonal matrix requires just computing the inverse of each diagonal block. By comparing the structure of the matrix $\underline{\mathbf{H}}_{\text{ff}}$ with the matrix $\underline{\mathbf{H}}_{\text{paf}}$, one observes that adapting some of the filter coefficients to the channel for achieving IA does not increase the complexity significantly as some sparse vectors are added to the problem, i.e., the last $2K$ elements of $\underline{\mathbf{q}}^{(k,l)}$ correspond to the adapted filter coefficients and they are sparse.

3.5.3 Performance analysis

In this section, the performances of the proposed IA algorithms described in Section 3.3.3 and Section 3.4.3 are investigated. The achieved sum rate per time slot

$$C = \frac{1}{2} \sum_{k=1}^K \text{ld} (1 + \gamma^{(k)}) \quad (3.59)$$

is considered as the performance measure. In the following, a three $K = 3$ cells scenario is considered. For $K = 3$ and $M = 2$, the required numbers of relays are $R \geq 2$ for the IA algorithm with fixed filters and $R \geq 1$ for the IA algorithm with adapted filters, respectively. Accordingly, $R = 3$ is chosen so that each cell contains a single relay with two antennas. For the IA algorithm with partially adapted filters, the fixed transmit filter coefficients are equal and they are adjusted such that equal energies are transmitted by the source nodes in the first time slot. By increasing the transmitted energy, the k -th fixed transmit filter coefficient $\underline{v}^{(k,1)}$ is scaled up such that part of transmitted energy is transmitted by the k -th source node in the first time slot. Furthermore, the corresponding fixed receive filter coefficient is scaled down as

$$\underline{u}^{(k,2)} = 1/\underline{v}^{(k,1)} \quad (3.60)$$

so that the transmitted energy is compensated and the sum MSE is reduced, i.e., this scaling of filter coefficients is not optimized. For the IA algorithm with fixed filters, the transmit filter coefficients are adjusted so that equal energies are transmitted by the source nodes in both time slots. To have the same fixed filter design, the receive filters as calculated as

$$\begin{pmatrix} \underline{u}^{(k,1)} \\ \underline{u}^{(k,2)} \end{pmatrix} = \begin{pmatrix} 1/\underline{v}^{(k,2)} \\ 1/\underline{v}^{(k,1)} \end{pmatrix}, \quad \forall k. \quad (3.61)$$

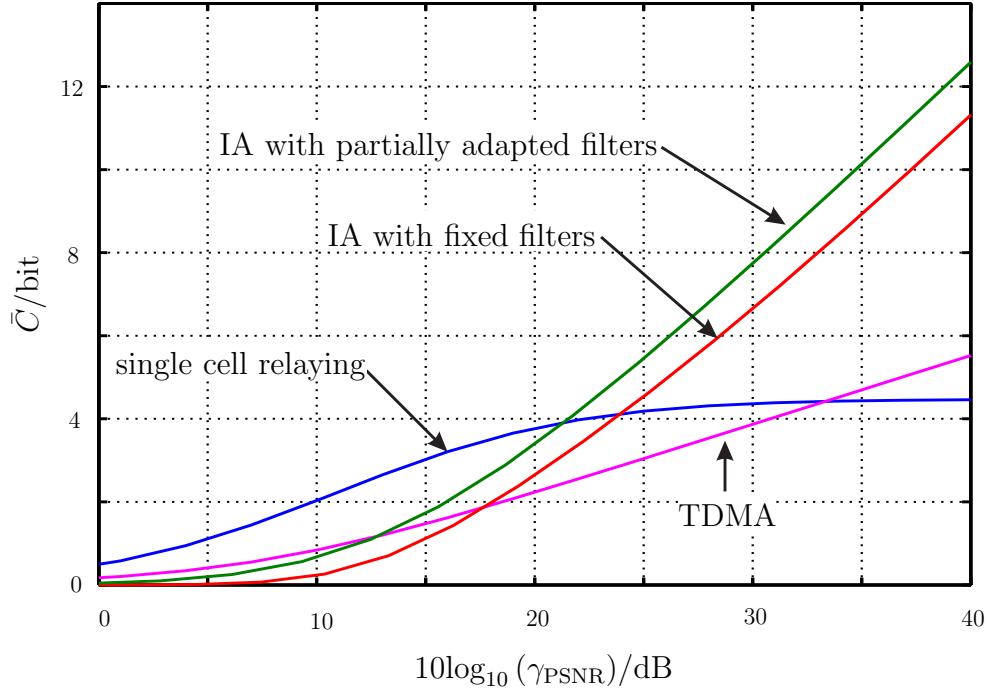


Fig. 3.2: Achieved sum rate as a function of PSNR for a scenario with $K = 3$, $R = 3$ and $M = 2$.

Two benchmark schemes are considered. The first one is the single cell relaying algorithm proposed in Section 2.2.1. Secondly, the time division multiple access (TDMA) algorithm is considered as a benchmark. For the TDMA algorithm, the transmission technique described in Section 2.1.2 is employed for the node pairs sequentially considering all the relays, i.e., six time slots are required to serve $K = 3$ node pairs using the TDMA algorithm. Fig. 3.2 shows the average achieved sum rate \bar{C} over a large number of channel realizations as a function of the PSNR. For low PSNRs, the interferences are low and thus the noise is dominant. Accordingly, the reference scheme, i.e., the single cell relaying algorithm, outperforms the IA algorithms. As the PSNR increases, the interference energies increase which limits the performances of the single cell relaying algorithm as it does not take the inter-cell interferences into account as described in Section 2.2.1. Therefore, the single cell relaying algorithm saturates at a certain sum rate at the high PSNR regime where the signal to interference ratio at every destination node does not change significantly as the PSNR increases. The IA algorithms outperform the single cell relaying algorithm at the high PSNR regime.

At high PSNRs, the slopes of the curves shown in Fig. 3.2 are related to the achieved DoFs. In a scenario with a single node pair with a single antenna and no relays, doubling the transmitted energy by the source node leads to one additional bit achieved at the destination node. For the performance of the IA algorithms at the high PSNR regime,

3/2 bits are achieved by doubling the PSNRs. Whereas, 1/2 bit is achieved when employing the TDMA algorithm and nothing is achieved using the single cell relaying algorithm.

It is observed from Fig. 3.2 that the IA algorithm with partially adapted filters outperforms the IA algorithm with fixed filters at all PSNRs because in the IA algorithm with partially adapted filters,

- part of the filter coefficients are adapted to achieve IA so there are more variables as compared to the IA algorithm with fixed filters and thus, the interference nullifying solution space is larger than the one when the filters are fixed.
- the limited noise energy retransmitted by the relays is always smaller than the one if the filters are fixed. Actually, the term limited noise retransmitted energy comes from the fact that the relays receive noise signals at the first time slot, preprocess them and retransmit them at the second time slot with a certain limited energy.
- the sum MSE is minimized which mitigates the noise especially at low and moderate PSNRs.

Chapter 4

Energy allocation for interference alignment systems

4.1 Preliminaries

In this chapter, the energy allocation in the framework of IA is investigated. As described in Section 3.2, the processing matrices at the relays and the directions of the transmit and receive filter vectors at the nodes are optimized to achieve IA. However, the norms of the transmit and receive filter vectors do not play a role in solving the IA problem. The norm $\|\underline{\mathbf{v}}^{(l)}\|$ of the l -th transmit filter vector determines the transmitted energy of the l -th source node. Because the IA problem is linearized and solved by fixing some or all coefficients of the transmit filters, the transmitted energies at the source nodes are a priori allocated either in the two time slots if the transmit filter coefficients in the two time slots are fixed or just in the first time slot if the transmit filter coefficients in the first time slot are fixed. Therefore, our goal is to optimize the energy allocation in conjunction with IA. Unfortunately, the problem of IA and energy allocation cannot be efficiently solved jointly, i.e., it is a non-convex problem. Consequently, it can be tackled in two steps:

Step 1: For an equal energy allocation among the source nodes, align the interferences using one of the IA algorithms proposed in Section 3.3 or in Section 3.4.

Step 2: For an IA solution, redistribute the total available energy among the source nodes and the relays aiming at maximizing the sum rate.

The first step is covered in Chapter 3 whereas the second step is the main focus in this chapter. It is assumed that the node pairs and the relays can employ N orthogonal resources for the transmission. There is no interference among different resources and thus, it can be seen as N parallel channels. Each source node aims at transmitting N different uncorrelated data symbols through the N parallel channels. Accordingly, the notations $\underline{h}_{\text{DS}}^{(k,l)}$, $\underline{\mathbf{h}}_{\text{RS}}^{(r,l)}$ and $\underline{\mathbf{h}}_{\text{DR}}^{(k,r)}$ of the channel coefficients introduced in Section 2.1 can be extended as $\underline{h}_{\text{DS}}^{(k,l,n)}$, $\underline{\mathbf{h}}_{\text{RS}}^{(r,l,n)}$ and $\underline{\mathbf{h}}_{\text{DR}}^{(k,r,n)}$ to include the resource index $n = 1, \dots, N$.

After applying an IA solution, the transmit filter of the l -th source node in the n -th resource, the receive filter of the k -th destination node in the n -th resource and the

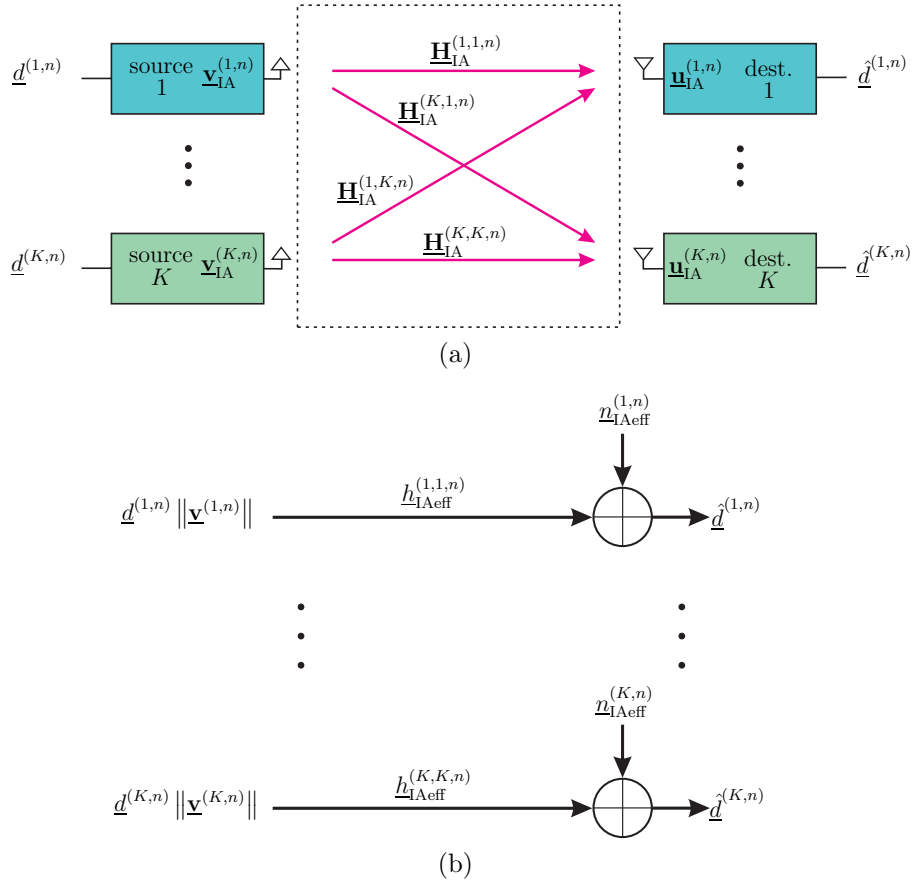


Fig. 4.1: Effective channel in the n -th resource between the source nodes and the destination nodes after applying an IA solution: (a) including the relays, (b) including the filters and the relays.

processing matrix of the r -th relay in the n -th resource are denoted as $\mathbf{v}_{\text{IA}}^{(l,n)}$, $\mathbf{u}_{\text{IA}}^{(k,n)}$ and $\mathbf{G}_{\text{IA}}^{(r,n)}$, respectively. Furthermore, the resulting effective channel between the l -th source node and the k -th destination node in the n -th resource including the relays is calculated as

$$\mathbf{H}_{\text{IA}}^{(k,l,n)} = \begin{pmatrix} h_{\text{DS}}^{(k,l,n)} & 0 \\ \sum_{r=1}^R \mathbf{h}_{\text{DR}}^{(k,r,n)} \mathbf{G}_{\text{IA}}^{(r,n)} \mathbf{h}_{\text{RS}}^{(r,l,n)} & h_{\text{DS}}^{(k,l,n)} \end{pmatrix}. \quad (4.1)$$

For the l -th source node in the n -th resource, the transmit filter vector can be described as

$$\mathbf{v}_{\text{IA}}^{(l,n)} = \left\| \mathbf{v}_{\text{IA}}^{(l,n)} \right\| \tilde{\mathbf{v}}_{\text{IA}}^{(l,n)}, \quad (4.2)$$

where $\left\| \mathbf{v}_{\text{IA}}^{(l,n)} \right\|$ and $\tilde{\mathbf{v}}_{\text{IA}}^{(l,n)}$ are the norm and the unit vector of the l -th transmit filter vector $\mathbf{v}_{\text{IA}}^{(l,n)}$ in the n -th resource, respectively. Fig. 4.1a shows the effective channel in the n -th resource between the source nodes and the destination nodes including the relays for an IA solution. It shows that the norms $\left\| \mathbf{v}_{\text{IA}}^{(l,n)} \right\|$, $l = 1, \dots, K$ of the

transmit filter vectors can be freely adapted while the interferences are still aligned at the destination nodes. The vector of the transmitted energies of the l -th source node in all resources is defined as

$$\mathbf{E}^{(l)} = (E^{(l,1)}, \dots, E^{(l,N)})^T, \quad (4.3)$$

where

$$E^{(l,n)} = E_d \left\| \mathbf{v}_{\text{IA}}^{(l,n)} \right\|^2. \quad (4.4)$$

Hence, the transmitted energies $E^{(l,n)}$ with $l = 1, \dots, K$ at the source nodes can be optimized to enhance the performance without affecting the IA.

For a certain resource n , the effective channel between the l -th source node and the k -th destination node including the temporal filters and the relays can be calculated as

$$\underline{h}_{\text{IAeff}}^{(k,l,n)} = \mathbf{u}_{\text{IA}}^{(k,n)*T} \mathbf{H}_{\text{IA}} \mathbf{v}_{\text{IA}}^{(l,n)}. \quad (4.5)$$

It can be noted that when IA is achieved, $\underline{h}_{\text{IAeff}}^{(k,l,n)} = 0$ for $l \neq k$ and $\underline{h}_{\text{IAeff}}^{(k,k,n)} \neq 0$. For a certain resource n , the effective received noise signal, see the last term of (2.4), at the output of the receive filter $\mathbf{u}_{\text{IA}}^{(k,n)}$ of the k -th destination node is calculated as

$$\underline{n}_{\text{IAeff}}^{(k,n)} = \mathbf{u}_{\text{IA}}^{(k,n)*T} \left(\begin{array}{c} \underline{n}_{\text{D}}^{(k,1,n)} \\ \sum_{r=1}^R \mathbf{h}_{\text{DR}}^{(k,r,n)} \mathbf{G}_{\text{IA}} \mathbf{u}_{\text{R}}^{(r,n)} + \underline{n}_{\text{D}}^{(k,2,n)} \end{array} \right). \quad (4.6)$$

Thanks to the linearity of the system, the effective channel between the source nodes and the destination nodes including the temporal filters and the relays for any resource n can be seen as an interference free channel when an IA solution is applied as shown in Fig. 4.1b. By substituting (4.5) and (4.6) in (2.13) and due to the fact that there are no interference links in the effective channel, the received SNR at the k -th destination node in the n -th resource is calculated as

$$\gamma_{\text{IA}}^{(k,n)} = E^{(k,n)} \frac{\left| \underline{h}_{\text{IAeff}}^{(k,k,n)} \right|^2}{\left(\sigma_{\text{IAeff}}^{(k,n)} \right)^2} \quad (4.7)$$

with the effective noise power

$$\left(\sigma_{\text{IAeff}}^{(k,n)} \right)^2 = \mathbb{E} \left\{ \underline{n}_{\text{IAeff}}^{(k,n)*} \underline{n}_{\text{IAeff}}^{(k,n)} \right\} \quad (4.8)$$

calculated at the output of the receive filter of the k -th destination node in the n -th resource. Furthermore, the total energy retransmitted by the relays of (2.15) for a single

resource can be adopted to consider the N resources and written as a function of the transmitted energies $E^{(l,n)}$, $l = 1, \dots, K$ of the source nodes as

$$\begin{aligned}
E_{\text{Rtot}} &= \sum_{n=1}^N \sum_{r=1}^R \text{tr} \left(\underline{\mathbf{G}}_{\text{IA}}^{(r,n)} \underline{\mathbf{C}}_{\text{r}}^{(r,n)} \underline{\mathbf{G}}_{\text{IA}}^{(r,n)*\text{T}} \right) \\
&= \sum_{n=1}^N \sum_{r=1}^R \text{tr} \left(\underline{\mathbf{G}}_{\text{IA}}^{(r,n)} \left(E_{\text{d}} \sum_{l=1}^K \left| \underline{v}_{\text{IA}}^{(l,1,n)} \right|^2 \underline{\mathbf{h}}_{\text{RS}}^{(r,l,n)} \underline{\mathbf{h}}_{\text{RS}}^{(r,l,n)*\text{T}} + \sigma^2 \mathbf{I}_M \right) \underline{\mathbf{G}}_{\text{IA}}^{(r,n)*\text{T}} \right) \\
&= \sum_{n=1}^N \sum_{r=1}^R \text{tr} \left(\underline{\mathbf{G}}_{\text{IA}}^{(r,n)} \left(E_{\text{d}} \sum_{l=1}^K \left| \underline{v}_{\text{IA}}^{(l,1,n)} \right|^2 \underline{\mathbf{h}}_{\text{RS}}^{(r,l,n)} \underline{\mathbf{h}}_{\text{RS}}^{(r,l,n)*\text{T}} \right) \underline{\mathbf{G}}_{\text{IA}}^{(r,n)*\text{T}} \right) \\
&\quad + \sigma^2 \sum_{r=1}^R \text{tr} \left(\underline{\mathbf{G}}_{\text{IA}}^{(r,n)} \underline{\mathbf{G}}_{\text{IA}}^{(r,n)*\text{T}} \right) \\
&= \sum_{n=1}^N \sum_{l=1}^K E_{\text{d}} \left| \underline{v}_{\text{IA}}^{(l,1,n)} \right|^2 \sum_{r=1}^R \text{tr} \left(\underline{\mathbf{G}}_{\text{IA}}^{(r,n)} \underline{\mathbf{h}}_{\text{RS}}^{(r,l,n)} \underline{\mathbf{h}}_{\text{RS}}^{(r,l,n)*\text{T}} \underline{\mathbf{G}}_{\text{IA}}^{(r,n)*\text{T}} \right) \\
&\quad + \sigma^2 \sum_{r=1}^R \text{tr} \left(\underline{\mathbf{G}}_{\text{IA}}^{(r,n)} \underline{\mathbf{G}}_{\text{IA}}^{(r,n)*\text{T}} \right) \\
&= \sum_{n=1}^N \left(\sum_{l=1}^K \beta_{\text{IA}}^{(l,n)} E^{(l,n)} + \left(\sigma_{\text{IAtx}}^{(n)} \right)^2 \right), \tag{4.9}
\end{aligned}$$

where

$$\beta_{\text{IA}}^{(l,n)} = \left| \underline{v}_{\text{IA}}^{(l,1,n)} \right|^2 \sum_{r=1}^R \text{tr} \left(\underline{\mathbf{G}}_{\text{IA}}^{(r,n)} \underline{\mathbf{h}}_{\text{RS}}^{(r,l,n)} \underline{\mathbf{h}}_{\text{RS}}^{(r,l,n)*\text{T}} \underline{\mathbf{G}}_{\text{IA}}^{(r,n)*\text{T}} \right) \tag{4.10}$$

scales the l -th source node transmitted energy in the n -th resource to the useful retransmitted energy of the relays corresponding to the l -th source node and

$$\left(\sigma_{\text{IAtx}}^{(n)} \right)^2 = \sigma^2 \sum_{r=1}^R \text{tr} \left(\underline{\mathbf{G}}_{\text{IA}}^{(r,n)} \underline{\mathbf{G}}_{\text{IA}}^{(r,n)*\text{T}} \right) \tag{4.11}$$

is the limited energy corresponds to the retransmitted noise of the relays in the n -th resource, i.e., the relays receive noise signals at the first time slot, preprocess them and retransmit them at the second time slot with a certain limited energy.

The energy allocation on the top of IA solutions for a single resource $N = 1$ is considered in the next section. In Section 4.3, the energy allocation on the top of IA solutions in the case of $N > 1$ is studied.

4.2 Energy allocation for a single resource in an interference alignment system

In this section, the energy allocation on the top of an IA solution in a single resource is investigated. Basically, the communication among the node pairs and the relays takes place through a single shared resource $N = 1$. As there is only a single resource, the resources indices are skipped in the analysis of this section. As described in the previous section, the effective channel including the filters and the relays is an interference free channel if an IA solution is applied. Using (4.7) and (4.9), the energy allocation optimization problem aiming at maximizing the sum rate with a total energy constraint can be stated as

$$\left(E_{\text{opt}}^{(1)}, \dots, E_{\text{opt}}^{(K)} \right) = \arg \max_{(E^{(1)}, \dots, E^{(K)})} \left\{ \frac{1}{2} \sum_{k=1}^K \text{ld} \left(1 + E^{(k)} \frac{|h_{\text{IAeff}}^{(k,k)}|^2}{(\sigma_{\text{IAeff}}^{(k)})^2} \right) \right\} \quad (4.12)$$

subject to

$$\sum_{k=1}^K E^{(k)} + \sum_{k=1}^K \beta_{\text{IA}}^{(k)} E^{(k)} + \sigma_{\text{IAtx}}^2 = E_{\text{tot}}, \quad (4.13)$$

and

$$E^{(k)} \geq 0, \forall k. \quad (4.14)$$

The first term and the second term of (4.13) describe the transmitted useful energy of the source nodes and of the relays, respectively. Furthermore, the limited energy of the noise retransmitted by the relays is represented by the third term of (4.13). It is to be noted that the total energy E_{tot} has to exceed the retransmitted noise energy σ_{IAtx}^2 of the relays. Otherwise, there is not enough energy for transmitting the useful signals, i.e., the relays will retransmit just the noise signals received at the first time slot to the destination nodes as the relay processing matrices are already set for an IA solution.

The optimization problem of (4.12)–(4.14) is convex as the objective function is a concave function and the constraints of (4.13)–(4.14) form a convex set. The Lagrange of the optimization problem of (4.12)–(4.14) can be written as

$$\begin{aligned} L(E^{(1)}, \dots, E^{(K)}, \lambda) &= \frac{1}{2} \sum_{k=1}^K \text{ld} \left(1 + E^{(k)} \frac{|h_{\text{IAeff}}^{(k,k)}|^2}{(\sigma_{\text{IAeff}}^{(k)})^2} \right) \\ &+ \lambda \left(\sum_{k=1}^K (1 + \beta_{\text{IA}}^{(k)}) E^{(k)} + \sigma_{\text{IAtx}}^2 - E_{\text{tot}} \right), \end{aligned} \quad (4.15)$$

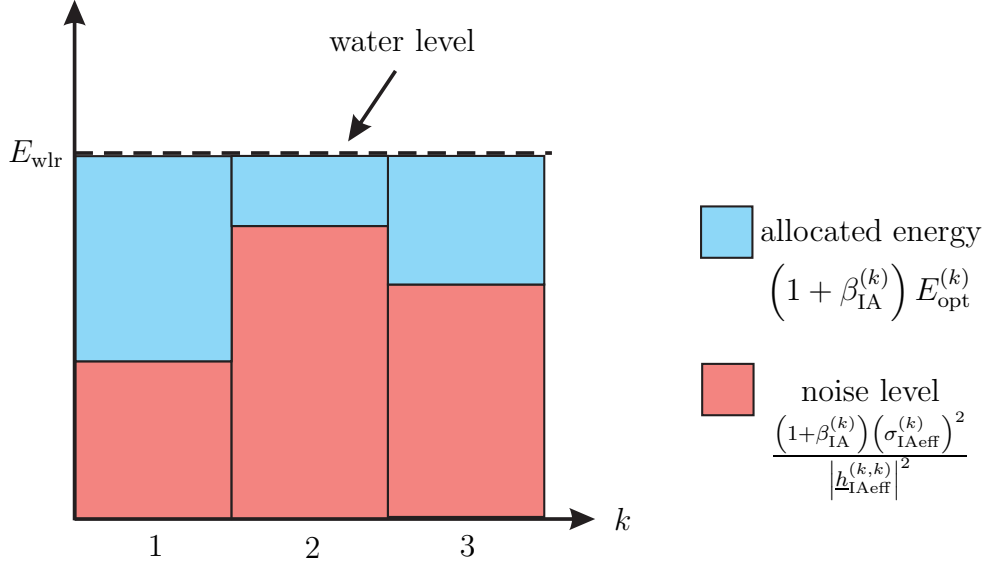


Fig. 4.2: Energy allocation among three source nodes and the relays using the rate maximization waterfilling algorithm.

where λ denotes the Lagrangian multiplier. The first order optimality conditions are

$$\frac{\partial \mathcal{L}}{\partial E^{(k)}} \stackrel{!}{=} 0, \quad (4.16)$$

and

$$\frac{\partial \mathcal{L}}{\partial \lambda} = \sum_{k=1}^K \left(1 + \beta_{\text{IA}}^{(k)}\right) E^{(k)} + \sigma_{\text{IAtx}}^2 - E_{\text{tot}} \stackrel{!}{=} 0. \quad (4.17)$$

By taking the derivative of (4.15) with respect to $E^{(k)}$ and setting the result to zero, one can solve for $E^{(k)}$ as

$$E^{(k)} = \frac{-1}{2 \ln(2) \lambda \left(1 + \beta_{\text{IA}}^{(k)}\right)} - \frac{\left(\sigma_{\text{IAeff}}^{(k)}\right)^2}{\left|\underline{h}_{\text{IAeff}}^{(k,k)}\right|^2}. \quad (4.18)$$

Substituting (4.18) in (4.17) yields

$$\frac{-1}{2 \ln(2) \lambda} = \frac{1}{K} \left(\sum_{k=1}^K \frac{\left(1 + \beta_{\text{IA}}^{(k)}\right) \left(\sigma_{\text{IAeff}}^{(k)}\right)^2}{\left|\underline{h}_{\text{IAeff}}^{(k,k)}\right|^2} - \sigma_{\text{IAtx}}^2 + E_{\text{tot}} \right). \quad (4.19)$$

By substituting (4.19) in (4.18), the optimum energy allocation at each source node k is calculated using an algorithm called the rate maximization waterfilling algorithm with

$$E_{\text{opt}}^{(k)} = \frac{1}{\left(1 + \beta_{\text{IA}}^{(k)}\right)} E_{\text{wlr}} - \frac{\left(\sigma_{\text{IAeff}}^{(k)}\right)^2}{\left|\underline{h}_{\text{IAeff}}^{(k,k)}\right|^2}, \quad k \in \Omega_{\text{WFr}}, \quad (4.20)$$

where

$$E_{\text{wlr}} = \frac{1}{K'} \left(\sum_{k \in \Omega_{\text{WFr}}} \frac{(1 + \beta_{\text{IA}}^{(k)}) (\sigma_{\text{IAeff}}^{(k)})^2}{|h_{\text{IAeff}}^{(k,k)}|^2} - \sigma_{\text{IAtx}}^2 + E_{\text{tot}} \right) \quad (4.21)$$

is the water level and Ω_{WFr} is the set of the indices of the node pairs which contribute non-negative energy values $E_{\text{opt}}^{(k)} \geq 0$ when considered in (4.20) and (4.21). K' denotes the size of the set Ω_{WFr} . The second term of (4.20) represents the noise level of each node pair. Waterfilling is a well known optimum energy allocation algorithm for maximizing the sum rate with a total energy constraint in interference free channels firstly introduced by Claude Shannon in [Sha49].

The rate maximization waterfilling algorithm is illustrated graphically in Fig. 4.2. In the rate maximization waterfilling algorithm, the total useful energy $E_{\text{tot}} - \sigma_{\text{IAtx}}^2$ is poured on the top of the noise levels $(1 + \beta_{\text{IA}}^{(k)}) (\sigma_{\text{IAeff}}^{(k)})^2 / |h_{\text{IAeff}}^{(k,k)}|^2$, $k = 1, \dots, K$, till the water level E_{wlr} is reached. Accordingly, the less the noise level at a certain destination node k , the more energy $(1 + \beta_{\text{IA}}^{(k)}) E_{\text{opt}}^{(k)}$ is allocated for the k -th data symbol.

4.3 Energy allocation for multiple orthogonal resources in an interference alignment system

4.3.1 Motivation and problem statement

In this section, the case when the source nodes transmit to the destination nodes through N orthogonal resources is considered. In other words, each source node transmits simultaneously N uncorrelated data symbols to its corresponding destination node through N parallel channels. As discussed in Section 4.1, the effective channel in any resource between the source nodes and the destination nodes including the filters and the relays can be considered as an interference free channel after applying an IA solution. This idea can be extended to multiple orthogonal resource scenarios assuming the received noise signals of different resources being uncorrelated.

The achieved rate at the k -th destination node in the n -th resource is calculated as

$$c^{(k,n)} = \frac{1}{2} \text{ld} \left(1 + \gamma_{\text{IA}}^{(k,n)} \right). \quad (4.22)$$

Also, the achieved sum rate at the k -th destination node in all the resources is calculated as

$$C^{(k)} = \sum_{n=1}^N c^{(k,n)}. \quad (4.23)$$

After applying an IA algorithm simultaneously in every resource, the overall effective channel including the filters and the relays becomes an interference free channel so that the rate maximization waterfilling algorithm, introduced in the previous section, can be applied for maximizing the sum rate. To exploit the fact that the nodes and the relays can access multiple orthogonal resources simultaneously, the energy allocation is optimized aiming at maximizing the overall sum rate while maintaining equal individual rates achieved by each destination node. The energy allocation optimization problem aiming at maximizing the sum rate with a total energy constraint and a fairness constraint can be stated as

$$\left(\mathbf{E}_{\text{opt}}^{(1)}, \dots, \mathbf{E}_{\text{opt}}^{(K)}\right) = \arg \max_{\left(\mathbf{E}^{(1)}, \dots, \mathbf{E}^{(K)}\right)} \left\{ \sum_{k=1}^K C^{(k)} \right\} \quad (4.24)$$

subject to

$$\sum_{n=1}^N \left(\sum_{k=1}^K \left(1 + \beta_{\text{IA}}^{(k,n)}\right) E^{(k,n)} + \left(\sigma_{\text{IAtx}}^{(n)}\right)^2 \right) = E_{\text{tot}}, \quad (4.25)$$

$$C^{(k)} = \frac{1}{K} \sum_{k=1}^K C^{(k)}, \quad k = 1, \dots, K, \quad (4.26)$$

and

$$E^{(k,n)} \geq 0, \forall k, n. \quad (4.27)$$

The sum rate $\sum_{k=1}^K C^{(k)}$ when considered as a function of the allocated energies $E^{(k,n)}$ with $k = 1, \dots, K$ and $n = 1, \dots, N$ is a concave function. Furthermore, the total energy constraint of (4.25) is an affine set. But the fairness constraint of (4.26) is not a convex set. The fairness constraint of (4.26) forms a difference of two convex functions (DC) set [Tuy98]. Therefore, the optimization problem of (4.24)–(4.27) is non-convex. Rather than applying a DC programming tool which is computationally expensive for solving the optimization problem of (4.24)–(4.27), a problem decomposition among the node pairs is applied [AW10] as will be shown in the next section.

4.3.2 Fairness constrained maximum sum rate energy allocation

In this section, the optimization problem of (4.24)–(4.27) is analyzed and solved. Basically, it can be decomposed into a master problem and K subproblems. Each subproblem corresponds to a node pair. Basically, the k -th subproblem finds the energy allocation $\mathbf{E}_{\text{req}}^{(k)}$ for the k -th source node required to achieve a $\frac{1}{K}$ portion of the target sum rate C_{tar} , i.e., the total fairness constraint of (4.26) is implicitly satisfied by feeding

the subproblems with $\frac{1}{K}C_{\text{tar}}$. To find $\mathbf{E}_{\text{req}}^{(k)}$ at the k -th source node, an energy allocation optimization problem aiming at minimizing the total energy used for transmitting the N data symbols correspond to the k -th source node with a sum rate constraint per destination node is formulated as

$$\mathbf{E}_{\text{req}}^{(k)} = \arg \min_{\mathbf{E}^{(k)}} \left\{ \sum_{n=1}^N \left(1 + \beta_{\text{IA}}^{(k,n)} \right) E^{(k,n)} \right\} \quad (4.28)$$

subject to

$$\frac{1}{2} \sum_{n=1}^N \text{ld} \left(1 + E^{(k,n)} \frac{|h_{\text{IAeff}}^{(k,k,n)}|^2}{\left(\sigma_{\text{IAeff}}^{(k,n)} \right)^2} \right) = \frac{1}{K} C_{\text{tar}}, \quad (4.29)$$

and

$$E^{(k,n)} \geq 0, \forall n. \quad (4.30)$$

From (4.25), $\left(\sigma_{\text{IAtx}}^{(n)} \right)^2$ is not a function of the optimized variables $E^{(k,n)}$ for $n = 1, \dots, N$, $k = 1, \dots, K$ and thus, it is omitted from the objective function of (4.28). It can be observed that the optimization problem of (4.28)–(4.30) is the inverse problem of the optimization problem of (4.12)–(4.14) in the sense that this problem minimizes the total energy with a sum rate constraint whereas the one in (4.12)–(4.14) maximizes the sum rate with a total energy constraint. The objective function $\sum_{n=1}^N \left(1 + \beta_{\text{IA}}^{(k,n)} \right) E^{(k,n)}$ is linear and the sum rate constraint of (4.29) is a convex set. It can be noted that the optimum $\mathbf{E}_{\text{req}}^{(k)}$ can be always achieved for the constraint of (4.29) with equality because the objective function is linear. The Lagrange of the optimization problem of (4.28)–(4.30) is calculated as

$$\mathbf{L}(\mathbf{E}^{(k)}, \lambda) = \sum_{n=1}^N \left(1 + \beta_{\text{IA}}^{(k,n)} \right) E^{(k,n)} + \lambda \left(\frac{1}{2} \sum_{n=1}^N \text{ld} \left(1 + E^{(k,n)} \frac{|h_{\text{IAeff}}^{(k,k,n)}|^2}{\left(\sigma_{\text{IAeff}}^{(k,n)} \right)^2} \right) - \frac{1}{K} C_{\text{tar}} \right), \quad (4.31)$$

where λ denotes the Lagrangian multiplier. The two first order optimality conditions can be stated as

$$\frac{\partial \mathbf{L}}{\partial E^{(k,n)}} = \left(1 + \beta_{\text{IA}}^{(k,n)} \right) + \frac{\lambda}{2 \ln(2)} \frac{1}{\frac{\left(\sigma_{\text{IAeff}}^{(k,n)} \right)^2}{|h_{\text{IAeff}}^{(k,k,n)}|^2} + E^{(k,n)}} \stackrel{!}{=} 0 \quad (4.32)$$

and

$$\frac{\partial \mathbf{L}}{\partial \lambda} = \frac{1}{2} \sum_{n=1}^N \text{ld} \left(1 + E^{(k,n)} \frac{|h_{\text{IAeff}}^{(k,k,n)}|^2}{\left(\sigma_{\text{IAeff}}^{(k,n)} \right)^2} \right) - \frac{1}{K} C_{\text{tar}} \stackrel{!}{=} 0. \quad (4.33)$$

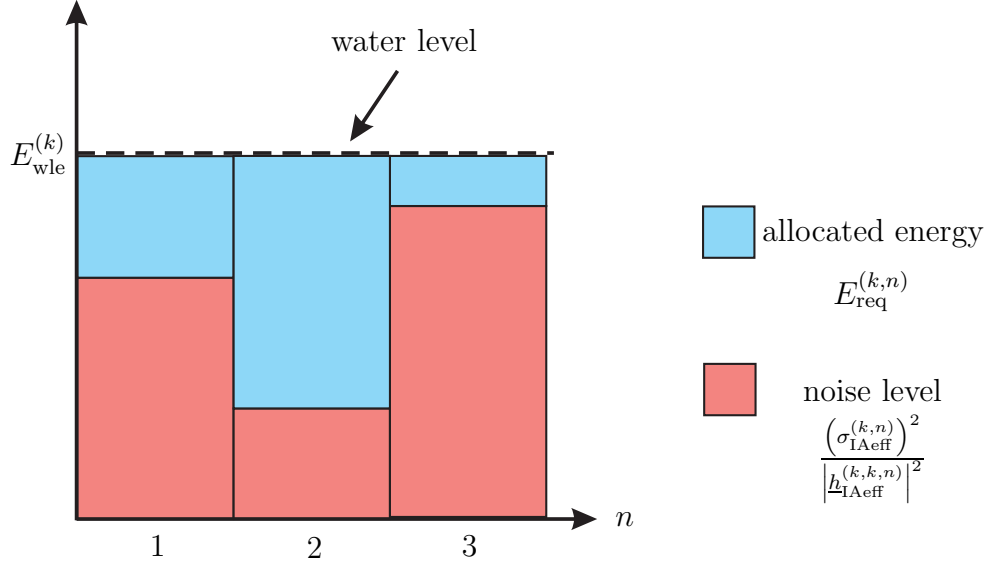


Fig. 4.3: Energy allocation for the k -th source node in its three resources using the energy minimization waterfilling algorithm.

Solving (4.32) for $E^{(k,n)}$ yields

$$E^{(k,n)} = \frac{-\lambda}{2\ln(2) \left(1 + \beta_{\text{IA}}^{(k,n)}\right)} - \frac{\left(\sigma_{\text{IAeff}}^{(k,n)}\right)^2}{\left|h_{\text{IAeff}}^{(k,k,n)}\right|^2}. \quad (4.34)$$

Substituting (4.34) in (4.33) yields

$$\frac{-\lambda}{2\ln(2) \left(1 + \beta_{\text{IA}}^{(k,n)}\right)} = 2^{\frac{2}{N^2 K} C_{\text{tar}} - \frac{1}{N} \sum_{n=1}^N \text{ld} \left(\frac{\left|h_{\text{IAeff}}^{(k,k,n)}\right|^2}{\left(\sigma_{\text{IAeff}}^{(k,n)}\right)^2} \right)}. \quad (4.35)$$

By substituting (4.35) in (4.34), the optimum energy allocation $E_{\text{req}}^{(k,n)}$ with $n = 1, \dots, N$ required to achieve $\frac{1}{K} C_{\text{tar}}$ is calculated for each resource n using an algorithm called the energy minimization waterfilling algorithm with

$$E_{\text{req}}^{(k,n)} = E_{\text{wle}}^{(k)} - \frac{\left(\sigma_{\text{IAeff}}^{(k,n)}\right)^2}{\left|h_{\text{IAeff}}^{(k,k,n)}\right|^2}, \quad n \in \Omega_{\text{WFe}}^{(k)}, \quad (4.36)$$

and the water level of the k -th node pair is calculated as

$$E_{\text{wle}}^{(k)} = 2^{\frac{2}{N^2 K} C_{\text{tar}} - \frac{1}{N'} \sum_{n \in \Omega_{\text{WFe}}^{(k)}} \text{ld} \left(\frac{\left|h_{\text{IAeff}}^{(k,k,n)}\right|^2}{\left(\sigma_{\text{IAeff}}^{(k,n)}\right)^2} \right)}, \quad (4.37)$$

where $\Omega_{\text{WFe}}^{(k)}$ is the set of the indices of the resources which contribute non-negative energy values $E_{\text{req}}^{(k,n)} \geq 0$ when considered in (4.36) and (4.37). Furthermore, N' denotes

the size of the set $\Omega_{\text{WFe}}^{(k)}$. The second term of (4.36) represents the noise level of each resource n . The energy minimization waterfilling algorithm intended to solve the k -th subproblem with three resources is illustrated in Fig. 4.3.

For the master problem, it basically aims at satisfying the total energy constraint of (4.25) given the required energy allocations from the individual subproblems. It can be noted that the rate maximization waterfilling algorithm and the energy minimization waterfilling algorithm are equivalent in the sense that for a certain optimum energy allocation the sum rate and corresponding to the total energy are the same for both algorithms. The structure of the maximum sum rate function is described by the following proposition.

Proposition 2. *For an interference-free channel, the maximum sum rate when considered as a function of the total energy constraint is a strictly monotonic increasing concave function.*

The proof is shown in Appendix B.2. Accordingly, the inverse function, the minimum total energy when considered as a function of the target sum rate, is a strictly monotonic increasing convex function [Bin83, Khu02]. With the optimum energy allocation, the function

$$g_{\text{con}}(C_{\text{tar}}) = \sum_{n=1}^N \left(\sum_{k=1}^K \left(1 + \beta_{\text{IA}}^{(k,n)} \right) E_{\text{req}}^{(k,n)} + \left(\sigma_{\text{IAtx}}^{(n)} \right)^2 \right) - E_{\text{tot}} \quad (4.38)$$

maps the target sum rate to the energy required or superfluous using the energy minimization waterfilling algorithm at each subproblem. Moreover, g_{con} is a strictly monotonic increasing function and it is either convex if $g_{\text{con}} \geq 0$ or concave if $g_{\text{con}} < 0$ as depicted in Fig. 4.4.

As shown in Fig. 4.4, the optimum sum rate C_{opt} is the root of the $g_{\text{con}}(C_{\text{tar}})$ function. Furthermore, the optimum sum rate C_{opt} is

- upper bounded by the sum rate C_{WFr} achieved using the rate maximization waterfilling algorithm over all resources and all node pairs $C_{\text{opt}} \leq C_{\text{WFr}}$, i.e., waterfilling does not consider the fairness constraint so it reaches the maximum sum rate of the channel, and
- lower bounded by zero as the sum rate is a non-negative real variable $C_{\text{opt}} \geq 0$.

A conventional numerical methods can be applied to find the root of the $g_{\text{con}}(C_{\text{tar}})$ function. Numerical methods such as the bisection method or Newton-Raphson method

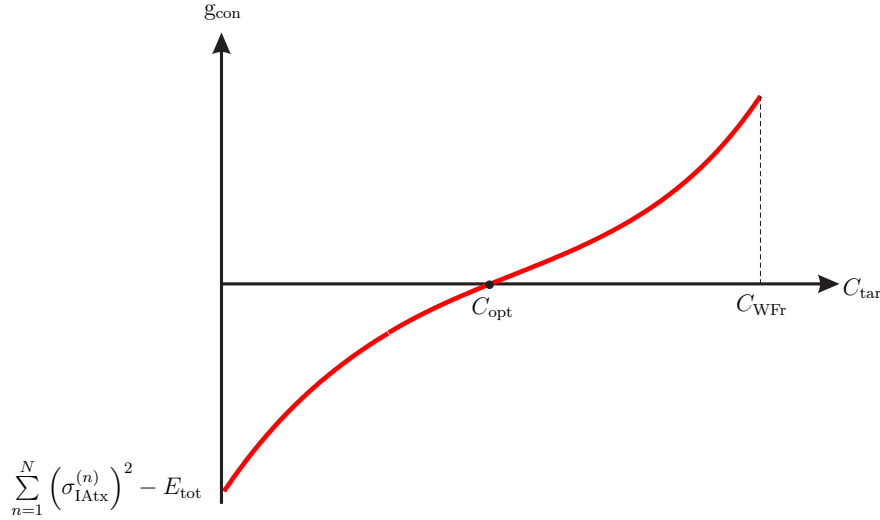


Fig. 4.4: A simple sketch of the function $g_{\text{con}}(C_{\text{tar}})$.

[JIJ07], are iterative methods. Accordingly, an iterative algorithm called the max-fair algorithm is proposed. In every iteration, a target sum rate is equally split among the K subproblems. Each subproblem applies the energy minimization waterfilling algorithm to find the optimum energy allocation required to achieve $\frac{1}{K}C_{\text{tar}}$ and feeds the result back to the master problem. Using the information feeded by the subproblems, the master problem moves a step forward towards the root of the function $g_{\text{con}}(C_{\text{tar}})$.

Concerning the convergence of the proposed max-fair algorithm, it is shown previously in this section that the subproblems are convex optimization problems and the $g_{\text{con}}(C_{\text{tar}})$ has a unique root. Therefore, a numerical method such as bisection or the Newton-Raphson can converge close to the root of $g_{\text{con}}(C_{\text{tar}})$. The convergence of the max-fair algorithm is based on the convergence of these numerical methods. The bisection method and the Newton-Raphson method guarantee convergence with a linear rate and a quadratic rate, respectively [JIJ07].

4.4 Complexity and performance of the energy allocation algorithms

4.4.1 Complexity analysis

In this section, the computational complexities of the energy allocation algorithms proposed in the previous sections are investigated. It is assumed that an IA solution is a

priori computed and the corresponding values of $\underline{h}_{\text{IAeff}}^{(k,k,n)}$, $\left(\sigma_{\text{IAeff}}^{(k,n)}\right)^2$, $\beta_{\text{IA}}^{(k,n)}$ and $\left(\sigma_{\text{IAtx}}^{(n)}\right)^2$ for $k = 1, \dots, K$ and $n = 1, \dots, N$ are given. Therefore, the complexity of computing the rate maximization waterfilling algorithm, the energy minimization waterfilling algorithm and the max-fair algorithm are required to be studied.

In general, the complexity of a waterfilling algorithm is dominated by the process of sorting the noise levels. For single resource systems, the complexity of the rate maximization waterfilling algorithm of (4.20) is $\mathcal{O}(K \log_{10}(K))$.

In the multiple orthogonal resources case $N > 1$, the complexity of applying the max-fair algorithm strongly depends on the complexity of the numerical methods which usually apply iterative methods. However, the complexity of each iteration is dominated by the complexity of computing the energy minimization waterfilling algorithm. In each iteration, the energy minimization waterfilling algorithm is applied individually for each of the K subproblems and thus, the complexity of an iteration is $\mathcal{O}(KN \log_{10}(N))$.

4.4.2 Performance analysis

In this section, the performances of the proposed energy allocation algorithms are analyzed and discussed. This section is separated into two parts. The performance of the single resource systems is discussed first. Then, performances of the systems with multiple resources are considered.

Firstly, the performance of applying the rate maximization waterfilling algorithm on the top of IA solutions for $N = 1$ is investigated. To this end, the same simulation setup used for analyzing the performance of the IA algorithms in Section 3.5.3 is considered. To show the gain of optimizing the energy allocation in the context of IA, Fig. 4.5 shows the average sum rates achieved by the IA algorithms with equal energy allocation and with optimum energy allocation. At high PSNRs, the amount of the available energy is relatively high as compared to the noise levels and thus, equal energy allocation reaches the optimum sum rates. Comparing the sum rates achieved by the IA algorithms with and without optimizing the energy allocations, it can be observed that they are not exactly the same at high PSNRs but they are close to each other. This happens because of the unconsidered energies of the useful signals retransmitted by the relays when applying the equal energy allocation. At low and moderate PSNRs, the noise levels are comparable to the allocated energies and thus, the rate maximization waterfilling algorithm outperforms the equal energy allocation especially for the IA with partially adapted filters. The main reason that the IA algorithm with fixed filters

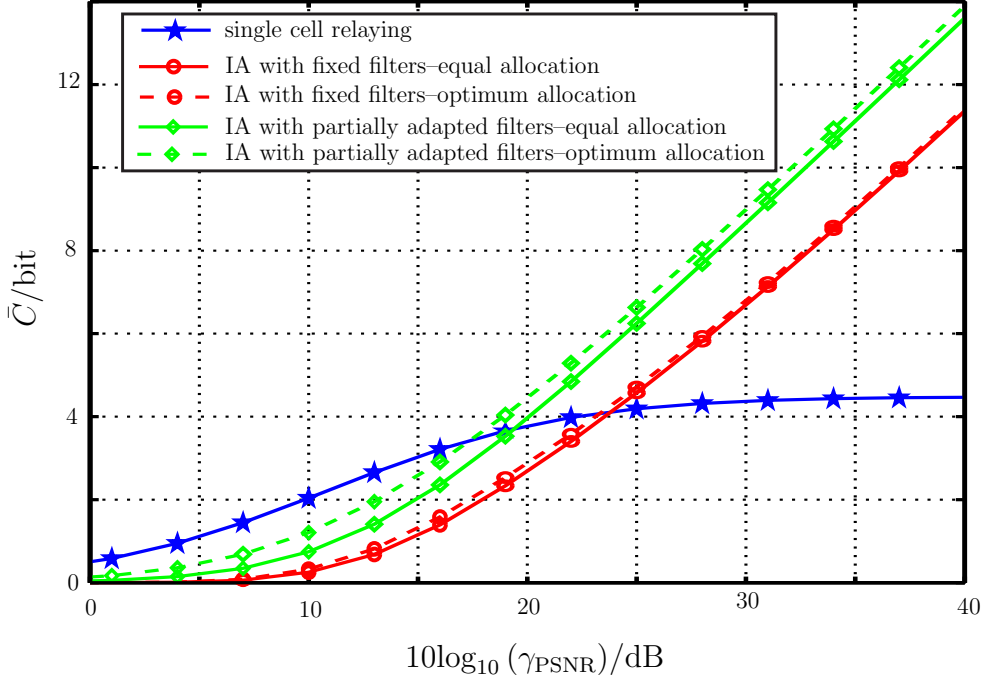


Fig. 4.5: Achieved sum rate as a function of PSNR for a scenario with $K = 3$, $R = 3$ and $M = 2$.

does not benefit from optimizing the transmitted energies is that it minimizes the total energy retransmitted by the relays including the limited retransmitted noise energy. This limited noise energy retransmitted by the relays dominates the received noises at the destination nodes. As Fig. 4.5 shows the average results over many channel realizations and because the average channel gains between the relays and different destination nodes are the same, the noise levels of different node pairs are comparable. As a result, waterfilling uses almost equal energies for transmitting the different data symbols.

Secondly, the performance of applying the max-fair algorithm on the top of the IA solution for $N > 1$ is investigated. For finding an IA solution in each resource, the homogeneous system of linear equations of (3.36) with partially adapted filters is considered. An IA solution is randomly picked. In the first step, the total energy constraint is equally split among the resources. For each resource, the picked IA solution is scaled to satisfy the energy constraint of the resource. In the second step, different energy allocation algorithms are applied to the effective channel including the filters and the relays.

Some conventional energy allocation algorithms are considered as benchmarks. Firstly, the rate maximization waterfilling algorithm proposed in Section 4.2 which allocates the energies over all resources at all nodes is considered. Secondly, the equal SNR

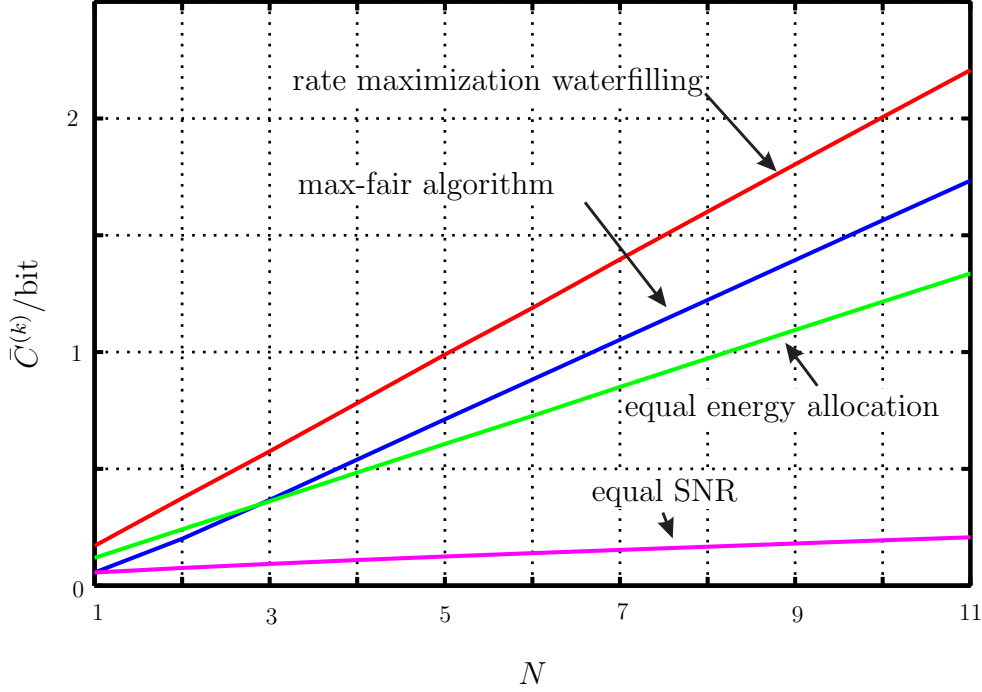


Fig. 4.6: Achieved sum rate at the k -th destination node as a function of the number of resources N for a scenario with $K = 3$, $R = 3$ and $M = 2$.

algorithm which equalizes the SNRs

$$\gamma^{(k,n)} = E^{(k,n)} \frac{|h_{\text{IAeff}}^{(k,k,n)}|^2}{\left(\sigma_{\text{IAeff}}^{(k,n)}\right)^2} = \gamma_{\text{eSNR}} \quad (4.39)$$

achieved at every destination node k in every resource n is considered. The last benchmark is the equal energy allocation which uses equal energies for transmitting all the KN data symbols

$$\left(1 + \beta_{\text{IA}}^{(k,n)}\right) E^{(k,n)} = \frac{E_{\text{tot}} - \sigma_{\text{IAtx}}^2}{KN}. \quad (4.40)$$

It is to be noted from (4.40) that the equal energy allocation algorithm takes into account the part of useful energy $\beta_{\text{IA}}^{(k,n)} E^{(k,n)}$ for $k = 1, \dots, K$, $n = 1, \dots, N$ retransmitted by the relays.

For a frequency selective channel, a scenario with $K = 3$, $R = 3$ and $M = 2$ is considered. Assuming the average PSNR per resource to be 10 dB, the average achieved sum rate $\bar{C}^{(k)}$ at the k -th destination node as a function of the number N of employed resources is shown in Fig. 4.6. It shows that the rate maximization waterfilling algorithm upper bounds the achieved rates for any number N of resources. The equal energy allocation achieves an average sum rates closes to the one achieved by the waterfilling if $N = 1$, i.e., equal energy allocation is the optimum at high PSNRs if IA is a priori

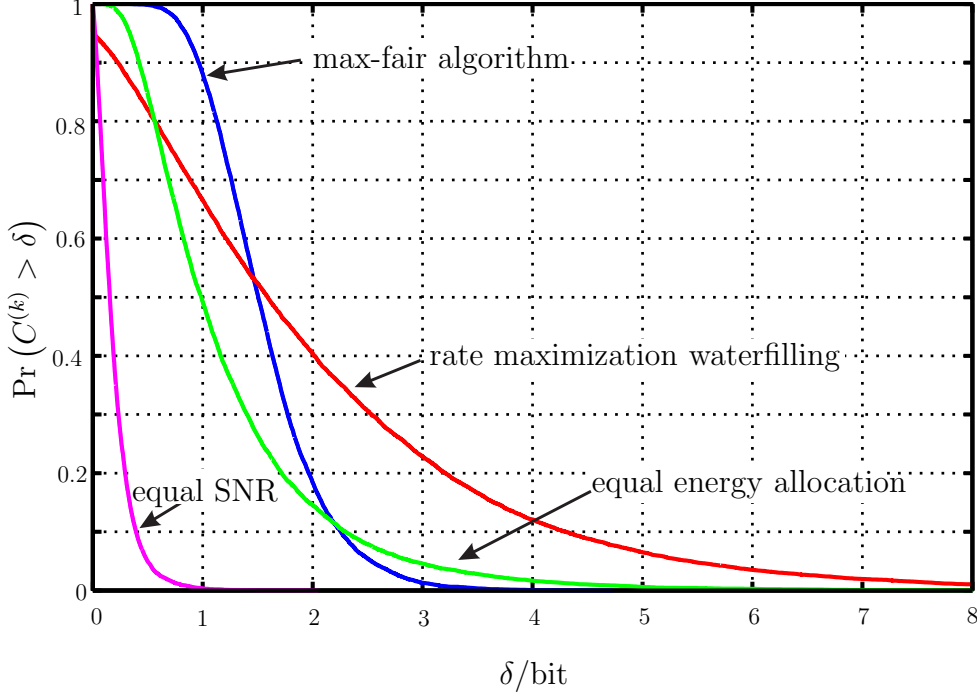


Fig. 4.7: CCDF of a destination node achieved sum rate for a scenario with $K = 3$, $R = 3$, $M = 2$ and $N = 10$.

applied. At $N > 1$, the equal energy allocation diverges from the maximum. The equal SNR algorithm always results in low sum rates per destination node as it aims at equalizing the rates among every resource of each destination node rather than equalizing the sum rate achieved by the individual destination nodes. Finally, the max-fair algorithm achieves the same rates as the equal SNR algorithm if $N = 1$ because it has no freedom to maximize the sum rate. For $N > 1$, the max-fair algorithm has a freedom to maximize the sum rate while maintaining equal sum rates per node pair. So, it outperforms the equal energy allocation when $N > 3$. Furthermore, it can be observed by comparing the achieved sum rates of the waterfilling and the max-fair algorithms in Fig. 4.6 that the slope of sum rate curve of the max-fair algorithm is smaller than the one of the waterfilling which can be translated as a price of fairness.

For the same setup with $N = 10$, the complementary cumulative distribution function (CCDF) of the sum rate per destination node is evaluated as shown in Fig. 4.7. Let

$$P_{\text{out}} = \Pr(C^{(k)} < C_{\text{out}}) \quad (4.41)$$

be the outage probability or the probability that the k -th destination node cannot correctly decode the received data symbol. Based on the definition of the outage probability, the outage capacity C_{out} is defined as the minimum sum rate per destination node achieved from the correctly received data symbols. Assuming an outage probability of $P_{\text{out}} = 0.1$, i.e., the usual assumption for the current communications systems,

the max-fair algorithm achieves the highest outage capacity of $C_{\text{out}} = 0.96$ bits and outperforms the waterfilling algorithm by 77%. It can be noted that at $P_{\text{out}} \leq 0.05$, the waterfilling algorithm achieves zero outage capacity. This is because of the fact that waterfilling does not serve node pairs with noise levels exceeding the water level.

Chapter 5

Interference mitigation

5.1 Preliminaries

Chapter 3 focused on the IA algorithms which fully cancel the interferences at the output of the receive filter of every destination node. In this chapter, algorithms which mitigate the interferences rather than cancel them are developed and investigated. As described in Section 1.2, IA is basically aiming at maximizing the DoFs of an interference network where the DoFs are defined at infinite SNRs. As a result, the IA algorithms achieve significantly high sum rates only at high SNRs as has been shown in Fig. 3.2.

In practice, energy is limited and most of the wireless systems operate at low or moderate SNR regimes. In these regimes, noise reduction is essential in addition to the interference reduction. Because the relays perform amplify and forward relaying, the noise signals, in addition to the useful signals, received at the relays are amplified and retransmitted to the destination nodes. This retransmission of the noise signals definitely affects the system performance especially at low and moderate SNR regimes. From the information theory perspective, treating interference as noise achieves the sum capacity of the Gaussian interference channels in the weak interference case [MK09, SKC09, AV09]. Following this principle, it can be concluded that keeping some weak unaligned interferences at the output of the receive filter of each destination node considered as noise would not harm the performance of the system. In some cases, it even leads to higher sum rates than the ones achieved using the IA algorithms especially at low SNRs.

This chapter concentrates on developing some interference mitigation (IM) algorithms which:

- unlike the IA algorithms, aim at achieving high performance at all SNRs.
- are able to balance between the noise reduction and the interference reduction. Accordingly, they can achieve a high sum rates at both low SNRs where the noise is dominant and at high SNRs where the interference is dominant.

- increase the powers of the received useful signals obtained at the output of the receive filters of every destination node in such a way that the individual SINRs at the destination nodes are increased.
- support any number of relays and relay antennas as IA is not required in these algorithms.
- require a reasonably low computational complexity.

Similar to the structure of Chapter 3, the contributions in this chapter are elaborated fundamentally in two sections. Section 5.2 proposes an IM algorithm assuming fixed transmit and receive filters. Section 5.3 proposes two IM algorithms assuming partially adapted transmit and receive filters.

5.2 Interference mitigation with fixed transmit and receive filters

In this section, an IM algorithm which reduces the total interference in the system is developed. Similar to Section 3.3, fixed transmit and receive filters are assumed and just the processing matrices of the relays are adapted to the channel aiming at mitigating the interferences. As discussed in Section 3.3.2, IA is feasible if the number of relays and relay antennas satisfies $M^2R \geq K(K-1)$, see (3.17). For a certain number M of antennas at the relays, it can be noted that the number R of required relays grows quadratically with the number K of node pairs which limits the practicality of the proposed IA algorithms in large networks. If the inequality of (3.17) does not hold which means

$$M^2R < K(K-1), \quad (5.1)$$

the system of linear equations of (3.15) has no solution and thus, IA is not feasible anymore. However, the few relays which are not enough to perform IA can be exploited for reducing the interferences rather than nullifying them. As a result, the system treats the remaining unaligned interferences as noise. The sum of the gains of all the effective interference links can be written as

$$\sum_{k=1}^K \sum_{l \neq k} \left| \underline{\mathbf{u}}^{(k)*T} \underline{\mathbf{H}}^{(k,l)} \underline{\mathbf{v}}^{(l)} \right|^2 = \left\| \underline{\mathbf{H}}_{\text{ff}} \underline{\mathbf{x}} + \underline{\mathbf{p}} \right\|^2, \quad (5.2)$$

where $\underline{\mathbf{H}}_{\text{ff}}$, $\underline{\mathbf{p}}$ and $\underline{\mathbf{x}}$ are introduced in Section 3.3.1. Every element in $\underline{\mathbf{H}}_{\text{ff}} \underline{\mathbf{x}}$ represents the effective interference link between a source node and a non-corresponding destination

node through the relays. Moreover, every element in $\underline{\mathbf{p}}$ represents the effective direct interference link between a source node and a non-corresponding destination node. To nullify the effective interference link between the l -th source node and the k -th destination node with $l \neq k$, the relay processing matrices are adapted such that at the k -th destination node, the interference received from the l -th source node through the relays is compensated by the one received directly from the l -th source node. If there are enough relays, all the effective interference links can be nullified as described in Section 3.3. If there are not enough relays, an approximate solution is found using the unconstrained optimization problem

$$\underline{\mathbf{x}}_{\text{IM}} = \arg \min_{\underline{\mathbf{x}}} \left\{ \|\underline{\mathbf{H}}_{\text{ff}} \underline{\mathbf{x}} + \underline{\mathbf{p}}\|^2 \right\}. \quad (5.3)$$

Because $\underline{\mathbf{H}}_{\text{ff}}^{*\text{T}} \underline{\mathbf{H}}_{\text{ff}}$ is a symmetric positive semidefinite matrix, the objective function of (5.2) is a convex quadratic function of $\underline{\mathbf{x}}$. Therefore, the optimization problem of (5.3) is convex. If the inequality of (5.1) holds, an approximate solution to the system of linear equations of (3.15) can be found by solving the optimization problem of (5.3) using the least squares method [AGKW12b] which results in

$$\underline{\mathbf{x}}_{\text{IM}} = -\underline{\mathbf{H}}_{\text{ff}}^+ \underline{\mathbf{p}}, \quad (5.4)$$

where

$$\underline{\mathbf{H}}_{\text{ff}}^+ = (\underline{\mathbf{H}}_{\text{ff}}^{*\text{T}} \underline{\mathbf{H}}_{\text{ff}})^{-1} \underline{\mathbf{H}}_{\text{ff}}^{*\text{T}} \quad (5.5)$$

denotes the left pseudo inverse of the matrix $\underline{\mathbf{H}}_{\text{ff}}$.

From the linear algebra perspective, the inhomogeneous system of linear equations of (3.15) can be characterized as follows:

- If there are enough relays and relay antennas for achieving IA, i.e., $M^2 R \geq K(K-1)$, $\underline{\mathbf{p}}$ is in the column space of $\underline{\mathbf{H}}_{\text{ff}}$ and the solution $\underline{\mathbf{x}}_{\text{IA}}$ is in the row space of $\underline{\mathbf{H}}_{\text{ff}}$.
- If there are not enough relays and relay antennas for achieving IA, i.e., $M^2 R < K(K-1)$, $\underline{\mathbf{p}}$ is not in the column space of $\underline{\mathbf{H}}_{\text{ff}}$ and there is no solution $\underline{\mathbf{x}}_{\text{IA}}$. An approximate solution $\underline{\mathbf{x}}_{\text{IM}}$ is found using the least squares method which is found by projecting $\underline{\mathbf{p}}$ onto the column space of $\underline{\mathbf{H}}_{\text{ff}}$. Accordingly, the approximate solution $\underline{\mathbf{x}}_{\text{IM}}$ is in the row space of $\underline{\mathbf{H}}_{\text{ff}}$. For a scenario with $K = 2$, $R = 1$ and $M = 1$, Fig. 5.1 illustrates the projection of the vector $-\underline{\mathbf{p}}$ onto the column space of $\underline{\mathbf{H}}_{\text{ff}}$.

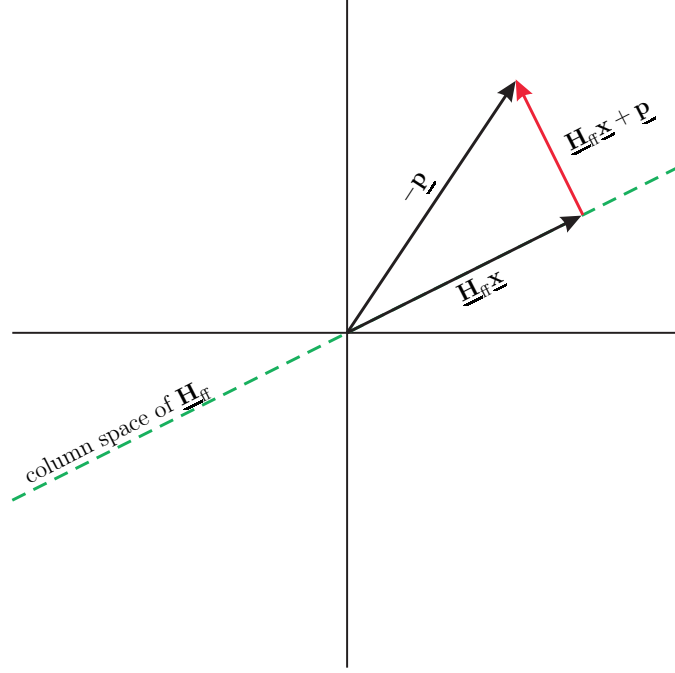


Fig. 5.1: Projecting the effective direct interference vector $-\underline{\mathbf{p}}$ into the column space of the $\underline{\mathbf{H}}_{\text{ff}}$ for a scenario with $K = 2$, $R = 1$ and $M = 1$.

5.3 Interference mitigation with partially adapted transmit and receive filters

5.3.1 Energy constrained minimum sum mean square error

5.3.1.1 Problem statement

In this section, an IM algorithm aiming at minimizing the sum MSE with a total energy constraint is developed. As described in Section 3.4.3, the estimated data $\hat{\underline{\mathbf{d}}}^{(k)}$ at a destination node k is a linear function of the unknown vector $\underline{\mathbf{y}}$ if the filters are partially adapted, see (3.40). As a result, the sum MSE described in (3.44) when considered as a function of $\underline{\mathbf{y}}$ is a convex quadratic function [ALG⁺13a]. With a total energy constraint, the sum MSE minimization problem can be stated as

$$\underline{\mathbf{y}}_{\text{MSE}} = \arg \min_{\underline{\mathbf{y}}} \{ \underline{\mathbf{y}}^{*\text{T}} \underline{\mathbf{A}} \underline{\mathbf{y}} - \underline{\mathbf{b}}^{*\text{T}} \underline{\mathbf{y}} - \underline{\mathbf{y}}^{*\text{T}} \underline{\mathbf{b}} \} \quad (5.6)$$

subject to

$$\underline{\mathbf{y}}^{*\text{T}} \begin{pmatrix} \underline{\Phi}' & \mathbf{0}_{M^2 R \times K} & \mathbf{0}_{M^2 R \times K} \\ \mathbf{0}_{K \times M^2 R} & E_{\text{d}} \mathbf{I}_K & \mathbf{0}_{K \times K} \\ \mathbf{0}_{K \times M^2 R} & \mathbf{0}_{K \times K} & \mathbf{0}_{K \times K} \end{pmatrix} \underline{\mathbf{y}} \leq E_{\text{tot}}^{(2)}, \quad (5.7)$$

where $\underline{\mathbf{A}}$ and $\underline{\mathbf{b}}$ are defined in Section 3.4.3. $\underline{\Phi}'$ is a block diagonal matrix with R diagonal blocks where the r -th diagonal block is calculated as $\mathbf{I}_M \otimes \underline{\mathbf{C}}_{\text{TR}}^{(r)}$. Because the transmit filter coefficients $\underline{v}^{(l,1)}$, $l = 1, \dots, K$ in the first time slot are fixed, the energy allocation in the first time slot is predetermined and hence, the total energy $E_{\text{tot}}^{(1)}$ transmitted in the first time slot is fixed. The remaining energy $E_{\text{tot}}^{(2)}$ will be allocated to the source nodes and to the relays in the second time slot by the constraint of (5.7). Concerning the optimization problem of (5.6)–(5.7), the objective function $\underline{\mathbf{y}}^{*\text{T}} \underline{\mathbf{A}} \underline{\mathbf{y}} - \underline{\mathbf{b}}^{*\text{T}} \underline{\mathbf{y}} - \underline{\mathbf{y}}^{*\text{T}} \underline{\mathbf{b}}$ is a convex quadratic function and the constraint of (5.7) is a convex quadratic set. As a result, the optimization problem of (5.6)–(5.7) is convex.

To solve the optimization problem of (5.6)–(5.7), the minimum of the sum MSE function without considering the constraint of (5.7) can be found first. Taking the general derivative of $\underline{\mathbf{y}}^{*\text{T}} \underline{\mathbf{A}} \underline{\mathbf{y}} - \underline{\mathbf{b}}^{*\text{T}} \underline{\mathbf{y}} - \underline{\mathbf{y}}^{*\text{T}} \underline{\mathbf{b}}$ over $\underline{\mathbf{y}}$ and setting the result to zero yields

$$\underline{\mathbf{A}}^{*\text{T}} \underline{\mathbf{y}} - \underline{\mathbf{b}} \stackrel{!}{=} \mathbf{0}. \quad (5.8)$$

Then, the unknown vector which yields the minimum sum MSE with no constraints is calculated as

$$\underline{\mathbf{y}}_{\text{uncon}} = (\underline{\mathbf{A}}^{*\text{T}})^{-1} \underline{\mathbf{b}}. \quad (5.9)$$

Two cases have to be distinguished:

- If the total energy constraint of (5.7) is satisfied by plugging in $\underline{\mathbf{y}}_{\text{uncon}}$, then $\underline{\mathbf{y}}_{\text{uncon}}$ is the optimum unknown vector for the constrained optimization problem of (5.6)–(5.7) as well.
- If the total energy constraint of (5.7) is not satisfied by plugging in $\underline{\mathbf{y}}_{\text{uncon}}$, then the optimization problem of (5.6)–(5.7) has to be solved considering the constraint of (5.7) with equality.

5.3.1.2 Quadratically constrained quadratic minimization problem

In this section, the optimization problem of (5.6)–(5.7) is studied and solved. The total energy constraint of (5.7) covers just the first $M^2R + K$ elements of $\underline{\mathbf{y}}$ related to the coefficients of the relay processing matrices and the coefficients of the transmit filters $\underline{v}^{(l,2)}$, $k = 1, \dots, K$ in the second time slot. Accordingly, the unknown vector $\underline{\mathbf{y}}$ can be split up into two vectors as

$$\underline{\mathbf{y}} = \left(\begin{array}{c} \underline{\mathbf{y}}_1 \\ \underline{\mathbf{y}}_2 \end{array} \right) \left. \vphantom{\begin{array}{c} \underline{\mathbf{y}}_1 \\ \underline{\mathbf{y}}_2 \end{array}} \right\} \begin{array}{l} M^2R+K \\ K \end{array}. \quad (5.10)$$

Similarly, $\underline{\mathbf{b}}$ is split up as

$$\underline{\mathbf{b}} = \left(\begin{array}{c} \underline{\mathbf{b}}_1 \\ \underline{\mathbf{b}}_2 \end{array} \right) \left. \vphantom{\begin{array}{c} \underline{\mathbf{b}}_1 \\ \underline{\mathbf{b}}_2 \end{array}} \right\} \begin{array}{l} M^2R+K \\ K \end{array}. \quad (5.11)$$

Moreover, the matrix $\underline{\mathbf{A}}$ is accordingly split up to four blocks $\underline{\mathbf{A}}_{11}$, $\underline{\mathbf{A}}_{12}$, $\underline{\mathbf{A}}_{21}$ and $\underline{\mathbf{A}}_{22}$ as

$$\underline{\mathbf{A}} = \left(\begin{array}{cc} \overbrace{\underline{\mathbf{A}}_{11}}^{M^2R+K} & \overbrace{\underline{\mathbf{A}}_{12}}^K \\ \underline{\mathbf{A}}_{21} & \underline{\mathbf{A}}_{22} \end{array} \right) \left. \vphantom{\begin{array}{cc} \underline{\mathbf{A}}_{11} & \underline{\mathbf{A}}_{12} \\ \underline{\mathbf{A}}_{21} & \underline{\mathbf{A}}_{22} \end{array}} \right\} \begin{array}{l} M^2R+K \\ K \end{array}. \quad (5.12)$$

From (5.10), the constraint of (5.7) can be rewritten as

$$\underline{\mathbf{y}}_1^{*\text{T}} \left(\begin{array}{cc} \underline{\Phi}' & \mathbf{0}_{M^2R \times K} \\ \mathbf{0}_{K \times M^2R} & E_d \mathbf{I}_K \end{array} \right) \underline{\mathbf{y}}_1 = E_{\text{tot}}^{(2)}. \quad (5.13)$$

The constraint of (5.13) forms a $M^2R + K$ dimensional ellipsoid. To simplify the optimization problem of (5.6)–(5.7), the constraint of (5.13) will be reformulated as a $M^2R + K$ dimensional sphere by decomposing the covariance matrix

$$\left(\begin{array}{cc} \underline{\Phi}' & \mathbf{0}_{M^2R \times K} \\ \mathbf{0}_{K \times M^2R} & E_d \mathbf{I}_K \end{array} \right) \quad (5.14)$$

using Cholesky factorization [TB97] into $\underline{\mathbf{T}} \underline{\mathbf{T}}^{*\text{T}}$, where $\underline{\mathbf{T}}$ is a lower triangular matrix. Because the covariance matrix of (5.14) is positive definite, $\underline{\mathbf{T}}$ is unique and invertible, i.e., $\underline{\Phi}'$ is a positive definite matrix because $\underline{\mathbf{C}}_{\text{tr}}^{(r)}$ is a positive definite matrix as described in (2.14). Then, the constraint of (5.13) can be written as an $M^2R + K$ dimensional sphere as

$$\underline{\mathbf{j}}^{*\text{T}} \underline{\mathbf{j}} = E_{\text{tot}}^{(2)}, \quad (5.15)$$

where

$$\underline{\mathbf{j}} = \underline{\mathbf{T}}^{*\text{T}} \underline{\mathbf{y}}_1. \quad (5.16)$$

By substituting $\underline{\mathbf{j}}$ in the optimization problem of (5.6)–(5.7), the Lagrange can be written as

$$\begin{aligned} \text{L} \left(\left(\begin{array}{c} \underline{\mathbf{j}} \\ \underline{\mathbf{y}}_2 \end{array} \right), \lambda \right) &= \left(\underline{\mathbf{j}}^{*\text{T}} \quad \underline{\mathbf{y}}_2^{*\text{T}} \right) \left(\begin{array}{cc} \underline{\mathbf{T}}^{-1} \underline{\mathbf{A}}_{11} (\underline{\mathbf{T}}^{*\text{T}})^{-1} & \underline{\mathbf{T}}^{-1} \underline{\mathbf{A}}_{12} \\ \underline{\mathbf{A}}_{21} (\underline{\mathbf{T}}^{*\text{T}})^{-1} & \underline{\mathbf{A}}_{22} \end{array} \right) \left(\begin{array}{c} \underline{\mathbf{j}} \\ \underline{\mathbf{y}}_2 \end{array} \right) \\ &\quad - \left(\underline{\mathbf{b}}_1^{*\text{T}} (\underline{\mathbf{T}}^{*\text{T}})^{-1} \quad \underline{\mathbf{b}}_2^{*\text{T}} \right) \left(\begin{array}{c} \underline{\mathbf{j}} \\ \underline{\mathbf{y}}_2 \end{array} \right) - \left(\underline{\mathbf{j}}^{*\text{T}} \quad \underline{\mathbf{y}}_2^{*\text{T}} \right) \left(\begin{array}{c} \underline{\mathbf{T}}^{-1} \underline{\mathbf{b}}_1 \\ \underline{\mathbf{b}}_2 \end{array} \right) \\ &\quad + \lambda \left(\underline{\mathbf{j}}^{*\text{T}} \underline{\mathbf{j}} - E_{\text{tot}}^{(2)} \right), \end{aligned} \quad (5.17)$$

where λ denotes the Lagrangian multiplier. Both the sum MSE of (3.44) and the total energy constraint of (5.15) are real functions and hence, λ is a real variable [BV04]. The first order optimality conditions are found by taking the general derivative of (5.17) with respect to $(\underline{\mathbf{j}}^T, \underline{\mathbf{y}}_2^T)^T$ and λ as follows

$$\begin{aligned} \frac{\partial L}{\partial \begin{pmatrix} \underline{\mathbf{j}} \\ \underline{\mathbf{y}}_2 \end{pmatrix}} &= \begin{pmatrix} (\underline{\mathbf{T}}^*)^{-1} \underline{\mathbf{A}}_{11}^T (\underline{\mathbf{T}}^T)^{-1} & (\underline{\mathbf{T}}^*)^{-1} \underline{\mathbf{A}}_{21}^T \\ \underline{\mathbf{A}}_{12}^T (\underline{\mathbf{T}}^T)^{-1} & \underline{\mathbf{A}}_{22}^T \end{pmatrix} \begin{pmatrix} \underline{\mathbf{j}}^* \\ \underline{\mathbf{y}}_2^* \end{pmatrix} \\ &\quad - \begin{pmatrix} (\underline{\mathbf{T}}^*)^{-1} \underline{\mathbf{b}}_1^* \\ \underline{\mathbf{b}}_2^* \end{pmatrix} + \lambda \begin{pmatrix} \underline{\mathbf{j}}^* \\ \mathbf{0} \end{pmatrix} \stackrel{!}{=} \mathbf{0} \end{aligned} \quad (5.18)$$

and

$$\underline{\mathbf{j}}^{*T} \underline{\mathbf{j}} - E_{\text{tot}}^{(2)} \stackrel{!}{=} 0, \quad (5.19)$$

respectively. Solving (5.18) for $(\underline{\mathbf{j}}^T, \underline{\mathbf{y}}_2^T)^T$ yields

$$\begin{pmatrix} \underline{\mathbf{j}} \\ \underline{\mathbf{y}}_2 \end{pmatrix} = \begin{pmatrix} \underline{\mathbf{T}}^{-1} \underline{\mathbf{A}}_{11}^{*T} (\underline{\mathbf{T}}^{*T})^{-1} + \lambda \mathbf{I}_{M^2 R + K} & (\underline{\mathbf{T}}^{*T})^{-1} \underline{\mathbf{A}}_{21}^{*T} \\ \underline{\mathbf{A}}_{12}^{*T} (\underline{\mathbf{T}}^{*T})^{-1} & \underline{\mathbf{A}}_{22}^{*T} \end{pmatrix}^{-1} \begin{pmatrix} \underline{\mathbf{T}}^{-1} \underline{\mathbf{b}}_1 \\ \underline{\mathbf{b}}_2 \end{pmatrix}, \quad (5.20)$$

where the Lagrangian multiplier λ has to be adapted for satisfying the total energy constraint of (5.19). In (5.18), two equalities are represented which can be explicitly written as

$$\underline{\mathbf{T}}^{-1} \underline{\mathbf{A}}_{11}^{*T} (\underline{\mathbf{T}}^{*T})^{-1} \underline{\mathbf{j}} + \underline{\mathbf{T}}^{-1} \underline{\mathbf{A}}_{21}^{*T} \underline{\mathbf{y}}_2 - \underline{\mathbf{T}}^{-1} \underline{\mathbf{b}}_1 + \lambda \underline{\mathbf{j}} = \mathbf{0} \quad (5.21)$$

and

$$\underline{\mathbf{A}}_{12}^{*T} (\underline{\mathbf{T}}^{*T})^{-1} \underline{\mathbf{j}} + \underline{\mathbf{A}}_{22}^{*T} \underline{\mathbf{y}}_2 - \underline{\mathbf{b}}_2 = \mathbf{0}. \quad (5.22)$$

Solving (5.22) for $\underline{\mathbf{y}}_2$ and substituting the result in (5.21) yields

$$\begin{aligned} \underline{\mathbf{T}}^{-1} \underline{\mathbf{A}}_{11}^{*T} (\underline{\mathbf{T}}^{*T})^{-1} \underline{\mathbf{j}} - \underline{\mathbf{T}}^{-1} \underline{\mathbf{A}}_{21}^{*T} (\underline{\mathbf{A}}_{22}^{*T})^{-1} \underline{\mathbf{A}}_{12}^{*T} (\underline{\mathbf{T}}^{*T})^{-1} \underline{\mathbf{j}} \\ + \underline{\mathbf{T}}^{-1} \underline{\mathbf{A}}_{21}^{*T} (\underline{\mathbf{A}}_{22}^{*T})^{-1} \underline{\mathbf{b}}_2 - \underline{\mathbf{T}}^{-1} \underline{\mathbf{b}}_1 + \lambda \underline{\mathbf{j}} = \mathbf{0}. \end{aligned} \quad (5.23)$$

Note that (5.23) is an equation with only $\underline{\mathbf{j}}$ as a vector of unknowns, i.e., $\underline{\mathbf{y}}_2$ satisfies the first order optimality condition of (5.18). Let

$$\underline{\mathbf{A}}' = \underline{\mathbf{T}}^{-1} \left(\underline{\mathbf{A}}_{11}^{*T} - \underline{\mathbf{A}}_{21}^{*T} (\underline{\mathbf{A}}_{22}^{*T})^{-1} \underline{\mathbf{A}}_{12}^{*T} \right) (\underline{\mathbf{T}}^{*T})^{-1} \quad (5.24)$$

and

$$\underline{\mathbf{b}}' = \underline{\mathbf{T}}^{-1} \left(\underline{\mathbf{b}}_1 - \underline{\mathbf{A}}_{21}^{*T} (\underline{\mathbf{A}}_{22}^{*T})^{-1} \underline{\mathbf{b}}_2 \right). \quad (5.25)$$

Then, (5.23) can be written in short as

$$(\underline{\mathbf{A}}' + \lambda \mathbf{I}_{M^2R+K}) \underline{\mathbf{j}} - \underline{\mathbf{b}}' = \mathbf{0}. \quad (5.26)$$

Using the Eigenvalue decomposition, the matrix $\underline{\mathbf{A}}'$ can be decomposed as

$$\underline{\mathbf{A}}' = \underline{\mathbf{Q}} \underline{\mathbf{\Lambda}} \underline{\mathbf{Q}}^{-1}, \quad (5.27)$$

where $\underline{\mathbf{\Lambda}}$ is a $(M^2R + K) \times (M^2R + K)$ diagonal matrix with the eigenvalues $\rho^{(1)}, \dots, \rho^{(M^2R+K)}$ of $\underline{\mathbf{A}}'$ at the main diagonal. Moreover, $\underline{\mathbf{Q}}$ is a $(M^2R + K) \times (M^2R + K)$ matrix where the i -th column is the eigenvector of $\underline{\mathbf{A}}'$ corresponding to the i -th eigenvalue $\rho^{(i)}$. Using (5.27), it follows

$$(\underline{\mathbf{A}}' + \lambda \mathbf{I}_{M^2R+K})^{-1} = (\underline{\mathbf{Q}} \underline{\mathbf{\Lambda}} \underline{\mathbf{Q}}^{-1} + \lambda \mathbf{I}_{M^2R+K})^{-1}. \quad (5.28)$$

Using the Woodbury matrix inversion lemma of (A.15), (5.28) can be simplified as

$$(\underline{\mathbf{Q}} \underline{\mathbf{\Lambda}} \underline{\mathbf{Q}}^{-1} + \lambda \mathbf{I}_{M^2R+K})^{-1} = \frac{1}{\lambda} \underline{\mathbf{Q}} \left(\mathbf{I}_{M^2R+K} - (\lambda \underline{\mathbf{\Lambda}}^{-1} + \mathbf{I}_{M^2R+K})^{-1} \right) \underline{\mathbf{Q}}^{-1}. \quad (5.29)$$

Substituting (5.29) in (5.26) yields

$$\underline{\mathbf{j}} = \frac{1}{\lambda} \underline{\mathbf{Q}} \left(\mathbf{I}_{M^2R+K} - (\lambda \underline{\mathbf{\Lambda}}^{-1} + \mathbf{I}_{M^2R+K})^{-1} \right) \underline{\mathbf{Q}}^{-1} \underline{\mathbf{b}}'. \quad (5.30)$$

To find λ which satisfies the total energy constraint, (5.30) is substituted in (5.15) as

$$\frac{1}{\lambda^2} \underline{\mathbf{t}}^{*\text{T}} \left(\mathbf{I}_{M^2R+K} - (\lambda \underline{\mathbf{\Lambda}}^{-1} + \mathbf{I}_{M^2R+K})^{-1} \right)^2 \underline{\mathbf{t}} = E_{\text{tot}}^{(2)}, \quad (5.31)$$

where

$$\underline{\mathbf{t}} = \underline{\mathbf{Q}}^{-1} \underline{\mathbf{b}}' = \left(\underline{t}^{(1)}, \dots, \underline{t}^{(M^2R+K)} \right)^{\text{T}}. \quad (5.32)$$

Equation (5.31) can be simplified as

$$\sum_{i=1}^{M^2R+K} \frac{|\underline{t}^{(i)}|^2}{(\lambda + \rho^{(i)})^2} - E_{\text{tot}}^{(2)} = 0. \quad (5.33)$$

By solving (5.33) for λ , one observes that there are several Lagrangian multipliers λ 's satisfying the total energy constraint of (5.33). To understand how several Lagrangian multipliers can satisfy the first order optimality condition of (5.19), a toy example of minimizing a quadratic function $f(x, y)$ under a unit circle $x^2 + y^2 = 1$ constraint is illustrated as a two dimensional contour plot shown in Fig. 5.2. Because the minimum point of the objective function f lays outside the constraint set, the optimum is achieved always with equality, i.e., at the circumference of the circle. Any point which satisfies the first order optimality conditions is called a stationary point. In a stationary point, the range of change of a function is zero. Therefore, it is not necessarily a minimum.

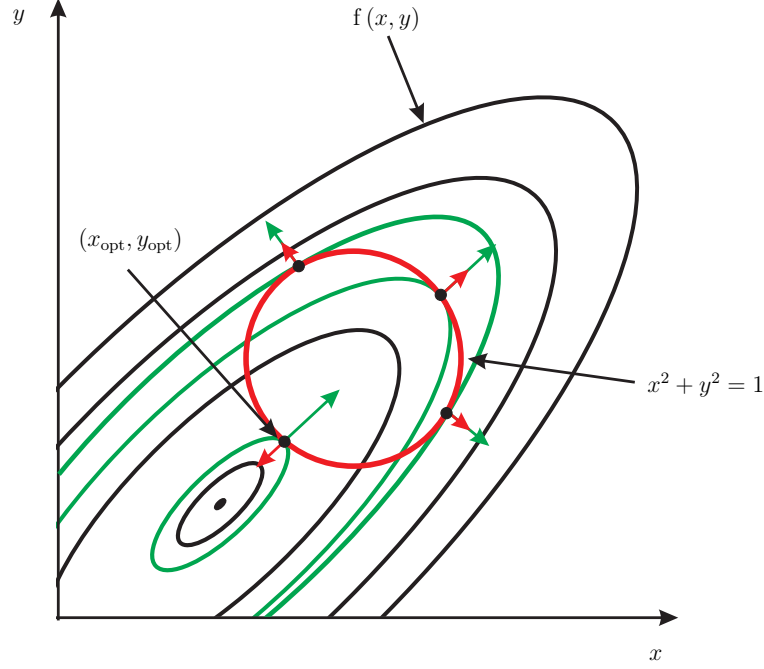


Fig. 5.2: Convex quadratic function minimization over a unit circle.

In a stationary point, the normal vectors of the objective function f and the constraint are aligned. In the example shown in Fig. 5.2, there are four stationary points each of which has a different Lagrangian multiplier λ . However, there is only one optimum point $(x_{\text{opt}}, y_{\text{opt}})$ with an optimum Lagrangian multiplier in which the directions of the normal vectors of the objective function f and the constraint are opposite to each other.

To find the optimum λ , the second order optimality condition should be satisfied. As $\underline{\mathbf{A}}$ is a positive semidefinite matrix, λ should be adapted in such a way that the Hessian of the Lagrange is kept positive semidefinite

$$\underline{\mathbf{i}}^{*\text{T}} \left(\frac{\partial^2 \mathcal{L}}{\partial \begin{pmatrix} \underline{\mathbf{j}} \\ \underline{\mathbf{y}}_2 \end{pmatrix} \partial \begin{pmatrix} \underline{\mathbf{j}}^{*\text{T}} \\ \underline{\mathbf{y}}_2^{*\text{T}} \end{pmatrix}} \right) \underline{\mathbf{i}} \geq 0, \quad (5.34)$$

for any non-zero column vector $\underline{\mathbf{i}}$. Moreover, $\underline{\mathbf{j}}$ corresponds to the total energy constraint and thus, corresponds to λ . Instead of taking the second derivative of (5.17), (5.26) is a function of only $\underline{\mathbf{j}}$ where $\underline{\mathbf{y}}_2$ satisfies the first order optimality condition of (5.22) and hence, (5.26) is equivalent to (5.18). The second order optimality condition in this case is obtained by taking the derivative of (5.26) with respect to $\underline{\mathbf{j}}$. Accordingly,

$$\underline{\mathbf{i}}^{*\text{T}} (\underline{\mathbf{A}}' + \lambda \mathbf{I}_{M^2 R + K}) \underline{\mathbf{i}} \geq 0 \quad (5.35)$$

should hold for any non-zero column vector \mathbf{i} . This condition implies that an optimum solution exists if the matrix $(\underline{\mathbf{A}}' + \lambda \mathbf{I}_{M^2R+K})$ is positive semidefinite. As a result, the eigenvalues of the matrix $(\underline{\mathbf{A}}' + \lambda \mathbf{I}_{M^2R+K})$ are lower bounded by zero. Because $\underline{\mathbf{A}}'$ is a positive semidefinite matrix, $\lambda \geq -\rho_{\min}$ holds where ρ_{\min} is the smallest eigenvalue of $\underline{\mathbf{A}}'$. Moreover, if $\lambda > -\rho_{\min}$ holds, the constraint of (5.33) is a monotonically decreasing function of λ in the interval $]-\rho_{\min}, \infty[$ [Tuy98]. Accordingly, there is only one zero of this function in the interval $]-\rho_{\min}, \infty[$ and hence, a unique optimum solution for λ_{opt} exists. With an initial value $\lambda_{\text{ini}} = -\rho_{\min} + \epsilon$ where ϵ is an arbitrary small positive value, a numerical equation solver can be used to find the optimum λ_{opt} which can be substituted in (5.20) to find the optimum solution of $\underline{\mathbf{j}}$ and $\underline{\mathbf{y}}_2$. Then, the optimum $\underline{\mathbf{y}}_{\text{MSE}}$ can be calculated using (5.16).

5.3.2 Energy constrained maximum sum rate

5.3.2.1 Problem statement and the concept of multi-convex optimization

In this section, an IM algorithm aiming at maximizing the sum rate with a total energy constraint is developed. Basically, the sum rate is a function of the individual SINRs obtained at the output of the receive filter of each destination node k . By partially adapting the filters, the received SINR at the k -th destination node of (2.13) can be rewritten as a function of the unknown vector $\underline{\mathbf{y}}$ as

$$\gamma^{(k)}(\underline{\mathbf{y}}) = \frac{E_d \underline{\mathbf{y}}^{*\text{T}} \underline{\mathbf{q}}^{(k,k)*\text{T}} \underline{\mathbf{q}}^{(k,k)} \underline{\mathbf{y}}}{\underline{\mathbf{y}}^{*\text{T}} \left(E_d \sum_{l \neq k} \underline{\mathbf{q}}^{(k,l)*\text{T}} \underline{\mathbf{q}}^{(k,l)} + \text{E} \{ \underline{\mathbf{z}}^{(k)} \underline{\mathbf{z}}^{(k)*\text{T}} \} \right) \underline{\mathbf{y}} + \sigma^2 |\underline{\mathbf{u}}^{(k,2)}|^2}, \quad (5.36)$$

where the vectors $\underline{\mathbf{q}}^{(k,l)}$ and $\underline{\mathbf{z}}^{(k)}$ are introduced in Section 3.4.1 and Section 3.4.3, respectively. The SINR of (5.36) is a ratio of two quadratic functions of $\underline{\mathbf{y}}$. With a total energy constraint, the sum rate (SR) maximization problem can be stated as

$$\underline{\mathbf{y}}_{\text{SR}} = \arg \max_{\underline{\mathbf{y}}} \left\{ \frac{1}{2} \sum_{k=1}^K \text{ld} (1 + \gamma^{(k)}(\underline{\mathbf{y}})) \right\} \quad (5.37)$$

subject to

$$\underline{\mathbf{y}}^{*\text{T}} \begin{pmatrix} \underline{\Phi}' & \mathbf{0}_{M^2R \times K} & \mathbf{0}_{M^2R \times K} \\ \mathbf{0}_{K \times M^2R} & E_d \mathbf{I}_K & \mathbf{0}_{K \times K} \\ \mathbf{0}_{K \times M^2R} & \mathbf{0}_{K \times K} & \mathbf{0}_{K \times K} \end{pmatrix} \underline{\mathbf{y}} \leq E_{\text{tot}}^{(2)}. \quad (5.38)$$

The sum rate function is not a concave function of $\underline{\mathbf{y}}$ because it is a sum of logarithmic functions of the individual SINRs where a SINR is a ratio of two quadratic functions

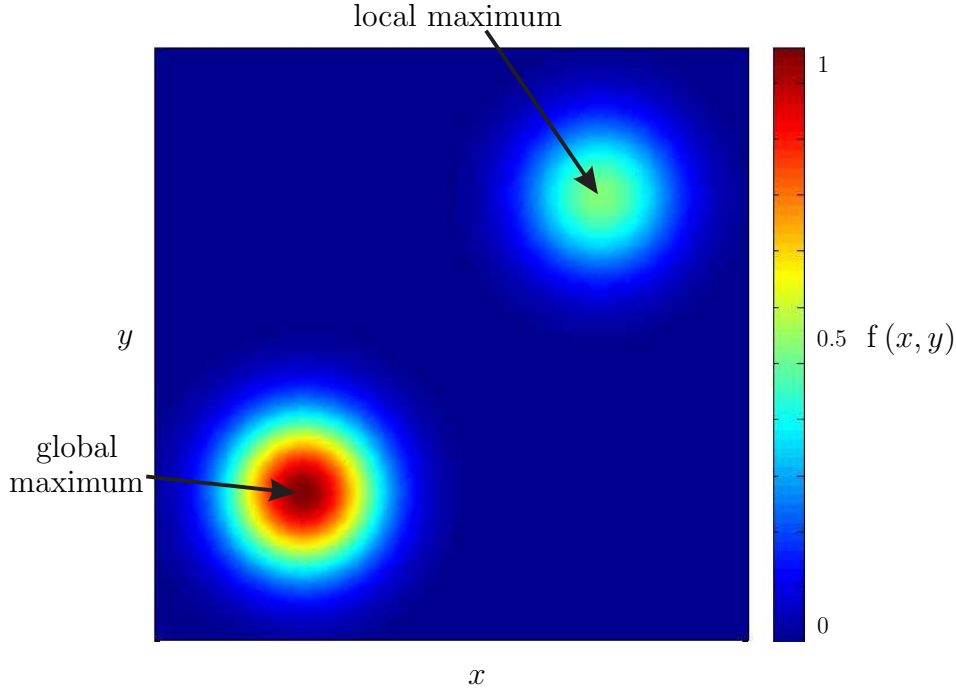


Fig. 5.3: A biconcave function $f(x, y)$ which is concave with respect to x for a certain y and it is concave with respect to y for a certain x .

of \underline{y} . The sum rate has several local maxima and a global maximum and hence, the optimization problem of (5.37)–(5.38) is a non-convex problem.

Before tackling the optimization problem of (5.37)–(5.38), the terms of multi-convex function and multi-convex optimization problem will be clarified.

Definition 1. *A function of a set of variables is a multi-convex function if the variables can be partitioned into different disjoint non-empty subsets such that the function is convex for each of these subsets of variables.*

From Definition 1, the definitions of multi-concave, multi-linear and multi-affine functions are obtained by replacing the property of being convex by concave, linear and affine, respectively. Fig. 5.3 shows a biconcave function $f(x, y)$ which is neither a convex nor a concave function of both x and y . However,

- for a fixed $x = x_{\text{fix}}$, $f(x_{\text{fix}}, y)$ is a concave function of y and
- for a fixed $y = y_{\text{fix}}$, $f(x, y_{\text{fix}})$ is a concave function of x .

There are many optimization problems in many different application areas where the objective functions can be reformulated as multi-convex or multi-concave functions. For

instance, the sum MSE in multiuser relay networks is a multi-convex function in the the transmit filters, the relay processing matrices and the receive filters. Furthermore, the multi-convex optimization problem can be defined as

Definition 2. *A non-convex problem for optimizing a set of variables is called a multi-convex optimization problem if the variables can be partitioned into different disjoint non-empty subsets such that the optimization problem is convex for each of these subsets of variables.*

As compared to a general non-convex optimization problem, the property of multi-convexity can be utilized for implementing a relatively low complexity algorithms which guarantee a local optimum achievement [GPK07]. Unfortunately, the sum rate maximization problem of (5.37)–(5.38) is not a multi-convex optimization problem. Nevertheless, the sum rate maximization problem of (5.37)–(5.38) will be reformulated as a multi-convex optimization problem by adding two sets of scaling factors [ALG⁺13b] as will be described in the following.

5.3.2.2 Signal to interference plus noise ratio

The main difficulty on reformulating the sum rate as a multi-concave function is that both the nominator and the denominator of the SINR are functions of $\underline{\mathbf{y}}$, see (5.36). To overcome this problem, a new term

$$\eta^{(k)}(\underline{\mathbf{y}}, \underline{\mathbf{w}}^{(k)}) = \frac{\mathbb{E} \left\{ \left| \underline{\mathbf{w}}^{(k)} \underline{\mathbf{d}}^{(k)} \right|^2 \right\}}{\mathbb{E} \left\{ \left| \hat{\underline{\mathbf{d}}}^{(k)} - \underline{\mathbf{w}}^{(k)} \underline{\mathbf{d}}^{(k)} \right|^2 \right\}}, \quad (5.39)$$

which describes the received SINR at a destination node k , is introduced. $\underline{\mathbf{w}}^{(k)}$ is a complex weighting factor. With the function

$$\begin{aligned} f_1^{(k)}(\underline{\mathbf{y}}, \underline{\mathbf{w}}^{(k)}) &= \mathbb{E} \left\{ \left| \hat{\underline{\mathbf{d}}}^{(k)} - \underline{\mathbf{w}}^{(k)} \underline{\mathbf{d}}^{(k)} \right|^2 \right\} \\ &= \underline{\mathbf{y}}^{*\text{T}} \left(\sum_l E_d \underline{\mathbf{q}}^{(k,l)} \underline{\mathbf{q}}^{(k,l)*\text{T}} + \mathbb{E} \{ \underline{\mathbf{z}}^{(k)} \underline{\mathbf{z}}^{(k)*\text{T}} \} \right) \underline{\mathbf{y}} + \sigma^2 \left| \underline{\mathbf{u}}^{(k,2)} \right|^2 \\ &\quad - E_d \underline{\mathbf{w}}^{(k)} \underline{\mathbf{q}}^{(k,k)*\text{T}} \underline{\mathbf{y}} - E_d \underline{\mathbf{w}}^{(k)*} \underline{\mathbf{y}}^{*\text{T}} \underline{\mathbf{q}}^{(k,k)} + E_d \left| \underline{\mathbf{w}}^{(k)} \right|^2, \end{aligned} \quad (5.40)$$

which is obtained using (3.40), $\eta^{(k)}(\underline{\mathbf{y}}, \underline{\mathbf{w}}^{(k)})$ can be rewritten as

$$\eta^{(k)}(\underline{\mathbf{y}}, \underline{\mathbf{w}}^{(k)}) = \frac{E_d \left| \underline{\mathbf{w}}^{(k)} \right|^2}{f_1^{(k)}(\underline{\mathbf{y}}, \underline{\mathbf{w}}^{(k)})}. \quad (5.41)$$

If $\underline{w}^{(k)}$ is fixed, $f_1^{(k)}(\underline{\mathbf{y}}, \underline{w}^{(k)})$ is a convex function of $\underline{\mathbf{y}}$ as $\sum_{l=1}^K E_d \underline{\mathbf{q}}^{(k,l)} \underline{\mathbf{q}}^{(k,l)*T} + E \{ \underline{\mathbf{z}}^{(k)} \underline{\mathbf{z}}^{(k)*T} \}$ is a positive semidefinite matrix, i.e., it has a similar structure as the matrix $\underline{\mathbf{A}}$ described in (3.45). By taking the generalized derivative of $\eta^{(k)}(\underline{\mathbf{y}}, \underline{w}^{(k)})$ with respect to $\underline{w}^{(k)}$ and setting the result to zero, the first order optimality condition is stated as

$$\frac{\partial \eta^{(k)}}{\partial \underline{w}^{(k)}} \stackrel{!}{=} 0. \quad (5.42)$$

A single stationary point is found by solving (5.42) for $\underline{w}^{(k)}$ and the optimum weighting factor is calculated as

$$\underline{w}_{\text{opt}}^{(k)} = \frac{\underline{\mathbf{y}}^{*T} \left(\sum_{l=1}^K E_d \underline{\mathbf{q}}^{(k,l)} \underline{\mathbf{q}}^{(k,l)*T} + E \{ \underline{\mathbf{z}}^{(k)} \underline{\mathbf{z}}^{(k)*T} \} \right) \underline{\mathbf{y}} + \sigma^2 |\underline{u}^{(k,2)}|^2}{E_d \underline{\mathbf{q}}^{(k,k)*T} \underline{\mathbf{y}}}. \quad (5.43)$$

By substituting (5.43) into (5.41), $\eta_{\text{opt}}^{(k)}$ with the optimum weighting factor is calculated as

$$\begin{aligned} \eta_{\text{opt}}^{(k)}(\underline{\mathbf{y}}) &= \frac{\underline{\mathbf{y}}^{*T} \left(\sum_{l=1}^K E_d \underline{\mathbf{q}}^{(k,l)} \underline{\mathbf{q}}^{(k,l)*T} + E \{ \underline{\mathbf{z}}^{(k)} \underline{\mathbf{z}}^{(k)*T} \} \right) \underline{\mathbf{y}} + \sigma^2 |\underline{u}^{(k,2)}|^2}{\underline{\mathbf{y}}^{*T} \left(\sum_{l \neq k} E_d \underline{\mathbf{q}}^{(k,l)} \underline{\mathbf{q}}^{(k,l)*T} + E \{ \underline{\mathbf{z}}^{(k)} \underline{\mathbf{z}}^{(k)*T} \} \right) \underline{\mathbf{y}} + \sigma^2 |\underline{u}^{(k,2)}|^2} \\ &= 1 + \gamma^{(k)}(\underline{\mathbf{y}}). \end{aligned} \quad (5.44)$$

Concerning the structure of the function $\eta^{(k)}(\underline{\mathbf{y}}, \underline{w}^{(k)})$ with respect to $\underline{w}^{(k)}$, this function has a singular point at $\underline{w}^{(k)} = 0$ where the first order derivative

$$\left. \frac{\partial \eta^{(k)}}{\partial \underline{w}^{(k)}} \right|_{\underline{w}^{(k)}=0} \quad (5.45)$$

is not defined. Accordingly, within the domain

$$\text{dom } \eta^{(k)}(\underline{\mathbf{y}}, \underline{w}^{(k)}) = \begin{cases} \text{Re } \{ \underline{w}^{(k)} \} \in \mathbb{R}_+ & \text{if } \text{Re } \{ \underline{\mathbf{y}}^{*T} \underline{\mathbf{q}}^{(k,k)} \} \geq 0, \\ \text{Re } \{ \underline{w}^{(k)} \} \in \mathbb{R}_- & \text{if } \text{Re } \{ \underline{\mathbf{y}}^{*T} \underline{\mathbf{q}}^{(k,k)} \} < 0, \\ \text{Im } \{ \underline{w}^{(k)} \} \in \mathbb{R}_+ & \text{if } \text{Im } \{ \underline{\mathbf{y}}^{*T} \underline{\mathbf{q}}^{(k,k)} \} \geq 0, \\ \text{Im } \{ \underline{w}^{(k)} \} \in \mathbb{R}_- & \text{if } \text{Im } \{ \underline{\mathbf{y}}^{*T} \underline{\mathbf{q}}^{(k,k)} \} < 0, \end{cases} \quad (5.46)$$

where \mathbb{R}_+ denotes the set of all the non-negative real numbers and \mathbb{R}_- denotes the set of all the non-positive real numbers, $\eta^{(k)}(\underline{\mathbf{y}}, \underline{w}^{(k)})$ is a concave function with respect to $\underline{w}^{(k)}$ because

- from (5.41), the extreme values of $\eta^{(k)}(\underline{\mathbf{y}}, \underline{w}^{(k)})$ range from zero for $\underline{w}^{(k)} = 0$ and one for $\underline{w}^{(k)} = \infty$ and

- there is a single stationary point and it is greater than or equal to one, see (5.44) and note that $\gamma^{(k)}(\underline{\mathbf{y}}) \geq 0$.

The main property of $\eta^{(k)}(\underline{\mathbf{y}}, \underline{\mathbf{w}}^{(k)})$ is that just its the denominator is a function of $\underline{\mathbf{y}}$ whereas both the nominator and the denominator of $\gamma^{(k)}(\underline{\mathbf{y}})$ are functions of $\underline{\mathbf{y}}$.

5.3.2.3 Sum rate maximization based on multi-convex optimization

From the result of (5.44), the vector of the unknowns $\underline{\mathbf{y}}$ as well as the weighting vector

$$\underline{\mathbf{w}} = (\underline{\mathbf{w}}^{(1)}, \dots, \underline{\mathbf{w}}^{(K)})^T \quad (5.47)$$

can be jointly optimized for maximizing the sum rate. Based on this idea, using

$$f_2(\underline{\mathbf{y}}, \underline{\mathbf{w}}) = \frac{1}{2} \sum_{k=1}^K \text{ld}(\eta^{(k)}(\underline{\mathbf{y}}, \underline{\mathbf{w}})), \quad (5.48)$$

the optimization problem of (5.37)–(5.38) can be reformulated as

$$(\underline{\mathbf{y}}_{\text{SR}}, \underline{\mathbf{w}}_{\text{opt}}) = \arg \max_{\underline{\mathbf{y}}, \underline{\mathbf{w}}} \{f_2(\underline{\mathbf{y}}, \underline{\mathbf{w}})\} \quad (5.49)$$

subject to

$$\underline{\mathbf{y}}^{*T} \begin{pmatrix} \underline{\Phi}' & \mathbf{0}_{M^2R \times K} & \mathbf{0}_{M^2R \times K} \\ \mathbf{0}_{K \times M^2R} & E_d \mathbf{I}_K & \mathbf{0}_{K \times K} \\ \mathbf{0}_{K \times M^2R} & \mathbf{0}_{K \times K} & \mathbf{0}_{K \times K} \end{pmatrix} \underline{\mathbf{y}} \leq E_{\text{tot}}^{(2)}. \quad (5.50)$$

Clearly, the objective function $f_2(\underline{\mathbf{y}}, \underline{\mathbf{w}})$ is concave with respect to $\underline{\mathbf{w}}$ as $\eta^{(k)}(\underline{\mathbf{y}}, \underline{\mathbf{w}}^{(k)})$ is a concave function of $\underline{\mathbf{w}}^{(k)}$ and the logarithm is a concave monotonic increasing function [BV04]. From (5.41), the objective function $f_2(\underline{\mathbf{y}}, \underline{\mathbf{w}})$ can be rewritten as

$$f_2(\underline{\mathbf{y}}, \underline{\mathbf{w}}) = \frac{1}{2} \sum_{k=1}^K \text{ld}(E_d |\underline{\mathbf{w}}^{(k)}|^2) - \frac{1}{2} \sum_{k=1}^K \text{ld}(f_1^{(k)}(\underline{\mathbf{y}}, \underline{\mathbf{w}}^{(k)})). \quad (5.51)$$

In (5.51), only the second term depends on $\underline{\mathbf{y}}$. Although $f_1^{(k)}(\underline{\mathbf{y}}, \underline{\mathbf{w}}^{(k)})$ with fixed $\underline{\mathbf{w}}^{(k)}$ is a convex function of $\underline{\mathbf{y}}$, the function $\text{ld}(f_1^{(k)}(\underline{\mathbf{y}}, \underline{\mathbf{w}}^{(k)}))$ with fixed $\underline{\mathbf{w}}^{(k)}$ is not necessarily a convex function of $\underline{\mathbf{y}}$ [Con78]. Therefore, a new objective function which has the function $f_1^{(k)}(\underline{\mathbf{y}}, \underline{\mathbf{w}}^{(k)})$ not inside the logarithm is needed. K additional scaling factors are introduced and the optimization problem of (5.49)–(5.50) is reformulated as a multi-convex optimization problem. Consider the function

$$f_3(\underline{\mathbf{y}}, \underline{\mathbf{w}}, \mathbf{o}) = \frac{1}{2} \sum_{k=1}^K \left(\text{ld}(o^{(k)}) + \text{ld}(E_d |\underline{\mathbf{w}}^{(k)}|^2) - \frac{o^{(k)}}{\ln(2)} f_1^{(k)}(\underline{\mathbf{y}}, \underline{\mathbf{w}}^{(k)}) \right), \quad (5.52)$$

where

$$\mathbf{o} = (o^{(1)}, \dots, o^{(K)})^T \quad (5.53)$$

is a vector of positive real variables

$$o^{(k)} > 0, \quad \forall k. \quad (5.54)$$

To show the equivalence between $f_2(\underline{\mathbf{y}}, \underline{\mathbf{w}})$ and $f_3(\underline{\mathbf{y}}, \underline{\mathbf{w}}, \mathbf{o})$, the first order optimality condition

$$\frac{\partial f_3}{\partial o^{(k)}} \stackrel{!}{=} 0 \quad (5.55)$$

with respect to $o^{(k)}$ is investigated. A single stationary point

$$o_{\text{opt}}^{(k)} = \frac{1}{f_1^{(k)}(\underline{\mathbf{y}}, \underline{\mathbf{w}}^{(k)})} \quad (5.56)$$

is found by solving (5.55) for $o^{(k)}$. By substituting (5.56) into (5.52), one obtains

$$f_3(\underline{\mathbf{y}}, \underline{\mathbf{w}}, \mathbf{o}_{\text{opt}}) = f_2(\underline{\mathbf{y}}, \underline{\mathbf{w}}) - \frac{K}{2 \ln(2)}. \quad (5.57)$$

Accordingly, the optimization problem of (5.49)–(5.50) is equivalently stated as

$$\left(\underline{\mathbf{y}}_{\text{SR}}, \underline{\mathbf{w}}_{\text{opt}}, \mathbf{o}_{\text{opt}} \right) = \arg \max_{\underline{\mathbf{y}}, \underline{\mathbf{w}}, \mathbf{o}} \{ f_3(\underline{\mathbf{y}}, \underline{\mathbf{w}}, \mathbf{o}) \} \quad (5.58)$$

subject to

$$\underline{\mathbf{y}}^{*T} \begin{pmatrix} \underline{\Phi}' & \mathbf{0}_{M^2 R \times K} & \mathbf{0}_{M^2 R \times K} \\ \mathbf{0}_{K \times M^2 R} & E_d \mathbf{I}_K & \mathbf{0}_{K \times K} \\ \mathbf{0}_{K \times M^2 R} & \mathbf{0}_{K \times K} & \mathbf{0}_{K \times K} \end{pmatrix} \underline{\mathbf{y}} \leq E_{\text{tot}}^{(2)}. \quad (5.59)$$

The optimization problem of (5.58)–(5.59) is a non-convex problem in the vectors $\underline{\mathbf{y}}$, $\underline{\mathbf{w}}$ and \mathbf{o} when they are jointly optimized. However, if $\underline{\mathbf{w}}$ and $\underline{\mathbf{y}}$ are fixed, the objective function $f_3(\underline{\mathbf{y}}, \underline{\mathbf{w}}, \mathbf{o})$ is concave in \mathbf{o} , i.e., the logarithm is a concave monotonic increasing function. Based on the discussion of the concavity of $\eta^{(k)}(\underline{\mathbf{y}}, \underline{\mathbf{w}}^{(k)})$ with respect to $\underline{\mathbf{w}}^{(k)}$ on the previous section, the objective function $f_3(\underline{\mathbf{y}}, \underline{\mathbf{w}}, \mathbf{o})$ is concave in $\underline{\mathbf{w}}$ if $\underline{\mathbf{y}}$ is fixed and the optimized \mathbf{o}_{opt} is used. Furthermore, if both $\underline{\mathbf{w}}$ and \mathbf{o} are fixed, just the last term of (5.52) is required to be considered as an objective function. Accordingly, the optimization problem of (5.58)–(5.59) can be reformulated as

$$\underline{\mathbf{y}}_{\text{SR}} = \arg \min_{\underline{\mathbf{y}}} \left\{ \underline{\mathbf{y}}^{*T} \underline{\mathbf{A}} \underline{\mathbf{y}} - \underline{\mathbf{b}}^{*T} \underline{\mathbf{y}} - \underline{\mathbf{y}}^{*T} \underline{\mathbf{b}} \right\} \quad (5.60)$$

subject to

$$\underline{\mathbf{y}}^{*T} \begin{pmatrix} \underline{\Phi}' & \mathbf{0}_{M^2 R \times K} & \mathbf{0}_{M^2 R \times K} \\ \mathbf{0}_{K \times M^2 R} & E_d \mathbf{I}_K & \mathbf{0}_{K \times K} \\ \mathbf{0}_{K \times M^2 R} & \mathbf{0}_{K \times K} & \mathbf{0}_{K \times K} \end{pmatrix} \underline{\mathbf{y}} \leq E_{\text{tot}}^{(2)}, \quad (5.61)$$

where

$$\bar{\mathbf{A}} = \sum_{k=1}^K o^{(k)} \left(E_d \sum_l \underline{\mathbf{q}}^{(k,l)} \underline{\mathbf{q}}^{(k,l)*\text{T}} + E \{ \underline{\mathbf{z}}^{(k)} \underline{\mathbf{z}}^{(k)*\text{T}} \} \right) \quad (5.62)$$

is a positive semidefinite matrix because the scaling factors $o^{(k)}$, $\forall k$ are positive, see (5.54), and

$$\bar{\mathbf{b}} = E_d \sum_{k=1}^K o^{(k)} \underline{\mathbf{w}}^{(k)*} \mathbf{q}^{(k,k)}. \quad (5.63)$$

As compared to (3.45) and (3.46), $\bar{\mathbf{A}}$ and $\bar{\mathbf{b}}$ are the weighted sum version of \mathbf{A} and \mathbf{b} , respectively. This means that when all the scaling factors are set to one $o^{(k)} = \underline{w}^{(k)} = 1$ for $k = 1, \dots, K$, $\bar{\mathbf{A}} = \mathbf{A}$ and $\bar{\mathbf{b}} = \mathbf{b}$ follow. The optimization problem of (5.60)–(5.61) is convex as the objective function $\underline{\mathbf{y}}^{*\text{T}} \bar{\mathbf{A}} \underline{\mathbf{y}} - \bar{\mathbf{b}}^{*\text{T}} \underline{\mathbf{y}} - \underline{\mathbf{y}}^{*\text{T}} \bar{\mathbf{b}}$ is a convex quadratic function and the constraint of (5.61) is a convex quadratic set. The structure of the problem of (5.60)–(5.61) is similar to the one of the sum MSE minimization problem (5.6)–(5.7) and it can be solved as described in Section 5.3.1.

Based on the above discussion, the optimization problem of (5.58)–(5.59) is a convex problem of either $\underline{\mathbf{y}}$ or \mathbf{o} individually and for the optimum \mathbf{o}_{opt} , it is a convex problem of $\underline{\mathbf{w}}$. In the other words, it is a multi-convex optimization problem and it is equivalent to the sum rate maximization problem of (5.37)–(5.38) in the sense that both of them have the same extreme points, i.e., the same global maximum and the same local maxima for optimum weights $\underline{\mathbf{w}}_{\text{opt}}$ and \mathbf{o}_{opt} .

Finally, an iterative algorithm which alternately maximizes the objective function $f_3(\underline{\mathbf{y}}, \underline{\mathbf{w}}, \mathbf{o})$ over $\underline{\mathbf{y}}$, $\underline{\mathbf{w}}$ and \mathbf{o} is described. Let ϵ be an arbitrary small tolerance value. The sum rate maximization algorithm is summarized as follows:

- 1: set initial values for $\underline{\mathbf{w}}^{(0)}$ and $\mathbf{o}^{(0)}$
- 2: in every iteration i
- 3: calculate $\underline{\mathbf{y}}^{(i)}$ given $\underline{\mathbf{w}}^{(i-1)}$ and $\mathbf{o}^{(i-1)}$
 - ▷ see Section 5.3.1.2 for solving (5.60)–(5.61)
- 4: calculate $\underline{\mathbf{w}}^{(i)}$ given $\underline{\mathbf{y}}^{(i)}$ ▷ using (5.43)
- 5: calculate $\mathbf{o}^{(i)}$ given $\underline{\mathbf{y}}^{(i)}$ and $\underline{\mathbf{w}}^{(i)}$ ▷ using (5.56)
- 6: stop if $|f_3(\underline{\mathbf{y}}^{(i)}, \underline{\mathbf{w}}^{(i)}, \mathbf{o}^{(i)}) - f_3(\underline{\mathbf{y}}^{(i-1)}, \underline{\mathbf{w}}^{(i-1)}, \mathbf{o}^{(i-1)})| \leq \epsilon$

The initial values for the scaling vectors \mathbf{w} and \mathbf{o} can be set to ones such that the initial point is the sum MSE solution. From the multi-convex optimization literature, this alternate optimization algorithm always converges to a local optimum [GPK07].

5.3.2.4 Some comments on the sum rate maximization algorithm

In this section, the idea of formulating the sum rate maximization problem as a multi-convex optimization problem is shown that it is quite general and it can be applied to many different systems. By tracing back the analysis in the previous section, one can observe that $f_3(\underline{\mathbf{y}}, \underline{\mathbf{w}}, \mathbf{o})$ becomes a concave function of the unknown vector \mathbf{y} for fixed $\underline{\mathbf{w}}$ and \mathbf{o} because for all k , $f_1^{(k)}(\underline{\mathbf{y}}, \underline{\mathbf{w}}^{(k)})$ is a convex function of \mathbf{y} for a fixed $\underline{\mathbf{w}}^{(k)}$. Furthermore, $f_1^{(k)}(\underline{\mathbf{y}}, \underline{\mathbf{w}}^{(k)})$ becomes a convex function of \mathbf{y} for a fixed $\underline{\mathbf{w}}^{(k)}$ because the estimated data symbol $\hat{\underline{\mathbf{d}}}^{(k)}$ is a linear function of the unknown vector \mathbf{y} . As a conclusion, the key system requirement for formulating the sum rate maximization problem as a multi-convex optimization problem is to have the estimated data symbols being multi-linear functions of the system variables.

For the considered scenario with fully adapted filters, one can write the k -th estimated data symbol $\hat{\underline{\mathbf{d}}}^{(k)}$ as multi-linear function of the transmit filters, the receive filters and the relay coefficients. In this case, a multi-concave objective function f_3 of the transmit filters, the receive filters, the relay coefficients, the scaling vector $\underline{\mathbf{w}}$ and the scaling vector \mathbf{o} can be formulated.

5.4 Complexity and performance of the interference mitigation algorithms

5.4.1 Complexity analysis

In this section, the complexity of applying the proposed IM algorithms is investigated. Appendix C introduces the main assumptions used for the complexity analysis. Also, the complexities of some basic linear algebra operations which are used for calculating the complexity of the proposed IM solutions are summarized in Table C.1.

The IM algorithm with fixed filters proposed in Section 5.2 basically requires calculating the left pseudo inverse of $\underline{\mathbf{H}}_{\text{ff}}$. By taking the complexity of calculating $\underline{\mathbf{H}}_{\text{ff}}$ into account, see Table 3.1, the complexity of calculating $\underline{\mathbf{x}}_{\text{IM}}$ is $\mathcal{O}(R^2 M^4 K^2)$, i.e., keep in mind that $M^2 R < K(K - 1)$.

For the proposed IM algorithms with partially adapted filters, the complexity of computing $\underline{\mathbf{A}}$ and $\underline{\mathbf{b}}$ listed in Table 3.1 are taken into account. Note that $\underline{\mathbf{A}}$ and $\underline{\mathbf{b}}$ have the

same complexity as $\underline{\mathbf{A}}$ and $\underline{\mathbf{b}}$, respectively. The complexities of computing the minimum sum MSE solution and the maximum sum rate solution are dominated by the complexity of computing the matrices listed in Table 5.1. The lower triangular matrix $\underline{\mathbf{T}}$ is computed by applying the Cholesky decomposition to the covariance matrix of (5.14). Because (5.14) is a block diagonal matrix with two blocks where the second diagonal block is a diagonal matrix, the complexity of computing the matrix $\underline{\mathbf{T}}$ is dominated by the complexity of applying the Cholesky decomposition to the first diagonal block $\underline{\Phi}'$, i.e., $\underline{\Phi}'$ is a block diagonal matrix as well and the decomposition can be done separately for each diagonal block. Furthermore, the complexity of computing $\underline{\mathbf{j}}$ and $\underline{\mathbf{y}}_2$ in (5.20) is dominated by the complexity of computing the matrix $\underline{\mathbf{T}}^{-1} \underline{\mathbf{A}}_{11}^{*\text{T}} (\underline{\mathbf{T}}^{*\text{T}})^{-1}$.

For the sum rate maximization algorithm proposed in Section 5.3.2, the complexities of computing $\underline{w}_{\text{opt}}^{(k)}$ in (5.43) and $o_{\text{opt}}^{(k)}$ in (5.56) are dominated by the complexity of computing $\underline{\mathbf{y}}^{*\text{T}} \left(\sum_{l=1}^K E_d \underline{\mathbf{q}}^{(k,l)} \underline{\mathbf{q}}^{(k,l)*\text{T}} + E \{ \underline{\mathbf{z}}^{(k)} \underline{\mathbf{z}}^{(k)*\text{T}} \} \right) \underline{\mathbf{y}}$ which is listed in Table 5.1. Furthermore, the complexities of computing the vectors $\underline{\mathbf{w}}^{(i)}$, $\underline{\mathbf{o}}^{(i)}$ and $\underline{\mathbf{y}}^{(i)}$ at the i -th iteration are listed in Table 5.2. For a fair complexity comparison between the sum MSE minimization algorithm and the sum rate maximization algorithm and because the optimum Lagrangian multiplier λ_{opt} is found using a numerical solver as described in Section 5.3.1.2, the complexities of computing $\underline{\mathbf{y}}_{\text{MSE}}$ and $\underline{\mathbf{y}}_{\text{SR}}^{(i)}$ are calculated for a certain λ .

For a certain Lagrangian multiplier λ , the complexity of the sum MSE minimization algorithm and the complexity of a single iteration of the sum rate maximization algorithm are shown in Table 5.3. It can be noted that the complexity of both algorithms grows cubically with respect to the number R of relays, polynomially with an order of six with respect to the number M of antennas at the relays and polynomially with an

Expression	Complexity
$\underline{\Phi}'$	$\mathcal{O}(RM^2K)$
$\underline{\mathbf{T}}$	$\mathcal{O}(RM^2K + RM^6)$
$\underline{\mathbf{T}}^{-1}$	$\mathcal{O}(RM^2K + RM^6)$
$\underline{\mathbf{T}}^{-1} \underline{\mathbf{A}}_{11}^{*\text{T}} (\underline{\mathbf{T}}^{*\text{T}})^{-1}$	$\mathcal{O}(R^2M^4K^2 + RM^2K^3 + R^3M^6 + K^4)$
$\underline{\mathbf{y}}^{*\text{T}} \left(\sum_{l=1}^K E_d \underline{\mathbf{q}}^{(k,l)} \underline{\mathbf{q}}^{(k,l)*\text{T}} + E \{ \underline{\mathbf{z}}^{(k)} \underline{\mathbf{z}}^{(k)*\text{T}} \} \right) \underline{\mathbf{y}}$	$\mathcal{O}(R^2M^4K + RM^2K^2 + R^3M^6 + K^3)$

Table 5.1: Complexity of computing the matrices involved in calculating the minimum sum MSE solution and the maximum sum rate solution.

Expression	Complexity
$\underline{\mathbf{w}}^{(i)}$ in (5.43) and (5.47)	$\mathcal{O}(R^2 M^4 K^2 + RM^2 K^3 + R^3 M^6 K + K^4)$
$\mathbf{o}^{(i)}$ in (5.56) and (5.53)	$\mathcal{O}(R^2 M^4 K^2 + RM^2 K^3 + R^3 M^6 K + K^4)$
$\underline{\mathbf{y}}^{(i)}$ in (5.60)–(5.61) with a certain λ	$\mathcal{O}(R^2 M^4 K^2 + RM^2 K^3 + R^3 M^6 + K^4)$

Table 5.2: Complexity of computing the vectors involved in a single iteration i of the maximum sum rate algorithm.

order of four with respect to the number K of node pairs.

By comparing the complexities of the two algorithms shown in Table 5.3, it can be observed that all the terms are the same except the last ones. This means that the sum rate maximization algorithm encounters a higher complexity than the one caused by the sum MSE minimization algorithm. The additional complexity grows linearly with the number K of node pairs and it is caused by computing $\underline{\mathbf{y}}^{*\text{T}} \left(\sum_{l=1}^K E_d \underline{\mathbf{q}}^{(k,l)} \underline{\mathbf{q}}^{(k,l)*\text{T}} + \text{E} \{ \underline{\mathbf{z}}^{(k)} \underline{\mathbf{z}}^{(k)*\text{T}} \} \right) \underline{\mathbf{y}}$ for each element k of the vectors $\underline{\mathbf{w}}^{(i)}$ and $\mathbf{o}^{(i)}$.

So far, the computational complexity of the sum rate maximization algorithm is studied for a single iteration. To have an impression on the number of iterations required for the convergence, Fig. 5.4 shows a histogram of the number I of iterations needed by the sum rate maximization algorithm with $\epsilon = 10^{-6}$ for a scenario with $K = 3$, $R = 3$ and $M = 2$. From the figure, one can observe that there are a high density of trails with $I < 100$ iterations.

Expression	Complexity	Remarks
$\underline{\mathbf{j}}$ and $\underline{\mathbf{y}}_2$ in (5.20)	$\mathcal{O}(R^2 M^4 K^2 + RM^2 K^3 + K^4 + R^3 M^6)$	for a certain λ
$\underline{\mathbf{w}}^{(i)}$, $\mathbf{o}^{(i)}$ and $\underline{\mathbf{y}}^{(i)}$ for a single iteration i	$\mathcal{O}(R^2 M^4 K^2 + RM^2 K^3 + K^4 + R^3 M^6 K)$	

Table 5.3: Complexity of computing the minimum sum MSE and the maximum sum rate.

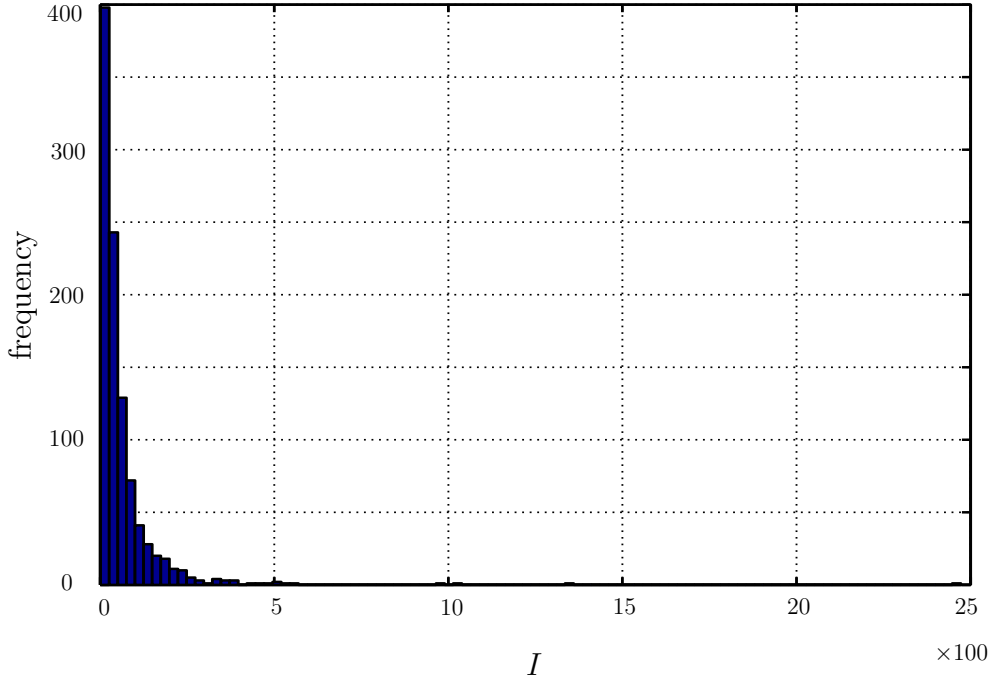


Fig. 5.4: A histogram of the number I of iterations needed by the sum rate maximization algorithm for a scenario with $K = 3$, $R = 3$ and $M = 2$.

5.4.2 Performance analysis

In this section, the performances of the proposed IM algorithms are investigated. The performance analyses of the IM algorithms are elaborated in two main categories:

- Under the assumption of fixed filters at the nodes, the performance of the IM algorithm proposed in Section 5.2 is investigated in conjunction with the IA algorithm previously proposed in Section 3.3.
- Under the assumption of partially adapted filters at the nodes, the performances of both the sum MSE minimization algorithm and the sum rate maximization algorithm proposed in Section 5.3 are investigated in conjunction with the IA algorithm proposed in Section 3.4.

Additionally, the single cell relaying algorithm proposed in Section 2.2.1 is considered as a reference scheme.

The first considered scenario consists of three node pairs $K = 3$ and multiple relays with a single antenna each $M = 1$. The transmit and the receive filters are adjusted as described in Section 3.5.3. Based on this scenario and from (3.17), IA is feasible

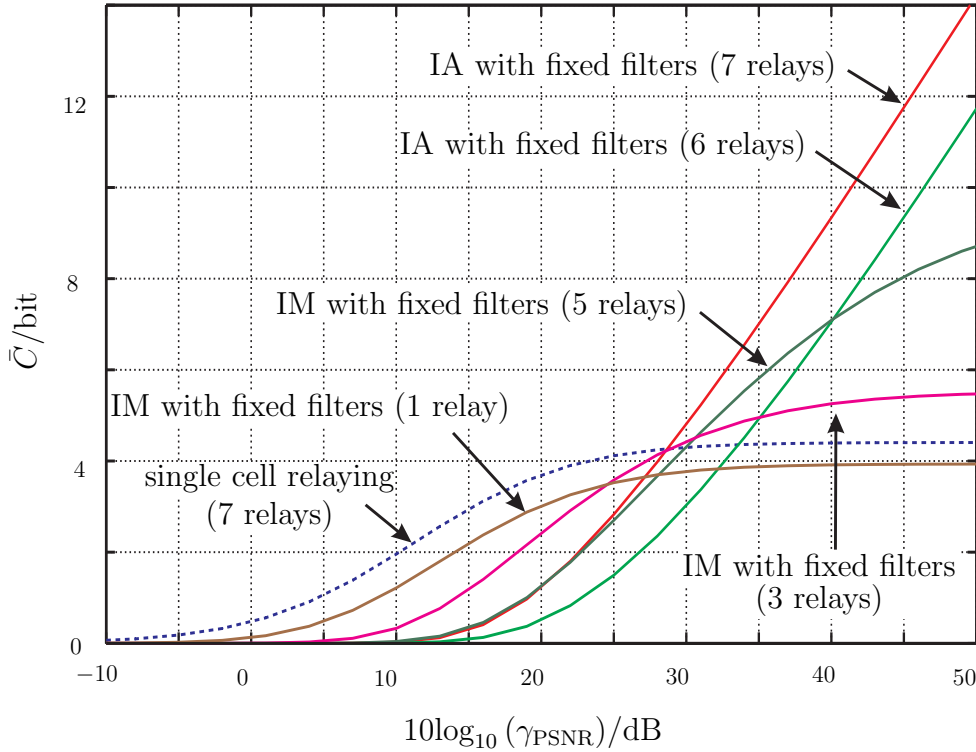


Fig. 5.5: Achieved sum rate as a function of PSNR for scenarios with $K = 3$, $M = 1$ and different number R of relays.

if $R \geq 6$. Fig. 5.5 shows the sum rate \bar{C} per time slot averaged over many different channel realizations and depicted as a function of the PSNR. It shows the sum rates achieved considering different numbers R of relays. If $R = 6$, IA is achievable and the inhomogeneous system of linear equations has a unique solution for the relay processing matrices. The IA algorithm with 6 relays achieves higher sum rates than the single cell relaying algorithm just at high PSNRs. In the low and moderate PSNR regimes, the IA algorithms perform worse than the single cell algorithm, i.e., the noise is dominant in these regimes. By adding one relay, the IA algorithm with 7 relays adjusts the relay processing matrices such that the retransmitted energies of the relays are minimized as described in Section 3.3.3. Minimizing the relay retransmitted energy means minimizing the total system energy and thus, higher sum rates are achieved as compared to the IA with 6 relays. Comparing the sum rates achieved using the IA algorithm with 7 relays to the one with 6 relays, one can notice that the required PSNRs are reduced by 5 dB and the sum rate is increased by around 3 bits. As described in Section 3.5.3, the slopes of the curves in the high PSNR regime are related to the achieved DoFs. Accordingly, the IA algorithm achieves 1.5 DoFs.

By reducing the number R of relays to five, IA is not feasible anymore but an approximate solution for the relay processing matrices can be found using the least squares

solution of (5.4). Accordingly, the interferences are not fully aligned at the interference subspace of every destination node and hence, the unaligned interferences are treated as noise. From Fig. 5.5, it can be observed that the IM algorithm with 5 relays achieves the same sum rates as the IA with 7 relays at the low and moderate PSNRs. This supports the previous statement in Section 5.1 that leaving some weak unaligned interferences at the destination nodes and treating them as noise can enhance the achieved sum rates at low and moderate PSNRs. At high PSNRs, the unaligned interference powers obtained at the output of the receive filters are significantly high which limits the achieved sum rates to a certain bound. By reducing the number R of relays further, the following can be observed:

- At low PSNRs, the achieved sum rates are increasing due to the fact that reducing the number of relays will reduce the energy required for the retransmission.
- At high PSNRs, the achieved sum rates saturate at smaller limiting values, i.e., more unaligned interference powers are obtained at the output of the received filters of every destination node when less relays are employed and thus, the SIR gets smaller. At these limiting values, the SIR remains constant even when the PSNR is increasing.

Finally, because the single cell relaying algorithm is supported by 7 relays, it outperforms the IM algorithm with 1 relay at all PSNRs.

To investigate the performances of the IM algorithms with partially adapted filters proposed in Section 5.3, a scenario with $K = 3$, $R = 3$ and $M = 2$ is considered. The fixed filter coefficients $\underline{u}^{(k,2)}$ and $\underline{v}^{(k,1)}$ with $k = 1, \dots, K$ are adjusted as described in Section 3.5.3. For the two energy constrained IM algorithms proposed in Section 5.3, the total energy constraint is split up equally over the time slots as

$$E_{\text{tot}}^{(1)} = E_{\text{tot}}^{(2)} = E_{\text{tot}}/2. \quad (5.64)$$

The average sum rates \bar{C} as a function of the PSNRs for the sum rate maximization algorithm, the sum MSE minimization algorithm, the IA algorithm proposed in Section 3.4.3 and the single cell relaying algorithm are shown in Fig. 5.6. From the figure, the following can be observed:

- The single cell relaying algorithm does not take the interference into account and thus, it performs poorly at the high PSNR regime. However, it outperforms the IA algorithm at the low SNRs, i.e., where noise is dominant. Also, zero DoF is achieved using this algorithm.

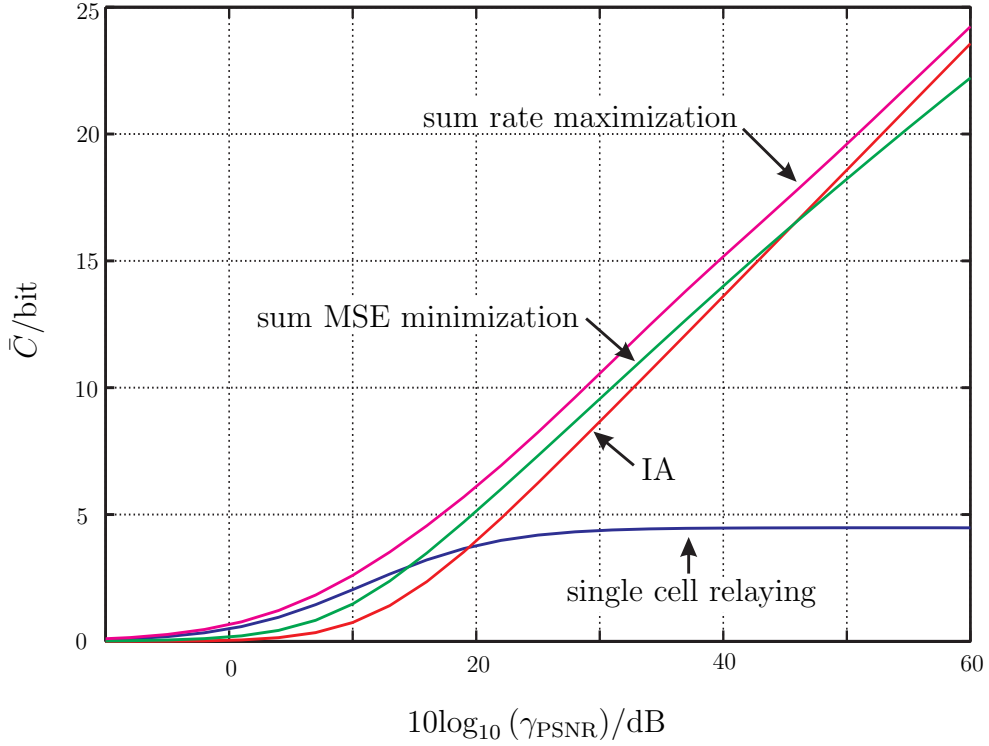


Fig. 5.6: Achieved sum rate as a function of the PSNR for a scenario with $K = 3$, $R = 3$ and $M = 2$.

- In contrast to the single cell relaying algorithm, the IA algorithm performs poorly at low PSNRs as it does not consider noise reduction when optimizing the filters and the relay processing matrices. However, it achieves $K/2 = 1.5$ DoFs.
- The sum MSE minimization algorithm outperforms the IA algorithm at the low and moderate PSNRs because it minimizes both noise power and interference power obtained at the output of the receive filter of every destination node. At high PSNRs, one can notice that it performs worse than the IA algorithm and it achieves only 1.3 DoFs. This happens because there are filter coefficients $\underline{u}^{(k,2)}$ and $\underline{v}^{(k,1)}$ with $k = 1, \dots, K$ being fixed a priori and thus, the feasible region of the total energy constraint does not necessarily include the zero sum MSE. In other words, achieving the zero sum MSE for some channel realizations may require infinite energy.
- The sum rate maximization algorithm outperforms all the other algorithms at all PSNRs. However, it achieves 1.4 DoFs because it is a suboptimal algorithm which guarantees only a local maximum of the sum rate rather than the global one.

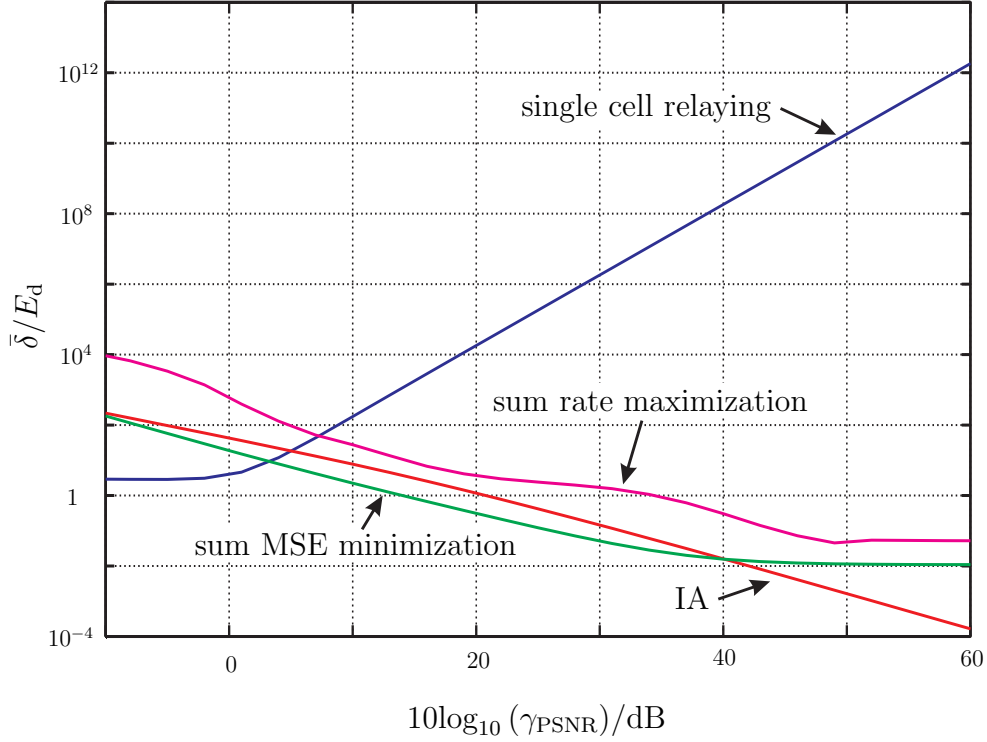


Fig. 5.7: The ratio of the average sum MSE and the average symbol energy as a function of the PSNR for a scenario with $K = 3$, $R = 3$ and $M = 2$.

For the same scenario and the same simulation setup, the ratio of the average sum MSE $\bar{\delta}$ and the average data symbol energy E_d is depicted as a function of the PSNR in Fig. 5.7. At low PSNRs, the received powers of the useful signals obtained at the output of the receive filters are weak as compared to the noise power and thus, low sum MSEs are achieved by all algorithms. As the PSNR increases, the unaligned interference power increases when applying the single cell relaying algorithm and thus, the achieved sum MSE is increased. However, the sum MSEs achieved by the other algorithms decrease as the PSNR increases and at high PSNRs,

- the IA algorithm asymptotically achieves a zero sum MSE because
 - it aims at minimizing the sum MSE.
 - the zero sum MSE is within the feasible region as described in Section 3.4.3.
- the sum MSE minimization algorithm saturates at $\bar{\delta}/E_d = 10^{-2}$ because of fixing some of the filter coefficients and thus for some channel realizations, infinite energies would be needed to achieve the zero sum MSE.
- the sum rate maximization algorithm saturates at $\bar{\delta}/E_d = 10^{-1.5}$ as it does not aim at minimizing the sum MSE.

Comparing Fig. 5.6 and Fig. 5.7, one can conclude that minimizing the sum MSE does not necessarily lead to high sum rates and maximizing the sum rate does not necessarily lead to low sum MSEs.

Chapter 6

Energy allocation for interference mitigation systems

6.1 Preliminaries

In this chapter, the energy allocation in the framework of interference mitigation (IM) is investigated. As discussed in Section 3.2, IA is realized by adapting the relay processing matrices and the directions of the transmit and the receive filter vectors to the channel aiming at obtaining no interferences at the output of the receive filter of each destination node. Moreover, it has been shown that the norms of the transmit filter vectors have no influence on the IA solution. Therefore, the norms of the transmit filter vectors or the energy allocation among the source nodes can be optimized for further enhancement of the performance of the IA system as discussed in Chapter 4. Optimizing the energy allocation on the top of an IA solution is equivalent to optimizing the energy allocation on an interference free channel with no relays where the waterfilling algorithm can be used for finding the optimum energy allocation. Unfortunately, the rate maximization waterfilling algorithm as shown in Fig. 4.5 does not improve the achieved sum rates significantly as compared to the one when using the equal energy allocation especially at high SNRs.

The previous chapter introduced different IM algorithms which implicitly reduce the interferences but not necessarily nullifying them. By applying an IM algorithm in a multi-cell scenario, some unaligned interferences remain at the output of the receive filter of each destination node. These unaligned interferences are considered as noise. Unlike the energy allocation optimization on the top of an IA solution, optimizing the energy allocation on the top of an IM solution is equivalent to optimizing the energy allocation in interference channels with no relays. For interference channels, energy allocation plays a key role in maximizing the performance where in general the equal energy allocation performs poorly.

As considered in Chapter 4, scenarios with either a single resource $N = 1$ or multiple orthogonal resources $N > 1$ are also considered. For scenarios with multiple orthogonal resources $N > 1$, there is no interference among different resources and thus, the effective channel between the source nodes and the destination nodes including the relays and the filters considering all the N resources can be seen as N parallel channels. It is

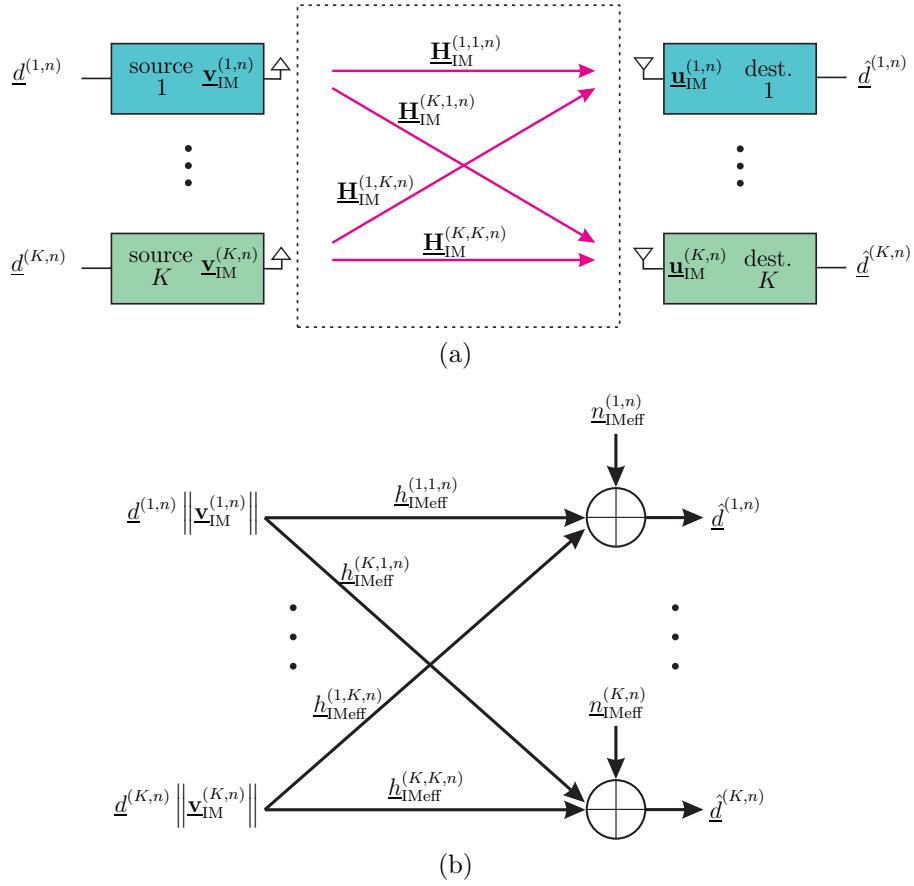


Fig. 6.1: Effective channel in the n -th resource between the source nodes and the destination nodes after applying an IM solution: (a) including the relays, (b) including the filters and the relays.

assumed that the nodes and the relays can always access the N resources simultaneously. Each source node wants to transmit N different uncorrelated data symbols through the N parallel channels to its corresponding destination node. Also, it is assumed that the received noise signals at different resources, different relays, different relay antennas and different destination nodes are uncorrelated.

After applying an IM solution, the transmit filter of the l -th source node in the n -th resource, the receive filter of the k -th destination node in the n -th resource and the processing matrix of the r -th relay in the n -th resource are denoted as $\mathbf{v}_{\text{IM}}^{(l,n)}$, $\mathbf{u}_{\text{IM}}^{(k,n)}$ and $\mathbf{G}_{\text{IM}}^{(r,n)}$, respectively. Then, the resulting effective channel between the l -th source node and the k -th destination node in the n -th resource including the relays is calculated as

$$\mathbf{H}_{\text{IM}}^{(k,l,n)} = \begin{pmatrix} h_{\text{DS}}^{(k,l,n)} & 0 \\ \sum_{r=1}^R \mathbf{h}_{\text{DR}}^{(k,r,n)} \mathbf{G}_{\text{IM}}^{(r,n)} \mathbf{h}_{\text{RS}}^{(r,l,n)} & h_{\text{DS}}^{(k,l,n)} \end{pmatrix}. \quad (6.1)$$

Furthermore, the transmit filter of the l -th source node in the n -th resource can be described as

$$\mathbf{v}_{\text{IM}}^{(l,n)} = \left\| \mathbf{v}_{\text{IM}}^{(l,n)} \right\| \tilde{\mathbf{v}}_{\text{IM}}^{(l,n)}, \quad (6.2)$$

where $\left\| \mathbf{v}_{\text{IM}}^{(l,n)} \right\|$ and $\tilde{\mathbf{v}}_{\text{IM}}^{(l,n)}$ are the norm and the unit vector of the l -th transmit vector $\mathbf{v}_{\text{IM}}^{(l,n)}$ in the n -th resource, respectively. The effective channel in the n -th resource between the source nodes and the destination nodes including the relays for an IM solution is shown in Fig. 6.1a. The vector of the allocated energies at the source nodes in the n -th resource is calculated as

$$\mathbf{E}^{(n)} = \left(E^{(1,n)}, \dots, E^{(K,n)} \right)^{\text{T}} \quad (6.3)$$

where

$$E^{(l,n)} = E_{\text{d}} \left\| \mathbf{v}_{\text{IM}}^{(l,n)} \right\|^2. \quad (6.4)$$

is the transmitted energy of the l -th source node in the n -th resource.

For a certain resource n , the effective channel between the l -th source node and the k -th destination node including the filters and the relays can be calculated as

$$\underline{h}_{\text{IMeff}}^{(k,l,n)} = \underline{\mathbf{u}}_{\text{IM}}^{(k,n)*\text{T}} \underline{\mathbf{H}}_{\text{IM}}^{(k,l,n)} \tilde{\mathbf{v}}_{\text{IM}}^{(l,n)}. \quad (6.5)$$

Moreover, the effective received noise signal, see (2.4), at the output of the receive filter $\underline{\mathbf{u}}_{\text{IM}}^{(k,n)}$ of the k -th destination node is calculated as

$$\underline{n}_{\text{IMeff}}^{(k,n)} = \underline{\mathbf{u}}_{\text{IM}}^{(k,n)*\text{T}} \left(\begin{array}{c} \underline{n}_{\text{D}}^{(k,1,n)} \\ \sum_{r=1}^R \underline{\mathbf{h}}_{\text{DR}}^{(k,r,n)} \underline{\mathbf{G}}_{\text{IM}}^{(r,n)} \underline{\mathbf{u}}_{\text{R}}^{(r,n)} + \underline{n}_{\text{D}}^{(k,2,n)} \end{array} \right). \quad (6.6)$$

Thanks to the linearity of the system, the effective channel between the source nodes and the destination nodes including the temporal filters and the relays for any resource n can be seen as an interference channel as shown in Fig. 6.1b. By substituting (6.5) and (6.6) in (2.13), the received SINR at the output of the receive filter of the k -th destination node in the n -th resource is calculated as

$$\gamma_{\text{IM}}^{(k,n)} = \frac{E^{(k,n)} \left| \underline{h}_{\text{IMeff}}^{(k,k,n)} \right|^2}{\sum_{l \neq k} E^{(l,n)} \left| \underline{h}_{\text{IMeff}}^{(k,l,n)} \right|^2 + \left(\sigma_{\text{IMeff}}^{(k,n)} \right)^2}, \quad (6.7)$$

with the noise power at the output of the receive filter of the k -th destination node in the n -th resource being calculated as

$$\left(\sigma_{\text{IMeff}}^{(k,n)} \right)^2 = \text{E} \left\{ \underline{n}_{\text{IMeff}}^{(k,n)*} \underline{n}_{\text{IMeff}}^{(k,n)} \right\}. \quad (6.8)$$

Note that the first term in the denominator of (6.7) describes the unaligned interference power remaining at the output of the receive filter of the k -th destination node in the n -th resource. Similar to the derivation of (4.9), the total energy retransmitted by the relays can be written as a function of the transmitted energies $E^{(l,n)}$, $l = 1, \dots, K$ of the source nodes as

$$E_{\text{Rtot}} = \sum_{n=1}^N \left(\sum_{l=1}^K \beta_{\text{IM}}^{(l,n)} E^{(l,n)} + \left(\sigma_{\text{IMtx}}^{(n)} \right)^2 \right), \quad (6.9)$$

where

$$\beta_{\text{IM}}^{(l,n)} = \left| \tilde{v}_{\text{IM}}^{(l,1,n)} \right|^2 \sum_{r=1}^R \text{tr} \left(\mathbf{G}_{\text{IM}}^{(r,n)} \mathbf{h}_{\text{RS}}^{(r,l,n)} \mathbf{h}_{\text{RS}}^{(r,l,n)*\text{T}} \mathbf{G}_{\text{IM}}^{(r,n)*\text{T}} \right) \quad (6.10)$$

scales the l -th source node transmitted energy in the n -th resource to the useful retransmitted energy of the relays corresponding to the l -th data symbol and

$$\left(\sigma_{\text{IMtx}}^{(n)} \right)^2 = \sigma^2 \sum_{r=1}^R \text{tr} \left(\mathbf{G}_{\text{IM}}^{(r,n)} \mathbf{G}_{\text{IM}}^{(r,n)*\text{T}} \right) \quad (6.11)$$

is the limited noise energy retransmitted by the relays in the n -th resource. Based on (6.3) and (6.10), the vector of the energies used by the source nodes and the relays for transmitting the K data symbols in the n -th resource is calculated as

$$\boldsymbol{\varepsilon}^{(n)} = \begin{pmatrix} \varepsilon^{(1,n)} \\ \vdots \\ \varepsilon^{(K,n)} \end{pmatrix} = \mathbf{E}^{(n)} + \begin{pmatrix} \beta_{\text{IM}}^{(1,n)} & & \mathbf{0} \\ & \ddots & \\ \mathbf{0} & & \beta_{\text{IM}}^{(K,n)} \end{pmatrix} \mathbf{E}^{(n)}, \quad (6.12)$$

where the first term and the second term of (6.12) describe the energies used for transmitting the K data symbols by the source nodes and the relays, respectively.

The rest of this chapter is organized as follows. The next section investigates the energy allocation on the top of an IM solution considering only a single resource $N = 1$. The energy allocation on the top of IM solutions using multiple resources $N > 1$ is studied in Section 6.3. Finally, the complexity and the performance analyses of the proposed algorithms are discussed in Section 6.4.

6.2 Energy allocation for a single resource in an interference mitigation system

6.2.1 Problem statement and reformulation

In this section, the energy allocation on the top of an IM solution in a single resource is investigated. Because the communication among the node pairs and the relays takes

place through a single shared resource $N = 1$, the resource index n is skipped in the following analysis. As described in the previous section, the effective channel including the filters and the relays is an interference channel as shown in Fig. 6.1b. Using (6.7) and (6.9), the energy allocation optimization problem aiming at maximizing the sum rate with a total energy constraint can be stated as

$$\mathbf{E}_{\text{opt}} = \arg \max_{\mathbf{E}} \left\{ \frac{1}{2} \sum_{k=1}^K \text{ld} \left(1 + \frac{E^{(k)} |h_{\text{IMeff}}^{(k,k)}|^2}{\sum_{l \neq k} E^{(l)} |h_{\text{IMeff}}^{(k,l)}|^2 + (\sigma_{\text{IMeff}}^{(k)})^2} \right) \right\} \quad (6.13)$$

subject to

$$\sum_{k=1}^K E^{(k)} + \sum_{k=1}^K \beta_{\text{IM}}^{(k)} E^{(k)} + \sigma_{\text{IMtx}}^2 = E_{\text{tot}}, \quad (6.14)$$

and

$$E^{(k)} \geq 0, \forall k. \quad (6.15)$$

The first term and the second term of (6.14) describe the energies of the useful signals transmitted from the source nodes and the relays, respectively. Because amplify and forward relaying are considered, part of the retransmitted signals of the relays is a retransmitted noise with a certain limited energy which is represented by the third term of (6.14). Moreover, the constraints of (6.14)–(6.15) form a convex set while the objective function $\frac{1}{2} \sum_{k=1}^K \text{ld} \left(1 + \gamma_{\text{IM}}^{(k)} \right)$ is not a concave function of $E^{(k)}$, $k = 1, \dots, K$, i.e., it has many local maxima and a global maximum. Therefore, the optimization problem of (6.13)–(6.15) is a non-convex problem. Generally speaking, the sum rate maximization problem in interference networks is a non-convex problem and it is still an open problem [LZ08, HL09].

The trick to solve the optimization problem of (6.13)–(6.15) is based on reformulating the objective function of the sum rate as a difference of two concave functions [AW12]. Define

$$g_1(\mathbf{E}) = \frac{1}{2} \sum_{k=1}^K \text{ld} \left(E^{(k)} |h_{\text{IMeff}}^{(k,k)}|^2 + \sum_{l \neq k} E^{(l)} |h_{\text{IMeff}}^{(k,l)}|^2 + (\sigma_{\text{IMeff}}^{(k)})^2 \right) \quad (6.16)$$

as a function of the received useful powers, received interference powers and the received noise powers. Also, let

$$g_2(\mathbf{E}) = \frac{1}{2} \sum_{k=1}^K \text{ld} \left(\sum_{l \neq k} E^{(l)} |h_{\text{IMeff}}^{(k,l)}|^2 + (\sigma_{\text{IMeff}}^{(k)})^2 \right) \quad (6.17)$$

be a function of the received interference powers and received noise powers. Because the logarithm is a concave monotonically increasing function, both $g_1(\mathbf{E})$ and $g_2(\mathbf{E})$

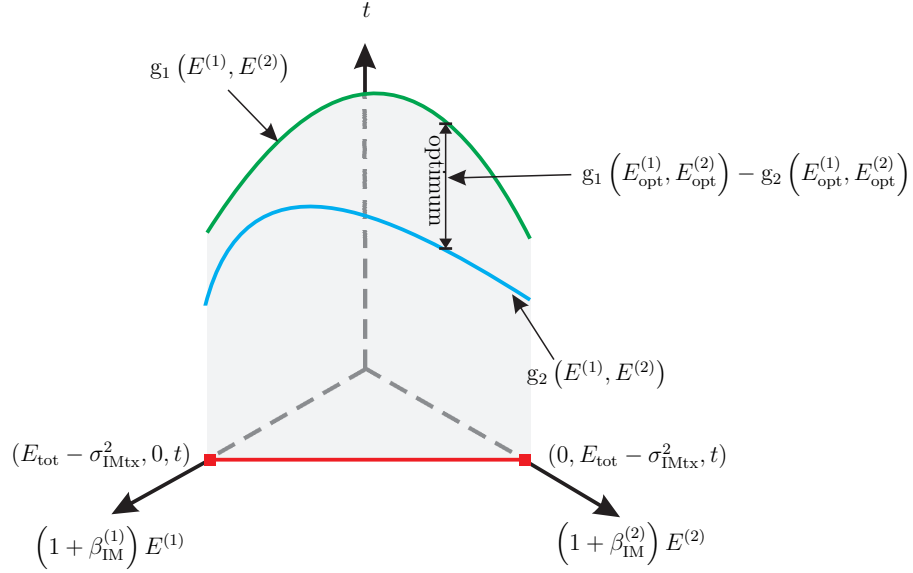


Fig. 6.2: Geometric representation of the DC problem of (6.18)–(6.20) for a two node pair scenario.

are concave functions of the allocated energies \mathbf{E} . Then, using the quotient property of the logarithms, the optimization problem of (6.13)–(6.15) can be reformulated as

$$\mathbf{E}_{\text{opt}} = \arg \max_{\mathbf{E}} \{g_1(\mathbf{E}) - g_2(\mathbf{E})\} \quad (6.18)$$

subject to

$$\sum_{k=1}^K \left(1 + \beta_{\text{IM}}^{(k)}\right) E^{(k)} + \sigma_{\text{IMtx}}^2 = E_{\text{tot}}, \quad (6.19)$$

and

$$E^{(k)} \geq 0, \forall k. \quad (6.20)$$

The new formulation of (6.18)–(6.20) fits in a class of the global optimization methods known as difference of two convex functions (DC) programming [HPTd91, HT99, HPT00]. The range of the functions $g_1(\mathbf{E})$ and $g_2(\mathbf{E})$ are in \mathbb{R} which can be represented as an additional dimension t as shown in Fig. 6.2. The DC problem of (6.18)–(6.20) can be illustrated considering a two node pair scenario shown in Fig. 6.2. For the two node pair scenario, the constraints of (6.19) and (6.20) form the line segment between $(E_{\text{tot}} - \sigma_{\text{IMtx}}^2, 0, t)$ and $(0, E_{\text{tot}} - \sigma_{\text{IMtx}}^2, t)$ for any $t \in \mathbb{R}$ where any point in this line represents a valid energy allocation. Within this feasible energy allocations region, the energy allocation which leads to the largest difference between $g_1(\mathbf{E})$ and $g_2(\mathbf{E})$ is the optimum one as illustrated in Fig. 6.2.

In the following, the new DC formulation of (6.18)–(6.20) is exploited aiming at finding

the global maximum sum rate efficiently instead of extensively searching over infinitely many possible energy allocations.

6.2.2 Branch and bound algorithm – basic idea

To solve the DC problem of (6.18)–(6.20), a branch and bound algorithm is proposed. Because the sum rate function over the feasible region has many maxima, the algorithm searches in different parts of the feasible region seeking for the global maximum sum rate rather than a local one. As the algorithm name indicates,

- the algorithm splits the closed region of the feasible energy allocations recursively into subregions. This process is called branching.
- Then for each subregion, the algorithm bounds the maximum sum rate from above and below. This process is called bounding.

Based on the recursive behavior of the algorithm, it can be implemented efficiently using a tree search mechanism. Basically, a breadth-first search over a full binary tree illustrated in Fig. 6.3 is done.

- The root of the tree corresponds to the whole feasible region.
- Each node i in the tree has two children with indices $2i$ and $2i + 1$.
- The subregion of the feasible energy allocation corresponding to the i -th tree node is split into two subregions corresponding to the children tree nodes $2i$ and $2i + 1$.
- Based on the bounding process which will be explained later in Section 6.2.4, a tree node i is considered as a leaf, i.e., it has no children, if one of the following two cases is satisfied.
 - It is guaranteed that the global maximum sum rate is not achievable using any of the energy allocations in the corresponding feasible subregion.
 - A local maximum sum rate which is close enough to the upper bound is found using an energy allocation in the corresponding feasible subregion.

This means that the branch and bound algorithm does not search the complete tree.

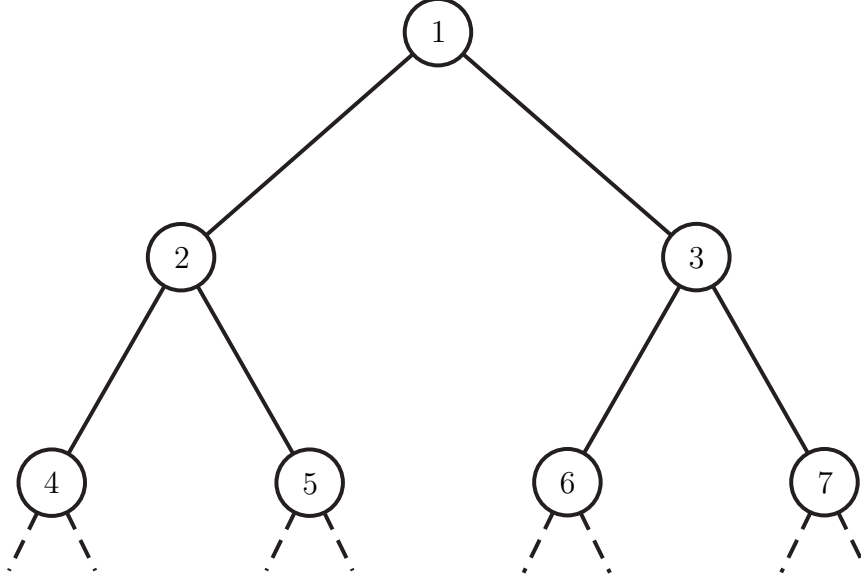


Fig. 6.3: A full binary tree where the root corresponds to the whole feasible region while any other tree node corresponds to part of the feasible region.

For every inspected tree node i , an upper bound $u_b^{(i)}$ and a lower bound $l_b^{(i)}$ of the maximum sum rate achieved within the respective feasible region are calculated. The computations of the bounds are described in Section 6.2.4.

Since the maximum sum rate is the objective, a lower bound is an achievable sum rate and the corresponding energy allocation is feasible. Additionally, the highest known lower bound, i.e., the lower bound which is closest to the global maximum sum rate, is an interesting one and needs to be updated throughout the search over the tree as

$$l_{\text{best}}^{(i)} = \max \left\{ l_{\text{best}}^{(i-1)}, l_b^{(i)} \right\}, \quad (6.21)$$

with

$$l_{\text{best}}^{(0)} = 0, \quad (6.22)$$

where i is the index of the currently inspected tree node. The energy allocation corresponding to the highest lower bound $l_{\text{best}}^{(i)}$ is denoted by $\mathbf{E}_{\text{best}}^{(i)}$. By inspecting the i -th tree node, three cases need to be distinguished:

1. If $u_b^{(i)} - l_{\text{best}}^{(i)} < 0$, the global maximum sum rate is not within this subregion of the i -th tree node as there exists an achievable sum rate $l_{\text{best}}^{(i)}$ which exceeds the upper bound of this subregion. Hence, there is no need to inspect the children of the i -th tree node which is considered as a leaf.

2. If $u_b^{(i)} - l_{\text{best}}^{(i)} > \epsilon$ with an arbitrary small tolerance value $\epsilon > 0$, the feasible subregion of the i -th tree node may contain an energy allocation corresponding to the global maximum but a lower bound which is close to the upper bound $u_b^{(i)}$ still has to be found. So, the two children tree nodes $2i$ and $2i + 1$ need to be inspected.
3. If $0 \leq u_b^{(i)} - l_{\text{best}}^{(i)} \leq \epsilon$, the lower bound $l_{\text{best}}^{(i)}$ is a local maximum of the sum rate within the feasible subregion of the i -th tree node with some acceptable precision if $\mathbf{E}_{\text{best}}^{(i)}$ is within the i -th tree node subregion and it can be a global maximum if no other tree nodes with higher lower bounds than $l_{\text{best}}^{(i)}$ are found later on during the search.

Finally, the algorithm terminates when no more tree nodes have to be inspected with a global optimum energy allocation $\mathbf{E}_{\text{best}}^{(I)}$ corresponding to $l_{\text{best}}^{(I)}$ where I denotes the index of the last inspected tree node.

In the next two sections, the branching and the bounding processes are described in detail.

6.2.3 Branching the feasible region

In this section, the process of splitting up the feasible region into subregions is described. At first, geometric shapes, namely a simplex and a face of a simplex are defined.

Definition 3. A K -simplex

$$\Psi = [\boldsymbol{\nu}^{(0)}, \dots, \boldsymbol{\nu}^{(K)}] \quad (6.23)$$

has $K + 1$ vertices $\boldsymbol{\nu}^{(k)}$, $k = 0, \dots, K$, in \mathbb{R}^K where $\boldsymbol{\nu}^{(0)}$ is the vertex at the origin as shown in Fig. 6.4. Now, let $\omega^{(k)}$ with $k = 0, \dots, K$ be scalars satisfying $\sum_{k=0}^K \omega^{(k)} = 1$ and $0 \leq \omega^{(k)} \leq 1$. Then, any point \mathbf{i} within the simplex Ψ can be represented uniquely as a weighted sum of the vertices as

$$\mathbf{i} = \sum_{k=0}^K \omega^{(k)} \boldsymbol{\nu}^{(k)}. \quad (6.24)$$

Note that column vectors are used to describe the coordinates of the point \mathbf{i} and the vertices $\boldsymbol{\nu}^{(k)}$ for all k . Examples of a 1-simplex, a 2-simplex and a 3-simplex are illustrated in Fig. 6.4.

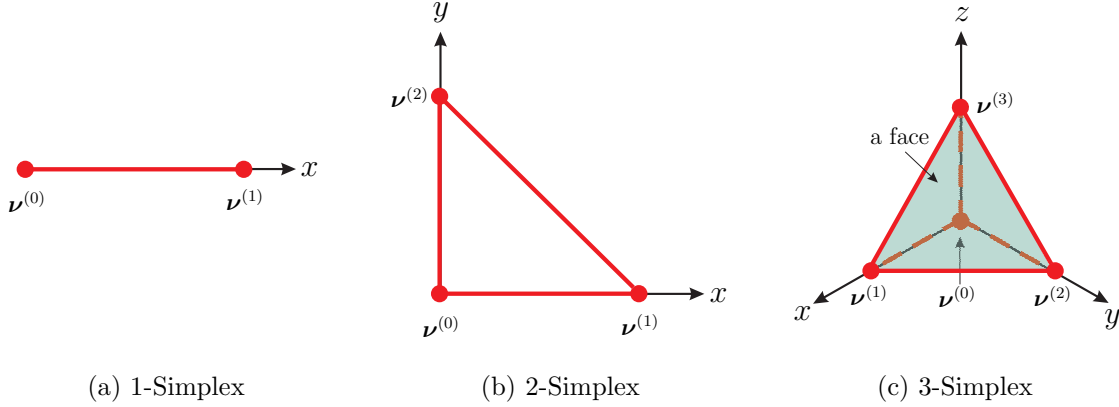


Fig. 6.4: Simplicies with (a) two vertices, (b) three vertices and (c) four vertices.

Definition 4. Let Ψ and Υ be two simplices. If the set of the vertices of Υ is a subset of the set of vertices of Ψ , then Υ is called a face of the simplex Ψ .

For instance, Fig. 6.4c shows a 2-dimensional face of the 3-simplex with the three vertices $\nu^{(1)}$, $\nu^{(2)}$ and $\nu^{(3)}$.

Basically, the region of the feasible energy allocations at the source nodes and the relays described by the constraint set of (6.19) and (6.20) forms a convex set with flat faces, i.e., it forms a $(K - 1)$ -dimensional polytope. Therefore, it can exactly be covered by a $(K - 1)$ -dimensional face $\Upsilon^{(1,K)}$ where $\Upsilon^{(i,K)}$ denotes a face corresponding to the i -th tree node, constructed from a K -simplex and having all the K -simplex vertices except the one at the origin as shown in the example of Fig. 6.5a. The K vertices of the initial face $\Upsilon^{(1,K)}$ are found by greedily using the total available useful energy $E_{\text{tot}} - \sigma_{\text{IMtx}}^2$ for transmitting only one of the K data symbols. Accordingly, the initial face is described as

$$\Upsilon^{(1,K)} = [\nu^{(1)}, \nu^{(2)}, \dots, \nu^{(K)}], \quad (6.25)$$

where the initial vertices are represented by the vectors

$$\nu^{(1)} = (E_{\text{tot}} - \sigma_{\text{IMtx}}^2, 0, \dots, 0)^{\text{T}}, \quad (6.26)$$

$$\nu^{(2)} = (0, E_{\text{tot}} - \sigma_{\text{IMtx}}^2, 0, \dots, 0)^{\text{T}}, \quad (6.27)$$

and

$$\nu^{(K)} = (0, \dots, 0, E_{\text{tot}} - \sigma_{\text{IMtx}}^2)^{\text{T}}. \quad (6.28)$$

In the branching process, a face which covers the whole or part of the feasible region is split into two smaller faces. In other words, the i -th face $\Upsilon^{(i,K)}$ is split over its longest

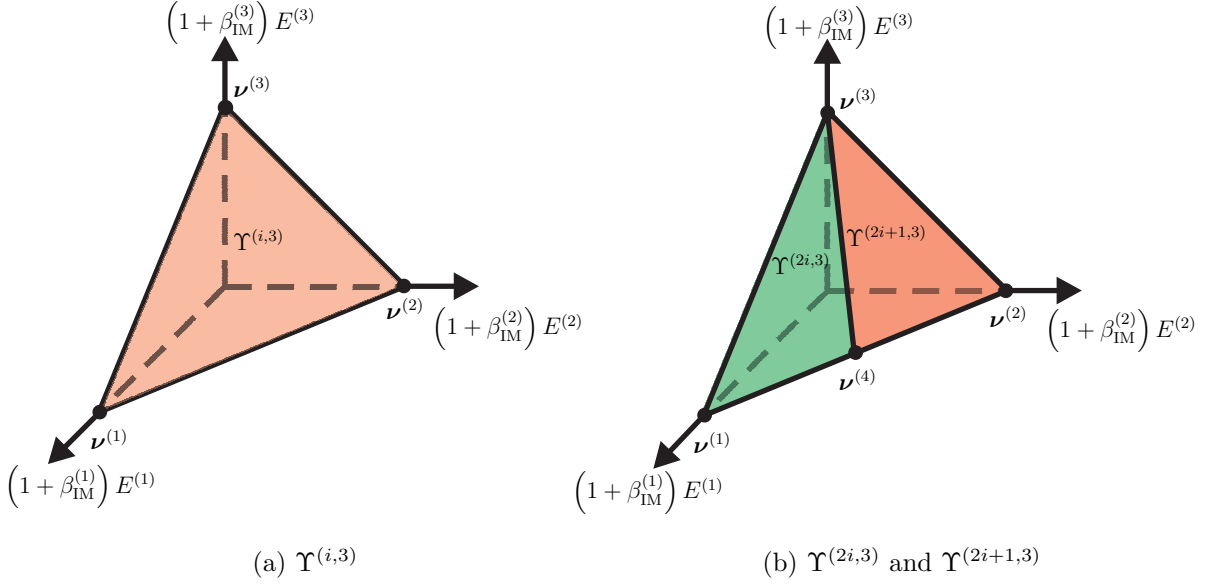


Fig. 6.5: An example of splitting a 2-dimensional face.

edge into the two faces $\Upsilon^{(2i,K)}$ and $\Upsilon^{(2i+1,K)}$. For instance, a total energy constraint of a three node pair $K = 3$ scenario forms 2-dimensional faces. This example is illustrated in Fig. 6.5. The i -th face can be described as

$$\Upsilon^{(i,3)} = [\nu^{(1)}, \nu^{(2)}, \nu^{(3)}]. \quad (6.29)$$

The i -th face is split over its longest edge, i.e., the edge between the vertices $\nu^{(1)}$ and $\nu^{(2)}$, into two faces described as

$$\Upsilon^{(2i,3)} = [\nu^{(1)}, \nu^{(3)}, \nu^{(4)}], \quad (6.30)$$

and

$$\Upsilon^{(2i+1,3)} = [\nu^{(2)}, \nu^{(3)}, \nu^{(4)}]. \quad (6.31)$$

The new vertex which is shared by the two new faces $\Upsilon^{(2i,3)}$ and $\Upsilon^{(2i+1,3)}$ is calculated as

$$\nu^{(4)} = \frac{1}{2} (\nu^{(1)} + \nu^{(2)}). \quad (6.32)$$

6.2.4 Bounding the maximum sum rate

For the i -th tree node with a subregion of feasible energy allocations defined by the $(K - 1)$ -dimensional face $\Upsilon^{(i,K)}$, an upper bound $u^{(i)}$ and a lower bound $l^{(i)}$ of the maximum sum rate are found in this section. For the discussion within this section,

- a single tree node i in the tree is considered for describing the bounding process. Therefore, the tree node index i is skipped.
- the energy $\varepsilon^{(k)}$ employed for transmitting the k -th data symbol is optimized instead of optimizing the transmitted energy $E^{(k)}$ by the k -th source node. There is a linear one to one mapping between these two energies

$$\varepsilon^{(k)} = \left(1 + \beta_{\text{IM}}^{(k)}\right) E^{(k)}. \quad (6.33)$$

By adding a new variable t to the DC problem of (6.18)–(6.20), it can be reformulated as a convex maximization problem stated as

$$(\boldsymbol{\varepsilon}_{\text{opt}}^{\text{T}}, t_{\text{opt}}) = \arg \max_{(\boldsymbol{\varepsilon}^{\text{T}}, t)} \{t - g_2(\boldsymbol{\varepsilon})\} \quad (6.34)$$

subject to

$$t - g_1(\boldsymbol{\varepsilon}) \leq 0, \quad (6.35)$$

$$\sum_{k=1}^K \varepsilon^{(k)} + \sigma_{\text{IMtx}}^2 = E_{\text{tot}}, \quad (6.36)$$

and

$$\varepsilon^{(k)} \geq 0, \forall k. \quad (6.37)$$

The objective function of $t - g_2(\boldsymbol{\varepsilon})$ and the constraint of (6.35) are a convex function and a convex set, respectively. Unfortunately, a convex maximization problem is a non-convex problem as well [HPT00]. The new feasible region described by the constraints of (6.35)–(6.37) is illustrated by the shaded area shown in Fig. 6.2. To find an upper bound of the maximum sum rate within the face $\Upsilon^{(i,K)}$, a linear relaxation of the convex maximization problem of (6.34)–(6.37) will be formulated. The main motivation of relaxing the convex maximization problem of (6.34)–(6.37) to a linear problem is that

- it is needed for finding a good upper bound of the maximum sum rate rather than the maximum sum rate itself.
- there are many efficient methods to solve a linear program with a reasonable complexity such as the simplex method and the active-set method [GMSW84, BJS09].

First, the nonlinear constraint of (6.35) is piece-wisely linearized. Accordingly, the function $g_1(\boldsymbol{\varepsilon})$ is linearly outer approximated using the tangents

$$(\boldsymbol{\varepsilon} - \boldsymbol{\varepsilon}_j)^{\text{T}} \partial g_1(\boldsymbol{\varepsilon}_j) + g_1(\boldsymbol{\varepsilon}_j), \quad \forall \boldsymbol{\varepsilon}_j \in \Omega \quad (6.38)$$

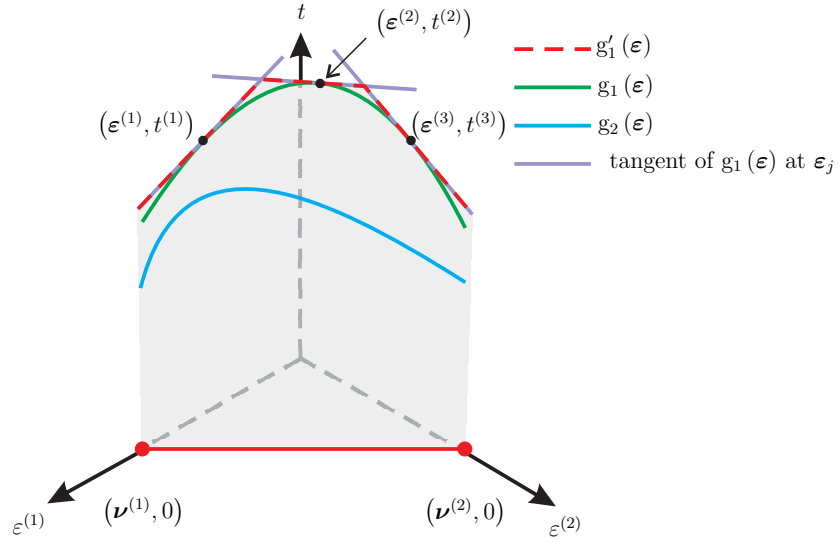


Fig. 6.6: The feasible region of the convex maximization problem of (6.34)–(6.37) forming a K -dimensional polytope when the function $g_1(\boldsymbol{\varepsilon})$ is linearly approximated.

of the function $g_1(\boldsymbol{\varepsilon})$ at different feasible energy allocations $\boldsymbol{\varepsilon}_j$ where Ω denotes a set of feasible energy allocations. Throughout the search over the tree, the energy allocation of the tree node vertices and added to the feasible energy allocation set Ω . The function

$$g'_1(\boldsymbol{\varepsilon}) = \min_{\boldsymbol{\varepsilon}_j \in \Omega} \left\{ (\boldsymbol{\varepsilon} - \boldsymbol{\varepsilon}_j)^T \partial g_1(\boldsymbol{\varepsilon}_j) + g_1(\boldsymbol{\varepsilon}_j) \right\} \quad (6.39)$$

- is piecewise linear and concave.
- is an outer approximation of $g_1(\boldsymbol{\varepsilon})$, i.e., $g'_1(\boldsymbol{\varepsilon}) \geq g_1(\boldsymbol{\varepsilon})$ with equality at all $\boldsymbol{\varepsilon}_j \in \Omega$.
- gets tighter to $g_1(\boldsymbol{\varepsilon})$ as the number of the different feasible energy allocations in the set Ω increases.

From $g'_1(\boldsymbol{\varepsilon}) \geq g_1(\boldsymbol{\varepsilon})$, it follows that

$$g'_1(\boldsymbol{\varepsilon}) - g_2(\boldsymbol{\varepsilon}) \geq g_1(\boldsymbol{\varepsilon}) - g_2(\boldsymbol{\varepsilon}). \quad (6.40)$$

Therefore, replacing $g_1(\boldsymbol{\varepsilon})$ by $g'_1(\boldsymbol{\varepsilon})$ in the optimization problem of (6.34)–(6.37) always yields an upper bound of the maximum sum rate. The shaded area in Fig. 6.6 represents the new feasible region defined by (6.35)–(6.37) considering a two node pair scenario. From Fig. 6.6, one can note that the feasible region is enlarged when considering $g'_1(\boldsymbol{\varepsilon})$ instead of $g_1(\boldsymbol{\varepsilon})$ and it has linear boundaries.

After linearizing the constraint of (6.35), the objective function of $t - g_2(\boldsymbol{\varepsilon})$ will be linearized as well. The function $g_2(\boldsymbol{\varepsilon})$ can be written as a function of the vertices by exploiting the simplex property of (6.24) as

$$g_2(\boldsymbol{\varepsilon}) = g_2\left(\sum_{k=1}^K \omega^{(k)} \boldsymbol{\nu}^{(k)}\right). \quad (6.41)$$

Based on the fact that $g_2(\boldsymbol{\varepsilon})$ is a concave function of $\boldsymbol{\varepsilon}$ and using the Jensen inequality,

$$g_2\left(\sum_{k=1}^K \omega^{(k)} \boldsymbol{\nu}^{(k)}\right) \geq \sum_{k=1}^K \omega^{(k)} g_2(\boldsymbol{\nu}^{(k)}) \quad (6.42)$$

follows with equality at the vertices, i.e., $\omega^{(k)} = 1$ while for $l \neq k$ $\omega^{(l)} = 0$, $k = 1, \dots, K$. It follows that the objective function is lower bounded as

$$t - g_2(\boldsymbol{\varepsilon}) \geq t - \sum_{k=1}^K \omega^{(k)} g_2(\boldsymbol{\nu}^{(k)}). \quad (6.43)$$

Using the simplex property of (6.24), the weighting factors $\omega^{(k)}$ for $k = 1, \dots, K$ can be considered as the optimizing variables instead of the allocated energies $\boldsymbol{\varepsilon}$. Fig. 6.7 illustrates how $g_1'(\boldsymbol{\varepsilon})$ outer approximates $g_1(\boldsymbol{\varepsilon})$ and how $\omega^{(1)} g_2(\boldsymbol{\nu}^{(1)}) + \omega^{(2)} g_2(\boldsymbol{\nu}^{(2)})$ lower bounds $g_2(\boldsymbol{\varepsilon})$. Using the linear approximated constraint of (6.39) and the linear approximated objective function of (6.43), the convex maximization problem of (6.34)–(6.37) is relaxed to a linear program stated as

$$\left(t_{\text{ub}}, \omega_{\text{ub}}^{(1)}, \dots, \omega_{\text{ub}}^{(K)}\right) = \arg \max_{(t, \omega^{(1)}, \dots, \omega^{(K)})} \left\{ t - \sum_{k=1}^K \omega^{(k)} g_2(\boldsymbol{\nu}^{(k)}) \right\} \quad (6.44)$$

subject to

$$t - g_1'\left(\sum_{k=1}^K \omega^{(k)} \boldsymbol{\nu}^{(k)}\right) \leq 0, \quad (6.45)$$

$$\mathbf{1}_{K \times 1} \left(\sum_{k=1}^K \omega^{(k)} \boldsymbol{\nu}^{(k)}\right) + \sigma_{\text{IMtx}}^2 = E_{\text{tot}}, \quad (6.46)$$

$$0 \leq \omega^{(k)} \leq 1, \quad \forall k, \quad (6.47)$$

and

$$\sum_{k=1}^K \omega^{(k)} = 1, \quad (6.48)$$

where $\mathbf{1}_{K \times 1}$ is a K -dimensional vector of ones. The linear program of (6.44)–(6.48) can be solved for finding an upper bound of the sum rate in this face $\Upsilon^{(i,K)}$ as illustrated in Fig. 6.7. Using the active-set method where any of the vertices $(\boldsymbol{\nu}^{(k)}, g_2(\boldsymbol{\nu}^{(k)}))$ can

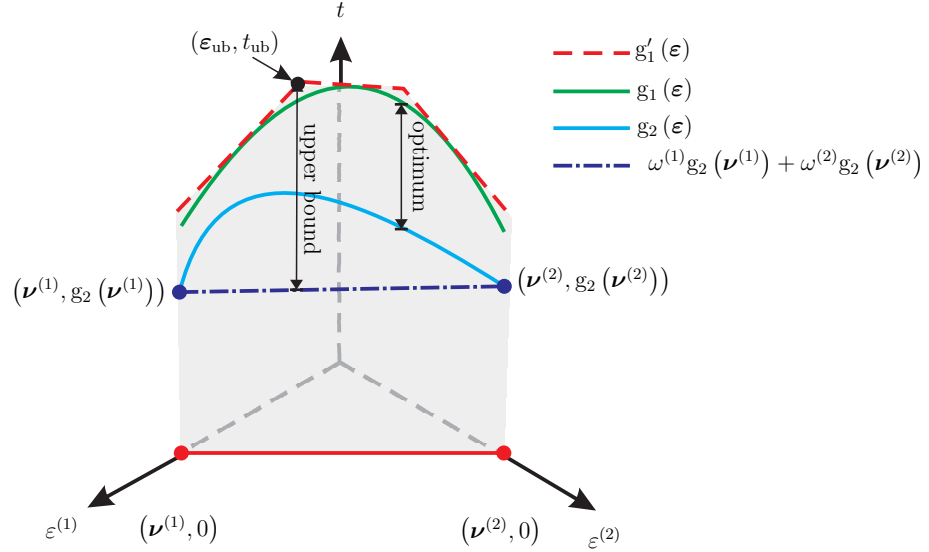


Fig. 6.7: The largest distance between $g'_1(\boldsymbol{\varepsilon})$ and $\sum_{k=1}^K \omega^{(k)} g_2(\boldsymbol{\nu}^{(k)})$ in the t direction always upper bounds the largest distance between $g_1(\boldsymbol{\varepsilon})$ and $g_2(\boldsymbol{\varepsilon})$.

be considered as an initial point [GMSW84], the linear program of (6.44)–(6.48) can be solved. Accordingly, the upper bound is calculated as

$$u_b^{(i)} = t_{\text{ub}} - \sum_{k=1}^K \omega_{\text{ub}}^{(k)} g_2(\boldsymbol{\nu}^{(k)}), \quad (6.49)$$

and the corner point at $g'_1(\boldsymbol{\varepsilon})$ corresponding to the upper bound is denoted as $(\boldsymbol{\varepsilon}_{\text{ub}}, t_{\text{ub}})$ where

$$\boldsymbol{\varepsilon}_{\text{ub}} = \sum_{k=1}^K \omega_{\text{ub}}^{(k)} \boldsymbol{\nu}^{(k)} \quad (6.50)$$

is a valid energy allocation which can be applied as a lower bound candidate.

Regarding to the lower bound $l_b^{(i)}$ of the maximum sum rate at the i -th tree node, any feasible energy allocation yields an achievable sum rate which represents a valid lower bound. Among all the possible lower bounds, the highest one is of interest as it is the closest to the maximum sum rate. To avoid using complex searching heuristics aiming at finding a good lower bound, the energy allocations at the vertices of the face $\Upsilon^{(i,K)}$ as well as the energy allocation found in (6.50) when calculating the i -th upper bound are considered for finding a lower bound $l_b^{(i)}$. Based on this, the lower bound is calculated as

$$l_b^{(i)} = \max \{g_1(\boldsymbol{\varepsilon}) - g_2(\boldsymbol{\varepsilon})\}, \quad (6.51)$$

and the corresponding energy allocation is calculated as

$$\boldsymbol{\varepsilon}_{\text{lb}} = \arg \max_{\boldsymbol{\varepsilon}} \{g_1(\boldsymbol{\varepsilon}) - g_2(\boldsymbol{\varepsilon})\}, \quad (6.52)$$

where

$$\boldsymbol{\varepsilon} \in \{\boldsymbol{\varepsilon}_{\text{ub}}, \boldsymbol{\nu}^{(1)}, \dots, \boldsymbol{\nu}^{(K)}\}. \quad (6.53)$$

Finally, the proposed branch and bound algorithm can be summarized as follows:

- 1: set $l_{\text{best}}^{(0)} = 0$
- 2: for every inspected tree node i
- 3: find $u_{\text{b}}^{(i)}$ ▷ using the linear program of (6.44)–(6.48)
- 4: find $l_{\text{b}}^{(i)}, \boldsymbol{\varepsilon}_{\text{lb}}^{(i)}$ ▷ using (6.51), (6.52)
- 5: update $l_{\text{best}}^{(i)} = \max \{l_{\text{best}}^{(i-1)}, l_{\text{b}}^{(i)}\}$
- 6: update the corresponding $\mathbf{E}_{\text{best}}^{(i)}$
- 7: **if** $u_{\text{b}}^{(i)} - l_{\text{best}}^{(i)} > \epsilon$ **then**
- 8: split $\Upsilon^{(i,K)}$ into $\Upsilon^{(2i,K)}$ and $\Upsilon^{(2i+1,K)}$
- 9: the children tree nodes with indices $2i$ and $2i + 1$ should be inspected
- 10: **end if**
- 11: stop if no more tree nodes to be inspected
- 12: $C_{\text{opt}} = l_{\text{best}}^{(I)}, \mathbf{E}_{\text{opt}} = \mathbf{E}_{\text{best}}^{(I)}$

where I is the index of the last inspected node. Concerning the convergence of the proposed branch and bound algorithm, see the discussion in [HPTd91].

6.3 Energy allocation for multiple orthogonal resources in an interference mitigation system

In this section, the energy allocation for multiple resource scenarios where IM solutions are applied at each resource is investigated. If $N > 1$, a source node transmits simultaneously N uncorrelated data symbols through the N orthogonal resources to its corresponding destination node. Due to the orthogonality of the resources, the effective channel including the relays and the filters can be seen as a parallel interference channel as shown in Fig. 6.8. Let

$$C^{(n)} = \frac{1}{2} \sum_{k=1}^K \text{ld} \left(1 + \gamma_{\text{IM}}^{(k,n)} \right) \quad (6.54)$$

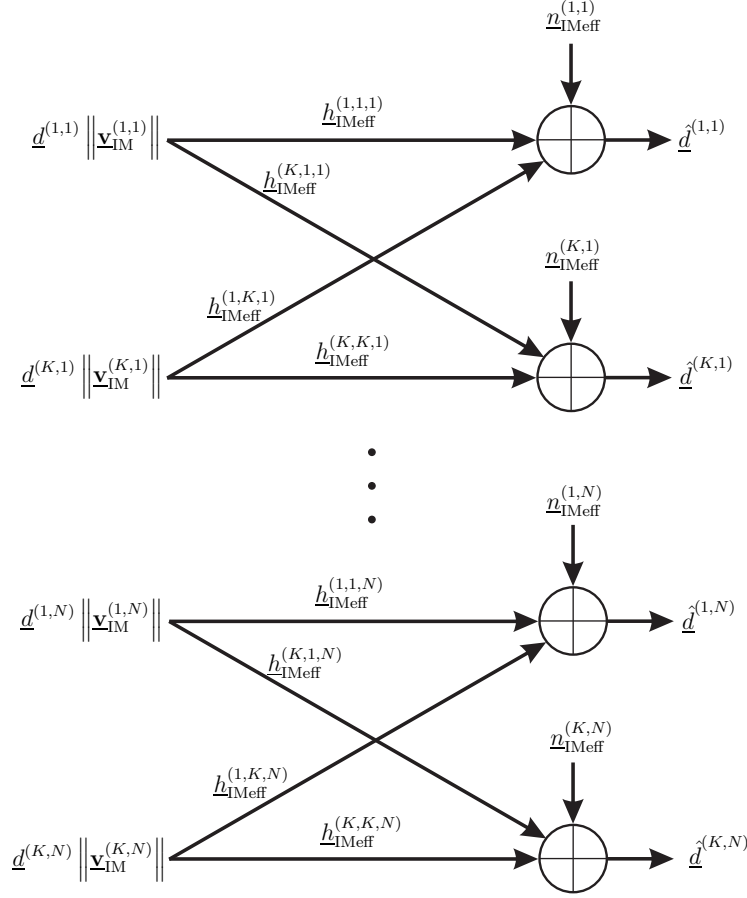


Fig. 6.8: Considering N orthogonal resources, the effective channel including the relays and the filters is a parallel interference channel.

be the sum rate achieved in the n -th resource. After applying an IM solution to each of the N parallel interference channels, the energy allocation optimization problem aiming at maximizing the sum rate with a total energy constraint can be written as

$$\left(\mathbf{E}_{\text{opt}}^{(1)}, \dots, \mathbf{E}_{\text{opt}}^{(N)} \right) = \arg \max_{\left(\mathbf{E}^{(1)}, \dots, \mathbf{E}^{(N)} \right)} \left\{ \sum_{n=1}^N C^{(n)} \right\} \quad (6.55)$$

subject to

$$\sum_{n=1}^N \left(\sum_{k=1}^K \left(1 + \beta_{\text{IM}}^{(k,n)} \right) E^{(k,n)} + \left(\sigma_{\text{IMtx}}^{(n)} \right)^2 \right) = E_{\text{tot}}, \quad (6.56)$$

and

$$E^{(k,n)} \geq 0, \forall k, n. \quad (6.57)$$

The optimization problem of (6.55)–(6.57) is a non-convex problem, i.e., the sum rate function has many local maxima and a global maximum. However, the branch and bound algorithm proposed in the previous section can be applied to find the global maximum sum rate. In this case, the complexity of the branch and bound algorithm

grows exponentially with the number N of resources because the dimensions of the feasible region increase linearly with N , i.e., the dimension of the face which describes the feasible region is $NK - 1$.

The objective function – the sum rate – is an additive function of the sum rates $C^{(n)}$ achieved in different resources. Because there are no interferences among different resources, the objective function can be decoupled into sub-objectives each of which is aiming at maximizing the sum rate in a certain resource. However, the constraint of (6.56) can not be decomposed among the resources as there is a total energy constraint E_{tot} rather than a per-resource energy constraint $E_{\text{totn}}^{(n)}$. If the optimum split of the total energy constraint among the resources is found, the optimization problem of (6.55)–(6.57) can be decomposed into N subproblems each subproblem corresponding to a single resource n which can be stated as

$$\mathbf{E}_{\text{opt}}^{(n)} = \arg \max_{\mathbf{E}^{(n)}} \{C^{(n)}\} \quad (6.58)$$

subject to

$$\sum_{k=1}^K \left(1 + \beta_{\text{IM}}^{(k,n)}\right) E^{(k,n)} + \left(\sigma_{\text{IMtx}}^{(n)}\right)^2 = E_{\text{totn}}^{(n)}, \quad (6.59)$$

and

$$E^{(k,n)} \geq 0, \forall k. \quad (6.60)$$

Accordingly, the branch and bound algorithm can be applied to each resource individually. In this case, the complexity of finding the global maximum sum rate grows linearly with the number N of resources. Unfortunately, the optimum split of the total energy among the resources is not known.

To find the optimum split of the total energy among the resources, the behavior of the optimum sum rate as a function of the total energy per resource has to be understood. Considering a single resource n , the Lagrange of the optimization problem of (6.58)–(6.60) can be written as

$$\mathbf{L}(\mathbf{E}^{(n)}, \lambda) = C^{(n)} - \lambda \left(\sum_{k=1}^K \left(1 + \beta_{\text{IM}}^{(k,n)}\right) E^{(k,n)} + \left(\sigma_{\text{IMtx}}^{(n)}\right)^2 - E_{\text{totn}}^{(n)} \right), \quad (6.61)$$

where λ denotes the Lagrangian multiplier. The dual function can be calculated as

$$\mathbf{d}(\lambda) = \max_{\mathbf{E}^{(n)}} \{\mathbf{L}(\mathbf{E}^{(n)}, \lambda)\}, \quad (6.62)$$

and the optimum Lagrangian multiplier is given by

$$\lambda_{\text{opt}} = \arg \min_{\lambda} \{\mathbf{d}(\lambda)\}. \quad (6.63)$$

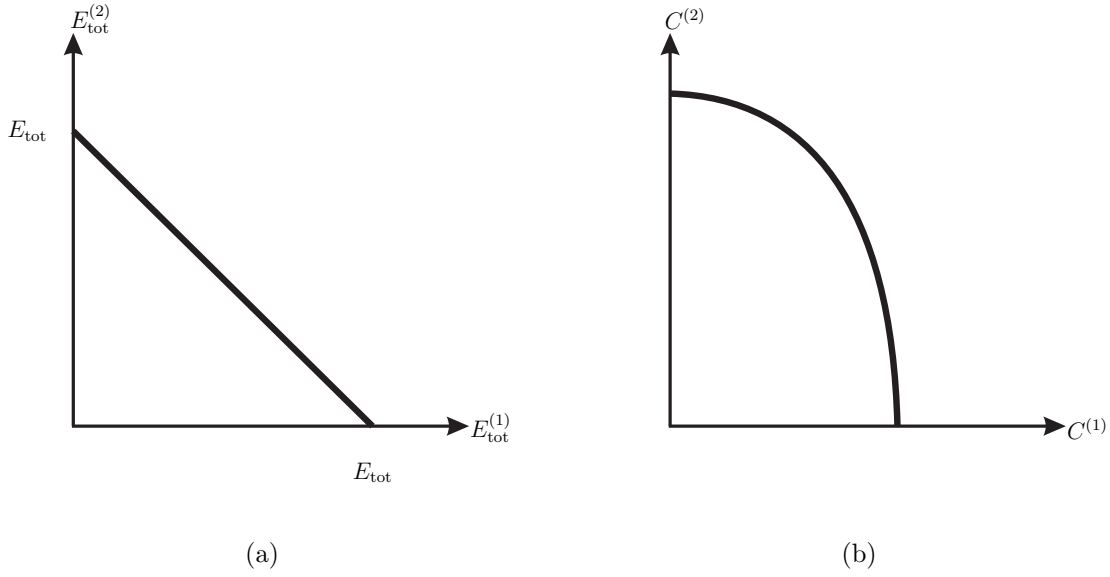


Fig. 6.9: (a) the possible total energy splits among a two resource scenario and (b) the resulting rate region after applying the branch and bound algorithm at each resource.

Now, let

$$f_{\text{dual}} \left(E_{\text{totn}}^{(n)} \right) = C_{\text{opt}}^{(n)} - \lambda_{\text{opt}} \left(\sum_{k=1}^K \left(1 + \beta_{\text{IM}}^{(k,n)} \right) E_{\text{opt}}^{(k,n)} + \left(\sigma_{\text{IMtx}}^{(n)} \right)^2 - E_{\text{totn}}^{(n)} \right) \quad (6.64)$$

be the optimum sum rate in the n -th resource as a function of the total energy constraint. The function $f_{\text{dual}} \left(E_{\text{totn}}^{(n)} \right)$ is a strictly monotonic increasing concave function, see the proof in Appendix B.2. In other words, the global maximum sum rate increases as the total energy increases. For a two resource scenario, Fig. 6.9a shows all the possible total energy splits among the two resources. Because the total energy constraint is considered only with equality, the energy splits form a line segment between the extreme points of allocating the total energy to one of the resources. For each energy split, the branch and bound algorithm can be applied to find the global maximum sum rate in every resource. Accordingly, the resulting rate region forms a convex envelope as shown in Fig. 6.9b.

In addition to the N subproblems of (6.58)–(6.60), the master problem which finds the optimum split of the total energy is stated as

$$\left(E_{\text{totn,opt}}^{(1)}, \dots, E_{\text{totn,opt}}^{(N)} \right) = \arg \max_{\left(E_{\text{totn}}^{(1)}, \dots, E_{\text{totn}}^{(N)} \right)} \left\{ \sum_{n=1}^N f_{\text{dual}} \left(E_{\text{totn}}^{(n)} \right) \right\} \quad (6.65)$$

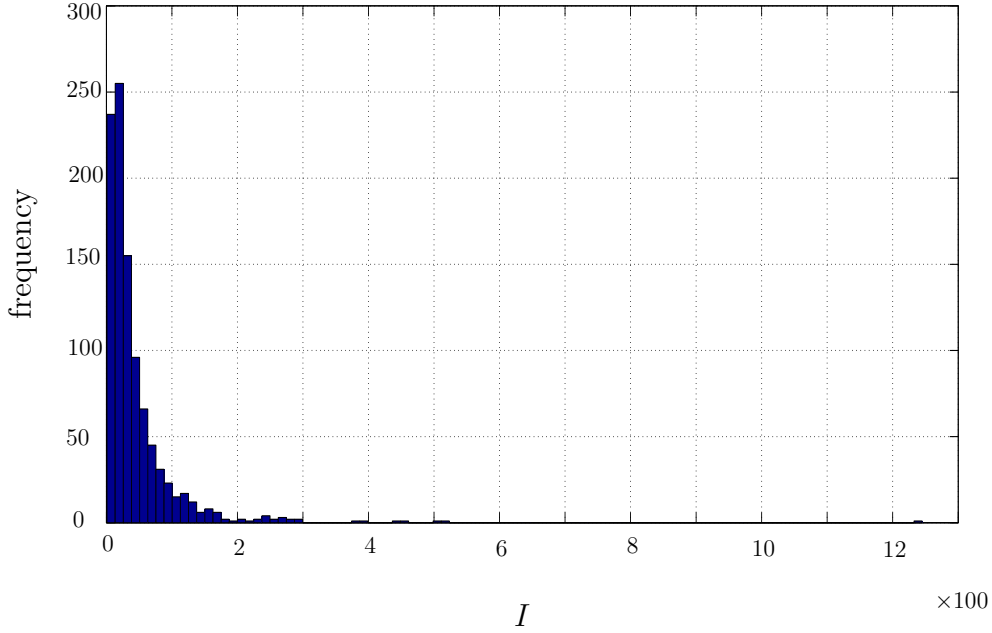


Fig. 6.10: A histogram of the number of inspected tree nodes I needed for a convergence to the global maximum sum rate for 1000 random snapshots.

subject to

$$\sum_{n=1}^N E_{\text{totn}}^{(n)} = E_{\text{tot}}, \quad (6.66)$$

and

$$E_{\text{totn}}^{(n)} \geq 0, \forall n. \quad (6.67)$$

The optimization problem of (6.65)–(6.67) is convex because the objective function of $\sum_{n=1}^N f_{\text{dual}}(E_{\text{totn}}^{(n)})$ is concave, i.e., see the proof in Appendix B.2 and the constraints of (6.66)–(6.67) form a convex set [AW11a]. Therefore, it can be solved using a conventional convex optimization tool.

6.4 Complexity and performance of the energy allocation algorithms

6.4.1 Complexity analysis

In this section, the complexity of the proposed branch and bound algorithm is investigated. The complexity of inspecting a tree node is dominated by calculating the upper

bound which requires solving a linear program. The complexity of solving a linear program using some of the conventional algorithms is discussed in [Meg89]. It is worth to mention that the complexity of solving the linear program increases as the number of inspected tree nodes increases. As the number of inspected tree nodes increases, the size of the set Ω of feasible energy allocations increases and thus, the number of tangents which approximate $g_1(\epsilon)$ increases. As a result, the number of constraints of (6.45) increases which increases the complexity of the linear program.

Actually, it is difficult to analytically study how the required number I of inspected nodes increases with the number K of node pairs. However, a simulation result depicting a histogram of the total number of inspected nodes I for a three node pairs $K = 3$ scenario with $N = 1$, $R = 3$, $M = 1$, $\gamma_{\text{PSNR}} = 30$ dB, $\epsilon = 10^{-6}$ and 1000 channel snapshots is shown in Fig. 6.10. As shown in the figure, the number I of inspected tree nodes varies between few tree nodes and around 1300 tree nodes. However, there is a high density of trials with $I < 100$ inspected tree nodes which shows that the proposed algorithm can be applied in realistic systems.

As discussed in Section 6.3, the optimization problem of (6.55)–(6.57) is decomposed among the resources into subproblems which can be solved simultaneously by applying the branch and bound algorithm to each subproblem. Accordingly, the complexity of the algorithm increases linearly with the number N of resources.

6.4.2 Performance analysis

In this section, the performance of the proposed branch and bound algorithm is investigated. A scenario with $K = 3$, $N = 1$, $R = 3$ and $M = 1$ is considered. Among the different IM algorithms proposed in Chapter 5, the one with fixed filters proposed in Section 5.2 is applied because the design of the relay coefficients depends only on the channel coefficients rather than the amount of the transmitted energies. In this case, the effective channel including the relays and the filters is independent of the PSNRs. Moreover, the coefficients of the transmit and receive filters are adjusted as described in Section 3.5.3. According to this setup, the effective channel including the relays and the filters is an interference channel as shown in Fig. 6.1b.

To assess the performance of the proposed branch and bound algorithm, well known energy allocation algorithms are considered as benchmarks. Firstly, the equal energy allocation algorithm which serves the data symbols transmitted by the source nodes

and the relays with equal energies

$$\varepsilon^{(k)} = \frac{E_{\text{tot}} - \sigma_{\text{retx}}^2}{K}, \quad \forall k. \quad (6.68)$$

The second benchmark is the SIR balancing which aims at maximizing the minimum SIR. This results in equal SIRs

$$\frac{E^{(k)} |h_{\text{IMeff}}^{(k,k)}|^2}{\sum_{l \neq k} E^{(l)} |h_{\text{IMeff}}^{(k,l)}|^2} = \gamma_{\text{SIRb}} \quad (6.69)$$

at all the destination nodes $k = 1, \dots, K$. Thirdly, the greedy energy allocation algorithm which uses all the available useful energy for transmitting a single data symbol k corresponding to the node pair with the highest ratio of the effective useful channel gain and the effective noise power

$$\varepsilon^{(k)} = \begin{cases} E_{\text{tot}} - \sigma_{\text{retx}}^2 & k = k_{\text{best}} \\ 0 & \text{otherwise,} \end{cases} \quad \forall k. \quad (6.70)$$

where

$$k_{\text{best}} = \arg \max_k \left\{ \frac{|h_{\text{IMeff}}^{(k,k)}|^2}{(\sigma_{\text{IMeff}}^{(k)})^2} \right\}, \quad \forall k. \quad (6.71)$$

The final reference energy allocation algorithm is the waterfilling algorithm described in Section 4.2 which ignores the interferences and maximizes the sum rate by allocating more energies to node pairs with low noise levels as illustrated in Fig. 4.2. Because the waterfilling algorithm does not consider the interferences, it is a suboptimum algorithm.

In the following simulation results, the sum rates achieved using the proposed branch and bound algorithm with $\epsilon = 10^{-6}$ as well as the benchmarks are calculated for many different channel snapshots with many different positions of the relays and the destination nodes after applying the IM algorithm described in Section 5.2. Fig. 6.11 depicts the achieved average sum rates as a function of the PSNRs. At low PSNRs, the energy is scarce and thus, the noise is dominant. As a consequence, using the whole available energy for the best node pair, e.g., applying the greedy allocation, is beneficial as compared to serving all the node pairs and generating more noise, i.e., using equal energy allocation and SIR balancing.

As the PSNR increases, the interference energy increases and becomes dominant. At the moderate PSNR regime, serving only the best node pair is not the optimum anymore,

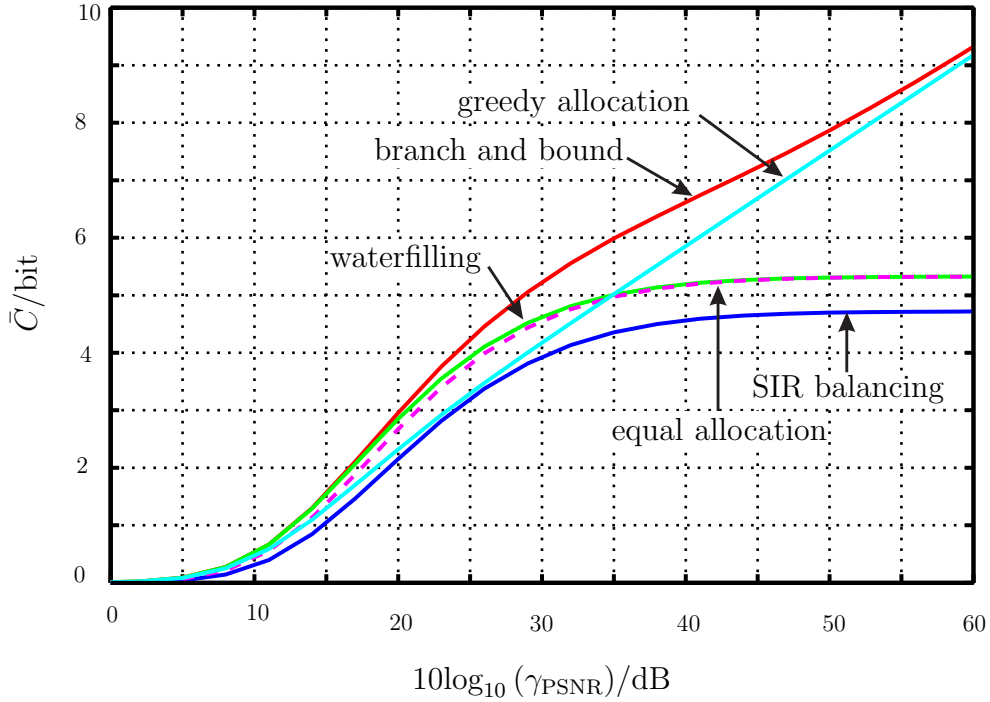


Fig. 6.11: Achieved sum rate as a function of PSNR for a scenario with $K = 3$, $N = 1$, $R = 3$ and $M = 1$ using different energy allocation algorithms.

i.e., greedy allocation is suboptimum. Also, serving all node pairs aiming at equalizing the SIR is the worst algorithm because it serves bad node pairs as well which generates more interference and hence, degrades the sum rate. Moreover, serving the node pairs with equal energies achieves a sum rate close to the maximum but as the interference increases, it diverges from the maximum. One can also note that at the moderate and high PSNR regimes, the sum rate achieved by the greedy allocation increases as the PSNRs increases but for other algorithms like equal energy allocation and SIR balancing which serve all nodes, it saturates at certain levels. Furthermore, waterfilling diverges from the maximum and uses almost the same amount of energies for transmitting all the data symbols because the noise levels are very small as compared to the transmitted energies. Therefore, waterfilling achieves the same sum rates as the equal energy allocation algorithm. Finally, at high PSNRs, a high interference is generated upon transmitting more than one data symbol. Therefore, greedy allocation achieves sum rate close to the global optimum. Furthermore, the branch and bound algorithm converges to the global maximum sum rate at the whole range of the PSNRs and it outperforms all the other algorithms.

For the same scenario and simulation setup, a CCDF of the sum rates achieved at $\gamma_{\text{PSNR}} = 35$ dB is depicted in Fig. 6.12. As shown in the figure, the branch and bound algorithm achieves always the highest sum rate for all channel snapshots. Furthermore,

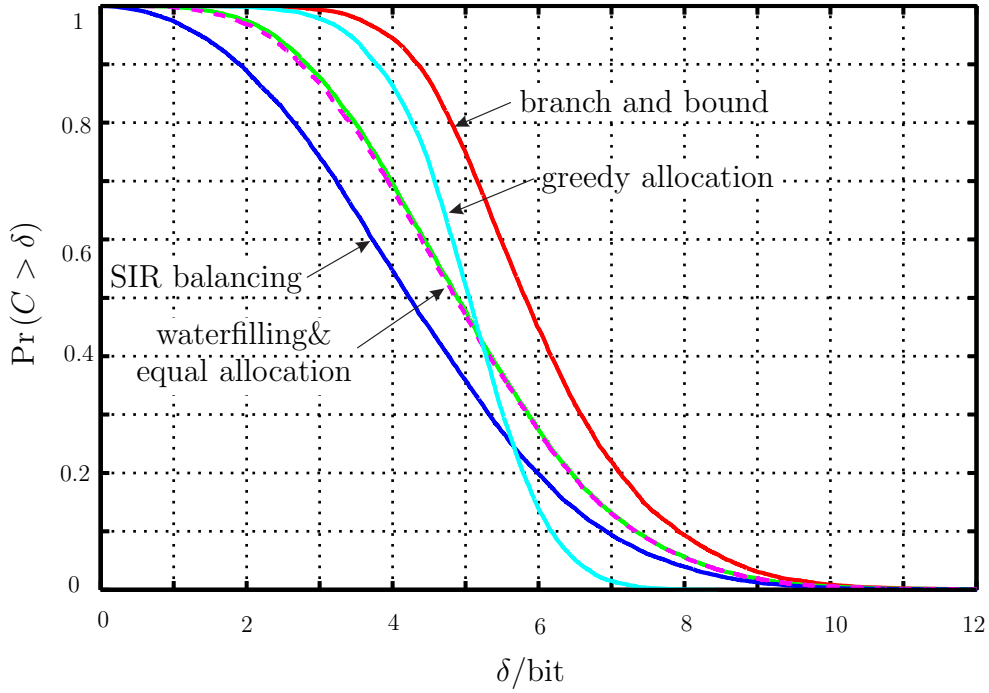


Fig. 6.12: CCDF of the achieved sum rates at a PSNR of 35 dB in a scenario with $K = 3$, $N = 1$, $R = 3$ and $M = 1$ for different energy allocation algorithms.

an outage capacity of $C_{\text{out}} = 4.4$ bits is achieved by the branch and bound algorithm for an outage probability of 10%. In terms of outage capacity, the branch and bound algorithm outperforms the conventional energy allocation algorithms, namely

- the equal energy allocation algorithm which is usually considered in downlink transmission and
- the SIR balancing algorithm which is usually considered in uplink transmission

by 36.4% and 56.8%, respectively.

Chapter 7

Summaries

7.1 Summary in English language

In future multiuser wireless systems, the limited system resources have to be extensively reused for serving several users. This results in received interferences at the users which limit the performance of the system. To demonstrate the interference problem in multiuser systems, a scenario with several source-destination node pairs communicating unidirectionally through a shared medium is considered. The communication among the nodes is assisted by some relays and takes place in two time slots. The source nodes transmit twice and the destination nodes receive twice during the two time slots and thus, they have two dimensional temporal transmit and receive filters, respectively. The present dissertation focuses on investigating how the relay and the filter coefficients can be smartly adjusted such that the system performance is enhanced.

For the considered scenario, interference alignment (IA) achievement is the first investigated problem. Basically, aligning the interferences at the destination nodes requires solving a multivariate system of polynomial equations. This system of equations is linearized by fixing the filter coefficients and hence, just the relay coefficients are optimized for achieving IA. The feasibility study of this IA algorithm shows that it requires a number of relays which increases quadratically with the number of node pairs. Moreover, the case of not having enough relays for achieving IA is studied. In this case, an interference mitigation (IM) algorithm which optimizes the relay coefficients aiming at minimizing the total interferences is proposed. Using this IM algorithm, the receive filters will not fully nullify the interferences and therefore, the remaining interferences are treated as noise. From the numerical results, one can conclude that the performance of the IA algorithm is good only at high signal to noise ratios (SNRs) while at low and moderate SNRs it performs poorly as compared to other conventional algorithms. Compared to the IA algorithm, a significant sum rate improvement in the low and moderate SNR regime is achieved when allowing some weak interferences being treated as noise using the IM algorithm.

The number of relays required for achieving IA can be reduced by adapting part of the filter coefficients to the channel in addition to the relay coefficients. By partially adapting the filters, the IA problem remains linear because the direct links are exploited.

The IA solutions form a multi-dimensional solution space of a homogenous system of linear equations. A closed form solution which selects the IA solution with the minimum sum mean square error (MSE) is derived. Apart from achieving IA, other alternative objectives which additionally reduce the noise powers and improve the useful signal powers are studied. Firstly, the sum MSE minimization problem with a total energy constraint is studied. By partially adapting the filters, the sum MSE becomes a convex function of both the relay coefficients and the unfixed filter coefficients and hence, a quadratically constrained quadratic minimization problem is solved to find the minimum sum MSE for a given total energy constraint. Secondly, the non-convex sum rate maximization problem is investigated. Basically, it is reformulated as a multi-convex optimization problem just by adding two sets of scaling factors. In the numerical results, both the sum MSE minimization and sum rate maximization algorithms show an out-performance over the IA algorithms at all SNRs.

Thanks to the linearity of the system, the effective channel between the source nodes and the destination nodes including the relays and the filters can be considered as an interference free channel after applying an IA solution. Based on this idea, the optimum energy allocation among the source nodes and the relays can be found using the waterfilling algorithm. From the numerical results, one can conclude that optimizing the energy allocation is essential only at low and moderate SNRs because at high SNRs equal energy allocation achieves sum rates close to the optimum ones. After applying an IM solution, the effective channel between the source nodes and the destination nodes including the relays and the filters can be considered as an interference channel. In interference channels, optimizing the energy allocation plays a key role in improving the performance. By treating the interference as noise, the sum rate function is not a concave function of the allocated energies, i.e., the function has many local maxima and a global maximum. Basically, the sum rate function is written as a difference of two concave functions and the global maximum is found using the proposed branch and bound algorithm.

The investigations on the energy allocation are extended to consider systems supporting multiple orthogonal resources. If an IA algorithm is applied on every resource, an energy allocation algorithm which maximizes the sum rate while maintaining equal rates achieved by the individual destination nodes is proposed. The effective channel can be seen as a parallel interference channel when an IM algorithm is applied in every resource. For parallel interference channels, the fact that there are no interferences among the resources is exploited by decomposing the energy allocation optimization problem among the resources. The energy allocation problem decomposition significantly reduces the complexity of the energy allocation algorithm so that the complexity increases only linearly with the number of resources.

7.2 Kurzfassung in deutscher Sprache

In zukünftigen Mehrbenutzerfunksystemen müssen die begrenzten Systemressourcen intensiv wiederverwendet werden. Dadurch empfangen die Benutzer Interferenzsignale, sodass die Performanz des Funksystems begrenzt wird. Um die Interferenzproblematik in Mehrbenutzerfunksystemen zu modellieren, wird ein Szenario bestehend aus mehreren Paaren von Quell- und Zielknoten betrachtet. Die Knotenpaare kommunizieren unidirektional miteinander. Die Kommunikation zwischen den Knoten wird von einigen Relays unterstützt und findet in zwei Zeitschlitzen statt. Die Quell- und Empfangsknoten senden beziehungsweise empfangen einmal pro Zeitschlitz und haben somit zweidimensionale Sende- und zweidimensionale Empfangsfilter. Diese Dissertation konzentriert sich auf die Untersuchung, wie die Relay- und die Filterkoeffizienten intelligent angepasst werden können, sodass die Performanz des Funksystems erhöht wird.

Interference-Alignment (IA) ist das erste untersuchte Verfahren. Zum Ausrichten der Interferenzen an den Zielknoten benötigt man die Lösung eines multivariaten Polynomgleichungssystems. Dieses Gleichungssystem kann durch Fixieren der Filterkoeffizienten linearisiert werden und dann werden nur die Relaykoeffizienten zum Erzielen von IA optimiert. Die Machbarkeitsstudie des vorgeschlagenen IA-Algorithmus zeigt, dass die Anzahl der benötigten Relays quadratisch mit der Anzahl der Knotenpaare steigt. Wenn nicht genug Relays zur Verfügung stehen, wird ein Interference-Mitigation (IM)-Algorithmus zum Reduzieren der Gesamtinterferenz vorgeschlagen. Die verbleibende Interferenz wird als Rauschen behandelt. Die numerischen Ergebnisse zeigen, dass der IA-Algorithmus nur für ein hohes SNR eine gute Performanz erzielt. Für ein geringes und mittleres SNR zeigt der IA-Algorithmus eine schlechte Performanz im Vergleich zu konventionellen Algorithmen. Im Vergleich zum IA-Algorithmus erreicht der IM-Algorithmus eine Performanzverbesserung bei geringen und mittleren SNRs.

Die Anzahl der benötigten Relays für IA kann reduziert werden, indem zusätzlich zu den Relaykoeffizienten ein Teil der Filterkoeffizienten optimiert wird. In diesem Fall bleibt das IA Problem linear, da die Direktverbindung zwischen den Knotenpaaren ausgenutzt wird. Die IA-Lösungen bilden so einen mehrdimensionalen Lösungsraum eines homogenen, linearen Gleichungssystems. Weiterhin wird eine geschlossene Lösung zum Finden der IA-Lösung dem minimalen Summen-MSE abgeleitet. Abgesehen vom IA werden auch Methoden zum Reduzieren der Rauschleistung und zum Vergrößern der Nutzsignalleistung untersucht. Zuerst wird das Problem der Minimierung des Summen-MSE bei beschränkter Summenenergie untersucht. Mit teilweise fixierten Filtern ist der Summen-MSE eine konvexe Funktion der Relaykoeffizienten und der unfixierten Filterkoeffizienten. Somit ist ein quadratisch-beschränktes quadratisches Minimie-

rungsproblem zu lösen. Zweitens wird das nicht-konvexe Problem der Summenraten-Maximierung bei beschränkter Summenenergie untersucht. Durch das Hinzufügen zweier Mengen von Skalierungsfaktoren als multi-konvexes Optimierungsproblem formuliert werden. Die numerischen Ergebnisse zeigen, dass sowohl die Summen-MSE-Minimierung als auch die Summenraten-Maximierung für alle SNR eine bessere Performanz als der IA-Algorithmus erreichen.

Aufgrund der Linearität des Systems kann, nachdem eine IA-Lösung angewendet wurde, der effektive Kanal zwischen Quell- und Zielknoten inklusive der Relays und der Filter als ein interferenzloser Kanal betrachtet werden. Aus diesem Grund wird die optimale Energieallokation mit der Waterfilling-Algorithmus gefunden. Die numerischen Ergebnisse zeigen, dass eine Optimierung der Energieallokation nur bei geringem und mittlerem SNR notwendig ist. Bei einem hohen SNR erreicht eine Gleichverteilung der Energie fast die gleiche Summenrate wie eine optimale Energieallokation. Wenn eine IM-Lösung angewendet wird, kann der effektive Kanal zwischen Quell- und Zielknoten inklusive der Relays und der Filter als ein Interferenzkanal betrachtet werden. In Interferenzkanälen spielt die Optimierung der Energieallokation eine Schlüsselrolle für die Performanzverbesserung des Funksystems. Wird die Interferenz als Rauschen betrachtet, dann ist die Summenraten-Funktion nicht mehr konkav, d.h. die Funktion hat viele lokale Maxima und ein globales Maximum. Die Summenraten-Funktion kann als Differenz zweier konkaver Funktionen formuliert werden. Das globale Maximum wird dann durch den vorgeschlagenen Branch-and-Bound-Algorithmus gefunden.

Die Untersuchung der optimalen Energieallokation wird auch für Systeme mit mehreren orthogonalen Ressourcen durchgeführt. Es wird ein Algorithmus zur Energieallokation vorgeschlagen, der die Summenrate bei gleichen Raten an den Zielknoten maximiert. Hierbei wird davon ausgegangen, dass IA für jede Ressource angewendet wird. Der effektive Kanal kann als ein paralleler Interferenzkanal gesehen werden, wenn ein IM-Algorithmus auf alle Ressourcen angewendet wird. In parallelen Interferenzkanälen wird die Tatsache genutzt, dass die orthogonalen Ressourcen keine Interferenz untereinander haben. Das Problem der Energieallokation kann dann in Teilprobleme für die einzelnen Ressourcen zerlegt werden. Es wird gezeigt, dass durch die Problemzerlegung die Berechnungskomplexität signifikant verkleinert wird. Dabei erhöht sich die Komplexität nur linear mit der Anzahl der Ressourcen.

Appendix A

Linear algebra

A.1 The Kronecker product and the vectorization operator

The Kronecker product is frequently used in this work. Given the two matrices $\underline{\mathbf{X}} = [\underline{x}^{(i,j)}] \in \mathbb{C}^{I \times J}$ and $\underline{\mathbf{Z}} = [\underline{z}^{(m,n)}] \in \mathbb{C}^{M \times N}$, the Kronecker product of $\underline{\mathbf{X}}$ and $\underline{\mathbf{Z}}$ denoted as $\underline{\mathbf{X}} \otimes \underline{\mathbf{Z}}$ is given by

$$\underline{\mathbf{X}} \otimes \underline{\mathbf{Z}} = \begin{pmatrix} \underline{x}^{(1,1)} \underline{\mathbf{Z}} & \cdots & \underline{x}^{(1,J)} \underline{\mathbf{Z}} \\ \vdots & & \vdots \\ \underline{x}^{(I,1)} \underline{\mathbf{Z}} & \cdots & \underline{x}^{(I,J)} \underline{\mathbf{Z}} \end{pmatrix} \in \mathbb{C}^{IM \times JN}. \quad (\text{A.1})$$

The resulting matrix has IJ blocks of size MN each.

Furthermore, the vectorization operator $\text{vec}(\cdot)$ is often used in conjunction with the Kronecker product. The vectorization of the matrix $\underline{\mathbf{X}}$ is given by

$$\text{vec}(\underline{\mathbf{X}}) = (\underline{x}^{(1,1)}, \dots, \underline{x}^{(I,1)}, \underline{x}^{(1,2)}, \dots, \underline{x}^{(I,2)}, \dots, \dots, \underline{x}^{(1,J)}, \dots, \underline{x}^{(I,J)})^T. \quad (\text{A.2})$$

$\text{vec}(\underline{\mathbf{X}})$ is IJ dimensional column vector.

A.2 Some properties of the Kronecker product and the vectorization operator

In this section, some properties of the Kronecker product and the vectorization operator used in this work are listed. For more information, see [MN99, Tur05]. Define the matrices $\underline{\mathbf{Y}} = [\underline{y}^{(j,m)}] \in \mathbb{C}^{J \times M}$ and $\underline{\mathbf{W}} = [\underline{w}^{(n,t)}] \in \mathbb{C}^{N \times T}$. Then, there are some properties of the Kronecker product and the vectorization operator including

$$(\underline{\mathbf{X}} \otimes \underline{\mathbf{Z}}) (\underline{\mathbf{Y}} \otimes \underline{\mathbf{W}}) = \underline{\mathbf{X}} \underline{\mathbf{Y}} \otimes \underline{\mathbf{Z}} \underline{\mathbf{W}}, \quad (\text{A.3})$$

$$\alpha \underline{\mathbf{X}} \otimes \underline{\mathbf{Y}} = \underline{\mathbf{X}} \otimes \alpha \underline{\mathbf{Y}} = \alpha (\underline{\mathbf{X}} \otimes \underline{\mathbf{Y}}), \quad (\text{A.4})$$

$$(\underline{\mathbf{X}} \otimes \underline{\mathbf{Z}})^{-1} = \underline{\mathbf{X}}^{-1} \otimes \underline{\mathbf{Z}}^{-1}, \quad (\text{A.5})$$

with $I = J$, $M = N$ and both $\underline{\mathbf{X}}$ and $\underline{\mathbf{Z}}$ being invertible. Furthermore,

$$\text{vec}(\underline{\mathbf{X}} \underline{\mathbf{Y}} \underline{\mathbf{Z}}) = (\underline{\mathbf{Z}}^T \otimes \underline{\mathbf{X}}) \text{vec}(\underline{\mathbf{Y}}), \quad (\text{A.6})$$

$$\text{tr}(\underline{\mathbf{X}} \underline{\mathbf{Y}}) = \text{vec}(\underline{\mathbf{X}}^T)^T \text{vec}(\underline{\mathbf{Y}}), \quad (\text{A.7})$$

and

$$\text{tr}(\underline{\mathbf{X}} \underline{\mathbf{Y}} \underline{\mathbf{Z}}) = \text{vec}(\underline{\mathbf{X}}^T)^T (\mathbf{I} \otimes \underline{\mathbf{Y}}) \text{vec}(\underline{\mathbf{Z}}). \quad (\text{A.8})$$

Let $\underline{\mathbf{x}}$ and $\underline{\mathbf{y}}$ be M dimensional and N dimensional column vectors, respectively. Then, the equalities

$$\text{vec}(\underline{\mathbf{x}} \underline{\mathbf{y}}^T) = \underline{\mathbf{y}} \otimes \underline{\mathbf{x}} \quad (\text{A.9})$$

and

$$\underline{\mathbf{x}}^{*T} \underline{\mathbf{Z}} \underline{\mathbf{y}} = \text{tr}(\underline{\mathbf{Z}} \underline{\mathbf{y}} \underline{\mathbf{x}}^{*T}) \quad (\text{A.10})$$

$$= \text{vec}(\underline{\mathbf{Z}}^T)^T \text{vec}(\underline{\mathbf{y}} \underline{\mathbf{x}}^{*T}) \quad (\text{A.11})$$

$$= \text{vec}(\underline{\mathbf{Z}}^T)^T (\underline{\mathbf{x}}^* \otimes \underline{\mathbf{y}}) \quad (\text{A.12})$$

$$= (\underline{\mathbf{y}}^T \otimes \underline{\mathbf{x}}^{*T}) \text{vec}(\underline{\mathbf{Z}}) \quad (\text{A.13})$$

hold. Finally, the trace property

$$\text{tr}(\underline{\mathbf{X}} \underline{\mathbf{Y}} \underline{\mathbf{Z}}) = \text{tr}(\underline{\mathbf{Y}} \underline{\mathbf{Z}} \underline{\mathbf{X}}) = \text{tr}(\underline{\mathbf{Z}} \underline{\mathbf{X}} \underline{\mathbf{Y}}) \quad (\text{A.14})$$

is applied in this work.

A.3 Woodbury matrix inversion lemma

Let $\underline{\mathbf{W}}$ and $\underline{\mathbf{Y}}$ be square and invertible matrices. The Woodbury matrix inversion lemma [TS86] can be stated as

$$(\underline{\mathbf{W}} + \underline{\mathbf{X}} \underline{\mathbf{Y}} \underline{\mathbf{Z}})^{-1} = \underline{\mathbf{W}}^{-1} - \underline{\mathbf{W}}^{-1} \underline{\mathbf{X}} (\underline{\mathbf{Y}}^{-1} + \underline{\mathbf{Z}} \underline{\mathbf{W}}^{-1} \underline{\mathbf{X}})^{-1} \underline{\mathbf{Z}} \underline{\mathbf{W}}^{-1}. \quad (\text{A.15})$$

Appendix B

Proofs of propositions

B.1 Proof of Proposition 1

Proof. The Rayleigh quotient maximization problem of (2.38) can be equivalently formulated as a general eigenvalue problem [TB97]

$$\frac{E_d |\underline{v}^{(k,1)}|^2}{\sigma^2} \underline{\mathbf{a}}^{(k)} \underline{\mathbf{a}}^{(k)*\text{T}} \underline{\mathbf{w}} = \rho \left(\frac{1}{E_{\text{Ctot}} - E_d |\underline{v}^{(k,1)}|^2} \mathbf{I}_{R_c M^2 + 1} + \mathbf{B}^{(k)} \right) \underline{\mathbf{w}}, \quad (\text{B.1})$$

where the eigenvalue and the eigenvector are denoted by ρ and $\underline{\mathbf{w}}$, respectively. For a fixed transmit energy $E_d |\underline{v}^{(k,1)}|^2$ in the first time slot, the maximum SNR in the second time slot is

$$\max \{ \gamma^{(k,2)} \} = \rho_{\max}, \quad (\text{B.2})$$

where ρ_{\max} is the largest eigenvalue of the problem of (B.1).

For the eigenvalue problem of (B.1), there is only a single nonzero eigenvalue and a single eigenvector because the rank of the vector $\underline{\mathbf{a}}^{(k)}$ is one. Accordingly,

$$\begin{aligned} & \text{rank} \left(\left(\frac{1}{E_{\text{Ctot}} - E_d |\underline{v}^{(k,1)}|^2} \mathbf{I}_{R_c M^2 + 1} + \mathbf{B}^{(k)} \right)^{-1} \underline{\mathbf{a}}^{(k)} \underline{\mathbf{a}}^{(k)*\text{T}} \right) = \\ & \min \left\{ \text{rank} \left(\left(\frac{1}{E_{\text{tot}}^{(k)} - E_d |\underline{v}^{(k,1)}|^2} \mathbf{I}_{R_c M^2 + 1} + \mathbf{B}^{(k)} \right)^{-1} \right), \text{rank} (\underline{\mathbf{a}}^{(k)}), \text{rank} (\underline{\mathbf{a}}^{(k)*\text{T}}) \right\} = 1. \end{aligned} \quad (\text{B.3})$$

Therefore, there is a single eigenvalue calculated as

$$\rho = \rho_{\max} = \frac{E_d |\underline{v}^{(k,1)}|^2}{\sigma^2} \text{tr} \left(\left(\frac{1}{E_{\text{Ctot}} - E_d |\underline{v}^{(k,1)}|^2} \mathbf{I}_{R_c M^2 + 1} + \mathbf{B}^{(k)} \right)^{-1} \underline{\mathbf{a}}^{(k)} \underline{\mathbf{a}}^{(k)*\text{T}} \right). \quad (\text{B.4})$$

Using (A.10), (B.4) can be rewritten as

$$\rho = \frac{E_d |\underline{v}^{(k,1)}|^2}{\sigma^2} \underline{\mathbf{a}}^{(k)*\text{T}} \left(\frac{1}{E_{\text{Ctot}} - E_d |\underline{v}^{(k,1)}|^2} \mathbf{I}_{R_c M^2 + 1} + \mathbf{B}^{(k)} \right)^{-1} \underline{\mathbf{a}}^{(k)}. \quad (\text{B.5})$$

Without loss of generality, the rest of the derivation considers single antenna $M = 1$ relays. By substituting the values of $\underline{\mathbf{a}}^{(k)}$ and $\mathbf{B}^{(k)}$ for $M = 1$, (B.5) can be rewritten as

$$\begin{aligned} \rho &= \frac{\left| \underline{h}_{\text{DS}}^{(k,k)} \right|^2}{\sigma^2} \left(E_{\text{Ctot}} - E_{\text{d}} \left| \underline{v}^{(k,1)} \right|^2 \right) \\ &+ \sum_{r=1}^{R_c} \frac{1}{\sigma^2} \frac{E_{\text{d}} \left| \underline{v}^{(k,1)} \right|^2 \left| \underline{h}_{\text{RS}}^{(r,k)} \right|^2 \left(E_{\text{Ctot}} - E_{\text{d}} \left| \underline{v}^{(k,1)} \right|^2 \right) \left| \underline{h}_{\text{DR}}^{(k,r)} \right|^2}{\sigma^2 + E_{\text{d}} \left| \underline{v}^{(k,1)} \right|^2 \left| \underline{h}_{\text{RS}}^{(r,k)} \right|^2 + \left(E_{\text{Ctot}} - E_{\text{d}} \left| \underline{v}^{(k,1)} \right|^2 \right) \left| \underline{h}_{\text{DR}}^{(k,r)} \right|^2}. \end{aligned} \quad (\text{B.6})$$

Let $E^{(1)}$ and $E^{(2)}$ be the transmitted energy in the first and the second time slots, respectively. Also, let $x = \frac{\left| \underline{h}_{\text{DS}}^{(k,k)} \right|^2}{\sigma^2}$, $y^{(r)} = \frac{\left| \underline{h}_{\text{RS}}^{(r,k)} \right|^2}{\sigma^2}$ and $z^{(r)} = \frac{\left| \underline{h}_{\text{DR}}^{(k,r)} \right|^2}{\sigma^2}$. Then, the sum SNR as a function of the transmitted energy in the first time slot with a total energy constraint can be written as

$$\gamma^{(k)}(E^{(1)}) = \gamma^{(k,1)} + \rho \quad (\text{B.7})$$

$$= xE^{(1)} + xE^{(2)} + \sum_{r=1}^{R_c} \frac{y^{(r)} E^{(1)} z^{(r)} E^{(2)}}{1 + y^{(r)} E^{(1)} + z^{(r)} E^{(2)}}. \quad (\text{B.8})$$

Because there is a total energy constraint, one can rewrite the transmitted energy in the first time slot as

$$E^{(1)} = \kappa E_{\text{Ctot}}, \quad (\text{B.9})$$

and in the second time slot as

$$E^{(2)} = (1 - \kappa) E_{\text{Ctot}}, \quad (\text{B.10})$$

where $0 \leq \kappa \leq 1$. By substituting (B.9) and (B.10) in (B.8), the sum SNR as a function of κ is written as

$$\gamma^{(k)}(\kappa) = E_{\text{Ctot}} \left(x + \sum_{r=1}^{R_c} \frac{y^{(r)} \kappa z^{(r)} (1 - \kappa)}{\frac{1}{E_{\text{Ctot}}} + y^{(r)} \kappa + z^{(r)} (1 - \kappa)} \right). \quad (\text{B.11})$$

To show the concavity of $\gamma^{(k)}(\kappa)$ in the domain of $0 \leq \kappa \leq 1$, it is sufficient to proof the concavity of the function

$$f^{(r)}(\kappa) = \frac{y^{(r)} \kappa z^{(r)} (1 - \kappa)}{\frac{1}{E_{\text{Ctot}}} + y^{(r)} \kappa + z^{(r)} (1 - \kappa)} \quad (\text{B.12})$$

for all $r = 1, \dots, R_c$ [BV04]. As the sufficient condition

$$\frac{\partial^2 f^{(r)}}{\partial \kappa^2} \leq 0 \quad (\text{B.13})$$

holds in the domain of $0 \leq \kappa \leq 1$ for any r , the function $f^{(r)}(\kappa)$ is concave and thus $\gamma^{(k)}(\kappa)$ is a concave function. This completes the proof. \square

B.2 Proof of Proposition 2

Proof. First, the concavity of the sum rate when considered as a function of the total energy constraint will be proved [AW11a, YL06]. Consider the optimization problem

$$\left(\mathbf{E}_{\text{opt}}^{(1)}, \dots, \mathbf{E}_{\text{opt}}^{(K)}\right) = \underset{(\mathbf{E}^{(1)}, \dots, \mathbf{E}^{(K)})}{\arg \max} \{C\} \quad (\text{B.14})$$

subject to

$$\sum_{n=1}^N \left(\sum_{k=1}^K \left(1 + \beta_{\text{IA}}^{(k,n)}\right) E^{(k,n)} + \left(\sigma_{\text{IAtx}}^{(n)}\right)^2 \right) = E_{\text{tot}}. \quad (\text{B.15})$$

The Lagrange of the optimization problem of (B.14)–(B.15) can be written as

$$\text{L}(\mathbf{E}^{(1)}, \dots, \mathbf{E}^{(K)}, \lambda) = C - \lambda \left(\sum_{n=1}^N \left(\sum_{k=1}^K \left(1 + \beta_{\text{IA}}^{(k,n)}\right) E^{(k,n)} + \left(\sigma_{\text{IAtx}}^{(n)}\right)^2 \right) - E_{\text{tot}} \right), \quad (\text{B.16})$$

where λ denotes the Lagrangian multiplier. The dual function can be calculated as

$$\text{d}(\lambda) = \max_{(\mathbf{E}^{(1)}, \dots, \mathbf{E}^{(K)})} \{\text{L}(\mathbf{E}^{(1)}, \dots, \mathbf{E}^{(K)}, \lambda)\} \quad (\text{B.17})$$

and the optimum Lagrangian multiplier is given by

$$\lambda_{\text{opt}} = \arg \min_{\lambda} \{\text{d}(\lambda)\}. \quad (\text{B.18})$$

Let

$$\text{f}(E_{\text{tot}}) = C_{\text{opt}} - \lambda_{\text{opt}} \left(\sum_{n=1}^N \left(\sum_{k=1}^K \left(1 + \beta_{\text{IA}}^{(k,n)}\right) E_{\text{opt}}^{(k,n)} + \left(\sigma_{\text{IAtx}}^{(n)}\right)^2 \right) - E_{\text{tot}} \right) \quad (\text{B.19})$$

be the optimum sum rate as a function of the total energy constraint. For $0 \leq \nu^{(n)} \leq 1$ with $n = 1, \dots, N$ and $\sum_{n=1}^N \nu^{(n)} = 1$. (B.19) can be rewritten as

$$\text{f}\left(\sum_{n=1}^N \nu^{(n)} E_{\text{totn}}^{(n)}\right) = C_{\text{opt}} - \lambda_{\text{opt}} \left(\sum_{n=1}^N \left(\sum_{k=1}^K \left(1 + \beta_{\text{IA}}^{(k,n)}\right) E_{\text{opt}}^{(k,n)} + \left(\sigma_{\text{IAtx}}^{(n)}\right)^2 \right) - \sum_{n=1}^N \nu^{(n)} E_{\text{totn}}^{(n)} \right), \quad (\text{B.20})$$

where $E_{\text{totn}}^{(n)}$ is the total energy at the n -th resource. Using the property of addition $C = \sum_{n=1}^N C^{(n)}$ of the rates where $C^{(n)}$ denotes the sum rate of the n -th resource, (B.20) becomes

$$\text{f}\left(\sum_{n=1}^N \nu^{(n)} E_{\text{totn}}^{(n)}\right) = \sum_{n=1}^N \left(C_{\text{opt}}^{(n)} - \lambda_{\text{opt}} \left(\sum_{k=1}^K \left(1 + \beta_{\text{IA}}^{(k,n)}\right) E_{\text{opt}}^{(k,n)} + \left(\sigma_{\text{IAtx}}^{(n)}\right)^2 \right) + \lambda_{\text{opt}} \nu^{(n)} E_{\text{totn}}^{(n)} \right), \quad (\text{B.21})$$

which fulfills the following inequality

$$f\left(\sum_{n=1}^N \nu^{(n)} E_{\text{totn}}^{(n)}\right) \geq \sum_{n=1}^N \nu_n f\left(E_{\text{totn}}^{(n)}\right). \quad (\text{B.22})$$

The equality holds when $\nu^{(n)} = 1$ and $\nu^{(m)} = 0$ for any other $m \neq n$. This proves the concavity of the function $f(E_{\text{tot}})$.

Secondly, the optimum sum rate is a strictly monotonic increasing function of the total energy constraint because of two reasons:

- The optimum sum rate is a logarithmic function where the logarithm is a monotonically increasing function.
- The optimum sum rate is a function of the optimum individual SNRs which is a strictly monotonic increasing function. This can be shown by the following argument. Considering the optimum energy allocation using the waterfilling algorithm, if the total energy constraint is increased, the water level is increased and thus, the individual SNRs are increased.

This completes the proof. □

Appendix C

Computational complexity

C.1 Complexity measure

When analyzing a complexity of an algorithm in terms of time, one needs to use an abstract measure independent of the central processing unit (CPU) type, the programming language and the programming style. Therefore, basic operations employed in an algorithm such as addition, subtraction, multiplication and division are usually considered in the complexity analysis. The complexity of an algorithm is a function of the number of input variables. Some operations like multiplication and division encounter a faster complexity growth with the dimensions of the input variables as compared to other operations like addition and subtraction.

The big-O notation $\mathcal{O}(\cdot)$, which describes the asymptotic behavior of an operation, a function or an algorithm is used as a complexity measure. Let $f(n)$ and $g(n)$ be real functions that map the size of an algorithm input variables n to its time complexity. Then,

$$g(n) \in \mathcal{O}(f(n)) \tag{C.1}$$

if

$$g(n) \leq c f(n), \tag{C.2}$$

where c is a positive real constant [NN11].

For instance, a polynomial which includes several terms, just the term with the highest order is considered in the complexity calculation because it has the fastest growth as compared to other terms. Furthermore, constant coefficients are ignored in the complexity analysis which is a reasonable assumption as we are interested in the asymptotic behavior.

C.2 Complexity of some mathematical operations and functions

In this section, the complexity of some basic mathematical operations used for calculating the computational complexity of the proposed algorithms is listed. Define the

matrices $\underline{\mathbf{X}} = [\underline{x}^{(i,j)}] \in \mathbb{C}^{I \times J}$, $\underline{\mathbf{Y}} = [\underline{y}^{(j,m)}] \in \mathbb{C}^{J \times M}$ and $\underline{\mathbf{Z}} = [\underline{z}^{(m,n)}] \in \mathbb{C}^{M \times N}$. The matrix $\underline{\mathbf{X}}$ is assumed to be full rank. Let $\underline{\mathbf{x}}$ and $\underline{\mathbf{y}}$ be column vectors of dimensions I and J , respectively. Let $\underline{\mathbf{L}}$ be a square lower triangular matrix of size $J \times J$. The complexities of some basic linear algebra operations are listed in Table C.1. For each operation, the number of complex multiplications is calculated and the corresponding complexity is shown. Part of the operations shown in Table C.1 are obtained from [Mac08, GV96].

Given the matrix $\underline{\mathbf{X}}$ with $J = I$, the matrix $\mathbf{I}_J \otimes \underline{\mathbf{X}}$ can be computed efficiently using a single finite loop with J iterations. Two nested finite loops each of which having J iterations are required for calculating the matrix $\underline{\mathbf{X}} \otimes \mathbf{I}_J$.

For a full rank tall matrix $\underline{\mathbf{X}}$, the complexity of the left pseudo inverse matrix

$$\underline{\mathbf{X}}^+ = (\underline{\mathbf{X}}^{*\text{T}} \underline{\mathbf{X}})^{-1} \underline{\mathbf{X}}^{*\text{T}} \quad (\text{C.3})$$

is calculated from Table C.1 as

$$\mathcal{O}(IJ^2 + J^3). \quad (\text{C.4})$$

Because $J < I$, (C.4) becomes

$$\mathcal{O}(IJ^2). \quad (\text{C.5})$$

Operation/function	Expression	Number of multiplications	Complexity
Product	$\underline{x} \underline{y}$	1	$\mathcal{O}(1)$
Division	$\underline{x}/\underline{y}$	1	$\mathcal{O}(1)$
Vector scaling	$\underline{x} \underline{y}$	J	$\mathcal{O}(J)$
Inner product	$\underline{\mathbf{x}}^{*\text{T}} \underline{\mathbf{y}}$ with $J = I$	J	$\mathcal{O}(J)$
Self outer product	$\underline{\mathbf{y}}^{*\text{T}} \underline{\mathbf{y}}$	J	$\mathcal{O}(J)$
Outer product	$\underline{\mathbf{x}} \underline{\mathbf{y}}^{*\text{T}}$	IJ	$\mathcal{O}(IJ)$
Tensor product	$\underline{\mathbf{x}} \otimes \underline{\mathbf{y}}$	IJ	$\mathcal{O}(IJ)$
Matrix scaling	$\underline{\mathbf{x}} \underline{\mathbf{Y}}$	JM	$\mathcal{O}(JM)$
Matrix-vector product	$\underline{\mathbf{X}} \underline{\mathbf{y}}$	IJ	$\mathcal{O}(IJ)$
Matrix-matrix product	$\underline{\mathbf{X}} \underline{\mathbf{Y}}$	IJM	$\mathcal{O}(IJM)$
Gram matrix generation	$\underline{\mathbf{X}} \underline{\mathbf{X}}^{*\text{T}}$	$\frac{I^2 J + IJ}{2}$	$\mathcal{O}(I^2 J)$
	$\underline{\mathbf{X}}^{*\text{T}} \underline{\mathbf{X}}$	$\frac{IJ^2 + IJ}{2}$	$\mathcal{O}(IJ^2)$
Matrix inversion	$\underline{\mathbf{X}}^{-1}$ with $J = I$	$\frac{J^3 + 3J}{2}$	$\mathcal{O}(J^3)$
Cholesky decomposition, see [KM11]	$\underline{\mathbf{X}} = \underline{\mathbf{L}} \underline{\mathbf{L}}^{*\text{T}}$ with $J = I$	$\frac{1}{6} J^3$	$\mathcal{O}(J^3)$
Triangular matrix inversion	$\underline{\mathbf{L}}^{-1}$	$\frac{J^3}{6} + \frac{J^2}{2} + \frac{J}{3}$	$\mathcal{O}(J^3)$
Left pseudo inverse	$\underline{\mathbf{X}}^+ = (\underline{\mathbf{X}}^{*\text{T}} \underline{\mathbf{X}})^{-1} \underline{\mathbf{X}}^{*\text{T}}$ with $J < I$		$\mathcal{O}(IJ^2)$
Kronecker product	$\underline{\mathbf{X}} \otimes \underline{\mathbf{Z}}$	$IJMN$	$\mathcal{O}(IJMN)$
	$\mathbf{I}_J \otimes \underline{\mathbf{X}}$ with $J = I$		$\mathcal{O}(J)$
	$\underline{\mathbf{X}} \otimes \mathbf{I}_J$ with $J = I$		$\mathcal{O}(J^2)$

Table C.1: Complexity of some mathematical operations and functions.

Appendix D

Acronyms and symbols

Acronyms

BS	Base Station
CCDF	Complementary Cumulative Distribution Function
CPU	Central Processing Unit
CSI	Channel State Information
DC	Difference of two Convex functions
DoF	Degree of Freedom
HK	Han and Kobayashi
IA	Interference Alignment
IC	Interference Channel
i.i.d.	independent identically distributed
IM	Interference Mitigation
MIMO	Multiple Input Multiple Output
MRC	Maximum Ratio Combining
MSE	Mean Square Error
OFDM	Orthogonal Frequency Division Multiplexing
PSNR	Pseudo Signal to Noise Ratio
SINR	Signal to Interference plus Noise Ratio
SIR	Signal to Interference Ratio
SNR	Signal to Noise Ratio
SR	Sum Rate

TDMA Time Division Multiple Access

TV Television

Frequently used symbols

$c^{(k,n)}$ achieved rate at the k -th destination node in the n -th resource

C sum rate

$C^{(k)}$ sum rate achieved at the k -th destination node

$C^{(n)}$ sum rate achieved in the n -th resource

C_{out} outage capacity

$\mathbf{C}_{\text{nn}}^{(k)}$ covariance matrix of the received noise signals at the k -th destination node

$\underline{\mathbf{C}}_{\text{rr}}^{(r)}$ covariance matrix of the received signals at the r -th relay

$\underline{d}^{(l)}$ transmitted data symbol of the l -th source node

$\underline{d}^{(l,n)}$ transmitted data symbol of the l -th source node in the n -th resource

$\underline{\hat{d}}^{(k)}$ estimated data symbol at the k -th destination node

$\underline{\hat{d}}^{(k,n)}$ estimated data symbol at the k -th destination node in the n -th resource

d_{dof} degrees of freedom

$\underline{e}^{(k,\tau)}$ received signal at the k -th source node in the τ -th time slot

$\underline{\mathbf{e}}_{\text{R}}^{(r)}$ received vector at the r -th relay

$E^{(k,n)}$ allocated energy at the k -th source node in the n -th resource

$\mathbf{E}^{(k)}$ vector of allocated energies at the k -th source node in all resources

$\mathbf{E}^{(n)}$ vector of allocated energies at the source nodes in the n -th resource

E_{d} average energy of the transmitted data symbols

E_{Ctot} total energy per cell

E_{Rtot} total energy transmitted by the relays

E_{Rx}	received energy in an antenna
E_{tot}	total energy constraint
$E_{\text{tot}}^{(\tau)}$	total energy used in the τ -th time slot
$E_{\text{totk}}^{(k)}$	total energy used for transmitting the k -th data symbol
E_{Tx}	transmitted energy of an antenna
f_c	carrier frequency
$\mathbf{G}^{(r)}$	processing matrix of the r -th relay
$\mathbf{h}_{\text{DR}}^{(k,r)}$	channel vector between the r -th relay and the k -th destination node
$\mathbf{h}_{\text{DR}}^{(k,r,n)}$	channel vector between the r -th relay and the k -th destination node in the n -th resource
$h_{\text{DS}}^{(k,l)}$	channel coefficient between the l -th source node and the k -th destination node
$\underline{h}_{\text{DS}}^{(k,l,n)}$	channel coefficient between the l -th source node and the k -th destination node in the n -th resource
$\mathbf{h}_{\text{RS}}^{(r,l)}$	channel vector between the l -th source node and the r -th relay
$\mathbf{h}_{\text{RS}}^{(r,l,n)}$	channel vector between the l -th source node and the r -th relay in the n -th resource
$\mathbf{H}^{(k,l)}$	effective channel between the l -th source node and the k -th destination node
I	number of iterations
\mathbf{I}	identity matrix
K	number of node pairs
L	Lagrange function
M	number of relay antennas
$\underline{n}_{\text{D}}^{(k,\tau)}$	received noise signal at the k -th destination node in the τ -th time slot
$\mathbf{n}_{\text{R}}^{(r)}$	received noise vector at the r -th relay
N	number of resources
P_{out}	outage probability

q	distance from a transmit antenna
q_0	minimum distance between a source node and a relay or a destination node
R	number of relays
R_c	number of relays in a considered cell
$\underline{s}^{(l,\tau)}$	transmitted signal of the l -th source node in the τ -th time slot
$\underline{u}^{(k,\tau)}$	receive filter coefficient of the k -th destination node in the τ -th time slot
$\underline{\mathbf{u}}^{(k)}$	receive filter of the k -th destination node
$\underline{v}^{(l,\tau)}$	transmit filter coefficient of the l -th source node in the τ -th time slot
$\underline{\mathbf{v}}^{(l)}$	transmit filter of the l -th source node
$\underline{\mathbf{x}}$	vector of the relay coefficients
$\underline{\mathbf{y}}$	vector of the relay coefficients and the unfixed filter coefficients
$\gamma^{(k)}$	SINR at the k -th destination node
$\gamma^{(k,\tau)}$	SNR at the k -th destination node in the τ -th time slot
γ_{PSNR}	PSNR pseudo SNR
δ	sum MSE
$\delta^{(k)}$	MSE at the k -th destination node
ϵ	arbitrary small positive value
$\epsilon^{(k,n)}$	energy used for transmitting the k -th data symbol in the n -th resource
$\boldsymbol{\epsilon}^{(n)}$	vector of used energies for transmitting the data symbols in the n -th resource
λ	lagrangian multiplier
$\underline{\boldsymbol{\lambda}}$	vector of lagrangian multipliers
ξ	effective channel gain between a node pair including the relays
$\rho^{(i)}$	the i -th eigenvalue
σ^2	noise variance at a receive antenna
v_c	speed of light

Bibliography

- [Aei73] Aein, J.: Power balancing in systems employing frequency reuse. *COM-SAT Technical Review*, vol. 3, 1973, pp. 277–299.
- [AGKW12a] Al-Shatri, H.; Ganesan, R. S.; Klein, A.; Weber, T.: Interference alignment using a MIMO relay and partially-adapted transmit/receive filters. *Proc. IEEE Wireless Communications & Networking Conference*, Paris, France, 2012, pp. 459–464.
- [AGKW12b] Al-Shatri, H.; Ganesan, R. S.; Klein, A.; Weber, T.: Perfect versus imperfect interference alignment using multiple MIMO relays. *Proc. 9th International Symposium on Wireless Communication Systems*, Paris, France, 2012, pp. 679–680.
- [Ahl74] Ahlswede, R.: The capacity region of a channel with two senders and two receivers. *The Annals of Probability*, vol. 2, 1974, pp. 805–814.
- [ALG⁺13a] Al-Shatri, H.; Li, X.; Ganesan, R. S.; Klein, A.; Weber, T.: Closed-form solutions for minimizing sum MSE in multiuser relay networks. *Proc. IEEE 77th Vehicular Technology Conference*, Dresden, Germany, 2013, pp. 1–5.
- [ALG⁺13b] Al-Shatri, H.; Li, X.; Ganesan, R. S.; Klein, A.; Weber, T.: Multi-convex optimization for sum rate maximization in multiuser relay networks. *Proc. 24th International Symposium on Personal, Indoor and Mobile Radio Communications*, London, UK, 2013, pp. 1–5.
- [AN82] Alavi, H.; Nettleton, R.: Downstream power control for a spread spectrum cellular mobile radio system. *Proc. IEEE Global Telecommunications Conference*, Miami, USA, 1982, pp. 84–88.
- [APW09] Al-Shatri, H.; Palleit, N.; Weber, T.: Transmitter power allocation for optimizing sum capacity interference channels. *Proc. 14th International OFDM-Workshop*, Hamburg, Germany, 2009, pp. 73–77.
- [AV09] Annapureddy, V. S.; Veeravalli, V.: Gaussian interference networks: Sum capacity in the low-interference regime and new outer bounds on the capacity region. *IEEE Transactions on Information Theory*, vol. 55, 2009, pp. 3032–3050.
- [AW10] Al-Shatri, H.; Weber, T.: Fair power allocation for sum-rate maximization in multiuser OFDMA. *Proc. International ITG/IEEE Workshop on Smart Antennas*, Bremen, Germany, 2010, pp. 350–354.
- [AW11a] Al-Shatri, H.; Weber, T.: Globally optimizing power allocation for maximum sum-rate in OFDM-based systems. *Proc. 16th International OFDM-Workshop*, Hamburg, Germany, 2011, pp. 26–30.

- [AW11b] Al-Shatri, H.; Weber, T.: Interference alignment aided by non-regenerative relays for multiuser wireless networks. *Proc. 8th International Symposium on Wireless Communication Systems*, Aachen, Germany, 2011, pp. 271–275.
- [AW12] Al-Shatri, H.; Weber, T.: Achieving the maximum sum rate using D.C. programming in cellular networks. *IEEE Transactions on Signal Processing*, vol. 60, 2012, pp. 1331–1341.
- [BCT11] Bresler, G.; Cartwright, D.; Tse, D.: *Settling the Feasibility of Interference Alignment for the MIMO interference channel: the Symmetric Square Case*. <http://arxiv.org/abs/1104.0888v1>, 2011.
- [Bel76] Bell, A. G.: *Improvement in Telegraphy*. US Patent 174,465, 1876.
- [BGN00] Byrd, R.; Gilbert, J.; Nocedal, J.: A trust region method based on interior point techniques for nonlinear programming. *Mathematical Programming*, vol. 89, 2000, pp. 149–185.
- [BHN99] Byrd, R.; Hribar, M.; Nocedal, J.: An interior point algorithm for large-scale nonlinear programming. *SIAM Journal on Optimization*, vol. 9, 1999, pp. 877–900.
- [Bin83] Binmore, K. G.: *Mathematical Analysis: A Straightforward Approach*. 2nd edition. Cambridge University Press, 1983.
- [BJS09] Bazaraa, M.; Jarvis, J.; Sherali, H.: *Linear Programming and Network Flows*. 4th edition. Wiley, 2009.
- [BKW⁺09] Berger, S.; Kuhn, M.; Wittneben, A.; Unger, T.; Klein, A.: Recent advances in amplify-and-forward two-hop relaying. *IEEE Communications Magazine*, vol. 47, 2009, pp. 50–56.
- [BNC⁺12] Bhat, P.; Nagata, S.; Campoy, L.; Berberana, I.; Derham, T.; Liu, G.; Shen, X.; Zong, P.; Yang, J.: LTE-Advanced: an operator perspective. *IEEE Communications Magazine*, vol. 50, 2012, pp. 104–114.
- [BNzOP06] Blcskei, H.; Nabar, R.; zgr Oyman; Paulraj, A.: Capacity scaling laws in MIMO relay networks. *IEEE Transactions on Wireless Communications*, vol. 5, 2006, pp. 1433–1444.
- [BPT10] Bresler, G.; Parekh, A.; Tse, D.: An approximate capacity of the many-to-one and one-to-many Gaussian interference channels. *IEEE Transactions on Information Theory*, vol. 56, 2010, pp. 4566–4592.
- [BV04] Boyd, S.; Vandenberghe, L.: *Convex Optimization*. Cambridge University Press, 2004.
- [CAAdCC08] Christensen, S. S.; Agarwal, R.; de Carvalho, E.; Cioffi, J.: Weighted sum-rate maximization using weighted MMSE for MIMO-BC beamforming design. *IEEE Transactions on Wireless Communications*, vol. 7, 2008, pp. 4792–4799.

- [Car75] Carleial, A.: A case where interference does not reduce capacity. *IEEE Transactions on Information Theory*, vol. 21, 1975, pp. 569–570.
- [Car78] Carleial, A.: Interference channels. *IEEE Transactions on Information Theory*, vol. 24, 1978, pp. 60–70.
- [Car83] Carleial, A.: Outer bounds on the capacity of interference channels. *IEEE Transactions on Information Theory*, vol. 29, 1983, pp. 602–606.
- [CC10] Chen, S.; Cheng, R.: Achieve the degrees of freedom of K -user MIMO interference channel with a MIMO relay. *Proc. IEEE Global Telecommunications Conference*, Miami, USA, 2010, pp. 1–5.
- [Cha66] Chang, R.: High speed multichannel data transmission with bandlimited orthogonal signals. *Bell System Technical Journal*, vol. 45, 1966, pp. 1775–1796.
- [Cim85] Cimini, L.: Analysis and simulation of a digital mobile channel using orthogonal frequency division multiplexing. *IEEE Transaction on Communications*, vol. 33, 1985, pp. 665–675.
- [CJ08] Cadambe, V.; Jafar, S.: Interference alignment and degrees of freedom of the K -user interference channel. *IEEE Transactions on Information Theory*, vol. 54, 2008, pp. 3425–3441.
- [CJ09] Cadambe, V.; Jafar, S.: Degrees of freedom of wireless networks with relays, feedback, cooperation, and full duplex operation. *IEEE Transactions on Information Theory*, vol. 55, 2009, pp. 2334–2344.
- [CMGG08] Chong, H. F.; Motani, M.; Garg, H. K.; Gamal, H. E.: On the hankobayashi region for the interference channel. *IEEE Transactions on Information Theory*, vol. 54, 2008, pp. 3188–3195.
- [Con78] Conway, J.: *Functions of One Complex Variable*. vol. 1. 2nd edition. Springer, 1978.
- [Cos85] Costa, M.: On the Gaussian interference channel. *IEEE Transactions on Information Theory*, vol. 31, 1985, pp. 607–615.
- [CS12] Chaaban, A.; Sezgin, A.: On the generalized degrees of freedom of the Gaussian interference relay channel. *IEEE Transactions on Information Theory*, vol. 58, 2012, pp. 4432–4461.
- [CT65] Cooley, J.; Tukey, J.: An algorithm for the machine calculation of complex fourier series. *Mathematics of Computation*, vol. 19, 1965, pp. 297–301.
- [CT06] Cover, T.; Thomas, J.: *Elements of Information Theory*. 2nd edition. John Wiley and Sons Ltd., 2006.
- [CTP⁺07] Chiang, M.; Tan, C. W.; Palomar, D.; O’Neill, D.; Julian, D.: Power control by geometric programming. *IEEE Transactions on Wireless Communications*, vol. 6, 2007, pp. 2640–2650.

- [CYM⁺06] Cendrillon, R.; Yu, W.; Moonen, M.; Verlinden, J.; Bostoen, T.: Optimal multiuser spectrum balancing for digital subscriber lines. *IEEE Transactions on Communications*, vol. 54, 2006, pp. 922–933.
- [DPSB08] Dahlman, E.; Parkvall, S.; Skold, J.; Beming, P.: *3G Evolution: HSPA and LTE for Mobile Broadband*. 2nd edition. Academic Press, 2008.
- [EAH09] Ellenbeck, J.; Al-Shatri, H.; Hartmann, C.: Performance of decentralized interference coordination in the LTE uplink. *Proc. IEEE 70th Vehicular Technology Conference*, Anchorage, USA, 2009, pp. 1–5.
- [Etk09] Etkin, R.: New sum-rate upper bound for the two-user Gaussian interference channel. *Proc. IEEE International Symposium on Information Theory*, Seoul, Korea, 2009, pp. 2582–2586.
- [ETW08] Etkin, R.; Tse, D.; Wang, H.: Gaussian interference channel capacity to within one bit. *IEEE Transactions on Information Theory*, vol. 54, 2008, pp. 5534–5562.
- [EW10] Eşli, C.; Wittneben, A.: A hierarchical AF protocol for distributed orthogonalization in multiuser relay networks. *IEEE Transactions on Vehicular Technology*, vol. 59, 2010, pp. 3902–3915.
- [FvFH95] Foley, J.; van Dam, A.; Feiner, S.; Hughes, J.: *Computer Graphics: Principles and Practice in C*. 2nd edition. Addison Wesley Professional, 1995.
- [GAWK13] Ganesan, R. S.; Al-Shatri, H.; Weber, T.; Klein, A.: Iterative MMSE filter design for multi-pair two-way multi-relay networks. *Proc. IEEE International Conference on Communications*, Budapest, Hungary, 2013, pp. 4522–4526.
- [GCJ11] Gomadam, K.; Cadambe, V.; Jafar, S.: A distributed numerical approach to interference alignment and applications to wireless interference networks. *IEEE Transactions on Information Theory*, vol. 57, 2011, pp. 3309–3322.
- [GG11] Guillaud, M.; Gesbert, D.: Interference alignment in the partially connected K -user MIMO interference channel. *Proc. IEEE International Symposium on Information Theory*, Barcelona, Spain, 2011, pp. 1095–1099.
- [GLZ12] Glazunov, A.; Lai, Z.; Zhang, J.: *LTE-Advanced and Next Generation Wireless Networks: channel Modeling and propagation*. Chap. Outdoor-Indoor Channels, pp. 123–151. John Wiley and Sons Ltd., 2012.
- [GMGK09] Ghozlan, H.; Mohasseb, Y.; Gamal, H. E.; Kramer, G.: The MIMO wireless switch: Relaying can increase the multiplexing gain. *Proc. IEEE International Symposium on Information Theory*, Seoul, Korea, 2009, pp. 1448–1452.

- [GMSW84] Gill, P.; Murray, W.; Saunders, M.; Wright, M.: Procedures for optimization problems with a mixture of bounds and general linear constraints. *ACM Transactions on Mathematical Software*, vol. 10, 1984, pp. 282–298.
- [GPK07] Gorski, J.; Pfeuffer, F.; Klamroth, K.: Biconvex sets and optimization with biconvex functions: a survey and extensions. *Mathematical Methods of Operations Research*, vol. 66, 2007, pp. 373–407.
- [GV96] Golub, G.; Van Loan, C.: *Matrix Computations*. 3rd edition. Addison Wesley Professional, 1996.
- [GVG94] Grandhi, S.; Vijayan, R.; Goodman, D.: Distributed power control in cellular radio systems. *IEEE Transactions in Communications*, vol. 42, 1994, pp. 226–228.
- [GVGZ93] Grandhi, S.; Vijayan, R.; Goodman, D.; Zander, J.: Centralized power control in cellular radio systems. *IEEE Transactions on Vehicular Technology*, vol. 42, 1993, pp. 466–468.
- [GZ94] Grandhi, S.; Zander, J.: Constrained power control in cellular radio systems. *Proc. IEEE 44th Vehicular Technology Conference*, vol. 2, Stockholm, Sweden, 1994, pp. 824–828.
- [HCM⁺12] Hoymann, C.; Chen, W.; Montojo, J.; Golitschek, A.; Koutsimanis, C.; Shen, X.: Relaying operation in 3GPP LTE: Challenges and solutions. *IEEE Communications Magazine*, vol. 50, 2012, pp. 156–162.
- [HK81] Han, T. S.; Kobayashi, K.: A new achievable rate region for the interference channel. *IEEE Transactions on Information Theory*, vol. 27, 1981, pp. 49–60.
- [HL09] Hayashi, S.; Luo, Z.-Q.: Spectrum management for interference-limited multiuser communication systems. *IEEE Transactions on Information Theory*, vol. 55, 2009, pp. 1153–1175.
- [HPT00] Horst, R.; Pardalos, P.; Thoai, N.: *Introduction to Global Optimization*. vol. 48 in *Nonconvex Optimization and its Applications*. 2nd edition. Kluwer Academic Publishers, 2000.
- [HPTd91] Horst, R.; Phong, T.; Thoai, N.; de Vries, J.: On solving a D.C. programming problem by a sequence of linear programs. *Journal of Global Optimization*, vol. 1, 1991, pp. 183–203.
- [HT99] Horst, R.; Thoai, V.: DC programming: Overview. *Journal of Optimization Theory and Applications*, vol. 103, 1999, pp. 1–43.
- [Ibe04] Ibenkahla, M.: *Signal Processing for Mobile Communications Handbook*. 1st edition. CRC Press, 2004.

- [Jaf11] Jafar, S.: *Interference Alignment – A New Look at Signal Dimensions in a Communication Network*. vol. 7 in *Foundations and Trends in Communications and Information Theory*. Now, 2011.
- [JIJ07] Jain, M.; IYengar, S.; Jain, R.: *Numerical Methods for Scientific and Engineering Computation*. 5th edition. New Age International Pvt Ltd. Publishers, 2007.
- [JS08] Jafar, S.; Shamai, S.: Degrees of freedom region of the MIMO X channel. *IEEE Transactions on Information Theory*, vol. 54, 2008, pp. 151–170.
- [Khu02] Khuri, A.: *Advanced Calculus with Applications in Statistics*. 2nd edition. Wiley-Interscience, 2002.
- [KM11] Krishnamoorthy, A.; Menon, D.: *Matrix inversion using Cholesky decomposition*. abs/1111.4144, 2011.
- [Kra04] Kramer, G.: Outer bounds on the capacity of Gaussian interference channels. *IEEE Transactions on Information Theory*, vol. 50, 2004, pp. 581–586.
- [Kra06] Kramer, G.: Review of rate regions for interference channels. *Proc. International Zurich Seminar on Communications*, Zurich, Switzerland, 2006, pp. 162–165.
- [KX10] Kumar, K. R.; Xue, F.: An iterative algorithm for joint signal and interference alignment. *Proc. IEEE International Symposium on Information Theory*, Austin, USA, 2010, pp. 2293–2297.
- [LAG⁺13] Li, X.; Al-Shatri, H.; Ganesan, R. S.; Klein, A.; Weber, T.: Feasibility conditions for relay-aided interference alignment in partially connected networks. *Proc. IEEE Vehicular Technology Conference*, Dresden, Germany, 2013, pp. 1–5.
- [LD10] Liu, S.; Du, Y.: A general closed-form solution to achieve interference alignment along spatial domain. *Proc. IEEE Global Telecommunications Conference*, Miami, USA, 2010, pp. 1–5.
- [LJ11] Lee, N.; Jafar, S.: *Aligned Interference Neutralization and the Degrees of Freedom of the 2 User Interference Channel with Instantaneous Relay*. arXiv:1102.3833v1, 2011.
- [LPGD⁺11] López-Pérez, D.; Güvenç, I.; De La Roche, G.; Kountouris, M.; Quek, T.; Zhang, J.: Enhanced intercell interference cooperation challenges in heterogeneous networks. *IEEE Wireless Communications Magazine*, vol. 18, 2011, pp. 22–30.
- [LZ08] Luo, Z.-Q.; Zhang, S.: Dynamic spectrum management: Complexity and duality. *IEEE Journal of Selected Topics in Signal Processing*, vol. 2, 2008, pp. 57–73.

- [Mac08] Maciel, T.: *Suboptimal Resource Allocation for Multi-User MIMO-OFDM System*. PhD thesis, Elektrotechnik und Informations-technik der Technischen Universität Darmstadt, 2008.
- [MB07] Morgenshtern, V.; Blcskei, H.: Crystallization in large wireless networks. *IEEE Transactions on Information Theory*, vol. 53, 2007, pp. 3319–3349.
- [Meg89] Megiddo, N.: *Advances in economic theory*. Chap. On the complexity of linear programming, pp. 225–268. Econometric Society Monographs. Cambridge University Press, 1989.
- [MHM11] Monzingo, R.; Haupt, R.; Miller, T.: *Introduction to adaptive arrays*. 2nd edition. SciTech Publishing, 2011.
- [MK09] Motahari, A. S.; Khandani, A. K.: Capacity bounds for the Gaussian interference channel. *IEEE Transactions on Information Theory*, vol. 55, 2009, pp. 602–642.
- [MN99] Magnus, J.; Neudecker, H.: *Matrix Differential Calculus with Applications in Statistics and Econometrics*. 2nd edition. Wiley, 1999.
- [MOGMAK09] Motahari, A.; Oveis-Gharan, S.; Maddah-Ali, M.-A.; Khandani, A.: *Real Interference Alignment: Exploiting the Potential of Single Antenna Systems*. cs.IT/0908.2282v2, 2009.
- [MXF⁺10] Ma, S.; Xing, C.; Fan, Y.; Wu, Y.-C.; Ng, T.-S.; Poor, H.: Iterative transceiver design for MIMO AF relay networks with multiple sources. *Proc. Military Communications Conference*, Princeton, USA, 2010, pp. 369–374.
- [NA83] Nettleton, R.; Alavi, H.: Power control for a spread spectrum cellular mobile radio system. *Proc. IEEE Vehicular Technology Conference*, Toronto, Canada, 1983, pp. 242–246.
- [NGJV09] Nazer, B.; Gastpar, M.; Jafar, S.; Vishwanath, S.: Ergodic interference alignment. *Proc. IEEE International Symposium on Information Theory*, Seoul, Korea, 2009, pp. 1769–1773.
- [NMK10] Nourani, B.; Motahari, A.; Khandani, A.: Relay-aided interference alignment for the quasi-static interference channel. *Proc. IEEE International Symposium on Information Theory*, Austin, USA, 2010, pp. 405–409.
- [NN11] Neapolitan, R.; Naimipour, K.: *Foundations of Algorithms*. 4th edition. Jones and Bartlett Publishers, 2011.
- [PD10] Papailiopoulos, D. S.; Dimakis, A. G.: Interference alignment as a rank constrained rank minimization. *Proc. IEEE Global Communications Conference*, Miami, USA, 2010, pp. 1–6.

- [PJ09] Peters, S. W.; Jr., R. W. H.: Interference alignment via alternating minimization. *Proc. IEEE International Conference on Acoustics, Speech, and Signal Processing*, Taipei, Taiwan, 2009, pp. 2445–2448.
- [PP02] Papoulis, A.; Pillai, S. U.: *Probability, Random Variables and Stochastic Processes*. 4th edition. McGraw-Hill, 2002.
- [PR80] Peled, R.; Ruiz, A.: Frequency domain data transmission using reduced computational complexity algorithms. *Proc. IEEE International Conference on Acoustics, Speech and Signal Processing*, Denver, USA, 1980, pp. 964–967.
- [QZH09] Qian, L. P.; Zhang, Y. J.; Huang, J.: MAPEL: Achieving global optimality for non-convex wireless power control problem. *IEEE Transactions on Wireless Communications*, vol. 8, 2009, pp. 1553–1563.
- [RCK92] Ruiz, A.; Cioffi, J.; Kasturia, S.: Discrete multiple tone modulation with coset coding for the spectrally shaped channel. *IEEE Transactions on Communications*, vol. 40, 1992, pp. 1012–1029.
- [RLL12] Razaviyayn, M.; Lyubeznik, G.; Luo, Z.-Q.: On the degrees of freedom achievable through interference alignment in a MIMO interference channel. *IEEE Transactions on Signal Processing*, vol. 60, 2012, pp. 812–821.
- [RW07] Rankov, B.; Witteneben, A.: Spectral efficient protocols for half-duplex fading relay channels. *IEEE Journal on Selected Areas in Communications*, vol. 25, 2007, pp. 379–389.
- [Sas04] Sason, I.: On the achievable rate region for the Gaussian interference channel. *IEEE Transactions on Information Theory*, vol. 50, 2004, pp. 1345–1355.
- [Sat77] Sato, H.: Two-user communication channels. *IEEE Transactions on Information Theory*, vol. 23, 1977, pp. 295–304.
- [Sat81] Sato, H.: The capacity of the Gaussian interference channel under strong interference. *IEEE Transactions on Information Theory*, vol. 27, 1981, pp. 786–788.
- [Sha49] Shannon, C.: Communication in the presence of noise. *Proceedings of the IRE*, vol. 37, 1949, pp. 10–21.
- [She95] Shenker, S.: Fundamental design issues for the future internet. *IEEE Journal on Selected Areas in Communications*, vol. 13, 1995, pp. 1176–1188.
- [SHMV08] Shen, M.; Høst-Madsen, A.; Vidal, J.: An improved interference alignment scheme for frequency selective channels. *Proc. International Symposium on Information Theory*, Toronto, Canada, 2008, pp. 559–563.

- [SKC09] Shang, X.; Kramer, G.; Chen, B.: A new outer bound and the noisy-interference sum-rate capacity for Gaussian interference channels. *IEEE Transactions on Information Theory*, vol. 55, 2009, pp. 689–699.
- [SLTW10] Shen, H.; Li, B.; Tao, M.; Wang, X.: MSE-based transceiver designs for the MIMO interference channel. *IEEE Transactions on Wireless Communications*, vol. 9, 2010, pp. 3480–3489.
- [SRLH11] Shi, Q.; Razaviyayn, M.; Luo, Z.-Q.; He, C.: An iteratively weighted MMSE approach to distributed sum-utility maximization for a MIMO interfering broadcast channel. *IEEE Transactions on Signal Processing*, vol. 59, 2011, pp. 4331–4340.
- [SSB⁺09] Schmidt, D.; Shi, C.; Berry, R.; Honig, M.; Utschick, W.: Minimum mean squared error interference alignment. *Proc. 43rd Asilomar Conference on Signals, Systems and Computers*, Pacific Grove, USA, 2009, pp. 1106–1110.
- [TB97] Trefethen, L.; Bau III, D.: *Numerical Linear Algebra*. 1st edition. SIAM, 1997.
- [TCS11] Tan, C. W.; Chiang, M.; Srikant, R.: Maximizing sum rate and minimizing MSE on multiuser downlink: Optimality, fast algorithms and equivalence via max-min SINR. *IEEE Transactions on Signal Processing*, vol. 59, 2011, pp. 6127–6143.
- [TGR09] Tresch, R.; Guillaud, M.; Riegler, E.: On the achievability of interference alignment in the K -user constant MIMO interference channel. *Proc. IEEE/SP 15th Workshop on Statistical Signal Processing*, Cardiff, UK, 2009, pp. 277–280.
- [TH11] Truong, K.; Heath Jr., R.: Interference alignment for the multiple-antenna amplify-and-forward relay interference channel. *Proc. 45th Asilomar Conference on Signals, Systems and Computers*, Pacific Grove, USA, 2011, pp. 1288–1292.
- [TS86] Tylavsky, D.; Sohie, G.: Generalization of the matrix inversion lemma. *Proceedings of the IEEE*, vol. 74, 1986, pp. 1050–1052.
- [Tur05] Turkington, D.: *Matrix Calculus and zero-one Matrices: Statistical and Econometric Applications*. 1st edition. Cambridge University Press, 2005.
- [Tuy98] Tuy, H.: *Convex Analysis and Global Optimization*. vol. 22 in *Nonconvex Optimization and Its Applications*. Springer, 1998.
- [Tuy00] Tuy, H.: Monotonic optimization: Problems and solution approaches. *SIAM Journal on Optimization*, vol. 11, 2000, pp. 464–494.
- [TV05] Tse, D.; Viswanath, P.: *Fundamentals of wireless communications*. 1st edition. Cambridge University Press, 2005.

- [UK08] Unger, T.; Klein, A.: Duplex schemes in multiple antenna two-hop relaying. *EURASIP Journal on Advances in Signal Processing*, vol. 2008, 2008, pp. 92:1–92:14.
- [WE71] Weinstein, S.; Elbert, P.: Data transmission by frequency-division multiplexing using the discrete fourier transform. *IEEE Transactions on Communication Technology*, vol. 19, 1971, pp. 628–634.
- [WMNO06] Waltz, R.; Morales, J.; Nocedal, J.; Orban, D.: An interior algorithm for nonlinear optimization that combines line search and trust region steps. *Mathematical Programming*, vol. 107, 2006, pp. 391–408.
- [WT08] Weng, Y.; Tuninetti, D.: On Gaussian interference channels with mixed interference. *Proc. of the Information Theory and Applications Workshop*, San Diego, USA, 2008, pp. 1–5.
- [YGC01] Yu, W.; Ginis, G.; Cioffi, J.: An adaptive multiuser power control algorithm for VDSL. *Proc. IEEE Global Telecommunications Conference*, vol. 1, San Antonio, USA, 2001, pp. 394–398.
- [YGC02] Yu, W.; Ginis, G.; Cioffi, J.: Distributed multiuser power control for digital subscriber lines. *IEEE Journal on Selected Areas in Communications*, vol. 20, 2002, pp. 1105–1115.
- [YGJK10] Yetis, C. M.; Gau, T.; Jafar, S. A.; Kayran, A. H.: On feasibility of interference alignment in MIMO interference networks. *IEEE Transactions on Signal Processing*, vol. 58, 2010, pp. 4771–4782.
- [YHXM09] Yang, Y.; Hu, H.; Xu, J.; Mao, G.: Relay technologies for WiMax and LTE-Advanced mobile systems. *IEEE Communications Magazine*, vol. 47, 2009, pp. 100–105.
- [YL06] Yu, W.; Lui, R.: Dual methods for nonconvex spectrum optimization of multicarrier systems. *IEEE Transactions on Communications*, vol. 54, 2006, pp. 1310–1322.
- [Zan92a] Zander, J.: Distributed cochannel interference control in cellular radio systems. *IEEE Transactions on Vehicular Technology*, vol. 41, 1992, pp. 305–311.
- [Zan92b] Zander, J.: Performance of optimum transmitter power control in cellular radio. *IEEE Transactions on Vehicular Technology*, vol. 41, 1992, pp. 57–62.

Thesen

- The performance of current multiuser wireless systems is limited by the interference.
- A multiuser wireless system is not interference limited anymore if interference alignment (IA) is applied.
- Relays can be employed in multiuser wireless systems for interference reduction rather than for the conventional task of range extensions.
- Realizing IA using relays is a more realistic approach than other approaches like using many time extensions or using many antennas at the communicating nodes.
- In multiuser relay networks, exploiting the direct links among the node pairs expands the dimensions of the transmit and the receive signal spaces.
- For a multiuser relay network, IA is a tri-affine problem of the transmit filter, the receive filter and the relay coefficients. By either fixing all the filter coefficients or fixing part of the filter coefficients, this tri-affine IA problem is linearized. Fixing part of the filter coefficients does not affect the dimensionality of the IA solution space.
- At low and moderate SNRs, leaving some weak interferences and treating them as noise leads to higher rates as compared to the ones achieved by fully canceling the interferences, i.e., by doing IA.
- IA nullifies the interferences in the system but it does not consider reducing the received noise powers. However, other approaches such as minimizing the sum MSE is promising as it keeps a compromise between the noise reduction and the interference reduction.
- In multiuser relay networks, the sum MSE is a tri-convex function of the transmit filter, the receive filter and the relay coefficients. Fixing part of the filter coefficients leads the sum MSE to be a convex function of the relay coefficients and the unfixed filter coefficients.
- Maximizing the sum rate is the ultimate goal in improving the system performance. The sum rate maximization problem is a non-convex problem but by adding two sets of scaling factors, it can be reformulated as a multi-convex optimization problem.

- For any multiuser communications system, the sum rate maximization problem can be equivalently formulated as a multi-convex optimization problem if the estimated data symbols can be written as multi-linear functions of the system variables.
- For a multiuser relay network, optimizing the energy allocation among the source nodes and the relays after applying an IA solution is equivalent to optimizing the energy allocation in interference free channels.
- Optimizing the energy allocation on the top of an IA solution does not improve the system performance significantly especially at high SNRs.
- For multiuser relay networks, optimizing the energy allocation among the source nodes and the relays is equivalent to optimizing the energy allocation in interference channels after applying a transmission scheme which mitigates the interferences but not fully nullifying them.
- Energy allocation in interference channels plays a key role in improving the system performance.
- In interference channels, the sum rate is not a concave function of the allocated energies rather it is a difference of two concave functions. This structure of the difference of two concave functions can be exploited to find the global maximum sum rate efficiently.

Selbstständigkeitserklärung

Ich erkläre, diese Arbeit selbständig angefertigt und die benutzten Unterlagen vollständig angegeben zu haben.

Rostock, den 05. November 2013

M.Sc. Hussein Al-Shatri

Lebenslauf

Persönliche Daten

Name	Hussein Al-Shatri
Geburtsdatum	01.01.1980
Geburtsort	Jeddah, Saudi-Arabien
Anschrift	Schweriner Straße 10, 18069 Rostock
Staatsangehörigkeit	Jemenitisch
Familienstand	Verheiratet

Schulbildung

1994–1997	Secondary School, Jeddah, Saudi-Arabien
1991–1994	Intermediate School, Jeddah, Saudi-Arabien
1985–1991	Primary School, Jeddah, Saudi-Arabien

Studium

10/2006–10/2008	Master-Studium (Communications Engineering) an der Technischen Universität München
09/1998–07/2003	Bachelor-Studium (Electronics and Communications Engineering) an der Hadhramout University of Science and Technology, Mukalla, Jemen

Berufserfahrung

02/2009–03/2014	Wissenschaftlicher Mitarbeiter am Institut für Nachrichtentechnik der Universität Rostock
10/2003–06/2006	Assistant Lecturer am Department of Electronics and Communications Engineering an der Hadhramout University of Science and Technology, Mukalla, Jemen

Rostock, den 05. November 2013

